Theory of extragalactic radio sources

Mitchell C. Begelman

Joint Institute for Laboratory Astrophysics, University of Colorado and National Bureau of Standards, Boulder, Colorado 80309 and Department of Astrophysical, Planetary, and Atmospheric Sciences, University of Colorado, Boulder, Colorado 80309

Roger D. Blandford

Theoretical Astrophysics, California Institute of Technology, Pasadena, California 91125

Martin J. Rees

Institute of Astronomy, Madingley Road, Cambridge CB3 OHA England

Powerful extragalactic radio sources comprise two extended regions containing magnetic field and synchrotron-emitting relativistic electrons, each linked by a jet to a central compact radio source located in the nucleus of the associated galaxy. These jets are collimated streams of plasma that emerge from the nucleus in opposite directions, along which flow mass, momentum, energy, and magnetic flux. Methods of using the observations diagnostically to infer the pressures, densities, and fluid velocities within jets are explained. The jets terminate in the extended radio components, where they interact strongly with the surrounding medium through a combination of shock waves and instabilities. Jets may expand freely, be confined by external gas pressure, or be pinched by toroidal magnetic fields. Shear flows are known to be Kelvin-Helmholtz unstable and thus may be responsible for some of the observed oscillation of jets about their mean directions and for creating the turbulence and shock waves needed to accelerate the relativistic electrons. Larger-scale bending may be caused by changes in the jet axis within the nucleus, gravitational interaction of the radio galaxy with a companion galaxy, or rapid motion of the source through dense intergalactic gas. The compact radio sources also exhibit a jet morphology and contain more direct clues as to the origins of jets; in particular, the variations sometimes observed imply bulk flows that are relativistic. It is widely believed that nuclear activity is ultimately ascribable to gas accreting onto a massive black hole. The accretion can proceed in several different fashions, depending upon whether or not the gas has angular momentum and whether or not the radiation emitted is sufficiently intense to influence the dynamics of the flow. Several distinct mechanisms for jet production in the context of black holes have been proposed. (Alternative mechanisms involving dense star clusters and massive spinning stars are also reviewed.) Supersonic jets may be collimated along the spin axis of a gas cloud surrounding the source of the lighter jet gas. Magnetic fields may be crucial in collimating jets, especially if they are wrapped around the jet by orbiting gas and can thereby collimate the outflow through the pinch effect. In fact, the spin energy of the black hole could also be extracted by magnetic torques, in which case the jet would contain electrons and positrons and carry a large electromagnetic Poynting flux. Statistical investigations of active galaxies also furnish valuable information on their nature and evolutionary behavior. The formation of particular kinds of sources appears to be correlated with environmental effects and cosmic epoch. In addition, the brightest compact radio sources on the sky, which probably involve relativistic motion, may be intrinsically faint objects beamed in our direction. There is now compelling evidence for the continuous fueling of extragalactic radio sources through jets emerging from the nucleus of the associated galaxy. The morphological classification of radio sources is interpreted in terms of the powers, speeds, and surroundings of jets. The ratio of the mass accretion rate to the mass of the hole may determine whether an active nucleus will be primarily a thermal object like an optical quasar or a nonthermal object like a radio galaxy. The authors outline a unified model of nuclear activity and assess what future progress may stem from observational developments (especially the proposed very long baseline array), experimental approaches (such as wind tunnel simulations), and theoretical studies (in particular, large-scale numerical hydrodynamical computing).

CONTENTS

Copyright ©1984 The American Physical Society

LIST OF SYMBOLS

B	magnetic flux density
d	jet diameter
I_ν	radiation intensity
J	spin angular momentum of black hole
Jy	jansky (1 Jy$=10^{-23}$ ergs cm^{-2} s^{-1} Hz^{-1})
H_0	Hubble constant (100 km s^{-1} Mpc^{-1} assumed)
L_E	Eddington luminosity ($L_E=4\pi GMM_p c/\sigma_T$)
M	mass (of central object)
$\dot{M}$	mass inflow rate
$M_\odot$	solar mass ($1M_\odot=2\times10^{33}$ g)
n_e	electron density
P_ν	spectral power at frequency ν
p	pressure
pc	parsec (1 pc$=3.09\times10^{18}$ cm)
R	radius (of central object)
r	radius (along jet)
r_g	gravitational radius of black hole ($r_g=GM/c^2$)
S_ν	flux density at frequency ν, measured in Jy
V	volume
VLA	Very Large Array. A radio interferometer in New Mexico, operated by the National Radio Astronomy Observatory
VLBI	very-long-baseline interferometry
v	speed (v_j=jet speed)
z	redshift
α	spectral index $-d\ln I_\nu/d\ln\nu$
α^*	viscosity parameter (shear stress/pressure)
β	slope of the pressure-radius relation $-d\ln p/d\ln r$
γ	Lorentz factor (γ_j=jet Lorentz factor)
θ	opening angle of jet ($\theta\sim d/r$)
ρ	gas density (ρ_e=density outside jet)
Υ	density of extragalactic objects. Number per unit comoving cubic Hubble radius
Ω	cosmological density parameter ($\Omega=8\pi G\bar{\rho}/3H_0^2$)
Ω_g	gyrofrequency ($\Omega_g=eB/mc$)

I. INTRODUCTION

A. Prologue

A few percent of the known galaxies in the universe contain hyperactive central regions. Compared with the size of a galaxy (tens of kiloparsecs)[1] the seat of this activity is extraordinarily compact, as indicated by rapid variability of the radiation flux on time scales as short as minutes. Yet the power output of an *active galactic nucleus,* in some of its more dramatic manifestations, can exceed the luminosity of a thousand normal galaxies (i.e., $\sim 10^{46}$ ergs s^{-1}) and equal the mass-energy equivalent of several solar masses per year.

The manifestations of nuclear activity are extremely diverse. The zoo of active galaxies includes *quasars,*[2] *Seyfert galaxies, radio galaxies, BL Lac objects,* etc., each type characterized by a set of observed properties and each subdivided to exhibit internal correlations. Active galactic nuclei are observed throughout the whole electromagnetic spectrum from 100-MHz radio waves to 100-MeV gamma rays. In this review, we are concerned with the subset of active galaxies that show powerful radio emission on length scales from parsecs to megaparsecs. These radio sources are believed to be powered by the associated galactic nuclei and involve energies that can exceed 10^{61} ergs, the mass equivalent of a million suns. This energy can be a substantial fraction, perhaps 10%, of the total energy an active nucleus radiates during its lifetime.

It is unlikely that mass can be converted into energy with better than a few (up to ten) percent efficiency; therefore, the more powerful active galactic nuclei must have "processed" upwards of $10^8 M_\odot$ through a region which is not much larger than the solar system.[3] Most of the mass which is not converted to energy will collect at the bottom of the gravitational potential well, and it is the belief of most astrophysicists that this process leads inevitably to the formation of a massive black hole, which is not merely the by-product of activity in a galactic nucleus, but is in fact the "prime mover" responsible for producing the energetic phenomena which we observe. No other entity can convert mass to energy with such a high efficiency, or within such a small volume.

It is beyond the scope of this article to describe completely the role that black holes may play in active galactic nuclei, and we shall confine our attention to those properties directly relevant to the production of radio sources. Although we shall necessarily adopt a radio-astronomical perspective, we wish to emphasize that such "spectral chauvinism" has no place in the modern study of active galaxies and that a complete defense of the black hole hypothesis involves observations and ideas not reviewed below.

Over the past ten years radio observations have shown us unexpected phenomena which have revolutionized our ideas about the structure and energetics of active galactic nuclei. Specifically, they have revealed that many galactic nuclei produce what appear to be collimated *jets* of plasma, which traverse the vast distances spanned by the extended radio emission. We shall argue that the concept of the jet is crucial to understanding all active nuclei, not just those associated with strong radio sources. However, it is the behavior of the jets themselves and the associated radio lobes that we can observe directly and of which we have the most detailed knowledge. Consequently, most theoretical work has been directed towards describing the radio sources without particular reference to their origins. Our review will reflect this bias.

B. Development of extragalactic radio astronomy

The study of active galactic nuclei, and especially extragalactic radio sources, has evolved somewhat unsystematically and carries a great deal of historical baggage, such as complex classifications schemes which will surely become streamlined as the field matures. Objects which were once thought to be different are now being found to be related. For this reason, we shall begin our discussion with a brief sketch of the major observational and theoretical developments that led to our current viewpoint.

1. Observations

The first nonoptical branch of the electromagnetic spectrum to be opened up for extensive astronomical investigation was at radio wavelengths. (Excellent accounts of the early development of radio astronomy are given by Hey, 1971; Kraus, 1976; and Edge and Mulkay, 1976.) By the early 1950s it was apparent that there were a large number of cosmic radio sources that were essentially unresolved—the radio "stars"—and a vigorous debate ensued as to whether they were galactic or extragalactic objects. When the positions were sufficiently well measured to permit optical identifications, it became clear that many sources were indeed associated with external *radio galaxies* (e.g., Baade and Minkowski, 1954), and it was suggested that the radio emission might be caused by galaxy-galaxy collisions. A difficulty with this idea was soon apparent from the earliest interferometric studies. In particular, Jennison and Das Gupta (1953) discovered that Cygnus A, the most powerful nearby extragalactic

---

[1] 1 parsec (pc) $= 3.09 \times 10^{18}$ cm $\simeq 3$ light years.

[2] The term "quasar" originally referred to "quasistellar" extragalactic objects, i.e., objects with bright starlike optical images. However, more and more quasars have been shown to exhibit low-surface-brightness extensions, and there seems no reason to doubt that all quasars reside in the centers of galaxies. For this reason we prefer to define quasars as those active galactic nuclei that are bright enough optically to outshine their host galaxies. They usually exhibit broad emission lines and large redshifts, implying great cosmological distances and powers.

[3] $1 M_\odot$ = one solar mass $= 2 \times 10^{33}$ g.

source, is *extended,* and in fact comprises two blobs of intense radio emission straddling the optical galaxy. As radio interferometers improved in sensitivity and resolution, many more examples of "double" radio sources were found (e.g., Maltby and Moffet, 1963), including several for which no obvious galactic identification could be made.

The picture became more complicated in 1963 with the discovery of *quasars* (Schmidt, 1963). Optically, quasars appear stellar, although they are apparently very distant and thus extremely powerful—often more luminuous than a thousand galaxies. As the radio band was extended to higher frequencies, a new class of extragalactic radio source was identified and found to be common. These *compact* radio sources were essentially pointlike, frequently variable, and usually identified with quasars or similar optical sources (e.g., Dent, 1965). Many extended sources were also associated with quasars, and most straddled radio cores.

In fact, quasars were first discovered in the course of making optical identifications of sources in radio surveys, and it was initially thought that all quasars were *radio loud.* However, the close connection between radio galaxies and quasars was obscured somewhat when astronomers developed techniques for optically identifying quasars through the properties of their continuum spectra and characteristic *broad emission lines* ($\Delta\lambda/\lambda \sim 0.03$) (Davidson and Netzer, 1979). It was found that these optically selected quasars were similar to their radio-selected counterparts in optical properties, but that ~ 90—$95\,\%$ of them were *radio quiet* (but, as we shall see, not silent). From an optical standpoint, radio-quiet quasars are basically high-luminosity *Type I Seyfert galaxies* (Seyfert, 1943; Weedman, 1977). Seyfert galaxies are spiral galaxies that possess bright nuclei and exhibit broad emission lines. They generally possess weak radio sources. By contrast, from a radio standpoint, the (radio-loud) quasars are related to radio galaxies, which are all elliptical.

Not all compact radio sources are quasars, however. It was discovered in the early 1970s that many of the most variable radio sources were associated with *BL Lac objects,* named after the eponymous "variable star" *BL Lacertae* (Schmitt, 1968; Blake, 1970). The optical identifications were generally stellar but, in contrast to quasars, did not exibit emission lines. Most of these *BL Lac* objects are low-redshift elliptical galaxies (Wolfe, 1978). Their power-law optical continua are unusually highly polarized, in contrast to those of most quasars (Angel and Stockman, 1980). *BL Lac* objects appear to be related to a subset (about 10%) of radio quasars that are termed *optically violently variable* (OVV).

The construction in the late 1960s through 1970s of large aperture-synthesis (linked) radio *interferometers* at Cambridge, England; Westerbork, Holland; Greenbank, West Virginia; and especially the Very Large Array (VLA) near Socorro, New Mexico; resulted in considerable improvements in resolution ($\lesssim 1$ arc sec) and sensitivity (down to 10^{-5} flux units or janskys, where 1 Jy $\equiv 10^{-23}$ ergs s^{-1} cm^{-2} Hz^{-1}). The resolution is somewhat better than that achieved by the largest ground-based optical telescopes. In addition, radio telescopes are far more sensitive than optical telescopes in terms of energy flux in a broad-band signal, typically by a factor of over a hundred. It is largely for this reason that they have played such a prominent role in the development of modern astronomy. A radio interferometer essentially measures the Fourier transform of the radio source brightness distribution, which can be inverted to produce a map of the source. Large samples of radio sources such as the 3CR catalog were routinely mapped and their spectra and polarizations studied. Attempts at morphological classification and statistical studies then became possible. Notable events during the early to mid 1970s include the discovery of *radio trails* (also called "head-tail galaxies"—Miley *et al.,* 1972), the Fanaroff-Riley (1974) classification scheme for strong and "relaxed" doubles, the discovery of the *hot spots* in the lobes of Cygnus A (Miley and Wade, 1971; Hargrave and Ryle, 1974), and the recognition of "bridges" linking extended radio structure with the compact nucleus in some radio doubles—the latter were the forerunners of jets (van Breugel and Miley, 1977; Waggett, Warner, and Baldwin, 1977). It was not until the advent of the VLA that the dynamic range and resolution were sufficient to reveal the ubiquity of highly collimated, low-surface-brightness jets (see Sec. I.D.1).

The technique of *very-long-baseline interferometry* (VLBI) was developed simultaneously with the construction of the modern generation of linked radio interferometers. VLBI differs from conventional interferometry in that the antenna spacing or baseline b can be as large as the Earth. This means that the angular resolution achievable at a characteristic wavelength $\lambda \sim 2$—10 cm, given approximately by (λ/b), is typically measured in milliarc-seconds (mas). In the late 1960s through the mid 1970s, such resolution was achieved at the cost of a greatly reduced sensitivity (~ 0.1 Jy) and dynamic range, because the large distances between antennae give rise to uncertainties in the phase relationships at opposite ends of the baseline. This and the poor coverage of the Fourier transform plane meant that detailed mapping was impossible, and the best that could be hoped for was a fit to a "model" consisting of two or three point sources. Unsatisfactory as they were, these primitive techniques enabled Cohen, Kellermann, Moffet, Shapiro, and coworkers (Moffet *et al.,* 1971; Cohen *et al.,* 1971; Whitney *et al.,* 1971) to discover *superluminal expansion,* although their results were not universally accepted until confirmed by more sophisticated VLBI observations nearly a decade later. By comparing observations made at different epochs, they found that features in their models of certain quasars appeared to be separating at speeds much greater than the speed of light.

VLBI came into its own in 1978, when it became practical to recover most of the phase information from a system of three of more antennae by using *closure phase* (Jennison, 1958; Readhead and Wilkinson, 1978). Since then, and with the design of broad-band correlators, ~ 3 mJy sensitivity levels are now possible. Current VLBI maps

are as sensitive and detailed as maps made using the linked interferometers of ten years ago. Using VLBI it has been possible to probe the structure of the more powerful compact radio sources on scales as small as a few parsecs (still about 10^5 times larger than the size of a hypothetical associated black hole), to map jets in many of these sources, and to observe their structures changing with time.

A related technique is radio-linked interferometry, pioneered at Jodrell Bank, England. The Multi-Element Radio-Linked Interferometer (MERLIN), with maximum baselines measured in hundreds of kilometers, is capable of producing maps with resolution (typically 0.01—0.1 arc sec) and dynamic range intermediate between that of the VLA and intercontinental VLBI.

There have also been developments in other wavebands. Optical identifications of large samples of distant radio sources are now fairly complete. In addition, several prominent regions of extended radio emission have recently been detected at optical wavelengths using modern detectors and at x-ray energies using the Einstein satellite.

2. Theory

The theoretical development of extragalactic radio astronomy has proceeded along two lines—one concentrating on the extended sources and the other focusing on compact sources and *radio-loud* quasars—which, until recently, have remained quite separate. Both lines of research did, however, adopt a common fundamental postulate proposed by Alfvén and Herlofsen (1950) and Shklovsky (1953), that the basic emission mechanism in most observed radio sources is incoherent synchrotron emission, produced by a nonthermal population of relativistic electrons gyrating in a magnetic field. Important results of synchrotron theory and associated diagnostics are outlined in Appendix A, and these form the basis for most statements that have been made about physical conditions within radio sources.

The earliest theories of extended sources associated double structure with mysterious explosions occurring within the nuclei of galaxies and involving the ejection of clouds of magnetized plasma (e.g., van der Laan, 1963; De Young and Axford, 1967; Sturrock and Feldman, 1968; Mills and Sturrock, 1970), or condensed objects (e.g., Burbidge, 1967). These theories were to some extent analogies drawn with solar flares and supernova remnants. One immediate difficulty with explosion models is the so-called adiabatic loss problem. In dynamical expansion, the internal energy associated with the relativistic electrons is converted into bulk kinetic energy, and the electron energies scale in proportion to the cube root of the background density. GeV electrons in the extended components would need to have been unacceptably energetic in the nucleus if they had been transported adiabatically. It was therefore clear that some of the bulk kinetic energy must be channeled back into particle acceleration, (e.g., through shocks or turbulence) *in situ*. This conclusion was put on a firmer footing with the discovery of the hot spots in Cygnus A in which the radiative lifetimes of the emitting electrons are shorter than the crossing times. An additional problem involved the energy content of the emitting regions. It had been shown as early as 1958 (Burbidge, 1958) that a source like Cygnus A must contain at least 10^{59} ergs in the energy of relativistic particles and magnetic fields, yet there was no evidence of such energetic explosions having occurred.

The "slingshot" model (Saslaw, Valtonen, and Aarseth, 1974; De Young, 1976; Valtonen, 1979) attempted to deal with these difficulties by supposing that compact objects (e.g., massive black holes) are responsible for particle acceleration within the extended components. The compact objects form in a three-body system. This is dynamically unstable, and the system breaks up into a binary and a single object flying apart in opposite directions. Adiabatic losses are minimized because the gas associated with the compact objects is gravitationally confined; the required energy reserve may be supplemented through accretion of gas onto the compact object. However, failure to detect pointlike sources within the extended components, together with the discovery of jets (see below), has led to a decline in the popularity of this type of model.

To some researchers, the evidence for ongoing activity in the nuclei associated with double radio sources suggested a direct energetic connection between the nuclear and extended regions of emission. Partly for this reason, it was proposed that the internal energy of radio sources might be supplied continuously from the nucleus through *beams, channels,* or *exhausts* (Rees, 1971; Longair, Ryle, and Scheuer, 1973; Scheuer, 1974; Blandford and Rees, 1974). In this class of models adiabatic losses are unimportant because most of the energy is transported in the form of bulk kinetic energy. Reconversion into random energy occurs at a "working surface" at the end of the channel, which is a natural site for particle acceleration. Blandford and Rees associated the hot spots with the working surface. Because of the continuous nature of the energy flow, the energy necessary for the extended emission could be stored up during the course of the source's evolution.

Let us now turn to the compact sources. An important early clue to the nature of these objects came from observations of radio outbursts in many quasars, with characteristic rise and decay times of months to a few years. These outbursts were commonly described in terms of an adiabatically expanding sphere of radius R in which the particle energies decay $\propto R^{-1}$ and the field strength decreases $\propto R^{-2}$. This soon proved inadequate. The original model (Kellermann and Pauliny-Toth, 1966; van der Laan, 1966; Shklovsky, 1960) had no dynamical basis, and objections similar to those raised against explosive models of extended components can be sustained. Furthermore, its detailed spectral predictions are not in accord with observations of individual outbursts (e.g., Altschuler and Wardle, 1976).

Variability time scales were taken as direct indicators

of a size limits on the compact components, through light-travel-time arguments. However, when the resulting dimensions were used to estimate radiation energy densities within the sources, it appeared that the source models would fall prey to the "inverse Compton catastrophe" (Hoyle, Burbidge, and Sargent, 1966), in which relativistic electrons cool catastrophically by Compton up-scattering their own synchrotron photons. At first, this appeared to threaten the entire incoherent synchrotron interpretation of the radio emission, but Rees (1966,1967a) pointed out that highly relativistic motion of some of the emitting material along the line of sight would cause the observer to underestimate the actual size of the source, thus overestimating the importance of Compton cooling. A further corollary of ultrarelativistic motion is the possibility of superluminal expansion, and this prediction was confirmed by the earliest VLBI experiments (see Sec. I.B.1).

These, then, were some of the theoretical issues at the time that the VLA and closure-phase VLBI began to reveal the presence of jets on all scales. To set the stage for our current theoretical viewpoint, we next summarize the observed properties of extragalactic radio sources as we perceive them in 1984.

FIG. 1. Prototypical "edge-brightened" strong double source Cygnus A (3C405), showing the characteristic hot spots, lobes, and nucleus (cf. Fig. 10). This radio image, made with the VLA operating at $\lambda=6$ cm, has a resolution of 0".7. Data from Perley, Cowan, and Dreher, in preparation; image supplied by R. A. Perley.

C. Observations of extragalactic radio sources—examples and trends

We do not intend in this article to give a detailed review of the observations. The current observational situation for extended sources may be found by consulting Miley (1980), Fomalont (1981), and especially Bridle and Perley (1984). Recent VLBI observations of compact sources are reviewed by Kellermann and Pauliny-Toth (1981) and Pauliny-Toth (1981). The most recent reviews of the whole field are contained in the proceedings of IAU Symposium No. 97 (edited by Heeschen and Wade, 1982) and IAU Symposium No. 110 (edited by Kellermann and Setti, 1984). We style this section "Examples and Trends" because many of the generalizations we describe based on VLA and VLBI data do not yet have the statistical weight of "complete" samples behind them. However, there are now sufficiently many examples of each phenomenon that we are unlikely to be led seriously astray if we test our theories against these trends.

Extended radio sources, in which most of the radio power at $\sim$GHz frequencies comes from regions $\gtrsim 3$ kpc in size, have structures that are loosely correlated with their absolute powers. The more powerful double sources with radio powers $\gtrsim 10^{42}$ ergs s^{-1} are typically 100—300 kpc in linear extent, and tend to be *edge brightened* (Fig. 1) (Fanaroff and Riley, 1974; Readhead and Hewish, 1976; Miley, 1980). That is to say, the regions of highest surface brightness, known as *hot spots,* are located at the outer extremities of two extended radio components (lobes) that usually straddle the optical identification. Hot spots contribute a larger fraction of the total radio luminosity in the more powerful radio sources (Readhead and Longair, 1975; Jenkins and McEllin, 1977; Laing and Peacock, 1980). Weaker sources generally appear more complex and are *edge darkened* (Fig. 2); however, they can be much larger than strong doubles in linear extent, with sizes ranging up to ~ 5 Mpc (e.g., 3C236; Willis, Strom, and Wilson, 1974). The radio power of the central component appears to be correlated with the total radio luminosity. Furthermore, the strength of the optical emission lines and nonthermal continuum radiation from the nucleus of the associated galaxy also appears to be

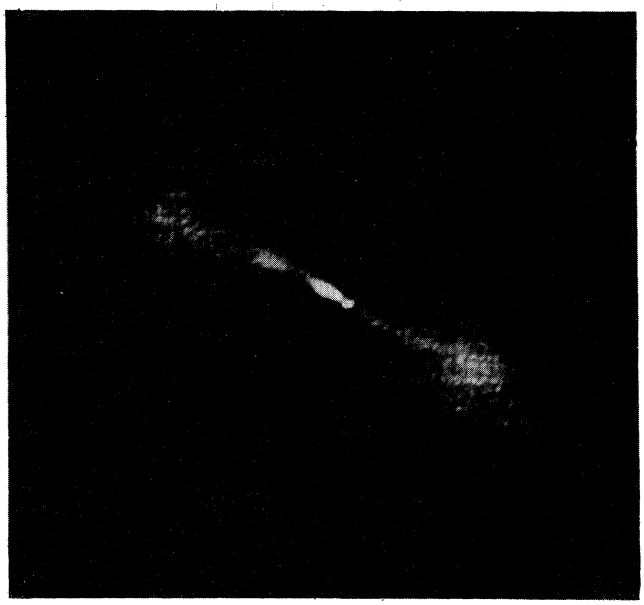

FIG. 2. Image of the weak "edge-darkened" radio source $2354+471$, made using the VLA at $\lambda=20$ cm. Data from Burns and Gregory (1982), image supplied by J. O. Burns.

similarly correlated with the source structure (Hine and Longair, 1979; Wilkinson, Hine, and Sargent, 1981).

Most extended sources are now known to be triple rather than double as they were first described. They display a compact *core* prominent at high frequencies and positionally identified with the nucleus of the associated galaxy or quasar, in addition to the two outer components.

Observationally, a *jet* is a thin feature that appears to emanate from the nucleus and to end in one of the regions of extended emission. The first known extragalactic jet, emanating from the giant elliptical M87, was discovered optically by Curtis (1918), and is now well mapped in the radio (Biretta, Owen, and Hardee, 1983). Jets are observed in both radio galaxies and quasars. In the case of radio galaxies, jets are disproportionately common amongst the weaker sources (e.g., M84) in which case they are usually seen with comparable brightness on both sides of the nucleus and are frequently quite distorted (Fig. 3). Extreme cases of this trend are supplied by the Seyfert galaxies within whose nuclei are found very faint twisted jets up to a few kpc in length (Wilson, 1982). In radio galaxies of intermediate power, jets are typically either one sided or one jet is much brighter than the other. These jets are much straighter and better collimated than those associated with weaker radio galaxies. A good example is NGC 6251 (Fig. 4). Jets are much harder to find in the most powerful radio galaxies [although an exception to this "rule" must be made in the case of Hercules A (Dreher and Feigelson, 1984), which displays characteristics of both strong and weak sources (Fig. 5)]. An extremely faint jet has just been found connecting the nucleus to one lobe in the prototypical example, Cygnus A (Perley, 1984), and in this case the collimation is extraordinarily good—the opening angle is smaller than 2°.

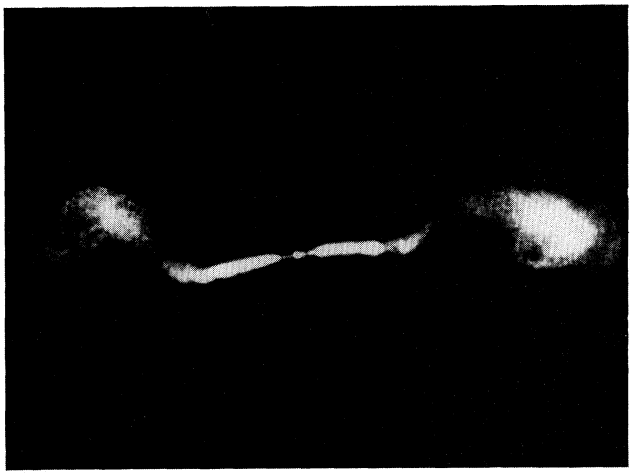

FIG. 3. Prominent jets and a high degree of symmetry are characteristic of the weaker radio sources, such as 3C449. The reflection (*C*-type) symmetry may result from the orbital motion of the parent galaxy around a companion, which is visible on optical photographs. This VLA image, made at $\lambda = 22$ cm, has a resolution of 1″.4. Data from Cornwell and Perley, in preparation; image supplied by R. A. Perley.

However, powerful one-sided jets are quite common in the radio quasars (Bridle and Perley, 1984). Even when the jet is invisible, the nucleus and the outer hot spots are often impressively collinear, suggesting that the jet is extremely straight (Hargrave and McEllin, 1975).

Jets are often surrounded by low-surface-brightness *cocoons* that are believed to be filled with plasma that has already passed along the jet and through the head of the source. Many of the sources that do not exhibit jets do show *bridges*—patches of diffuse emission connecting the outer components with the galaxy.

Extreme distortion occurs in *radio trails* or "head-tail" sources and *wide-angle tails,* both of which are found almost exclusively in rich clusters of galaxies. Examples are NGC 1265 (Owen *et al.,* 1979; Fig. 6) and 3C465 (Burns, 1981; Eilek *et al.,* 1984; Fig. 7), respectively. Here it appears that the jets are being "swept back" by the motion of the galaxy through the intergalactic medium. The more symmetric examples are sometimes called "relaxed doubles" (Fig. 2). Other sources exhibit either reflection or inversion symmetry about the nucleus (Ekers, 1982). Reflection symmetry may reflect the orbital motion of the parent galaxy about a binary companion (e.g., 3C31; Burch, 1977b), while inversion symmetry may reflect precession of the jet axis (e.g., NGC 326; Ekers *et al.,* 1978) or buoyancy effects in the interstellar medium of a distorted galaxy. Sometimes more than one source of curvature may be present: in the radio trail 3C129, short-wavelength oscillations are superimposed on the swept-back jets (Rudnick and Burns, 1981). The one-sided jets seen in stronger sources, which are generally straighter, often show low-amplitude *wiggles* (e.g., NGC 6251; Saunders *et al.,* 1981; Fig. 4).

Not only are small cores being found in extended sources, the majority of compact sources are now found to be surrounded by extended emission prominent at low frequencies (Perley, Fomalont, and Johnston, 1982). This secondary emission is usually one sided, and the compact sources may simply be extended sources, seen end-on. The strongest support for this hypothesis comes from recent VLBI observations showing one-sided jets emanating from the nuclei of both extended and compact sources (Readhead, 1980, and references therein). In fact, most compact extragalactic sources that have been well resolved by VLBI (more than 20) show a jetlike feature with an unresolved bright spot at one end, a so-called *core-jet* structure (e.g., Readhead and Pearson, 1984; see Figs. 8 and 9). Where such structure occurs in the nucleus of an extended source, the component and extended structures are fairly well aligned (Fig. 4). This correlation may extend to very weak radio sources in the nuclei of normal galaxies (Jones, Sramaek, and Terzian, 1981). Where no extended jet is seen in an extended source, the compact jet usually lines up well with the extended lobe structure. However, in core-halo sources and compact doubles, the alignment is not so good (Readhead, Cohen, Pearson, and Wilkinson, 1978; Linfield, 1981a), and some VLBI jets appear to curve by as much as 40° in the first few milli-arc-seconds (Fig. 8). A subset of these exhibit

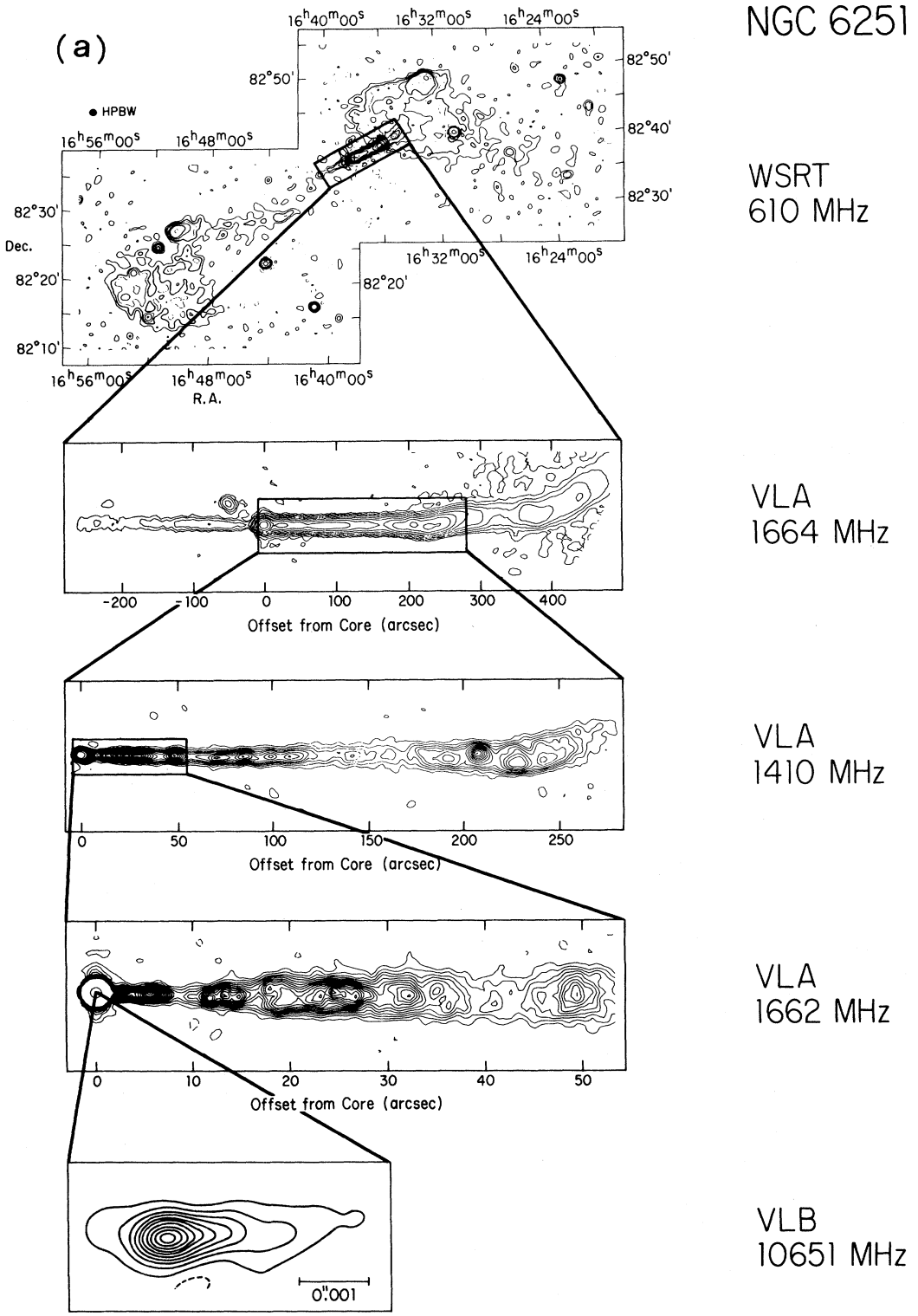

FIG. 4. (a) Montage showing the jet and counterjet of NGC 6251 over a wide range of angular scales. The large brightness asymmetry between jet and counterjet and the relative straightness of the jet are characteristic of moderately bright radio sources. The nuclear core-jet source (bottom panel) and the mean position angle of the large-scale jet are misaligned by $4.5° \pm 1°$. Top panel, Willis *et al.* (1982); second and third panels, Perley and Bridle, in preparation; fourth panel, Perley, Bridle, and Willis (1984); bottom panel, Cohen and Readhead (1979). Montage reproduced from Bridle and Perley (1984), with permission from the *Annual Review of Astronomy and Astrophysics,* Vol. 22, © 1984 by Annual Reviews, Inc. (b) Greyscale image of the jet in NGC 6251 made with the VLA at $\lambda = 22$ cm, with 2".1 resolution. Data from Perley, Bridle, and Willis (1984); image supplied by R. A. Perley.

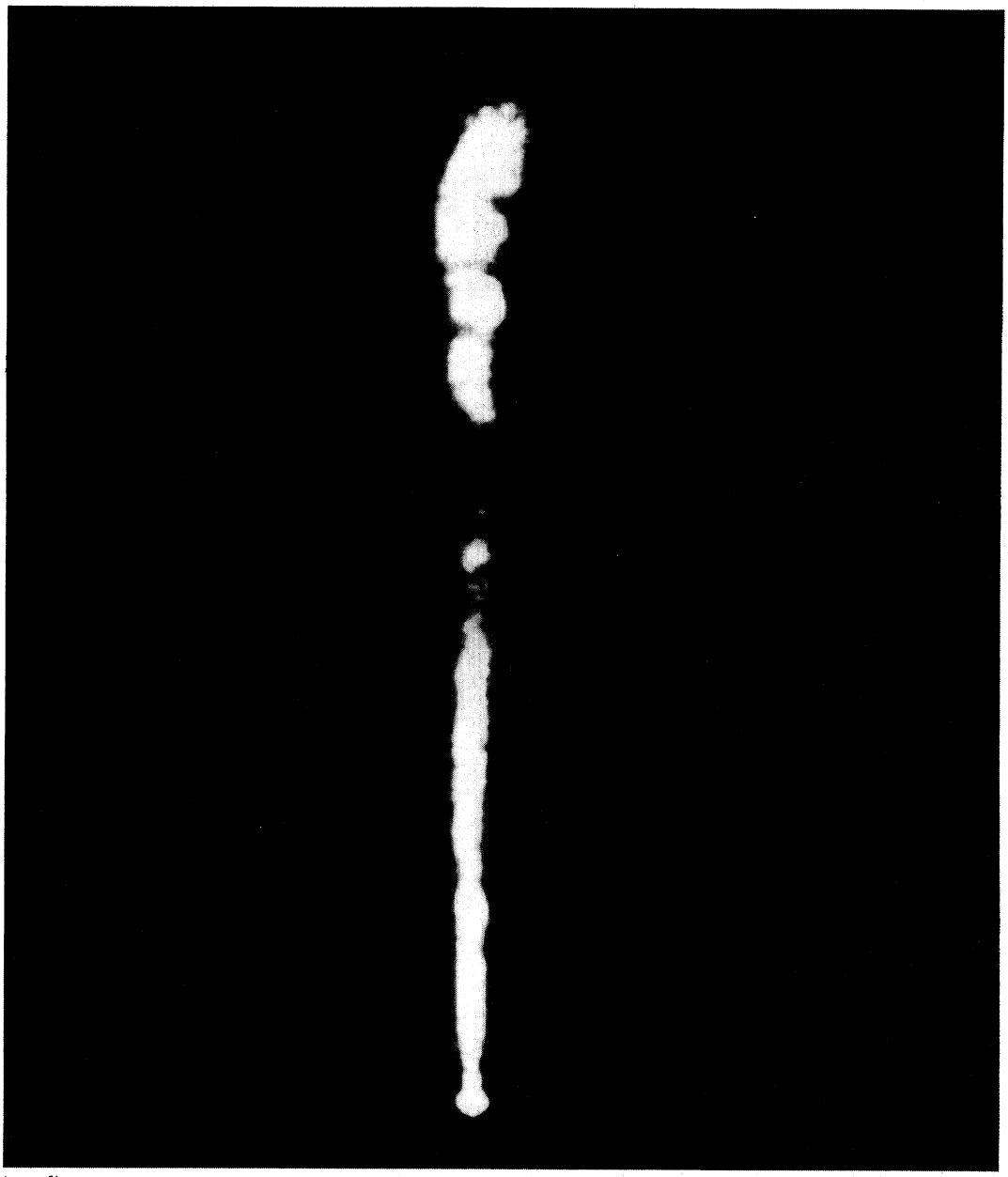

FIG. 4. *(Continued).*

apparent superluminal expansion, which probably indicates relativistic motion nearly along the line of sight (see Secs. II.A.4 and III.A.3 and Fig. 9). If core-halo sources are ordinary doubles viewed nearly along the jet axis, then the large apparent curvature of compact jets is easily understood as a slight physical curvature, exaggerated by projection.

Extragalactic radio sources are usually observed in the frequency range $\nu \sim 100$ MHz—10 GHz and have power-law spectra. The observed *flux density* S_ν obeys $S_\nu \propto \nu^{-\alpha}$ where α, the *spectral index,* lies in the range ~ 0.5—1 for the brighter regions of extended sources. Hot spots and jets tend to have flatter spectra $\alpha \lesssim 0.5$, and fainter regions of diffuse emission have steeper spectra $\alpha \gtrsim 0.8$—2. The spectra of extended components of sources in rich clusters are often very steep (Slingo, 1974a,1974b; Burns *et al.,* 1981). The high-frequency spectra of compact sources are usually flat, i.e., $\alpha \sim 0$. This explains why compact sources are found preferentially in higher-frequency surveys. Nonthermal optical and x-ray emission is of course observed from many compact radio cores, e.g., quasars, but it is only recently that optical emission has been detected from extended radio sources. As polarization measurements are not yet available, it is not known whether this radiation is synchrotron emission from extremely energetic electrons or arises from some

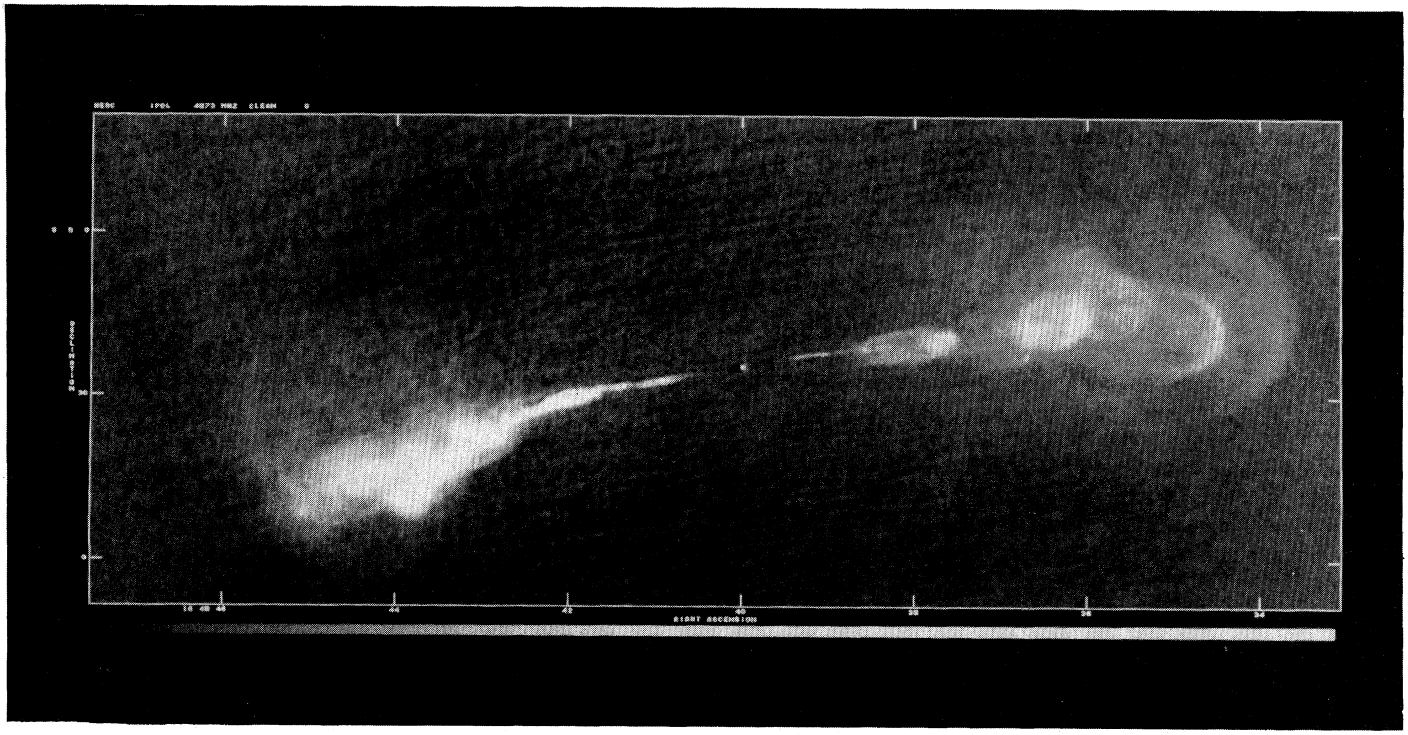

FIG. 5. The puzzling object Hercules A (3C348) displays characteristics of both the strong ("edge-brightened") and weak ("edge-darkened") sources, and may represent a transitional case. This 6-cm VLA image has a resolution of 0.″5. Data from Dreher and Feigelson (1984); image supplied by E. D. Feigelson.

other process. Several jets have also been traced in the optical and/or x-ray wavebands (e.g., Miley *et al.*, 1981; Butcher, van Breugel, and Miley, 1980; Schreier, Burns, and Feigelson, 1981; Feigelson *et al.*, 1981). Optical observations have revealed both continuum and line emission (Saslaw, Tyson, and Crane, 1978; van Breugel *et al.*, 1984). The line emission appears to be excited by nonthermal uv radiation. Indeed, the first known example of

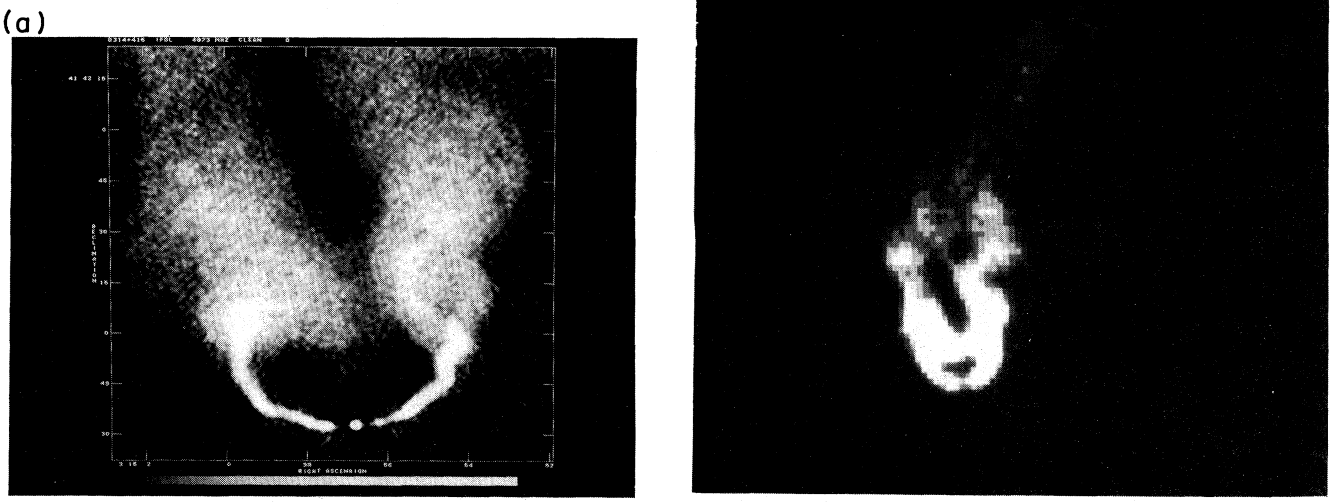

FIG. 6. (a) The jets in the prototypical radio trail NGC 1265 (3C83.1B) are believed to be swept back by the ram pressure of the intergalactic medium. The sharp edges above and below the inner jets are artifacts of the reproduction process. (VLA image at $\lambda=6$ cm, 1.″2 resolution.) (b) Traced over hundreds of kiloparsecs, the source has a tadpole-like appearance. (VLA image at $\lambda=20$ cm, $13''\times11''$ resolution.) Data from O'Dea and Owen, in preparation; images supplied by C. P. O'Dea.

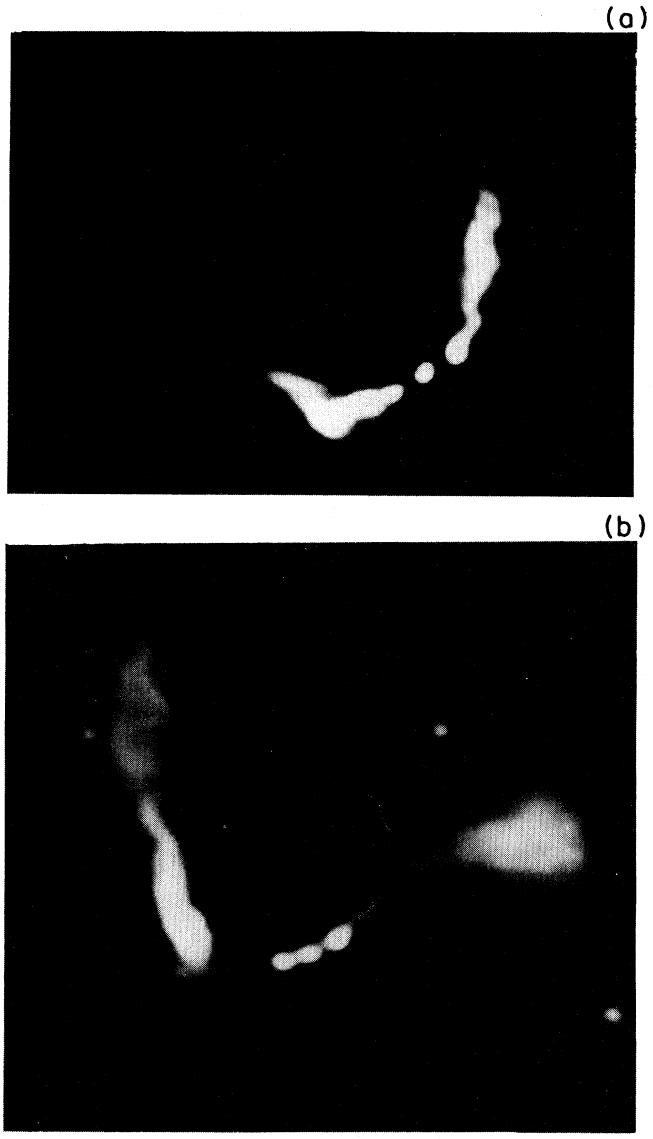

FIG. 7. 3C465 (a) and 1919 + 479 (b) are typical of the sources known as "wide-angle tails." Like radio trails (Fig. 6), wide-angle tails are found almost exclusively in rich clusters of galaxies, and the curvature is believed to result from interaction between the jets and the intracluster medium. Data on 3C465 (VLA at $\lambda=20$ cm with $9''.5\times12''$ resolution) from Eilek, Burns, O'Dea, and Owen, 1984; image supplied by C. P. O'Dea. Data on 1919 + 479 (VLA at $\lambda=20$ cm with 5″ resolution) from J. O. Burns (1981); image supplied by J. O. Burns.

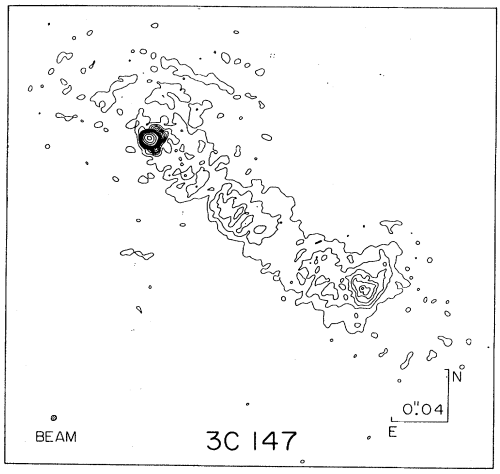

FIG. 8. The quasar 3C147 mapped at 1661 MHz by Simon, Readhead, and Wilkinson (1984), using a ten-station VLBI interferometer. Note the small beam size, indicating that the jet is well resolved. This source shows typical one-sided core-jet structure. Map supplied by R. S. Simon and T. J. Pearson.

an extragalactic jet was the one-sided optical jet in the elliptical galaxy M87 (Curtis, 1918), which is now known to have a radio counterpart (Biretta, Owen, and Hardee, 1983). M87, Centaurus A, and (more controversially) 3C273 have been detected as x-ray jets (Feigelson, 1983).

Linear polarization studies provide a further powerful probe of the physics of radio sources. Emission at radio frequencies is believed to originate with electrons of energies typically ≈ 100 MeV—10 GeV, gyrating in magnetostatic fields of strength $B\sim10^{-6}$—10^{-1} G. This emission is linearly polarized with the electric vector normal to the projection of the magnetic field direction (Appendix A). Measurements of strength and position angle of the polarization provide information on the degree of order and alignment of the magnetic fields. For radio jets, the pattern that is emerging is that for the powerful sources the fields are parallel to the jet axis, whereas for weaker jets the fields are perpendicular, although they are often parallel near the walls of the jet and close to the nucleus (Bridle, 1982; Fig. 12 below). Fields in hot spots tend to be transverse to the source axis (e.g., Dreher, 1979), whereas those in the diffuse outer regions are frequently observed to be aligned parallel to the boundaries of these regions. In the diffuse regions, degrees of polarization as large as 60%, close to the maximum possible for synchrotron radiation, are sometimes observed. This indicates that the field is highly organized on a large scale, rather than having a large fluctuating component. Furthermore, one can apply the theory of Faraday rotation (Appendix A Sec. 4) to multifrequency polarization measurements to place limits on the amount of thermal plasma mixed in with the radiating nonthermal electrons and along the line of sight. In some compact sources (e.g., *BL Lac*'s) these constraints are exceptionally tight and indicate that virtually all of the plasma is highly relativistic (Wardle, 1977).

A final, but crucial, observational development which must be noted is the discovery of small-scale jets within our galaxy. The most notable example is the peculiar object SS433 (e.g., Margon, 1982), in which the existence of a pair of precessing jets was inferred from optical spectra. The jets have since been mapped directly with the VLA (Hjellming and Johnson, 1981) and VLBI (Neill *et al.*, 1982), and their interaction with the interstellar medium has been studied through the structure of the associated extended radio source, W50 (Geldzahler, Pauls, and Salter, 1980). Other galactic objects now show evidence for

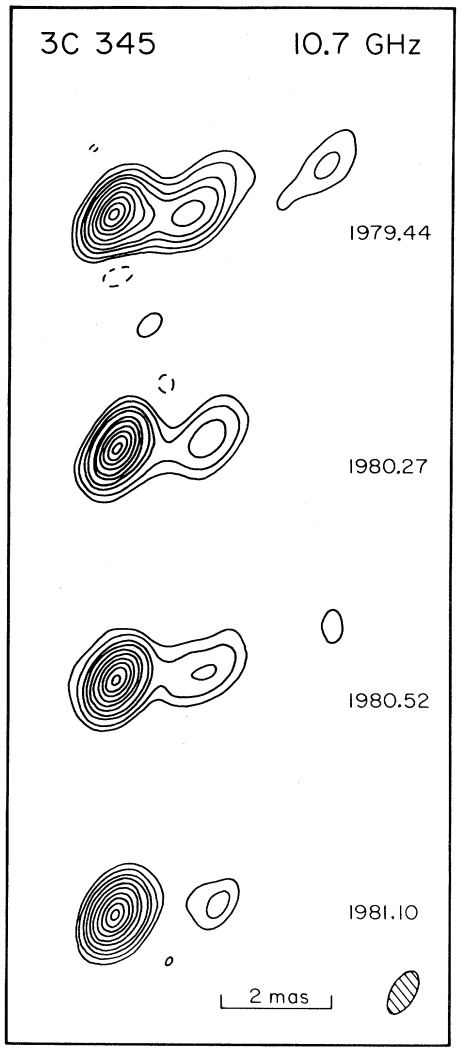

FIG. 9. Sequence of VLBI maps made by Unwin *et al.* (1983) at four epochs illustrate apparent superluminal expansion in the nucleus of 3C345. If 3C345 lies at the cosmological distance given by its redshift ($z=0.595$), then the two faint "knots" are separating from the bright "core" at an apparent projected speed of $\sim 8c$. At the assumed distance, the resolution (shown by the hatched restoring beam at lower right) is better than 4 pc. Reproduced, with permission, from Unwin *et al.* (1983), © 1983 by the American Astronomical Society.

jets, notably the x-ray source Scorpius X-1 (which has double radio lobes; Fomalont *et al.*, 1983), young stars (e.g., Mundt and Fried, 1983) and a number of molecular clouds (Schwarz, 1983). The importance of these local objects to an understanding of the jet phenomenon cannot be overestimated, not only because they are nearby, but also because they indicate that jets form under an enormous range of physical conditions.

In spite of this rapid recent progress on the observational front, we expect there will be comparable advances over the next five years as the full dynamic range of the VLA is exploited in mapping large samples, and if the proposed VLBI arrays are constructed (see Sec. V.B).

D. This review

Below, we summarize the main issues we shall cover in the remainder of this review.

1. Jets

As a result of the confirmation of the presence of jets, a synthesis of the research on extended and compact radio sources has begun to take shape. The observations cited earlier (Sec. I.C) have convinced most astronomers that jets are physical conduits along which mass, momentum, energy, and magnetic flux are supplied from the nucleus to the outer components. We shall adopt this point of view throughout the review, and we shall not discuss alternative models for extended sources further. Hybrid models are possible in which the sources are built up through a series of explosions (e.g., Christiansen, 1973; Christiansen, Pacholczyk, and Scott, 1981), but as there is little evidence for intermittency on any but the shortest length scales observed, these models are basically equivalent to the continuous-flow models on larger scales. Fortunately, in the case of compact sources, where the jets are often poorly resolved and their association with a collimated outflow correspondingly suspect, much of what we can infer is fairly independent of detailed geometrical and dynamical assumptions.

There are two crucial issues we need to address concerning jets. The first is, of course, how are they formed? The second is, how do they retain their coherence and collimation as they traverse interstellar and intergalactic space? The second issue is no less pressing than the first, since jetlike flows known on Earth are notoriously unstable. We treat jet propagation first, in Sec. II, because it has closer parallels to familiar physics. To do this, we need to know what physical parameters characterize an astrophysical jet, and we outline a simple gas dynamical or hydromagnetic description of a jet in Sec. II.A. Using a variety of diagnostics based on observations of radio emission, we can then make crude estimates of densities, pressures, and velocities in individual sources, and the results and validity of these estimates are summarized.

Given an energy flux ("luminosity"), momentum flux ("thrust"), and mass flux ("discharge"), it is straightforward to describe the evolution of a jet-powered radio source into a stationary background medium of specified density and temperature. This evolution plausibly accounts for the hot spots and radio lobes of the strong double radio sources such as Cygnus A, and is described in Sec. II.B. However, the observable properties of jets depend on additional internal degrees of freedom, such as the static pressure in the jet material and internal magnetic field. These internal properties and their observable consequences are discussed in Sec. II.C, where we address the collimation and stability of jets as well as the dissipative processes which render them visible. We make the case that most observed jets are pressure confined over most of their lengths, rather than being overpressured and in free expansion. The run of ordinary gas pressure in the

ambient medium is adequate to produce the observed degree of collimation in many cases; however, in some jets the internal pressure appears to be much greater than that in the ambient medium, and we explain how these jets may be confined by the tension of the magnetic field surrounding the jet.

In order for jets to produce the observed radio emission, relativistic electrons must be continually accelerated within them. Indeed, it appears that the local dissipation of bulk kinetic energy is responsible for much of the internal pressure in the jet. A number of processes are available for transferring energy from directed motion to random motion, including turbulence induced by the Kelvin-Helmholtz instability and magnetic stresses. We discuss some of the possibilities in Secs. II.C.5—II.C.8. The Kelvin-Helmholtz instability, in particular, is potentially capable of disrupting the entire jet, but we argue that its virulence is diminished by a combination of large jet Mach numbers, large or small density ratios between jets and their surroundings, and relativistic velocities.

In Sec. II.D. we treat the jets which are systematically curved and discuss the numerous mechanisms which may be responsible in different sources. The observed ability, in some radio trails, of jets to be bent through $\sim 90°$ without losing coherence is a testimony to their remarkable stability.

We have less detailed information on the compact radio sources and are consequently less confident that these are also jets. In Sec. III.A we describe some of the less model-dependent inferences that have been drawn about the physical conditions within compact radio sources and review the various attempts to model these sources, both with and without jets.

2. Black holes

The most fundamental problem posed by radio sources is: How can $\gtrsim 10^{61}$ ergs be generated in a galactic nucleus and channeled into the collimated plasma jets that we observe? It is now evident that these jets are just one manifestation of "violent activity" in galactic nuclei; extra clues therefore come from observations in all wavebands (especially optical and x ray) of the multifarious phenomena associated with quasars, Seyfert galaxies, and related classes of objects. The cumulative evidence insistently suggests that the inner regions of some galaxies have undergone a catastrophic gravitational collapse of $\gtrsim 10^8 M_\odot$ into a single compact entity—only this hypothesis accounts for the high luminosity and compactness (inferred from optical and x-ray variability), combined with the long-term stability implied by large-scale radio jets and radio sources. We make this case in Sec. III.B.

Conventional physics implies that the inevitable end point of a compact supermassive system must be gravitational collapse. This outcome is predicted by most theories of gravity—not solely by Einstein's general relativity. Flow patterns near black holes will be discussed in some detail later in this review (Secs. III.B.3 and III.C)—we believe that they offer the best hope of understanding the "prime mover" in all types of active galactic nuclei. When quantitative discussion requires it, we shall assume that the black holes are described by the Kerr metric; according to general relativity, any gravitational collapse settles down to a stationary state described exactly by this two-parameter family of metrics (Appendix C Sec. 4). However, we must emphasize that none of the data yet allow us to discriminate between general relativity and rival theories—all that can really be "diagnosed" is a very deep gravitational potential well. There are nevertheless some models for jet production where specific features of the Kerr metric play a crucial role. If such models are vindicated by further theoretical and observational work, then active galactic nuclei may offer the prospect of testing general relativity beyond the weak-field approximation.

It is likely that black holes have to be fueled with accreting gas in order to exhibit prominent nonthermal activity, as we discuss in Sec. III.C. A spinning black hole constitutes an excellent gyroscope, and the ingredients of accretion, angular momentum, entropy production, and possibly also magnetic fields are probably sufficient to ensure the production of collimated outflow near the black hole. However, the detailed mechanism is a matter for debate, and several distinct lines of research are currently being pursued: radiative acceleration under both optically thick and optically thin conditions, acceleration normal to thick and thin gas pressure-dominated disks, and acceleration involving hydromagnetic or electromagnetic stresses. Indeed, it is not even clear what is being accelerated; nonrelativistic thermal plasma, relativistic plasma, electron-positron plasma, or an optically thick, radiation-dominated gas are all possibilities. Furthermore, it seems highly unlikely that well-collimated jets with opening angles as small as 2° can be produced within a few Schwarzschild radii of the black hole, and in most models either external pressure or magnetic stresses must be invoked to achieve full collimation. Most important of all, we should not expect one particular mechanism to account for the observed heterogeneity of jet structure. These various possibilities are reviewed in Sec. III.D.

3. Unified model of active galactic nuclei

Radio properties provide only one of several criteria for classifying active galaxies. We give a précis of this confusing subject in Sec. IV.A. It has long been known that both the density and the luminosities of radio sources evolve very rapidly with redshift, in the sense that the probability of an individual galaxy's becoming a radio source or quasar was far higher in the past (by a factor of ~ 1000 at a redshift $z \sim 2$). This evolution is stronger for the more powerful sources. Our incomplete knowledge of source space densities and evolutionary properties is reviewed in Sec. IV.B. Extended radio sources appear to have been systematically smaller in the past, although this may be partly a selection effect (Sec. IV.C). If indeed a radio source is produced quite naturally whenever a mas-

sive black hole resides in the nucleus of a galaxy, then its evolution will be largely controlled by the manner and the rate at which the hole is supplied with gaseous fuel (Sec. IV.D). The evolution of the extended components will also be influenced by changes in the circumgalactic gas density and microwave background as we go backwards in cosmological time. Cosmological evolution in the properties of galaxy clusters (in which a few percent of galaxies and radio sources reside) may also be important (Sec. IV.D). Statistics of compact radio sources are probably skewed by relativistic beaming effects, and in Sec. IV.E we discuss the constraints that observations impose on the kinematics of jets, and indicate how "Doppler favoritism" can be incorporated into a unified classification scheme for active galaxies.

In Sec. V, we draw together the principal conclusions from Secs. II, III, and IV, and propose a tentative unification of the theory of active galactic nuclei, and particularly the extragalactic radio sources. Specifically, we suggest that the form of the nuclear emission depends primarily on the ratio of the mass supply rate $\dot{M}$ to the mass of the black hole M at the center of the nucleus. Flows with small $\dot{M}$ or large M tend to have low optical depth and to be inefficient at radiating away gravitational binding energy—these are radio sources which may produce powerful jets but which are weak optically. In the limit of small $\dot{M}$, much of the energy powering the source may be extracted electromagnetically from the spin of the black hole, and the resulting jet may be accelerated and collimated by magnetic stresses.

When $\dot{M}$ is large or M small, the flow tends to be radiative—this case represents the quasars and Seyfert galaxies, as well as other active galaxies which are strong optical and uv sources. Spiral galaxies, with their large specific angular momentum, may form smaller holes than ellipticals of comparable mass, which would account for the fact that Seyfert galaxies are spirals. Quasars, which sometimes exhibit strong extended radio emission and jets, may occur in both spirals and ellipticals; radio quasars may represent a transitional case in which both optically thick, radiation-dominated flow and optically thin, gas-dominated flow can coexist in the nucleus.

Our one-parameter family of models may account for the density evolution of quasars and strong radio sources with cosmological epoch. At early epochs, when gaseous "fuel" is plentiful, most sources would be seen as quasars. Quasars in elliptical galaxies would tend to be radio loud, while those in spirals would be radio quiet. As fuel became scarce, the optical and uv manifestations of activity would diminish, turning the ellipticals first into strong radio galaxies and later into weaker radio sources. The nuclei of spirals, with their smaller black holes, would be able to maintain optical and uv activity despite the decrease in $\dot{M}$, and they would simply weaken into Seyferts and eventually into normal spiral galaxies like our own. Indeed, our galaxy and other "normal" spiral galaxies do display nonthermal nuclear activity which may be due to a black hole of $\lesssim 10^6$ solar masses.

Of course, the picture described above is highly oversimplified, and it is likely that such factors as the angular momentum of the black hole and the properties of the ambient interstellar and intergalactic media also play important roles in determining the observable manifestations of nuclear activity. For example, the weakness of extended radio emission of Seyferts may be largely ascribed to the large angular momentum of the interstellar medium of the spiral, which hinders effective collimation. In sources with jets which we believe to be relativistic, e.g., the compact one-sided jets and superluminal sources, the orientation of the jet axis with respect to our line of sight will strongly affect the source's appearance, because radiation from jet material will be Doppler beamed in the direction of motion. Attempts to understand the luminosity function of bright compact sources may have to take into account the statistics of orientation, collimation, and velocity of the jet, as well as the jet's intrinsic radiative properties.

Although our proposed synthesis of active nuclear properties is highly conjectural and far from unique, we hope it will provide a framework for discussing the integrated properties of these objects. We conclude the review by discussing how future observations (Sec. V.B), experiments (Sec. V.C), and theoretical studies (Sec. V.D) should enhance our understanding of the physical processes underlying active galactic nuclei.

4. Format and scope of review

In order to make this review accessible to physicists unfamiliar with the standard techniques of theoretical radio astronomy, we present an appendix containing an abbreviated summary of radiative emission and transfer processes relevant to radio sources, an outline of the elements of gas dynamics and magnetohydrodynamics (MHD), and a description of relativistic effects associated with cosmological expansion of the universe, local source motions that approach c, and black holes. We also include a glossary of symbols which may be unfamiliar.

This review was planned in 1975 at a time when it was still possible to review theoretical ideas about the nature and creation of extragalactic radio sources comprehensively. In the eight years that have elapsed since this time the subject has grown faster than the authors' ability to keep up with it. This review is therefore not complete and in its emphasis reflects the biases of the authors. Specifically, we have endeavored to emphasize more recent theoretical papers that are written within the jet/massive black hole framework at the expense of work describing alternative models of radio sources. In particular, we give only representative references for those topics on which helpful review articles already exist. We apologize to those colleagues whose work is either omitted or misrepresented.

There are several substantive issues which have a direct bearing on models of powerful radio galaxies and quasars that we do not include in this review. These include radio

emission from the disks and halos of spiral galaxies, radio emission from rich clusters of galaxies, general models of active galactic nuclei, and the theory of galaxy formation.

Observations of extragalactic radio sources have now outrun the theory. We are uncertain about the fundamental composition, collimation, and speeds of jets. Most important of all, we do not know how jets are made. In view of this basic uncertainty it seems wisest to keep the discussion (with the exception of the Appendix) at the qualitative or elementary algebraic level. Of course, this does not reflect the level of technical detail in many of the papers that we review.

II. PHYSICS OF JETS

In this section, we adopt the view that powerful extragalactic radio sources are powered by narrow jets. We review existing ideas on the composition and properties of these jets, relating them as far as possible to observations.

A. Physical parameters

1. Fluid model

Consider first an idealized one-dimensional fluid model of a jet, that is to say, a nearly parallel flow of plasma along a channel embedded in a background medium. As most well-observed jets appear to be collimated within opening angles $\theta \lesssim 15°$, the assumption of parallel streamlines should be reasonably accurate. We suppose that there exists a well-defined bulk velocity and that there is no significant interpenetration of the jet and ambient materials. This hydrodynamical viewpoint is probably valid despite the fact that the mean free path for Coulomb collisions in the jet plasma is very large—typically larger than the width of the jet. This is because we know that jets contain substantial magnetic fields, and the associated Larmor radii and Debye lengths of the constituent ions and electrons are always at least 8 orders of magnitude smaller than the jets (e.g., Blandford and Rees, 1974). The magnetic field is crucial to making the flow fluidlike, just as it is in the solar wind. Jets are also believed to be basically charge-neutral, the electrons and the ions (or positrons) which neutralize them flowing outward with similar densities and speeds. This contrasts with the situation in most laboratory or terrestrial beams (e.g., Bekefi *et al.*, 1980). When large-scale magnetic stresses become dynamically important, MHD rather than gas dynamics is the relevant theoretical tool (see Sec. II.C.4, Appendix B Sec. 6).

At least four alternative descriptions to simple fluid flows have been proposed and may have some relevance. First, Rees (1971) proposed that jets comprise low-frequency, strong electromagnetic waves—generated by, for instance, a dense cluster of rapidly spinning pulsars in the galactic nucleus. The waves would be "self-focused" into a channel because their phase velocity increases with increasing density (Blandford, 1973a; Dobrowolny, Ferrari, and Massaglia, 1978; Ferrari, Massaglia, and Dobrowolny, 1980; Bodo, Ferrari, and Massaglia, 1981). However, it is now believed that monochromatic strong waves emitted by pulsars are subject to both resonant damping and a variety of parametric instabilities, even in quite underdense plasmas (e.g., Max, 1972; Arons, Max, and Norman, 1977), and the Poynting flux of a single wave will ultimately be shared between a variety of wave modes and particles so that a fluid description now seems more appropriate. Furthermore, interactions between waves of different frequencies lead to efficient particle acceleration (Blandford, 1973b; Arons *et al.*, 1975); a corollary of this is that the energy flux of broad-band low-frequency waves is quickly attenuated by being converted into particle energy.

In a second description (e.g., Jaffe and Perola, 1973; Earl, 1976; Sanders, 1974; Milgrom and Bahcall, 1978; Spangler, 1979), radio sources are formed by an expanding bundle of magnetic field lines. Relativistic electrons of energy $\gamma m_e c^2$ that stream along the field conserving their adiabatic invariants will move at smaller and smaller "pitch angles" φ to the magnetic field: $\sin\varphi \propto B^{1/2}$. The guiding center then moves with an increasing velocity and a corresponding Lorentz factor that increases up to γ. This acceleration is directly analogous to the adiabatic motion of a relativistic, supersonic fluid in an expanding channel (cf. Appendix B Sec. 3; Longair, Ryle, and Scheuer, 1973) and with a distribution of pitch angles; the center-of-momentum velocity can be thought of as a fluid velocity. However, the adiabatic invariants may be destroyed by radiative losses and wave-particle interaction (see Cesarsky, 1980 for a recent review), and it seems unlikely that relativistic particles can stream through hundreds of kiloparsecs of ambient plasma. There is a further difficulty with this model in that the magnetic pressure, which varies as the inverse square of the cross-sectional area of the flux tube, will generally be too large to be confined within the galactic nucleus. In addition, the large field implied within the nucleus causes catastrophic radiative losses. [Note that although small pitch angle motion in an expanding field is dynamically similar to fluid motion, the observed synchrotron radiation can be quite different (Appendix A Sec. 1).]

In a third approach, Benford (1978) developed the analogy with laboratory beams by assuming that the charge and the matter currents were strictly proportional but with a proportionality constant $\sim 10^{-10}(e/m_e)$ (as required by observations) rather than (e/m_e) as in laboratory applications. There seems to be no reason to adopt this assumption.

Finally, Christiansen and Scott (1977), Christiansen, Scott, and Vestrand (1978), Christiansen (1969,1971, 1973), and Christiansen, Pacholcyzk, and Scott (1977) have discussed the multiple ejection of "plasmons"—dense radio-emitting clouds—moving through the ambient medium. In one limit this can be considered as an extremely time-variable jet and as such is discussed further in Sec. II.C.8 (see also Sec. III.A.3).

The arguments for rejecting these alternative physical descriptions are not particularly strong. However, the most important dynamical inferences that we can hope to draw from observations of jets concern their overall speeds, discharges, thrusts, and powers. Such estimates are relatively insensitive to assumptions concerning the internal composition of the jets. Although most of the ensuing discussion will be framed in the language of a fluid model, many of the conclusions are directly relevant to nonfluid models.

2. Pressure

Most of the observed radio (and probably optical and x-ray) emission from jets is believed to come directly from incoherent synchrotron radiation of relativistic electrons (Appendix A). In the case of extended sources, the evidence for this derives from the ubiquity of nonthermal spectra and the substantial linear polarization. Alternative emission processes, usually involving the scattering of lower-frequency wave modes, have been proposed (e.g., Gailitis and Tsytovitch, 1964; Rees, 1971; Getmansev, 1971; Okoye, 1976; Windsor and Kellogg, 1974). It is straightforward to show that they lead to comparable or larger estimates for the jet powers, etc. For compact sources, the observational evidence is less persuasive, and alternative emission processes are quite possibly operating (see Sec. III.A.3).

From the theory of synchrotron radiation (Appendix A Sec. 1) we can obtain a lower bound on the internal pressure in a source of known spectral power P_ν and volume V, $p_{\min} \propto \nu^{2/7}(P_\nu/V)^{4/7}$. (For a typical spectral index $\alpha \sim 0.5$—0.7, $p_{\min}$ is insensitive to the cutoff frequencies assumed.) The pressure is minimized when there is rough equipartition between relativistic electron and magnetic energy densities; allowance can be made for any large contributions to the energy associated with relativistic protons or thermal plasma. This latter would be a serious omission in the ambient interstellar medium, in which the relativistic electron energy density may be as low as a few percent of the total energy density. The pressure is smallest when the radio emission uniformly occupies the visible outlines of the source (extended to a three-dimensional volume in the case of a jet by assuming cylindrical symmetry). The total energy ($\propto V^{3/7}$) can, however, be reduced if the source comprises many unresolved emitting regions occupying a small total fraction of the jet volume. The radiative lifetime of the relativistic electrons can be increased in this type of inhomogeneous magnetic field (Hughes, 1979). As we shall see, in many sources, confinement of the equipartition pressure is hard enough to explain, and as these possible complications only exacerbate the problem we shall henceforth assume that $p_{\min}$ provides a reliable estimate of the internal pressure.

In the jet associated with the galaxy NGC 6251, for example, $p_{\min}$ declines from $\sim 10^{-3}$ dyn cm^{-2} within the nucleus to $\sim 3\times 10^{-12}$ dyn cm^{-2} in the outermost parts (Perley, Bridle, and Willis, 1984). A typical value for the hot spots of a strong source, like Cygnus A, is $p_{\min} \sim 3\times 10^{-9}$ dyn cm^{-2}. For the lowest-surface-brightness regions detectable in large, weak sources, $p_{\min} \sim 10^{-14}$ dyn cm^{-2}. The associated equipartition field strengths are $B_{\rm eq} \sim (4\pi p_{\min})^{1/2}$ and range from 0.1 G in the compact components to 3×10^{-7} G in the weakest halos.

In order for our gas-dynamical model to be fully self-consistent, the pressure should not be taken strictly as a scalar; but even if roughly half the energy density is magnetic, a scalar pressure is still an adequate approximation unless there is a long-range order in the magnetic field on the scale of the jet, which would then require a MHD description (Sec. II.C.4).

3. Density

Jets probably contain some thermal plasma which, although it supplies most of the inertia, is generally too tenuous to reveal its presence directly through detectable line emission or bremsstrahlung. (Exceptions include SS433; Margon, 1982; Centaurus A; Schreier *et al.*, 1980; Coma A; Miley *et al.*, 1981.) If, in contrast to the assumptions in the preceding section, the magnetic field contains a large-scale ordered component, the plane of polarization of emitted synchrotron radiation will be rotated by the Faraday effect (Appendix A Sec. 4) through an angle $\Delta\varphi \propto \nu^{-2}\int n_e \mathbf{B}\cdot\mathbf{dl}$ where $\mathbf{dl}$ is an increment distance along the line of sight and n_e is the thermal electron density. Radiation emitted at different depths within the jet is rotated through different angles, and the net flux will be "depolarized" (e.g., Burn, 1966; Burch, 1979; Potash and Wardle, 1979). The rotation measure ($\mathrm{RM} = \Delta\varphi/\lambda^2$) is unaffected by clumping of the gas, provided that the clumps cover the source and that the field strength is uncorrelated with the clumps.

Under these assumptions, measurements of the degree of polarization as a function of frequency can often set an upper bound on the mass density of thermal plasma and occasionally yield a direct estimate. For example, in 3C31 (Burch, 1979; van Breugel, 1980) and 3C449 (Perley, Willis, and Scott, 1979), the estimated mean thermal electron density is $n_e \sim 10^{-2}$ cm^{-3}, comparable with upper limits estimated for other sources. Thus the pressure and densities in extended jets are not so different from those encountered in our interstellar medium, and we have every reason to expect that conditions will be just as complex. The gas may be localized within dense cool clouds where the field is stronger than average, or the magnetic field may reverse many times along the line of sight (Scheuer, 1967; Saslaw and Mitton, 1973). Faraday rotation measurements would then be quite misleading. The rms rotation measure random walks rather than increasing linearly with distance through the source, and attains a value smaller than the naive RM by a factor $\sim (l/l_B)^{-1/2}$, where l_B is the correlation length of the magnetic field. Depolarization then occurs at depths which are larger than the naive value by $\sim (l/l_B)$ (Burn,

1966). The degree of polarization depends on the field resolved normal to the line of sight, and high polarization can be maintained even if this component suffers reversals, as long as it tends to be stretched along one direction (e.g., Laing, 1980b; Spangler, 1983). The true density could be quite different from that indicated by naive analysis of polarization studies. To give an example, it has been claimed by Saunders *et al.* (1981) that NGC 6251 displays evidence of internal depolarization. This implies an internal plasma density which, in conjuction with the estimated energy flux along the beam, determines the velocity as 10^3–10^4 km s^{-1}. However, it is hard to distinguish observationally between depolarization which is internal, and that which could be due to a "screen" outside the jet over which the rotation measure varies on an angular scale comparable with the telescope beamwidth. The higher-resolution observations of Perley, Bridle, and Willis (1984) in fact attribute the depolarization to the external medium.

These arguments have also been applied to compact radio sources. Faraday rotation due to relativistic matter drops rapidly with increasing electron Lorentz factor γ (RM $\propto \langle \ln\gamma/\gamma^2 \rangle$; Sazonov, 1973a,1973b). The high degrees of polarization seen in some compact variable radio sources are possible only if the particle density is very small ($<10^{-3}$ cm^{-3}). In this case, either the plasma must be virtually devoid of electrons of energy $\lesssim 10$ MeV (Wardle, 1977; Jones and O'Dell, 1977a) or the emitting particles comprise equal densities of positrons and electrons (Sec. III.D.6).

4. Velocity

Unfortunately, the jet velocity is even more difficult to estimate observationally than the density. Only in the case of the galactic source SS433, where Doppler-shifted emission lines are observed, do we have a reliable determination of the jet speed (78 000 km s^{-1}, Margon, 1982). In the case of Coma A (Miley *et al.*, 1981), emission line redshifts relative to the galaxy have been measured, but their relationship to a jet speed is at present unclear. For the majority of jets, we must rely on indirect arguments that give velocity estimates ranging from ~ 300 km s^{-1} (comparable with the escape velocity from a galaxy) to the speed of light.

First we consider the case for relativistic jets. As we have seen, several of the brighter compact radio sources mapped by VLBI display a one-sided core-jet morphology, and some of these sources in addition show apparent superluminal expansion. These effects probably result from relativistic motion nearly along the line of sight toward the observer (Rees, 1966; Blandford, McKee, and Rees, 1977; Marscher and Scott, 1980); the apparent one-sidedness reflects the Doppler boosting of radiation from the approaching jet over that from the receding counterjet. This "Doppler favoritism" is particularly sensitive to orientation (e.g., Rees, 1978a; Shklovsky, 1977; Scheuer and Readhead, 1979; Behr *et al.*, 1976; Blandford and Königl, 1979b; Königl, 1981). The observed flux densities from the approaching and receding jets differ by a factor $[(1+v_j\cos\varphi/c)/(1-v_j\cos\varphi/c)]^{2+\alpha}$ where v_j is the jet velocity, α is the spectral index, and φ is the angle the jet makes with the line of sight (Appendix C Sec. 2). The apparent relative velocity v_{ob} between a feature moving with the jet speed and the source of the jet is $v_j\sin\varphi/(1-v_j\cos\varphi/c)$. For example, in 3C273 ($z=0.16$, and assuming $H_0=100$ km s^{-1} Mpc^{-1}, $\Omega=0.1$), $v_{ob}\sim 5c$ (Pearson *et al.*, 1981). A jet oriented at $\sim 10°$ to the line of sight with $\gamma_j \simeq 5$ could reproduce this expansion and be brighter by a factor ~ 6000 than a similar counterjet, which would therefore be unobservable. Although far more complicated geometries than this have been explored and are indeed likely (e.g., Blandford, 1984), a relativistic jet speed remains the basis for a general explanation of one-sided compact jets (see Sec. III.A.3 below).

There are other independent considerations which point to relativistic motion in some active galactic nuclei and compact radio sources. These include

(a) low-frequency variability (Sec. III.A.2),

(b) the "inverse Compton problem" (Sec. III.A.2),

(c) rapid changes in polarization and total intensity in *BL Lac* objects (Sec. III.A.2),

(d) Faraday rotation arguments that indicate that the radio-emitting gas is devoid of thermal plasma and has an internal sound speed $\sim c$ (Sec. II.A.3),

(e) a "natural" jet speed is of order the escape speed from the bottom of a relativistic potential well, i.e., $\sim c$ (Sec. III.B.3).

The one-sidedness of jets is also frequently mirrored in the small (few arc sec) extensions found around many compact radio sources (Perley, Fomalont, and Johnston, 1982) and in many (but, importantly, not all) of the extended radio jets (e.g., NGC 6251).

It appears that one-sidedness is associated with intermediate-power radio galaxies. The most powerful radio galaxies rarely show jets, and in most low-power sources, both jets can be seen. [Quasars, by contrast, often exhibit one-sided jets (Bridle and Perley, 1984).] Typically, unobserved counterjets are at least thirty times fainter than jets in these intermediate power sources, so it is natural to suppose that the more powerful extended jets may also be displaying relativistic beaming.

However, the relativistic interpretation leads to some complications.

(1) If large jets are beamed toward us, then their true lengths greatly exceed their projected lengths, making the extended sources, which are believed to be unbeamed, unusually large (Schilizzi and de Bruyn, 1983). In the particular case of Cygnus A, there is a one-sided nuclear jet which is believed not to be beamed towards us (Saikia and Wiita, 1982).

(2) Some one-sided jets show bends (see Sec. II.D). If the bulk flow follows the jet, then the smoothness of the brightness contours around the bend indicates a subrelativistic jet velocity (Potash and Wardle, 1980; Van Groningen, Miley, and Norman, 1980). This argument is extremely strong for the radio trails. [It also holds for ba-

sically linear jets, in which small bends are caused by slight changes in the direction of collimation in the nucleus (Linfield, 1981b).] One can also use a purely dynamical argument to rule out very high bulk Lorentz factors γ_j in curved jets: consideration of equilibrium in the moving frame shows that the "scale height" cannot exceed γ_j^{-2} times the radius of curvature. The observed ratio of jet diameter to radius of curvature then implies $\gamma_j < 5$ in these sources.

(3) Cygnus A has a one-sided radio jet which would require that $\varphi \lesssim 60°$ (Linfield, 1982), and yet the morphology of the extended radio lobes (Hargrave and Ryle, 1976) and the optical galaxy rotation curve (Simkin, 1979) both suggest that the jet axis lies close to the plane of the sky.

(4) In sources that show a high degree of reflection or inversion symmetry (see Sec. II.D), it is sometimes possible to give a (model-dependent) velocity estimate. For example, in radio trails like NGC 1265, v_j is typically estimated to be $\sim 10\,000$ km s^{-1} (see Sec. II.D.1). In addition, if the bending in 3C31 (Burch, 1977b; Blandford and Icke, 1978) and 3C449 (Perley *et al.*, 1979) results from acceleration of the parent galaxy in its orbit about a close companion, then the jet velocities in these sources are in the range 300—500 km s^{-1}.

(5) In sources where there is evidence for internal Faraday depolarization within a jet (see Sec. II.A.3), it is often possible to estimate both the density ρ_j and the sound speed s_j. The jet speed can then be computed either by estimating the thrust Π in the beam from the pressure in the hot spots (see the discussion of "waste energy problem" below) and using the relation $v_j \sim (\Pi_j / A\rho_j)^{1/2}$ where A is the cross-sectional area of the hot spot; or by assuming that the jet is free (see Sec. II.C.3), so that $v_j \sim Ms_j \sim 2\theta^{-1}s_j$ where θ is the jet opening angle and M_j the jet Mach number. Speeds estimated in this way generally lie in the range $v_j \sim 1000$—$10\,000$ km s^{-1}, again much less than c.

(6) A jet moving out through a galaxy is bound to sweep up a small amount of gas—that which is released (via stellar winds, etc.) from all the ordinary stars along its path (De Young, 1981). The jet gains internal energy as it shares its momentum with swept-up matter. This may decollimate low-powered jets even if they sweep up only a small fraction of their original mass. This material could even be sufficient to decelerate a low-powered ultrarelativistic jet (Phinney, 1983a).

(7) Relativistic velocities in large-scale jets often lead to the "waste energy" problem, first emphasized by Longair, Ryle, and Scheuer (1973). We can derive a lower bound on the thrust in the jet (Appendix B Sec. 3) by multiplying the minimum pressure in the hot spots by their apparent area. Typical values for strong doubles are $\sim 10^{34}$—10^{35} dyn. Further multiplication by $v_j/2$ gives a lower bound on the jet power. If $v_j \sim c$, then the jet powers are frequently much greater than the powers that appear to be dissipated as heat or radio luminosity in the extended components (cf. Hargrave and McEllin, 1975). Note, however, that if a jet emerges from the collimation region with speed $\sim c$, it may be decelerated by friction or entrainment to $v_j \ll c$ without losing too much of its bulk kinetic energy, provided the deceleration occurs at Mach number near unity (Begelman, 1982; see Sec. II.C.6). If, on the other hand, deceleration occurs precipitously at high Mach number, then the jet will leave behind c/v_j times as much thermal energy near the nucleus as it retains in kinetic energy. The waste energy that is difficult to dissipate in the radio components must then be dissipated in the nucleus.

(8) For Cygnus A, the power is $\gtrsim 10^{46}$ ergs s^{-1}, far greater than the known power from the nucleus (e.g., Hargrave and Ryle, 1974). If the jet speeds are subrelativistic, then we must seek an alternative explanation for their one-sidedness. One possibility is that they are made one sided and that the direction of outflow flips from side to side on a time scale long compared with the flow time to the outer components but short compared with the electron cooling time (Wiita and Siah, 1981; Saikia and Wiita, 1982; Shklovsky, 1982). Rudnick (1982) and Edgar and Rudnick (1983) have found a number of sources in which the regions of emission on either side appear to interleave when reflected through the nucleus, suggesting such a flip-flop of time scales $\gtrsim 10^7$ yr. Asymmetry on large scales may be associated with an asymmetric environment. The optical and x-ray emission associated with the jets in M87, Coma A, and Cen A appear to be one sided on account on the distribution of cool gas in the respective galaxies (De Young, Condon, and Butcher, 1980; Miley *et al.*, 1981). Another possibility is that jets may undergo some sort of turbulent transition if their effective Reynolds number exceeds some critical value. The turbulence would be translated into particle acceleration and field amplification and hence strong radio emission. If the probability of such a transition decreased with increasing jet power then the apparent correlation of jet properties with radio power could be understood. The fact that the one-sided compact jets are mostly elongated on the same side as the extended jets (Linfield, 1981a; Kellermann and Pauliny-Toth, 1981) indicates that if these are examples of low-speed sources then the asymmetry must be maintained over many decades of radius. Perhaps one jet undergoes a transition to turbulence in the nucleus and this is maintained all along its length.

Slow jet speeds also pose some observational problems.

(9) If in some sources the assumption of a relativistic jet speed makes them unusually large, the assumption of a speed near the lower range makes them surprisingly old, far older than the maximum cooling times of the emitting electrons (see Appendix A Sec. 6). To take an extreme example, if the expansion speed in the giant radio source 3C236 (angular size ~ 20 min) were only 300 km s^{-1}, then the source age would be $\gtrsim 0.5 H_0^{-1}$, and therefore comparable with the age of the universe.

(10) Similarly in some sources, while energy considerations provide an argument against large jet speeds, constraints on the mass discharge lead to problems with low speeds. Given an observational lower bound on the thrust, the discharge $\dot{M}$ is obtained after dividing by v_j. Again using Cygnus A as an example, a jet speed as low

as 1000 km s^{-1} would require a mass loss of $100M_\odot$ yr^{-1}. Over the lifetime of the radio source more than $10^{10}M_\odot$ of gas would have to be injected into the radio components. This is far more gas than is currently believed to be present within an elliptical galaxy (but see Sec. III.C.1), and such a high gas density will lead to a larger Faraday depolarization in the radio lobes than is observed.

With improved and more extensive observations, it should be possible to refine all these methods for estimating v_j. At the moment, it seems that relativistic speeds must be present in the superluminals and absent in the radio trails. We indeed favor relativistic speeds in the majority of strong and intermediate power sources, especially for sources like M87, NGC 315, and NGC 6251 that are one sided on the same side on both small and large scales. Note that one does not need to invoke a special orientation in order to get an apparently one-sided jet by Doppler favoritism, if the jets are relativistic. Even for a jet at 60° to the line of sight (the 50-percentile angle for random orientation), the factor is $3^{2+\alpha}\sim 20$ for $v\approx c$. If this last group of sources shows no evidence for even mild superluminal expansion, then we are placed in the uncomfortable position of having to postulate two separate explanations for one-sidedness. A further observational probe is to see if the lobes on the jet side in the one-sided sources are in any way systematically different (e.g., closer to the nucleus, brighter, more compact, etc.) than their counterparts on the other side (see Saikia, 1981). (If the lobe on the same side as the jet were systematically brighter, this could conceivably be due to Doppler effects, since speeds of $>0.1c$ may still occur even after the beams have been through a shock. A large asymmetry in the projected distances of the two components from the central source would be harder to interpret in terms of a relativistic jet, particularly if the component on the jet side were *nearer* to the galaxy.)

B. Interaction of jets with their environment

1. Advance of the head

As we described in Sec. I.C, the most powerful radio sources are $\sim$1—300 kpc in size, have simple double structure and well-defined outer hot spots. The weaker sources generally appear more complex and are edge darkened. We can interpret this naturally in terms of the advance of the head of a jet into the surrounding medium (Fig. 10). At early times, the jet is short and well collimated; the energy density at its end and the radiative efficiency are both high. At later times, when the jet is much longer, the collimation deteriorates and the radiative efficiency drops.

Jet material (density ρ_j) travels along a channel of its own making. The speed v_h with which the head of the channel advances into the surrounding medium (density ρ_e) is obtained by balancing the momentum flux in the jet against the momentum flux of the surrounding medium,

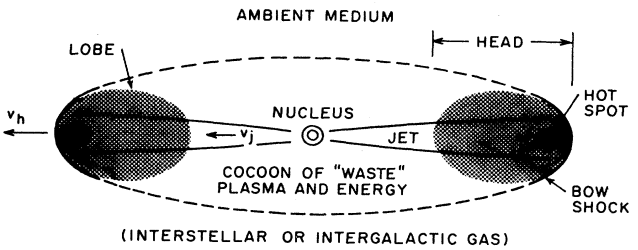

FIG. 10. Schematic diagram of a strong double radio source, such as Cygnus A (cf. Fig. 1), illustrating the nomenclature of visible (shaded) parts, and parts inferred to exist from the "twin-exhaust" theory of Blandford and Rees (1974). The nucleus, hot spots, and lobes are generally observed; one or both of the jets may be invisible and there is often no detectable radiation from the cocoon or ambient medium. The entire head is believed to move into the ambient medium at a speed v_h (Sec. II.B.1), which is much smaller than the jet speed v_j.

measured in the frame comoving with the advancing head. If v_h is supersonic with respect to the external gas but subrelativistic, then from Appendix B Secs. 1 and 2

$$v_h\sim[1+(\rho_e/\rho_j)^{1/2}]^{-1}v_j \tag{2.1}$$

for a nonrelativistic equation of state. When the jet density exceeds the external density, then clearly $v_h\sim v_j$. w_j and ρ_j should really be averaged over the head. If the beam is well focused into an area much smaller than the head but jitters around, then the momentum flux is effectively spread out and the local rate of advance can greatly exceed the long-time average (Scheuer, 1982; Wilson and Scheuer, 1983).

There is clear observational evidence that v_h is subrelativistic. If the regions of intense radio emission at the head of the jets (the hot spots) were moving with a relativistic speed, then a complete sample of radio sources would exhibit larger brightness and separation ratios between the advancing and receding components than is observed (Ryle and Longair, 1967; Mackay, 1971a,1971b,1973; Ingham and Morrison, 1975; Longair and Riley, 1979; Katgert-Miekelijn *et al.*, 1980; Gopal-Krishna, 1980b). In fact, using these arguments, Hargrave and Ryle (1974) have placed upper bounds $v_h\lesssim 0.1c$ on the typical head velocity in a large sample of relatively powerful double sources and made a direct estimate of $v_h\sim 0.03c$ for Cygnus A. We might expect double sources within clusters to be much smaller than those outside clusters, as has been claimed by Stocke (1979), in contrast to Hooley (1976).

In weaker "Type-II" doubles without well-defined lobes, v_h may be comparable with v_j, and most of the bulk kinetic energy may be dissipated through the channel walls rather than behind a strong shock at the head of the source. The jet may then terminate when its speed becomes sonic, and the region of greatest radio emissivity would then be located in the interior rather than at the outer extremity of the lobe. [This is particularly true of bent jets (see Secs. II.D.2 and II.D.3) where the jets have

to rebore a channel in response to motion of the source or the development of large-amplitude instability.]

2. Hot spots

Many Type-I radio sources are characterized by "hot spots"—regions of high radio surface brightness located at the outer extremities of the radio components (e.g., Miley and Wade, 1971; Hargrave and Ryle, 1974; Hargrave and McEllin, 1975; Readhead and Hewish, 1976; Kapahi and Schilizzi, 1979; Dreher, 1981). These hot spots are frequently collinear with the central compact radio component. Most hot spots appear to be a few kpc in size, elongated perpendicular to the source axis and exhibiting very sharp leading edges together with diffuse "tails" that extend backwards toward the central component. Taking projection effects into account, the intrinsic shape is almost certainly disklike (Dreher, 1981), which should be borne in mind when computing the equipartition fields. Frequently hot spots come in pairs (e.g., NGC 6251), perhaps suggesting a vortex ring seen in projection. Sometimes the hot spots in the two components are related by reflection or inversion about the central component (see Sec. II.D.3).

Radio spectral indices in hot spots lie in the range $0.5 \lesssim \alpha \lesssim 0.9$ (e.g., Hargrave and McEllin, 1975). The spectra of hot spots in the most powerful radio sources are often negatively curved (Laing and Peacock, 1980; Peacock, 1982). This is probably due to the combined effects of synchrotron self-absorption at low frequency and radiative loss at high frequency. Optical emission both in the continuum and in lines has been reported from hot spots in several sources (Tyson, Crane, and Saslaw, 1977; Saslaw, Tyson, and Crane, 1978; Simkin, 1978; Simkin and Ekers, 1979; Rudnick *et al.*, 1981). The optical luminosity from the hot spots typically is slightly less than the radio luminosity. The optical continuum emission is probably produced by the synchrotron process. Inverse Compton emission seems unlikely because the radio and microwave background radiation energy densities are typically a factor 10—100 smaller than the magnetic field energy density within hot spots (see Appendix A Sec. 6). The optical line emission could also arise from dense clouds ($n_e \approx 10^3$ cm^{-3}) of collisionally excited ionized gas, much as in a supernova remnant (Eilek *et al.*, 1984; Gopal-Krishna, 1980a). If this is the case, individual clouds must be excited many times as they traverse the hot spot. Otherwise the radiative efficiency will be only $\approx 10^{13}$ ergs g^{-1} and a prohibitive mass flow of $\approx 10^4 M_\odot$ yr^{-1} would be necessary.

Typical hot spot equipartition pressures in edge-brightened doubles range from $\approx 3\times 10^{-9}$ dyn cm^{-2} ($B \approx 10^{-4}$ G) for Cygnus A to $\sim 3\times 10^{-11}$ dyn cm^{-2} (e.g., Scott and Readhead, 1977). *In situ* particle acceleration must be occurring within the most powerful hot spots, since the synchrotron lifetimes of relativistic electrons emitting at radio frequencies are substantially shorter than the probable transit time of the jet from the nucleus (and indeed are often shorter than the light travel time).

Polarization observations of the outer edges of bright doubles generally indicate fields elongated parallel to the source boundary (Miley and van der Laan, 1973; Burch, 1979; Laing, 1981; Dreher, 1981), whereas the absence of strong depolarization suggests an upper bound to the electron density, $n_e \lesssim 10^{-4}$—10^{-3} cm^{-3}, a value inconsistent with simple "plasmoid" models (Hargrave and Ryle, 1974; Hargrave and McEllin, 1975; Dreher, 1981; Kerr *et al.*, 1981).

Hot spots are naturally interpreted as the "working surface" at the end of a jet (Blandford and Rees, 1974; Norman, Winkler, and Smarr, 1983; Fig. 11). This interpretation is still viable in sources which show multiple hot spots or hot spots which appear to lie behind the leading edge of the radio lobe (Laing, 1982). These effects may result from jitter in the jet orientation or segmenting of

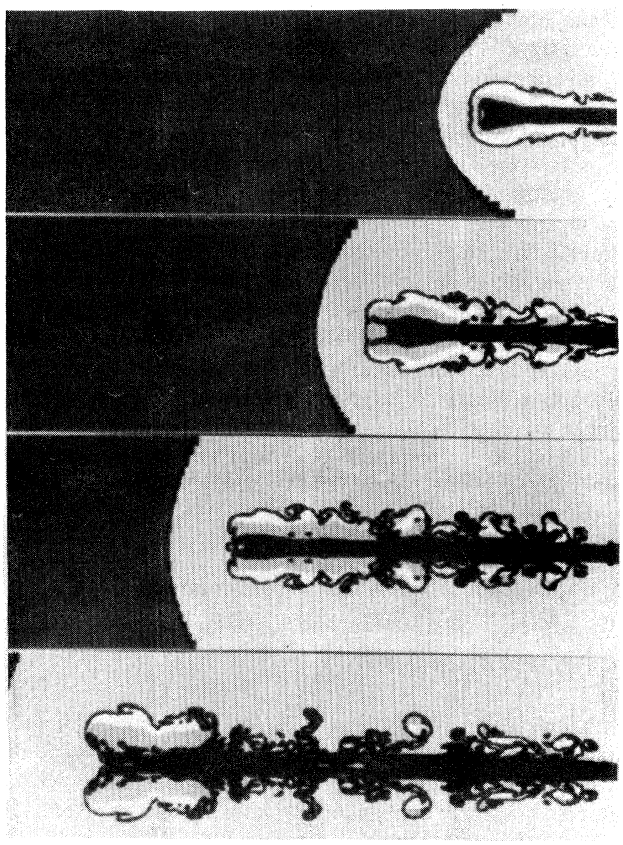

FIG. 11. Evolution of a Mach 3 pressure-matched jet of $\frac{1}{10}$ the ambient density, as determined by the two-dimensional hydrodynamical simulations of Norman, Winkler, and Smarr (1983). Various flow features are represented by different shades of grey as follows: unperturbed ambient medium, dark grey; bow shock, black; perturbed ambient medium, light grey; supersonic jet, black; backflowing cocoon gas, white; forward-flowing cocoon gas, grey; jet boundary, black. At early times a well-developed cocoon exists, which becomes Kelvin-Helmholtz unstable at later times. Reproduced, with permission, from Norman, Winkler, and Smarr (1983), © 1983 by D. Reidel Publishing Company.

the jet into several streams, which impinge at various places on the walls of a low-density cavity (cf. the "dentist's drill" model of Scheuer, 1982). The jet is decelerated at a strong collisionless shock where particle acceleration and field amplification can occur. The shock can be thought of as a Mach disk caused by an increase in the external pressure associated with the ram pressure of the surrounding medium. In fact numerical simulations indicate that there is a cylindrically symmetric triple shock structure. The inferred orientation of the magnetic field in hot spots (normal to the source axis) can be understood in terms of shock compression of an initially nearly random magnetic field (Laing, 1980b). The relativistic electrons and magnetic field pressure are balanced by the ram pressure of the intergalactic medium $\sim\rho_e v_h^2$. From the equipartition pressure in the hot spots and the upper limit $v_h \lesssim 0.1c$ a lower bound can be placed on the external density $\rho_e \gtrsim 10^{-28}$ g cm^{-3} (see Sec. II.B.1). In many sources x-ray observations can be used to argue that ρ_e is also not much larger than this (Sec. II.B.4). As typical radio spectral indices have $\alpha \gtrsim 0.5$, most of the relativistic electron internal energy is contained at the low-energy cutoff (see Appendix A Sec. 1), where the cooling time is probably long compared with the time to cross the hot spot, hence the flow will be effectively adiabatic even in the absence of the thermal plasma and relativistic protons. This is the origin of the "waste energy" problem described in Sec. II.A.4.

This inability of radiation processes to keep up with dissipation means that the shocked jet material is still hot when it emerges from the hot spot region where the pressures are largest. The flow is deflected upstream (i.e., back toward the nucleus), where it is left behind the advancing head (Norman *et al.*, 1981). The flow is separated from the shocked external medium by a contact discontinuity across which considerable mixing may occur. The strong shear near the contact discontinuity is quite probably responsible for the tangential field geometry (Laing, 1980b).

The structure of strong hydromagnetic shocks is unfortunately not well understood. As we describe in Sec. II.C.7, such shocks are capable of converting a significant fraction ($\gtrsim 0.01$) of the bulk kinetic energy flux measured in the frame of the shock into relativistic particles. In most mechanisms, the acceleration is achieved fairly close to the shock, and there need be no difficulty in accelerating electrons to optical-photon-emitting energies ($\gtrsim 1000$ GeV), even if these electrons are subsequently advected by the post-shock fluid out of the hot spot. At optical frequencies, the emitting electrons undoubtedly can cool in a time short compared with the escape time, and so we expect that the spectral index should increase by ~ 0.5 at some lower frequency. From the reported detections of optical emission this appears to be the case, although the steepening is not generally apparent from radio observations of hot spots (Hargrave and McEllin, 1975). Such spectral information can in principle provide an estimate of the escape time and hence the jet speed, and the existing scanty observations indicate pre-shock jet speeds $v_j \approx 0.1$–$0.5c$. An obvious observational test of the single-shock acceleration model is to see whether or not the optical emission is more compact and closer to the nucleus than the radio hot spot.

The magnetic field in the jet ahead of the shock is probably transverse to the flow. The magnetic energy density can then increase by a factor $\lesssim 16$ (if the post-shock pressure is mostly provided by thermal plasma) and $\lesssim 49$ if it is mostly relativistic electrons [Eqs. (B12) and (B16)]. This is probably adequate to account for the brightness of even the most powerful hot spots, though for very strong shocks (with Alfvén Mach numbers exceeding ≈ 6) this will lead to departure from equipartition in the immediate post-shock region. If, as proposed by some authors (De Young, 1980; Hughes and Allen, 1981), there are large-scale helical motions in the post-shock region, then the field energy density can be boosted from the post-shock value by dynamo action. Such motions might also be driven by Rayleigh-Taylor instability of the contact discontinuity separating the jet from the shocked external medium, as appears to occur in supernova remnants (Gull, 1975; Allen and Hughes, 1983).

A further possible point of contact with the observations is to try to reproduce the characteristic hot spot shape with the elongation perpendicular to the source axis and the tails extending back toward the nucleus. Calculations using axisymmetric numerical hydrodynamics (De Young, 1977; Rayburn, 1977; Norman *et al.*, 1981) have demonstrated the dependence of the model radio source on assumptions about the equation of state and volume emissivity as well as the conditions in the external medium. De Young claims that limb-brightened features rather than hot spots will be produced in the absence of thermal gas in the jet; however, comparison with observed radio brightness profiles is made on the assumption—not necessarily valid—that the magnetic field has its equipartition value, or a standard fraction thereof, everywhere.

3. Cocoons

The "radio lobes" or "tails" which surround each jet upstream of the hot spot may be radiation from material which has recently emerged from the hot spot (Fig. 10). These regions often have a greater total synchrotron luminosity than the accompanying hot spots, but their surface brightnesses are considerably lower, presumably as a result of adiabatic losses in magnetic and particle energies. Some sources show steepening of the synchrotron spectrum as one moves toward the nucleus from the hot spot, indicating that synchrotron losses have occurred (Miley, 1980, and references therein), while other sources show no evidence of steepening. Lack of steepening does not necessarily imply a long cooling time, however, because *in situ* acceleration may be occurring in the lobes.

Even when the surface brightness of the lobe becomes undetectably small, the lower-energy relativistic electrons (and any thermal plasma present) have lost very little of their energy. Thus most of the dissipated energy persists

as heat for the lifetime of the source, in a cocoon of light fluid enveloping the jets and often the entire double source (Scheuer, 1974). The lobes (which often extend much of the way back toward the nucleus, but sometimes—as in Cygnus A—drop sharply in surface brightness only a fraction of the way upstream) are simply the regions near the tips of the cocoon which are bright enough to be seen.

As a first approximation, evolution of the cocoon's shape is governed both by the advance of the head and by the cocoon's own pressure-driven sideways expansion into the ambient medium. Where both expansion rates are subsonic with respect to the cocoon material, the pressure is nearly uniform across the cocoon and smaller than that in the hot spot by as much as 2 orders of magnitude. The cocoon lengthens at a rate v_h, and expands sideways at a speed v_c determined by matching the cocoon pressure p_c against the ram pressure ($\rho_e v_c^2$) plus the static pressure (p_e) of the ambient medium at each point. Thus the evolution of the cocoon's shape depends on such uncertainties as the run of pressure and density in the ambient medium and the way in which the cross-sectional area of the working surface varies with time. Initially, the cocoon experiences rapid sideways expansion, until its width is

$$\sim \left[\eta \frac{\rho_e v_h^2 v_j}{p_c}\right]^{1/2} \tag{2.2}$$

times the width of the hot spot. Here η is the fraction of internal energy retained by the gas during its expansion from the hot spot to fill the cocoon, and has the value $(p_c/\rho_e v_h^2)^{1/2} \sim \frac{1}{3}$ for adiabatic expansion of an ultrarelativistic fluid (Blandford and Rees, 1974; Hargrave and McEllin, 1975; Scott, 1977a; Gopal-Krishna, 1977). Having reached the width given above, the cocoon subsequently widens more slowly than it lengthens.

The flow pattern depends crucially upon the jet Mach number and the density ratio between the jet and the external medium. This is clearly borne out by the axisymmetric numerical calculations of Norman *et al.* (1983) (Fig. 11) and Yokosawa, Ikeuchi, and Sakashita (1983). Heavy jets propagate almost ballistically and naturally are surrounded by small cocoons. Light jets proceed by shedding vortex rings and have large cocoons.

When sideways expansion becomes subsonic with respect to the ambient medium, it slows more drastically than when the expansion is supersonic, and may stop altogether if the increased length alone is able to store the additional energy in pressure balance with the ambient medium (Hargrave and McEllin, 1975). Since the rate of sideways expansion generally tends to decelerate, the effective gravity is outward, and the leading interface between the cocoon and the ambient medium is Rayleigh-Taylor stable provided that the deceleration is larger than any actual gravitational field. This condition might not be satisfied at late times, in which case Rayleigh-Taylor instability may be driven by the gravitational attraction of the parent galaxy (or, for large sources, that of a cluster). If the cocoon grows at an accelerating rate, owing for instance, to a steep ambient density gradient or to time dependence in the jet, then the contact discontinuity is unstable regardless of whether there is a gravitational field or not.

Numerical calculations by Norman *et al.* (1981) and Nepveu (1979a,1979b) (Fig. 11) indicate that Kelvin-Helmholtz instability can disrupt the cocoon within the relaxation zone which follows the bow shock. In this region, the shocked intergalactic medium flows back toward the beam. Significant mixing of the two fluids can occur here.

Buoyant rise of the cocoon (Gull and Northover, 1973; Scheuer, 1974; Gull, 1974) would also ensue if the jet were suddenly to turn off. It would be preceded by the collapse of the jet channel which, suddenly evacuated, would be filled in on the transverse sound crossing time for whatever material happened to surround it. This ambient or cocoon material could be driven into the jet channel at supersonic speeds, and the resulting shocks might effectively accelerate particles, which would then radiate. Adiabatic compression of relativistic particles and fields already within the cocoon could also provide observable synchrotron emission. The collapse of both the channel and the cocoon would proceed from the parent galaxy outward, decreasing in violence as it went because of the declining gravitational field. Hence the collapsing cocoon would tend to be pear-shaped, with the narrow end pointing toward the nucleus and surface brightness trailing off as one looks further out. The general qualitative features of this scenario suggest that those relaxed doubles which show no evidence for the presence of a jet or hot spots may be such dying sources. However, as Baldwin (1982) points out, simply turning off the hot spots and allowing the source to collapse hydrodynamically is probably incompatible with the observed scarcity of high-luminosity sources which do not have hot spots. Turning off the hot spots would leave the bulk of the source intact, and it would take so long for the source to fade that more high-luminosity sources without hot spots would be visible. An alternative model for relaxed doubles, involving unstable breakup of live jets, is outlined in Sec. II.C.5.

It is significant that cluster radio sources have steep spectra (see Sec. I.B; Slingo, 1974a,1974b). In these sources radiative cooling of the highest-energy electrons is probably more important than expansion loss. This is as expected, as the confining gas pressure within clusters greatly exceeds that outside clusters. Diffusion of relativistic electrons may be important when the cocoon is confined. As this is likely to be increasingly effective with increasing energy, we might expect to see larger cocoons at higher frequency.

Most of the kinetic energy output of extended radio sources goes into heating the intergalactic medium (IGM) through the expansion of the cocoon and the mixing of shocked cocoon material with the IGM. A lower bound on the volume heating rate is given by the total radio luminosity per volume of space, estimated locally to be $\varepsilon \sim 10^{46}$ ergs s^{-1} Gpc^{-3} (Schmidt, 1978). Over a Hubble time H_0^{-1}, this rate of energy output accounts for an en-

ergy density of only 10^{-19} ergs cm^{-3} (independent of H_0). Radio sources at $z \lesssim 1$ would not be able to heat an IGM to the high temperatures ($\sim 10^8$ K) observed in clusters unless the kinetic energy output exceeded ε by at least 10^4. Such inefficiency would require that the more powerful sources have powers as large as 10^{50} ergs s^{-1} and convert $10^{12} M_\odot$ entirely into energy during their lifetimes (see Lea and Holman, 1978).

However, the density evolution of strong radio sources with increasing z is drastic (see Sec. IV.B.1), and radio sources may have played an important role in heating the IGM at $z > 2$ (when there were more than 500 times as many strong sources as presently). The main heat input to the intergalactic medium may be uv radiation from quasars (Sherman, 1981). However, mechanical heating by radio sources may be more localized than heating by quasars. The emitting regions of the larger sources have volumes of up to several cubic Mpc, and energy outputs large enough to seriously affect the thermal balance of gas on these scales. At earlier cosmological epochs, the shocked IGM ahead of an expanding cocoon may have been sufficiently dense to allow it to cool, resulting in thermal and gravitational instabilities, as discussed by Ostriker and Cowie (1981) and Ikeuchi (1981) for the case of spherical explosions in the pregalactic universe. Thus, if jets propagated in the $z \gtrsim 5$ universe, they may have had a role in galaxy formation.

4. Nature of the ambient medium

Very little is known about the ambient medium encountered by jets within their parent elliptical galaxies. We can place hypothetical (and somewhat model-dependent) upper limits on the density and pressure at the jet source if the jet emerges from an accretion disk around a black hole (see Secs. III.C.2 and III.C.3). On VLBI scales ($\sim 10^5$ times larger than the black hole) we can use the minimum pressure in the jet to obtain a lower limit on the ambient pressure, if we assume that the jet is pressure confined. These estimates are of consequence in studying the collimation of jets, and are pursued further in Sec. II.C.1. On scales of kiloparsecs to hundreds of kiloparsecs, most jets have minimum pressures which are comparable with those believed to exist in the interstellar medium, typically 10^{-13}–10^{-11} dyn cm^{-2}. However, some jets have considerably higher pressures—notably 4C32.69, which has minimum pressures $\sim 2 \times 10^{-10}$ dyn cm^{-2} on scales as large as 180 kpc, and 3C273 often have knots of enhanced emission in which the minimum pressure may be as much as an order of magnitude larger than the mean pressure. Many jets, e.g., NGC 6251 and NGC 315, lie outside the cores of rich clusters where the intergalactic pressure is believed to be smaller than that in the jet.

If all jets were indeed in pressure equilibrium with their surroundings, then free-free emission in the confining gas should often lead to a strong x-ray source. In the case of 4C32.69 (Potash and Wardle, 1980), the expected luminosity exceeds 3×10^{45} ergs s^{-1}, but the distance of the source ($z = 0.7$) is so large that x-ray observations cannot definitely rule out pressure confinement. However, the observational constraints on the properties of any confining gas are now sufficiently strong that they make thermal confinement extremely unlikely. For example, Wardle and Potash (1982) point out that the x-ray emitting gas confining this and other quasar jets would have to be unusually hot ($kT > 10$ keV), compared to gas found elsewhere in clusters and galaxy halos, to avoid conflicting with existing x-ray data. If it turns out that pressure confinement is untenable, then jets are either free (see Sec. II.C.3) or magnetically confined (Sec. II.C.4). Dreher (1981) obtains even more stringent constraints, based on the lack of depolarization in the diffuse radio "bridge" surrounding the jet in 4C32.69.

C. Collimation, stability, and dissipation

1. Collimation by gas pressure

A jet flowing out from the nucleus of a galaxy may encounter steadily decreasing ambient pressure for several tens of kiloparsecs. Even if the jet is confined, this decrease in pressure will result in an increase in cross section, and the degree of collimation will either decrease or increase, depending on whether the diameter of the channel d increases more or less rapidly than the distance from the nucleus r (Blandford and Rees, 1974; Chan and Henriksen, 1980). This is well outside the region where supersonic flow begins, so the flux of bulk kinetic energy does not change significantly in this region if there is no entrainment. If in addition to a conserved flux of rest mass, we assume that the pressure in the jet varies with density as $p_j \propto \rho_j^\beta$ (not necessarily adiabatic), and the external pressure varies with distance r along the jet as $p_e \propto r^{-n}$, we find that the cone angle of the jet $\theta \sim d/r$ varies as $\theta \propto r^{(n-2\beta)/2\beta}$ for a nonrelativistic equation of state in the jet, and $\theta \propto r^{(n-4)/4}$ for a relativistic gas with $c_s \simeq c/\sqrt{3}$ (see Krantner, Henriksen, and Lake, 1983). The Mach number varies as $r^{(\beta-1)n/2\beta}$ and $r^{n/4}$, respectively, in these two cases. Collimation increases with decreasing n and increasing β, i.e., with a harder equation of state. The jet composed of ultrarelativistic fluid is easier to collimate, since the formula for θ corresponds to setting $\beta = 2$ in the nonrelativistic equation, although the equation of state in the comoving frame has $p \propto \rho^{4/3}$. If resistance to sideways compression is dominated by conserved angular momentum about the jet axis (left over from initial collimation in a disk—see Sec. III.D) or a longitudinal magnetic field, then the effective β also equals 2. A number of processes can result in an effective β smaller than the adiabatic index of the gas, including MHD effects, viscous heating, turbulent mixing, and shear instabilities as discussed below.

If most of the inertia is contained in its walls, then a jet can in principle be focused by an ambient external pressure (Eichler, 1982,1983). The focal length f can be estimated by equating the centrifugal pressure in the jet to

the external pressure and is roughly $f \sim (p_e/P)^{1/2}$ where P is the thrust (see Appendix B Sec. 3). However, this requires that the interior of the jet be kept at a lower pressure than the surroundings. As the convergence speed in the frame of the jet is necessarily supersonic, the flow must maintain a high symmetry in order to avoid internal shocks and consequent dissipation.

The most rapid drop in pressure probably occurs near the galactic nucleus, where ambient gas may form a nearly hydrostatic atmosphere around a compact central object or dense stellar core. For ambient gas with a polytropic equation of state $p_e \propto \rho_e^{\beta_e}$ surrounding a point mass, $n = \beta_e/(\beta_e - 1)$. Thus a jet of nonrelativistic gas with $\frac{4}{3} < \beta < \frac{5}{3}$ will be *decollimated* unless β_e exceeds $\frac{10}{7}$. Note that a radiation-dominated isentropic atmosphere ($\beta_e = \frac{4}{3}$) cannot enhance collimation, although the jet may have originated in a thick disk of radiation-dominated gas. Where convergence does occur within a hydrostatic atmosphere it is in general rather slow. Even for the favorable nonrelativistic case, $\beta_e = \beta = \frac{5}{3}$, θ varies as $r^{-1/4}$ and a 20-fold decrease in θ requires a drop in pressure by a factor $\sim 10^{-13}$. A jet of ultrarelativistic fluid needs a pressure drop by a factor $\sim 10^{-9}$ to achieve the same increase in collimation with $\beta_e = \frac{5}{3}$.

Semiempirical estimates of the factor by which the pressure changes between different values of r offer greater hope for effective pressure collimation. Radiation-dominated flow carrying an Eddington luminosity away from the vicinity of a $10^9 M_\odot$ black hole ($\sim 10^{14}$ cm) is unlikely to have a stagnation pressure exceeding 10^8 dyn cm^{-2}, while the pressure at ~ 1 pc is typically of order 10^{-3} dyn cm^{-2} for VLBI jets such as NGC 6251 (Readhead, Cohen, and Blandford, 1978), as well as for the broad emission line regions of quasars. This gives a mean value for n of about 2, resulting in considerably better collimation than one obtains with the $n = \frac{5}{2}$ hydrostatic atmosphere which corresponds to $\beta_e = \frac{5}{3}$. In the five decades of radius between the putative black hole and the radius where we see VLBI jets, the opening angle of the jet could decrease by more than a factor of 20 for $\beta > \frac{4}{3}$, with as much as a 300-fold decrease possible for a jet with an ultrarelativistic equation of state. This would be more than adequate to explain the apparent opening angles of $\theta \gtrsim 5°$ which have been observed in VLBI jets. However, cooling processes may prevent a quasistatic gas distribution with a smooth power-law run of pressure from being maintained close to the black hole, where the virial temperature exceeds 10^9 K.

There are further observational constraints on confining gas clouds on scales $r \lesssim 10$ pc within a galactic nucleus. A uniform sphere of gas with characteristic pressure $p \simeq 10^{-3} p_{-3}$ dyn cm^{-2} and temperature $10^7 T_7$ K will have an x-ray luminosity of $L_x \sim 3 \times 10^{43} \times p_{-3}^2 r_{pc}^3 T_7^{-3/2}$ ergs s^{-1}. Furthermore, if the gas cloud is hydrostatic and isothermal then the luminosity increases inversely with r as we approach the nucleus. Increasing the gas temperature reduces the luminosity, but at the expense of increasing the necessary central confining mass (Blandford and Rees, 1974; Wiita, 1978a; Readhead, Cohen, and Blandford, 1978; Smith, Smarr, Norman, and Wilson, 1981; Linfield, 1981b). There do not yet exist x-ray observations capable of definitely ruling out pressure confinement and collimation in any single compact source, but from what is known about other galaxies, it seems to be rather unlikely.

From ~ 1 pc to where the outer jets are seen (10—100 kpc), the pressure drops another factor $\sim 10^{-10}$ to values typical of interstellar and intergalactic media. The increase in distance scale is another five decades; hence the additional collimation may be comparable with that achieved in the inner region if the jet maintains the same effective β. In fact, the opening angle of a jet appears to be comparable on VLBI and kiloparsec scales, suggesting that the effective β is close to unity if the jet is confined, i.e., the net collimation need not be a strong function of pressure. Indeed, low values of β are suggested by the slow falloff of radio surface brightness along jets (see Sec. II.C.6). However, it should be noted that weak, two-sided jets often do appear to "flare" dramatically on scales of a few kpc, only to be recollimated further out (Bridle, 1982). This effect, which indicates that the collimation process is much more complex than the power-law models presented here, could be due to a sharp decrease in confining pressure (Bridle, Chan, and Henriksen, 1981) or some increase in dissipation, possibly related to the interpretation of radio "gaps" as regions of insignificant dissipation (Begelman, 1982, and Secs. II.C.6, and II.C.8). When a jet emerges from a confining cloud and enters a region of much lower pressure, it is said to be underexpanded, and a rarefaction wave will propagate into the center of the jet at the internal sound speed. Material through which the rarefaction has passed can expand supersonically, and when this material interacts with the ambient medium a reflected shock follows the rarefaction inward towards the center of the jet. When the shock wave converges at the center of the jet a "Mach disk" will form, and some of the jet's bulk kinetic energy will be dissipated (e.g., Courant and Friedrichs, 1948; Königl, 1980). Such features, which are frequently seen in numerical simulations (e.g., Norman, Winkler, and Smarr, 1983), are naturally identified with the inner bright spots in weak jets.

Converging jets may not retain a circular cross section as they propagate away from the nucleus. If the flow is isentropic and the jet cross section is elliptical at some radius then it will deviate increasingly from a circular cross section because the centrifugal force associated with the convergence is greater along the major axis of the jet cross section than along the minor axis (Smith and Norman, 1981).

In summary, there is direct evidence in the stronger sources that jets are collimated on extremely small scales ($\ll 1$ pc) and manage to maintain or increase their collimation as they propagate through several pressure scale heights. However, it is also possible that in some of the weaker radio sources the jet is collimated entirely on the

galactic scale (e.g., Chan and Henriksen, 1980; Sparke and Shu, 1980). If this were the case, then we would expect the jet to be aligned with the minor axis of the galaxy. Some correlation has been found (Bridle and Brandie, 1973; Guthrie, 1979; Palimaka *et al.*, 1979).

2. Cooling effects

Collimation can also result from radiative cooling of the gas within the jet. It is therefore important to compare the expansion time with the cooling time scale. Thermal gas, cooling by free-free emission (at temperatures in excess of $\sim 5\times 10^6$ K), will radiate away its internal energy in traversing a distance r if

$$v_j \lesssim 300 M_j^{1/5}(L_j/10^{42}\ \mathrm{ergs\,s^{-1}})^{1/2} r_{pc}^{-1/5}\theta_{-1}^{-2/5}\ \mathrm{km\,s^{-1}}\ ,$$

where the jet has a Mach number M_j and an opening angle $0.1\theta_{-1}$ rad (Schreier *et al.*, 1980; see also Hardee, Eilek, and Owen, 1980). X-ray emission is observed from the Cen A jet (Schreier *et al.*, 1980). If this is due to the free-free process, then the jet must be very slow. Line emission from gas at lower temperatures, which will presumably have a small filling factor, can be important only if the line-emitting clouds are continuously excited. Neither free-free emission nor line cooling directly affects the relativistic component of the jet, and increased collimation will result only if thermal pressure dominates the combined relativistic and magnetic pressures. A decrease in jet cross section due to thermal cooling will, however, adiabatically compress any relativistic component mixed with the thermal gas, thereby indirectly enhancing nonthermal emission.

The effects of nonthermal cooling are even harder to estimate, particularly if the jet becomes magnetically dominated. Note, however, that in the relativistic compact radio sources, radio-emitting electrons do not cool within the flow time.

Compact jets emitting synchrotron radiation may be thermally unstable, and this is a way of generating outflowing knots (Simon and Axford, 1967; Marscher, 1980b). However, all investigations of thermal instability in jets are handicapped by our ignorance of the details of the heating mechanism.

Most powerful radio galaxies reveal no evidence for emission from the associated nuclear region, in any waveband, with a power comparable to that believed to be carried by the jet. This indicates that if cooling is responsible for the collimation, it only occurs long after the jet has become highly supersonic.

3. Freedom or confinement?

Information about the ambient pressure gradient propagates into the jet at the internal sound speed s_j. If the jet moves through a background with pressure scale height $\sim r$, the necessary condition for the jet interior to remain in pressure balance with its surroundings is $\theta M_j \lesssim 2$, where M_j is the jet Mach number and $\theta \sim d/r$ is the opening angle. If this condition is not satisfied when a jet is moving into a region of higher pressure, then strong shocks are driven into the jet (Sanders, 1983). A jet moving into a region of lower pressure becomes overpressured relative to its surroundings, and thereafter expands freely.

For an ambient pressure run $p_j \propto r^{-n}$, θM_j scales as $r^{(n-2)/2}$, independent of β; hence a jet will eventually become free if $n>2$. We have argued that $n\sim 2$ may represent the mean slope of p_e between the jet source and ~ 100 kpc scales, but it is unlikely that $p_e \propto r^{-2}$ is a good approximation over any large range in r. It is more likely that the pressure drops sharply where the jet emerges from both the nucleus and the galaxy and varies less steeply than $p_e \propto r^{-2}$ elsewhere. The apparent flaring of some weak two-sided jets at distances of a few kpc from the nucleus (Bridle, 1982) may be evidence for a region where p decreases more rapidly than r^{-2} and where the jet may undergo a short stretch of free expansion. However, these jets all recollimate a few kpc farther out. [However, there is evidence that the flaring is associated with increased dissipation, so it may be largely the result of sudden heating of the jet, rather than a rapid decline in pressure with r (Bridle, 1982; Perley, Bridle, and Willis, 1984).]

If a jet becomes free at r_f, with $\theta M_j \sim 2$, a cylindrical rarefaction wave propagates inward, reaching the core when the jet has traveled a further distance $\sim r_f$. This is followed by a series of compression and rarefaction waves of decreasing amplitude. If the external pressure gradient is sufficiently steep, then the maximum pressure within the jet can exceed the mean jet pressure by a large factor. This furnishes one possible explanation for the knots observed in many jets (Königl, 1980).

Once these transients have decayed, the bulk of the jet expands with a constant opening angle $\theta \sim 2M_j^{-1}$, while the instantaneous Mach number varies as $M_j \propto r^{\beta-1}$, where we again set $\beta=2$ for a jet composed of adiabatic ultrarelativistic fluid (see Sec. II.C.1). If $\beta<1$ a free jet expands with ever increasing opening angle, while for $\beta>1$, the expansion is essentially ballistic after a few scale heights. During this expansion, a surface layer of the jet must remain in pressure balance with the ambient medium, since the jet surface is a contact discontinuity. For $n<2\beta$, this layer is at a higher pressure than the jet interior, and a shock propagates into the jet at a speed $v_{\rm sh} \sim (p_j/\rho_j)^{1/2} \propto r^{(2-n)/2}$ relative to the jet material. The shocked region would have a characteristic opening angle $\sim v_{\rm sh}/v_j \sim \theta (r/r_f)^{(2-n)/2}$. Thus a free jet which enters a region with $n<2$ is shocked back into pressure confinement after it has traveled a distance $\sim d$. For $2<n<2\beta$ the surface of the jet is an increasingly narrow shock front, while for $n>2\beta$ the jet surface is a rarefaction.

A variety of arguments have been advanced in favor of particular observed jets being free. These include

(a) apparently constant observed opening angles (e.g., NGC 6251; Readhead, Cohen, and Blandford, 1978; NGC 315; Bridle *et al.*, 1980);

(b) high equipartition pressure relative to likely intergalactic pressure (e.g., 4C32.69; Potash and Wardle, 1980);

(c) apparently ballistic motion in orbiting jets (e.g., 3C31; Blandford and Icke, 1978; 3C449; Perley *et al.*, 1979);

(d) amelioration of instability problems (see Sec. II.C.5);

(e) absence of limb darkening in observed jets.

However, many of the above sources now show evidence of continuing collimation (e.g., Willis *et al.*, 1981; Bridle *et al.*, 1980; Potash and Wardle, 1980; Saunders *et al.*, 1981; Bridle, 1982), which is clearly incompatible with free expansion. Moreover, in a source as strong as 4C32.69, the thrust estimated on the assumption that the jet is freely expanding ($\gtrsim pd^2$) is far larger than could reasonably be opposed by the ram pressure of the intergalactic medium. Finally, in a supersonic free jet with constant opening angle, the Mach number cannot decrease (i.e, $\beta < 1$) along the jet. In contrast, the variation of surface brightness with distance indicates that generally $\beta < 1$ (see Sec. II.C.6).

Therefore, there are in some instances serious problems associated with both pressure confinement and free expansion of jets. These difficulties motivate consideration of magnetic confinement, to which we now turn.

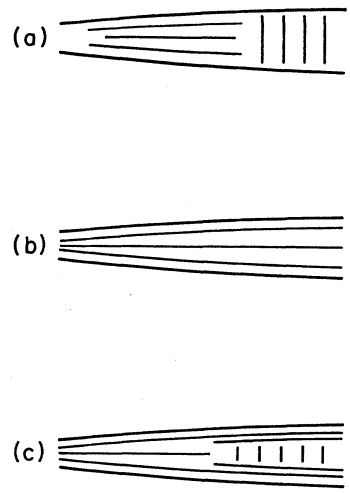

FIG. 12. Schematic diagram of typical magnetic field configurations inferred from polarization measurement of jets. Lines indicate the dominant field direction projected on the sky for (a) weak to moderately strong sources (e.g., NGC 315, NGC 6251), showing the transition from longitudinal to transverse direction expected for a frozen-in field in a sideways expanding jet; (b) strong sources (e.g., 4C32.69); (c) certain of the weaker sources (e.g., 3C31) (resolved transverse to the jet axis), for which there is evidence that the longitudinal field is being amplified by shear near the walls of the jet.

4. Magnetic collimation

The jet's magnetic field not only produces the synchrotron emission, but may also have a strong effect on the collimation, confinement, and stability of the jet. MHD (Appendix B Sec. 6) probably provides a better description of the macroscopic behavior here than in the case of laboratory plasmas because the particle Larmor radii are so much smaller than the transverse size of the jet. The resistivity parallel to the field, based upon Coulomb collisions, is essentially zero. Anomalous resistivity, however, may occur in regions of large shear and high magnetic field gradients, resulting in reconnection, dynamo action, and particle acceleration for which adequate theories do not yet exist. In the absence of resistivity, magnetic field lines can be thought of as being frozen into the plasma (e.g., Parker, 1979). If no field is entrained from the ambient medium, the magnetic flux in the jet is conserved along the jet trajectory, although the field strength may be amplified by internal shear. In the absence of a velocity gradient across the jet, the magnetic field parallel to the jet velocity (longitudinal field), $B_{||}$, scales with the jet diameter as $B_{||} \propto d^{-2}$, while the transverse field $B_{\perp}$ scales as $B_{\perp} \propto d^{-1}$. According to this naive scaling, the field should become predominantly transverse far from the source of the jet, regardless of its configuration closer in. Polarization studies exhibit this transition in several of the weaker jets (e.g., NGC 315 and 3C31, NGC 6251, 3C449), but not for the stronger ones (e.g., 4C32.69; Potash and Wardle, 1980), which generally have parallel magnetic fields (Fig. 12).

In the absence of entrainment, magnetic flux is convected outward from the source of the jet. As we shall discuss in Sec. III.D.5, magnetic fields may play a crucial role in the formation and initial collimation of the jet; hence it would not be surprising if much of the pressure near the source of the jet were contributed by magnetic fields. However, it is highly unlikely that the magnetic field is unidirectional in the outer jet. Field lines parallel to the jet may, if they are unidirectional, carry a net flux of up to $\sim 10^{34}$ G cm^2 near the horizon of a $10^9 M_\odot$ black hole, and $\sim 10^{37}$ G cm^2 at a distance of ~ 1 pc. By contrast, the product of the equipartition magnetic field strength and the jet cross-sectional area for outer jets ($\gtrsim 10$ kpc) is far larger, typically in the range 10^{39}–10^{41} G cm^2, and so $B_{||}$ presumably reverses many times across the jet. In the same vein, we note that a jet whose field is helical with $B_{||} \approx B_\varphi$ carries much more angular momentum than can reasonably have been supported by the nucleus. Likewise, there is evidence from single-dish observations that many compact sources have parallel magnetic fields (Aller *et al.*, 1981), and this too is unlikely to be unidirectional.

A transverse velocity gradient of magnitude $|\nabla v_j| \gtrsim v_j / r$, acting over any scale within the jet, would create sufficient shear to make the longitudinal field dominate (Fig. 13). If spread across the halfwidth of the jet, this much shear need only correspond to a maximum velocity difference of $\Delta v_j / v_j \gtrsim \theta/2$. If the shear reflects the overall velocity profile of the jet, as determined by a turbulent or viscous boundary layer, then the greatest amplification of parallel field might be expected to occur

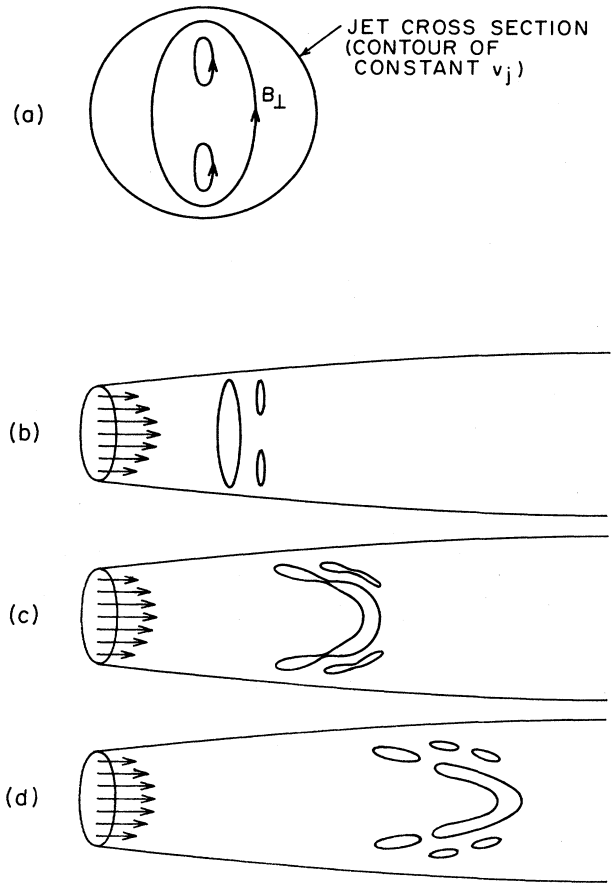

FIG. 13. Diagram illustrating the effects of shear on the evolution of a loop of magnetic field which is initially perpendicular to the jet axis. (a) Cross-sectional view, emphasizing the fact that creation of a longitudinal component ($B_{||}$) from a loop of transverse field ($B_\perp$) requires that the loop not coincide with a surface of constant jet velocity v_j. (b)—(d) Succession snapshots of the loops as they are stretched by the velocity field depicted at left until reconnection takes place. It is likely that jets in which longitudinal field dominates have field structures consisting of numerous stretched loops, as shown in (d); otherwise, the net flux carried by the jet would be too large.

near the jet boundary. Polarization maps of 3C31 indicate that this might be occurring (Fomalont *et al.*, 1980; Laing, 1981), but we should note that there is no accompanying increase in surface brightness at the edge of the jet (limb brightening), which one might expect if dissipation were a surface effect. [Such boundary layers need not show up in radio maps, though, because if there is strict equipartition, then the volume emissivity would be fixed by the pressure alone, and this is approximately constant across the jet. Electrons accelerated in the boundary layer could probably cross the jet on the expansion time scale (Eilek, 1982).] The direction of longitudinal field amplified by large-scale shear would reverse periodically as one moved in azimuth around the jet boundary. Shear on smaller scales might amplify $B_{||}$ more uniformly throughout the jet, for example, if the jet interior were turbulent. Both $B_{||}$ and $B_\perp$ would then reverse on small scales, helping to reduce the depolarizing effect of internal Faraday rotation as described in Sec. II.A.3.

A detailed investigation of turbulent amplification of magnetic field by De Young (1980) shows that, provided the stirring motions contain sufficient helicity (nonzero $\langle \mathbf{v}\cdot\nabla\times\mathbf{v}\rangle$), a small seed magnetic field can be amplified up to an energy density $\sim 5\%$ of the fluid kinetic energy density. In particular, magnetic energy density can flow from short wavelength to long wavelength, in contrast to what is assumed in most models of magnetic turbulence.

The flux conservation problem does not apply to $B_\perp$. Indeed, the values of the field strength inferred within both extended and compact radio sources are approximately consistent with the field having been advected away from the neighborhood of a black hole according to the scaling law $B_\perp \propto d^{-1}$. In fact, we expect that shear and entrainment will enable $B_\perp$ (and in the presence of sufficient shear, $B_{||}$ also) to fall more slowly with jet diameter than this. Hence the Alfvén speed increases along the expanding jet, and the effective value of β is less than unity. Unless the gas is heated and increases its temperature, the jet must become magnetically dominated and will approach local force-free equilibrium (i.e., $\nabla\times\mathbf{B}$ parallel to $\mathbf{B}$). Particle acceleration probably will be associated with this field readjustment (see Sec. II.C.7).

If the jet carries a net current, then it can be magnetically self-confined under the tension associated with the toroidal field lines (Fig. 14; Benford, 1978; Chan and Henriksen, 1980; Bicknell and Henriksen, 1980; Bridle, Chan, and Henriksen, 1981; cf. also Piddington, 1970; Sturrock and Barnes, 1972; Ozernoi and Usov, 1973a,1973b; Achterberg, Blandford, and Goldreich, 1983). The current involved is $\sim 10^{17} p_{-12}^{1/2} d_{\rm kpc}$ A, where $10^{-12} p_{-12}$ dyn cm^{-2} is the pressure. In an axisymmetric jet, with a purely toroidal field and no significant particle pressure, magnetic confinement can be achieved by rearranging the density profile in the external medium so that the toroidal field B_φ varies inversely with distance x from the axis. The magnetic stress then varies as x^{-2} and can be reduced to the value of the external pressure. The return current flows at larger radii still, and the stresses associated with it can be ignorably small. This approach towards force-free equilibrium results in a high compression of the core of the jet. Thus the above scaling must ultimately break down when the combined pressures due to the particles and the longitudinal field become comparable with that of the toroidal field. In this way, the pressure in the core of the jet can be substantially larger than in the external medium.

Other studies of magnetically self-confined equilibria undertaken in connection with astrophysical jets have either assumed the field to be generated by surface currents (Cohn, 1983), which implies that the jet confinement is entirely supplied by the cocoon, or made the *ad hoc* assumption of a self-similar helical equilibrium (Chan and Henriksen, 1980). As discussed earlier, the assumption of a unidirectional longitudinal field, required by the latter model, is probably unrealistic.

A more realistic approach to magnetic self-confinement

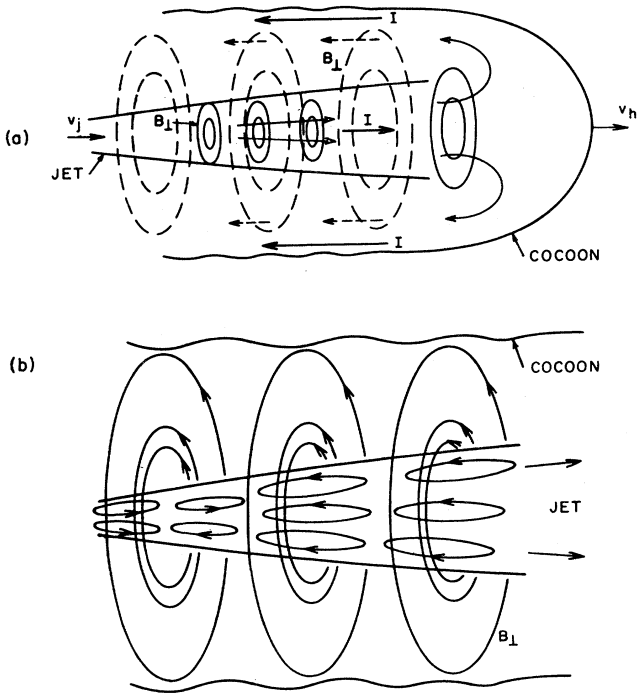

FIG. 14. Illustrative scheme for the development of magnetic confinement around a jet. (a) Jet production mechanism establishes current I along jet; equivalently, loops of $B_\perp$ are advected towards the head of the jet. These are deposited in the cocoon along with the jet material, and surround the jet with loops of external field. Time-dependent evolution of the cocoon causes a return current I to flow near the outer surface of the cocoon, excluding the field from the ambient medium. (b) Strong shear between jet and cocoon causes the field to become predominantly longitudinal inside the jet (cf. Fig. 13). Absence of shear amplification and viscous heating outside the jet allows $B_\perp$ to become dominant source of pressure in the cocoon. As a result, the field in the cocoon evolves towards a force-free configuration in which magnetic tension maintains the jet at a much higher pressure than the ambient medium. Only the highly dissipative jet is a sufficiently strong synchrotron source to be detected observationally; thus strong jets which appear to need magnetic confinement also appear to have longitudinal field.

will have to take into account contributions of particle pressure *as well* as the dynamical effects of both *longitudinal* and *toroidal* fields. Certain existing equilibria explored in connection with the fusion program have properties which make them attractive for jet confinement (Bateman, 1978; Taylor, 1974).

When a magnetically confined jet reaches the hot spot, the magnetic flux may be advected into the cocoon, where it will surround the jet as it continues to advance into the intergalactic medium. If $v_j \gg v_h$ then only a small fraction of the flux carried by the jet need be cast off around the jet in order to reduce the pressure from that in the jet to a much smaller value in the surrounding medium. Associated with the moving magnetic field is a Poynting energy flux $(B_\perp^2/4\pi)v_j$. For super-Alfvénic jet speeds, this is smaller than the bulk kinetic energy flux, but if the motion is sub-Alfvénic, then the deposition of magnetic energy in the hot spot can be regarded as Ohmic heating (Benford, 1978).

If there is no confining field in the external medium, and this medium behaves as a perfect conductor, then the time-dependent evolution of the jet and cocoon will induce a return current on the interface between the cocoon and ambient medium, which will exclude the field from the latter. However, complications may arise if turbulent mixing of cocoon and ambient medium (Norman *et al.*, 1983) allows the diffusion of the confining field (through anomalous resistivity and/or reconnection) into the gas surrounding the source. Furthermore, return currents may be distributed throughout the cocoon and on the surface of the jet.

In any case, (1) the toroidal field within the jet and cocoon probably consists of nested loops with the same field direction (perhaps determined by the spin of the central engine) and (2) the jet-plus-cocoon probably has a core-sheath structure, with pressure rising to a central plateau and leveling off (Fig. 14). Indeed, it appears that a core-sheath structure is required observationally in those powerful jets which seem to be most in need of magnetic confinement, since the polarization in these jets indicates that the field is predominantly *longitudinal.* A longitudinal field is unable to provide the tension necessary for self-confinement; hence, if these jets are self-confined, the confinement must occur in a sheath of low surface brightness surrounding a bright core in which longitudinal field dominates. Since the pressure in the sheath declines rapidly with distance from the jet axis, it should not be surprising that the sheath is fainter than the core of the jet. However, if no trace of a low-surface-brightness sheath were found in high-resolution, high-sensitivity maps of sources like 4C32.69, then this would suggest that conditions in the core differ markedly from those in the confining sheath. This could be the case, for example, if essentially all of the collimation is provided by a magnetic field threading the cocoon. The longitudinal field would then dominate only in the region of the most intense shear—the jet—which would also be the site of the strongest particle acceleration. A positive test of magnetic confinement by an invisible cocoon would be the detection of a flip in the sign of Faraday rotation from one side of the jet to the other. However, to date none of the candidates for magnetic collimation show evidence for either intrinsic Faraday rotation or depolarization, so the feasibility of this observational test remains to be demonstrated.

The existence of core-sheath structure in magnetically confined jets may be reflected in the observed high degree of collimation in the jet. The effective β for the sheath would be $\lesssim 1$. The core, however, is dominated by a combination of longitudinal field and particle pressures, all of which may have considerably higher β's. Since the equation of state in the core may be harder than that in the sheath, the collimation may be better for the core than for the sheath (Sec. II.C.1), and if it is the core that produces

the observed radio emission, the jet will appear to be well collimated. Note, however, that dissipation in the core may reduce β below the naive (adiabatic) value.

If the external pressure changes sufficiently rapidly, then the expansion of the jet may not be steady but oscillatory (Wesson and Lenmann, 1977; Chan and Henriksen, 1980). In the frame of the outflowing fluid, the compressive magnetic tension does not maintain equilibrium with the particle pressure. This may account for the variations in apparent jet width observed in some sources.

Magnetically confined plasma is notoriously unstable. However, the situation in a jet is different from that encountered in the laboratory because of the super-Alfvénic and supersonic streaming velocity. Formal stability analysis of even the simplest jet models is complex and handicapped by the absence of a suitable variational principle (Benford, 1981; Fiedler, 1982; Cohn, 1983); we must rely on heuristic arguments at this stage.

Kelvin-Helmholtz stability of the interface between the jet and the ambient medium would not be strongly influenced by the magnetic field, since the energy density is much smaller than the kinetic energy density which drives the Kelvin-Helmholtz instability (Sec. II.C.5). Unstable MHD modes (such as the pinch and kink instability) do not grow as rapidly as in a stationary plasma, although sufficiently short-wavelength unstable modes, localized within the jet interior, are not suppressed by the relative motion. Longitudinal magnetic field in the core of the jet can likewise act as a "backbone," provided that the correlation length for magnetic field reversal along the jet exceeds the wavelength of the perturbation. Instability may be suppressed for perturbations of large wavelength along the jet by the inertia of the ambient medium. Interchange modes with large azimuthal wave numbers cannot be suppressed in this way, but their growth is not as serious a threat to the integrity of the core.

Polarization observations of the outer parts of the jet in 3C31 (Fomalont *et al.*, 1980) indicate a magnetic geometry opposite to that just described, i.e., a perpendicular field in the body of the jet surrounded by a boundary layer containing a parallel field (see Sec. II.C.6). This may also be produced by electrons emitting in a toroidal field in a jet viewed from an inclination angle $\sim 45°$ (Fomalont *et al.*, 1980; Spangler, 1979; Laing, 1981).

It is clear that our understanding of the role of magnetic fields in jets is even more primitive than that of other aspects of the problem. Future high-resolution observations that reveal the variation of field direction and emissivity across the jet will furnish more insight than can theoretical guesswork at this stage.

5. Kelvin-Helmholtz instability

It is well known that the interface between two parallel flows with differing velocities is subject to the Kelvin-Helmholtz (KH) instability (e.g., Chandrasekhar, 1961; Gerwin, 1968). Since a jet surrounded by an ambient medium possesses such an interface, it is important to examine the effects of this instability on the propagation of a jet. In particular, the weak, edge-darkened sources may be fueled by jets that have been decelerated by surface instabilities, and the curvature of some jets (Sec. II.D below) may be caused by the nonlinear development of Kelvin-Helmholtz instabilities.

The KH instability, which occurs in inviscid fluid dynamics (or MHD), taps the relative kinetic energy between the jet and the ambient medium. In a linear analysis the tapped energy goes into sideways motion of the material near the interface (i.e., transverse waves), rather than directly into heat. To derive a dispersion relation one perturbs the interface and the fluid on either side, then solves the equations of motion subject to continuity of pressure and displacement of the interface. The nonlinear development of the instability, observed in experiments and numerical simulations, involves the formation of "rolls" or "cats' eyes," which obtain their vorticity (in the absence of viscosity) from the vorticity contained in the interface. If the change in velocity occurs gradually rather than discontinuously, the instability is not changed much for wavelengths longer than the scale height of the shear layer, but is suppressed for shorter wavelengths (Chandrasekhar, 1961). Shorter wavelengths are also suppressed by viscosity, and it is the competition between the spreading of a viscous boundary layer (Sec. II.C.6) and the growth by KH instability of successively longer (and hence deeper) perturbations that leads to a critical Reynolds number, above which the flow becomes turbulent (Batchelor and Gill, 1962; Lessen and Singh, 1973).

For perturbations of wavelength much smaller than the jet radius, the interface can be treated as a plane vortex sheet (Bodo and Ferrari, 1982; see Ferrari *et al.*, 1982 and Ray and Ershkovich, 1983 for the case of a shear layer with finite thickness). In ideal, compressible hydrodynamics, the dispersion relation for this initial configuration is a sixth-order polynomial in $\omega/k_{||}$, where ω is the (complex) frequency and $k_{||}$ the (complex) wave number parallel to the velocity (see, for example, Miles, 1958 for the compressible hydrodynamic case; Southwood, 1968, and Blake, 1972 for the inclusion of tangential magnetic field; Turland and Scheuer, 1976 or Blandford and Pringle, 1976 for the relativistic case). The instability is severe for subsonic and trans-sonic relative velocities, but for the highly supersonic case, instability is suppressed for all modes save those for which the wave vector $\mathbf{k}$ is nearly normal to the relative velocity. If the angle between these two vectors is δ, then the condition for instability in the compressible hydrodynamic case is $\cos\delta < \max[M_j^{-1}, M_e^{-1}]$, where M_e is the Mach number relative to the external sound speed.

Physically, this means that the relative velocity normal to the wavecrests has to be subsonic in the less dense fluid in order to support the coherent pressure perturbations necessary to drive the instability. Growth rates are also slower when the density ratio is far from unity, by a factor $\sim(\rho_j\rho_e)^{1/2}/(\rho_j+\rho_e)$. Southwood (1968) did not find magnetic field configurations which suppress all modes in a compressible system, and conjectured that unstable

modes always exist.

Turland and Scheuer (1976) and Blandford and Pringle (1976) found that the range of unstable modes is restricted by sound-travel-time effects in the relativistic case as well (Mach numbers scale with γ_j), and that observed growth rates for unstable modes may be slowed considerably by time dilation.

It is not at all clear whether this instability should be regarded as temporal growth for real $k_{||}$, as is normally assumed, or spatial growth for real ω. For slow growth, however, the imaginary parts are related through the phase velocity $\mathrm{Im}(\omega)/\mathrm{Im}(k_{||})=\omega/k_{||}$. In the case of spatial growth, we wiggle the jet at some point and watch the perturbations propagate downstream, while for temporal growth a perturbation imposed on the channel wall grows at the same rate everywhere.

Generally, if the two fluids have very different densities, the perturbation will be nearly comoving in the frame of the denser fluid, i.e., the one with the greater inertia. Thus, in a light jet immersed in dense ambient medium, an unstable temporal mode grows exponentially before it has traveled one wavelength downstream from its source, although the group speed of the wave is smaller than the jet speed by $\sim(\rho_j/\rho_e)^{1/2}$. On the other hand, a train of unstable sine waves can nearly move with a dense jet for $\sim(\rho_j/\rho_e)^{1/2}$ wavelengths before e-folding in amplitude.

For longer-wavelength modes, we must take into account the cylindrical geometry of the jet. If the jet is modeled as a uniform cylinder moving with constant velocity in pressure balance with a uniform medium, then the normal modes are Bessel functions in cylindrical radius (Gill, 1965). These are characterized by azimuthal dependence $\exp(im\varphi)$ with m a real integer, but the wave number $k_{||}$ along the jet may be complex. Modes with $m>1$ (fluting modes) increasingly resemble plane-parallel waves wound helically around the jet as m increases, and the nonrelativistic stability criterion approaches that for the plane-parallel case with $\cos\delta$ replaced by $k_{||}d/2m$, where d is the jet diameter. Relativistic modifications (Ferrari, Trussoni, and Zaninetti, 1978a,1978b,1979, 1980,1981; Hardee, 1979) are analogous to those found for the plane-parallel case. As in the plane-parallel case, the fastest-growing modes (spatially and/or temporally) are those which are not too far from marginal stability; hence for a given m the dominant modes have wavelengths $\lambda_{||}(\equiv 2\pi/k_{||})\sim(\pi d/m)\min(M_j,M_e)$. Since the growth rate is roughly proportional to $k_{||}$, modes with the largest m grow most quickly, but only affect the jet to a depth $\sim d/m$. Thus, while fluting modes may trigger the formation of a turbulent boundary layer (perhaps ultimately resulting in the particle acceleration and field amplification which make the jet visible), it is unlikely that they have a devastating effect on the coherence of the jet. Magnetic fields would further restrict the range of unstable wave numbers; a sufficiently broad shear layer could plausibly suppress all modes with $m>1$, but further investigations are needed to make these statements quantitative (Ferrari and Trussoni, 1983). Buoyancy effects which may be of importance for a light jet have been included by Achterberg (1982).

Far more threatening to overall jet stability are the $m=1$ and $m=0$ modes, which are similar in appearance to the kink and pinching modes of plasma physics. Since these modes penetrate to the core of the jet, they are not suppressed by a broad shear layer, nor can they be strongly influenced by a magnetic field unless $B^2/8\pi$ is comparable with the kinetic energy density. They may, however, be suppressed by rapid expansion of the jet (Hardee, 1983,1984). Stewart (1971), Hardee (1979), and Ray (1981) have examined the fundamental $m=0$ mode in detail, and find that for a narrow range of $\lambda_{||}\sim\pi d$ it can grow more quickly than other modes having the same $\lambda_{||}$, provided M_j is not much larger than unity and the ambient medium is considerably denser than the jet. The sausage (or pinch) is the only mode which alters the jet's cross-sectional area, resulting in alternating zones of compression and rarefaction which extend into the core of the jet. The knots of enhanced emission observed in some jets (e.g., 3C273, NGC 6251; Sec. II.C.8) could be manifestations of the nonlinear development of the $m=0$ mode (Hardee, 1979). More recent work by Cohn and Payne (1983,1984) indicates that higher-order "reflection modes" of the $m=0$ pinch grow more rapidly than the fundamental modes for high Mach numbers. For a Mach number M_j, the fastest growing $m=0$ mode has $\sim M_j^{-1}$ nodes inside the jet, and a wavelength $\sim\pi d$. These modes are less liable to disrupt a jet than the fundamental mode or $m=1$ mode, but they may be responsible for the development of periodically spaced knots. Evidence for the nonlinear development of these modes may be present in recent numerical simulations by Norman *et al.* (1982).

At Mach numbers substantially greater than unity, the $m=1$ mode with $\lambda_{||}\sim\pi d\min(M_j,M_e)$ grows fastest (Hardee, 1979,1981; Ray, 1981). For purely temporal perturbations in a low-density jet, the e-folding distance is approximately $\lambda_{||}$, while for a jet denser than its surroundings the perturbation e-folds in a distance $\sim(\rho_j/\rho_e)^{1/2}\lambda_{||}$. The linear kink mode alters neither the area nor the shape of the jet's cross section, unlike the pinch and flute modes, but it shifts the mean trajectory of the jet material, twisting it into a sinusoidal motion.

To determine whether these modes can disrupt jets, it will be necessary to examine their nonlinear development, which takes place after the sideways displacement of the wiggle becomes comparable with the jet radius. If the flow inside the channel remains coherent, then one may neglect the internal fluid properties of the jet and write an equation of motion for the channel as if it were a garden hose. Using this approximation, Benford (1981) found that the instability continued to grow in the nonlinear regime, although the growth rate for a low-density jet may be reduced from exponential to algebraic if the sideways motion is opposed by ram pressure in the ambient medium.

However, it appears that the garden hose approximation must break down before the nonlinear development has gone very far. In order for the flow inside the channel to remain coherent, a sound wave must be able to

cross the jet in less time than it takes the jet material to move sideways by one jet radius, in attempting to follow the channel. For the fastest-growing kink mode in supersonic jets, this condition is violated when the sideways displacement is comparable with the jet radius, and for longer wavelengths the maximum displacement scales linearly with $\lambda_{||}$. When the coherence condition is violated, pressure perturbations inside the jet can no longer remain in phase with wiggles in the jet channel, and the energy which would have gone into sideways motion is instead dissipated as heat. Since this limits the amplitude of the instability to a relatively small value, it may severely lessen the role of kink modes in disrupting jets.

Nevertheless, it is attractive to associate the quasi-periodic nonuniformities observed in some jets (e.g., 3C449, 3C31, M87) with the nonlinear development of kink modes (Owen, Hardee, and Bignell, 1980; Benford, 1981,1983). Our understanding of these instabilities, however, is far from complete. The most promising technique for studying the nonlinear development is through numerical calculations (Norman *et al.*, 1983; Nepveu, 1980,1982a,1982b). In addition, it is natural to identify relaxed doubles (Type-I sources) as radio sources in which the jet is destroyed by these instabilities before it reaches the interface with the ambient medium (Hardee, 1983). Either the jet is now much weaker than in the past, or it is simply inflating a larger buoyant bubble of hot plasma. In favor of the latter possibility we note that relaxed doubles are typically much larger than Type-I sources (Secs. I.C and II.B.1).

The condition for neglect of self-gravitation in the development of these modes is that the jet velocity exceed $\sim 500 L_{j45}^{1/5}\theta_{-1}^{-2/5}$ km s^{-1} where the kinetic energy flux is $10^{45}L_{j45}$ ergs s^{-1}. Velocities as slow as this have been proposed in some jets (Sec. II.A.4), although if this inequality is violated the discharges generally exceed $100M_{\odot}$ yr^{-1}. If gravitational instability were ever important, then fragmentation to smaller and smaller mass scales (down to stellar masses?) would probably ensue, at a rate dictated by cooling processes.

6. Viscosity and turbulence

So far our discussion has been framed in the language of perfect gas dynamics and MHD. However, the observationally determined value of the exponent in the pressure-density relation β (Sec. II.C.1) appears to be smaller than unity, substantially lower than the exponent in the "adiabatic" pressure-density relation for all jet constituents except a transverse magnetic field (Sec. II.C.4). If the gas is to maintain such a small value of β and equipartition is approximately valid, then there must be dissipation throughout the jet. Indeed the simple fact that we observe jets at all indicates that they are dissipative to some degree. Radiation times generally exceed expansion times in jets, and if the jet were expanding uniformly with a transverse field and $\alpha=0.5$, the surface brightness would decay as $I_\nu \propto r^{-19/6}$. Even if the electrons maintain equipartition, $I_\nu \propto r^{-5/2}$ (e.g., Valtonen, 1979). The surface brightness in observed jets decays far more slowly than this; typically $-(d\ln I_\nu/d\ln r)\equiv m$ lies in the range 0—1.5 (e.g., Waggett, Warner, and Baldwin, 1977; Bridle *et al.*, 1979; Bridle, 1982). Therefore, there must be substantial dissipation occurring throughout the jet. With this surface brightness law, the volume emissivity scales as $\theta^{-1}r^{-(m+1)}$ and the equipartition pressure scales as $p_{\rm eq}\propto\theta^{-4/7}r^{-4/7(m+1)}$, where $\theta(r)$ is the observable jet cone angle. Typically $p_{\rm eq}$ declines less steeply than $d^{-1.4}$; hence the effective sound speed increases in the expanding jet if the mass flux remains constant. The likeliest source of energy for this dissipation is the relative kinetic energy associated with shear within the jet and between the jet and the surrounding medium. This energy may be tapped by viscous stresses.

The equations of relativistic viscous flow in the one-dimensional approximation have been written down by Baan (1980). Unfortunately, as with accretion disks (e.g., Pringle, 1981), we have no good understanding of the viscosity mechanism. What is clear, however, is that conventional "molecular" viscosity, as well as thermal and electrical conductivities based on Coulomb mean free paths, are probably irrelevant. The relevant viscosity is associated with either fluid turbulence or magnetic fields.

Turbulence may arise as a consequence of instability at the wall of a jet and subsequent spreading of a turbulent boundary layer, or it may be caused by local instability within the jet (e.g., Henriksen, Bridle, and Chan, 1982). Surface instability is partly suppressed by high Mach number, large density contrast betwen the jet and the surrounding medium, and relativistic speeds—all conditions which may be present within astrophysical jets (see Sec. II.C.5). Internal instability may be driven by shear or internal magnetic fields. In the former case, it will grow at a rate determined by the velocity profile. However, in a collimating or decollimating jet, centrifugal forces associated with the curvature of the streamlines may promote local shear stability. For wavelengths shorter than the local density scale length, $|dx/d\ln\rho|\equiv H_\rho$, the Richardson criterion for stability is $H_\rho < 4H_v^2/R$, where $H_v=|dx/d\ln v|$ is the velocity scale length and R is the radius of curvature (Chandrasekhar, 1961; Bicknell and Melrose, 1982; Blandford and Payne, 1982). For stability, the density gradient must oppose the curvature. (Short-wavelength modes may be damped by viscosity.) This criterion is applicable only if the growth time is shorter than the expansion time, i.e., $d>(RH_\rho)^{1/2}$. It is also modified by the presence of a toroidal magnetic field. In any case, local instability can be avoided only in regions of low shear.

We can perhaps draw some guidance from laboratory investigations of jets (see Sec. V.C). Subsonic "submerged" jets (i.e., those with densities similar to the ambient medium) become turbulent when the Reynolds number $dv_j\rho/\eta$, where η is the coefficient of dynamical viscosity, exceeds $\sim$100—3000 (McNaughton and Sinclair, 1966; Lessen and Singh, 1973), and thereafter ex-

pand with a constant opening angle $\sim 25°$—$30°$. The sideways expansion is dictated by entrainment. For kinematic reasons, supersonic jets can expand with an opening angle not much larger than $2/M_j$. Here the expansion is due to the heating of jet material, presumably by viscous processes. There are experimental indications that the preturbulent range of a supersonic jet increases very rapidly with Mach number (e.g., Shirie and Seubold, 1967). With these experimental guidelines in mind, we can begin to examine simple phenomenological models of jet viscosity.

In accretion disks, a common prescription is to abandon the notion of molecular viscosity and estimate the shear stress by $\alpha^* p$, where α^* is a constant less then unity and a superscript $*$ has been appended to distinguish it from the spectral index. This is argued to be a good model of both magnetic (Eardley and Lightman, 1975) and turbulent (Shakura and Sunyaev, 1973) viscosity. It is obviously of some interest to see whether or not the large body of theory founded on the α^* hypothesis has any counterpart in the study of jets. Of course, such a prescription cannot be relevant near the center of the jet where the shear goes to zero and the shear stress must do likewise. (A similar situation arises where the innermost parts of accretion disks match onto more slowly rotating stars.) An alternative model for the viscosity involves the assumption of constant Reynolds number (Lynden-Bell and Pringle, 1974).

For simplicity let us make the equipartition hypothesis at all points in the jet and suppose that the viscosity is caused by small-scale instabilities that convect magnetic field across the jet. The field is then stretched in the direction of the jet velocity until reconnection occurs. The coherence length in the field is $\sim \alpha^* v_A / |dv/dx|$, and a necessary condition for applicability of the α^* prescription within a region is that the velocity difference across that region exceed the Alfvén speed. The magnetic shear stress is given by $\langle B_{||} B_{\perp} \rangle / 4\pi$ (where $B_{||}$ is the field component resolved parallel to the local velocity). In the more powerfully radiating jets $B_{||} \gg B_{\perp}$, and so the angle $B_{\perp}/B_{||}$ is simply $\sim \alpha^*$. The local rate of energy dissipation is then $\sim \alpha^* p (dv_j/dx)$. This can be equated to the particle acceleration power $\sim p v_j / r$ described in Sec. II.C.7. Now p must be approximately constant across the jet and, except for a free or magnetically confined jet, is equal to the external pressure. We therefore conclude that the velocity profile is roughly exponential, with a characteristic width $\sim \alpha^* r$. Observations indicate that $0.01 \lesssim \alpha^* \lesssim 0.1$. Clearly, in a jet dominated by viscous heating, and in which $\theta = d/r$ changes along its length, α^* cannot be constant (Begelman, 1982). Also, the changes in width and surface brightness (even allowing for projection) from jet to jet argue against any simple phenomenological scaling law.

A similar result is obtained if turbulent rather than magnetic viscosity is assumed. Here the mean free path of a turbulent element is $\sim \alpha^* s / |dv/dx|$ and the turbulent pressure is assumed to be in equipartition with the magnetic and particle pressures, as is generally argued to be the case in the interstellar medium (e.g., Spitzer, 1978). Clearly, observations of polarization from jets indicate that any turbulence must be anisotropic to some degree. One new feature introduced with turbulent viscosity is thermal conduction. Baan (1980) has computed jet profiles under the assumption that the ratio of the kinematic viscosity and thermal diffusivity (Prandtl number) is unity. Kahn (1983) has computed a velocity profile for a relativistic jet emphasizing the kinematical consequences of observing a range of speeds (i.e., Doppler boosts) in an individual jet.

Independent of the detailed viscosity mechanism, there is a limit on how rapidly a supersonic jet can decelerate and still remain supersonic. Again ignoring the inner and outer boundary conditions, and assuming that a substantial fraction of the internal energy is contained in the form of magnetic fields and low-energy particles that cannot radiate efficiently on the expansion time scale, one finds that in each expansion length a fraction $\lesssim M_j^{-2}$ of the bulk kinetic energy is converted into heat while the jet conserves thrust. This means that $|d \ln v_j / d \ln r| \lesssim M_j^{-2}$. To give a numerical example, suppose a jet is decelerated from a velocity $v_j = 10^5$ km s^{-1} to 10^4 km s^{-1} as it propagates from $r = 10$ pc to 100 kpc. The argument above implies that during most of this deceleration the jet must have a Mach number $\lesssim 2$. For such a jet, transverse confinement is imperative to achieve the observed degrees of collimation. By the same token, no observed jet can have $M_j > 4$ and have dissipated a substantial fraction of its kinetic energy by viscous stresses, unless it is also radiative.

There is not much evidence for the existence of thin boundary layers separating the jet from the surrounding gas. No jet yet observed has shown evidence for limb brightening, although several are well resolved across their widths. This may not be surprising if the radio-emitting electrons are able to diffuse across the jet before they cool. The volume emissivity, $\propto p^{7/4}$ on the equipartition hypothesis, is roughly constant across the jet. There is, however, evidence of a boundary layer in 3C31 and other jets from polarization data (Perley *et al.*, 1979).

If, as is usually the case, a jet cannot cool radiatively (or through the radiation of sound waves) on the expansion time scale, then the expansion rate is influenced by the rate of dissipation as well as the run of ambient pressure. If dissipation is concentrated in a thin boundary layer, then the thickness of the layer t must exceed a value fixed by balancing expansion losses with viscous heating. In the context of the α^* model, this requires $t \gtrsim (\alpha^*/\theta) d$. If $\theta \lesssim \alpha^*$, then the jet will expand as a result of heating until this becomes an approximate equality. If $\theta > \alpha^*$, the jet may continue to collimate adiabatically until $\theta \sim \alpha^*$. The expansion of the jet is thereafter dominated by viscous heating, and continues to expand with $\theta \sim \alpha^*$ regardless of the run of pressure $p(r)$, provided that α^* does not decrease too rapidly with increasing M_j (Begelman, 1982). Since a pressure-confined jet cannot expand with $\theta \gtrsim 2 M_j^{-1}$, a strongly heated jet will reduce its Mach number until $M_j \lesssim 2/\alpha^*$. The increased dynamical importance of dissipation after a jet is collimated to a sufficiently small angle may cause the relatively sudden

brightening of a jet that is too faint to see closer in to the nucleus, and thus explain the presence of "gaps" in many jets (Sec. II.C.8). A sudden enhancement in the dissipation rate may also account for the "flaring" of jets in some of the weaker two-sided sources (Bridle, 1982).

Whatever the thickness of the boundary layer, there is likely to be some entrainment of the external gas (De Young, 1981). The line emission which van Breugel and Heckman (1982) find to coincide with the outer contours of radio lobes may arise in newly entrained gas (De Young, 1982). Again, strongly supersonic jets should propagate with roughly constant thrust, hence any strong reduction in the mean jet speed through entrainment will lead to a large and in general unobserved dissipation of the jet's kinetic energy (see Sec. II.A.4). The flux of entrained mass is certainly limited by p/s_e, where s_e is the external sound speed (Bradshaw, 1977, quotes an entrainment rate of $\sim\frac{1}{4}\pi^2\rho_e l_{\rm edd} u_{\rm edd} R_j$ where $l_{\rm edd}$ is the dominant eddy size, $U_{\rm edd}$ the eddy speed, and R_j is the jet radius, for Mach number $M_j \lesssim 2$). Entrainment is therefore unimportant if $M_j > (s_j/\theta s_e)$ (Blandford and Rees, 1974).

Entrainment provides a possible explanation of slow, dense jets. Suppose that a jet entrains material steadily over some distance r. The rate of entrainment will be dictated by the viscosity. Under certain conditions (Begelman, 1982), the jet Mach number can be reduced to approximately unity without the jet's becoming decollimated or radiating a large power. Let us assume an α^* law. (Similar results were obtained with a "molecular" viscosity.) If we seek a self-similar scaling law, then we can equate the radial force due to the external pressure gradient acting over a pressure scale height $\sim pr^2\theta^2$ to both the jet thrust and the viscous force $\sim\alpha^* pr^2\theta$. From this we conclude that if entrainment proceeds in a self-similar fashion over several pressure scale heights, then $\theta\sim\alpha^*$. The energy flux $L\sim pv_j d^2$ is then approximately conserved, and the variations in Mach number, velocity, and mass discharge are related through the scalings $\dot{M}\propto M_j^2/v^2\propto M_j^2 p^2 r^4$ (Begelman, 1982).

7. Particle acceleration and radio emission

Acceleration of relativistic electrons occurs at four distinct locations in extragalactic radio sources—nucleus, jets, hot spots (see Sec. II.B.2), and the cocoons or tails of some sources (see Sec. II.B.3). As we have described, the observed spectral indices in these regions are different—indeed, there is not even a universal pattern found in all sources. Nuclei of compact sources have flat spectra, $-0.3\lesssim\alpha\lesssim 0.5$. There is now substantial evidence that these spectra result from the superposition of several (or even a continuum of) self-absorbed regions (e.g., Wittels, Shapiro, and Cotton, 1982) in which the optically thin spectra have indices closer to the standard value $\alpha\sim 0.7$ (e.g., Readhead and Wilkinson, 1980). The spectral indices of jets typically fall in the range $0.5<\alpha<0.7$ (Bridle, 1982). Spectral indices of hot spots are hard to measure but are typically $0.5\lesssim\alpha\lesssim 1$. Some, but not all, low-surface-brightness tails and cocoons (e.g., Jenkins and Scheuer, 1976) have very steep spectra $\alpha\gtrsim 1.2$, conventionally interpreted as the result of radiative losses.

It seems unlikely that the same acceleration mechanisms are at work in each of these four regions, nor is the relationship of the acceleration region to the emitting region generally the same. From a macroscopic point of view, particle acceleration is one of the principal means of dissipation available to a jet. Given a mechanism of prescribed efficiency, a jet presumably adjusts until the resulting pressure is dynamically consistent with quasisteady flow. For this reason, jets can provide a valuable probe of particle acceleration—inverting the argument, given a reliable theory of particle acceleration (derived from observations within the interplanetary and interstellar media), it should be possible to infer dynamical information and, in particular, the jet velocity.

Using the theory of synchrotron radiation (Appendix A Sec. 1), it is possible to infer the slope of the relativistic electron distribution function from the spectral index α, $N_\gamma\propto\gamma^{-(2\alpha+1)}$. This means that over the power-law region the electron energy is concentrated at the high-energy end for $\alpha<0.5$ and at the low-energy end for $\alpha>0.5$. If an extensive power law of slope $(2\alpha+1)$ is continuously accelerated within a region of constant magnetic field, then the observed synchrotron spectrum will have spectral index α up to a frequency for which the typical emitting electron [of energy $\propto(\nu/B)^{1/2}$] has a cooling time ($\propto\nu^{-1/2}B^{-3/2}$) comparable with the acceleration time. At higher frequencies, the spectral index will increase to $(\alpha+0.5)$ until the acceleration mechanism is no longer able to supply the electrons emitting at that frequency (e.g., Kardashev, 1966). Note that optically thin spectra with $\alpha<0.5$ cannot be produced continuously at frequencies where the cooling time is shorter than the acceleration time. This constraint perhaps applies within the jets themselves. As noted above, spectral indices in jets are generally measured to lie in the range $0.5\lesssim\alpha\lesssim 0.7$. Optical jets, when observed, have radio-optical spectral indices $\alpha_{\rm ro}\simeq 0.6$. From radio and optical observations, and on the assumption that the optical emission is synchrotron radiation, one can infer the frequency ν_b at which α increases by 0.5. For electrons radiating at frequencies below ν_b the main losses are due to expansion. Assuming that $\alpha\gtrsim 0.5$, the acceleration power is at least $p_{\rm min}v_j/r$, where $p_{\rm min}$ is the equipartition pressure deduced from radio observations. We can estimate r/v_j by equating it to the synchrotron cooling time in the equipartition field at the break frequency, $10^{13}\nu_{b_{13}}$ Hz. Numerically, the particle acceleration emissivity is

$$\epsilon_{\rm pa}\sim 10^{38} p_{-12}^{7/4}\nu_{b_{13}}^{1/2}\ {\rm ergs\,s^{-1}\,kpc^{-3}}\ , \tag{2.3}$$

which is a factor $\sim(\nu_b/\nu_{\rm min})^{2\alpha-1}$ larger than the radiated power, where $\nu_{\rm min}$ is the lower cutoff assumed in computing the equipartition pressure. If the jet is inhomogeneous or variable (as, for example, in the knots of M87) then the relevant dynamical time may be substantially less than r/v_j.

Many particle acceleration schemes have been proposed. In most of them the energy is drawn from large-scale motions using hydromagnetic or magnetosonic waves. We know most about the operation of these mechanisms from detailed observations of various locations within the solar system (e.g., solar flares, interplanetary shocks, planetary bow shocks, the terrestrial magnetotail). In general, provided the motion is "sufficiently violent," the acceleration efficiency is large, typically exceeding a few percent, and in one instance is argued to exceed $\sim 50\%$ (Eichler, 1981). These mechanisms also appear to be capable of accelerating particles up to energies where finite Larmor radius effects become important. For example, protons are accelerated up to energies ~ 20 MeV at the Earth's bow shock, where their Larmor radii are as large as the radius of curvature of the shock front. Similar comments can be made, with less confidence, about particle acceleration in supernova remnants in the interstellar medium, where the field strengths are similar but the scale is up to 9 orders of magnitude larger (reviewed in Blandford, 1981). Cosmic-ray protons with energies up to $\sim 10^{16}$ eV are probably accelerated in the interstellar medium. The disparity between Larmor radii and scale lengths is much stronger in extragalactic radio sources. Here the scale lengths are typically 10^{11} times the Larmor radius of a GeV particle. Relativistic electrons that radiate synchrotron radiation in the optical band have energies $\sim 10^4$ GeV, and where x-ray emission is observed, an even larger energy is implied. It should be possible to accelerate electrons to these energies provided only that the acceleration rate exceeds the radiative loss rate. As optically emitting electrons generally cool far more quickly than they escape from a region, this requires either that the acceleration time be a decreasing function of increasing energy or that the acceleration be localized in small regions within the emitting volume.

There is another important contrast to be drawn with the interplanetary and interstellar media. In these environments most of the energy goes into the nucleonic component. The energy density of cosmic-ray protons is a factor $k \gtrsim 30$ times the electronic component. If such a ratio were universal, then the equipartition pressures must be increased by a factor $k^{4/7}$, which exacerbates the confinement problem. However, there are also environments (e.g., the Crab nebula; Woltjer, 1972; the knots of Cassiopeia A; Bell, 1977) where we know that $k \lesssim 1$. Clearly, mechanisms that accelerate electrons with high efficiency are more suitable for extragalactic radio sources than those that preferentially accelerate protons.

Second-order Fermi acceleration has been invoked by several authors as a plausible particle acceleration mechanism (e.g., Pacholczyk and Scott, 1976; Christiansen, Pacholczyk, and Scott, 1976; Christiansen, Rolison, and Scott, 1979). In a Fermi process, the accelerating electron bounces continually off randomly moving clouds, magnetic inhomogeneities, or waves of speed v, possibly generated by large-scale instability. For a relativistic electron, each bounce gives an energy change, $|\Delta\gamma/\gamma| \sim v/c$. Energy increase is favored over decrease by a fractional amount v/c. Hence the acceleration time t_a is related to the collision time t_c by $t_a \sim \gamma/\dot{\gamma} \sim (c/v)^2 t_c$. The energy of an individual electron thus increases exponentially with time. Power-law distribution functions are then generated by combining this acceleration law with an energy-independent escape probability from the acceleration region. The resulting spectral index is a sensitive function of the ratio of the acceleration and escape time scales. In an expanding flow, adiabatic loss will further influence the spectrum. It would be surprising if as narrow a range of spectral indices as is observed could be produced in this manner. Furthermore, what empirical evidence we have of particle transport indicates that it is generally energy dependent.

This mechanism can be made more attractive if it operates in a flow process (e.g., Burn, 1976; Blandford and Rees, 1974; Achterberg, 1979). In this case, Fermi acceleration may be constrained to produce a power-law distribution of relativistic electrons. If the particles are injected at some fixed energy, and all the energy associated with the accelerating disturbances eventually is channeled into the particles, then the spectral index is fixed by the ratio of the turbulent energy density to the initial particle energy density.

First-order Fermi acceleration is more efficient than second-order acceleration and can occur at a strong shock front (Krimsky, 1977; Axford, Leer, and Skadron, 1977; Bell, 1978; Blandford and Ostriker, 1978; Eichler, 1979). These shocks probably occur in the hot spots at the ends of a jet, but may also be produced as a result of time dependence or inhomogeneity in the jet (see Sec. II.C.8). In this process particles are scattered in pitch angle by resonant Alfvén waves on either side of the shock front. If the shock speed is v, then a relativistic electron will cross the shock $\sim c/v$ times; each time it does so, it will gain energy (from the frame change) by an amount $\Delta\gamma/\gamma \sim v/c$. The net mean fractional energy gain is then of order unity. A simple calculation shows that low-energy incident electrons are transmitted as a power-law distribution, the slope of which is dictated by the shock compression r. In fact, $N_\gamma \propto \gamma^{-(r+2)/(r-1)}$. For a nonrelativistic, adiabatic strong shock, the compression satisfies $3 \lesssim r \lesssim 4$, and the exponent lies in the range 2—2.5, consistent with observations. Of course, this acceleration scheme could be far more complex than the simple linear theory described here (see Blandford, 1979; Axford, 1981). The structure of high-Mach-number shocks is not well understood, and it may be that there is in general no thin region through which the background flow is rapidly decelerated. Instead, the post-shock region might be strongly turbulent (e.g., Hughes and Allen, 1981; De Young, 1980) and most of the acceleration might occur well downstream of the shock transition. Furthermore, if the acceleration efficiency, which is controlled by the particle injection rate, is very high, then the cosmic-ray pressure itself is important in determining the shock structure and the jump conditions, and may also increase the speed of propagation of the scattering waves, thus impairing the acceleration efficiency.

Extended jets are unlikely to be permeated by high-Mach-number shocks; otherwise they would be disrupted. It seems far more probable that the ongoing particle acceleration be attributed to a continuous spectrum of weaker waves. Supersonic jets will be quite noisy and subject to small-scale Kelvin-Helmholtz instabilities. This will generate long-wavelength ($\lambda \gtrsim 1$ kpc) waves which can cascade down to shorter wavelengths and interact directly with the electrons (Bicknell and Melrose, 1982; Henriksen, Bridle, and Chan, 1982).

In a magnetoactive plasma there are three types of low-frequency mode: Alfvén waves and fast and slow magnetosonic waves. In the linear approximation, Alfvén waves are noncompressive and travel with a speed $a\cos\xi$ where a is the Alfvén speed $\sim 1000(B/10^{-5}\ \mathrm{G})(\rho/10^{-27}\ \mathrm{g\,cm^{-3}})^{-1/2}\ \mathrm{km\,s^{-1}}$ and ξ is the angle between $\mathbf{k}$ and $\mathbf{B}$. If the Alfvén speed exceeds the sound speed (a "low-beta" plasma) then the fast mode is compressive and travels with a speed $\sim a$; the slow mode is similar to a sound wave but will probably be strongly Landau damped by the background plasma under these conditions. In the absence of wave-particle interaction it is generally argued that an "inertial" range turbulence spectrum will be established through local three-wave coalescence processes. The appropriate spectrum is $(\delta B/B)^2 \propto k^{-1.5}$ (Kraichnan, 1965; Cesarsky, 1980) where $\delta B^2/4\pi$ is to be interpreted as the wave energy density within an octave of k. [A different approach has been followed by Eilek (1979), who has argued that waves are created at all k at a rate proportional to the relevant fluid instability growth rate.]

There are two relevant wave-particle interactions (Melrose, 1980; Kulsrud and Ferrari, 1971; Lacombe, 1976,1977,1979; Eilek, 1979; Achterberg, 1979; Benford, Ferrari, and Trussoni, 1980; Fedorenko, 1980; Bicknell and Henriksen, 1980; Eilek and Henriksen, 1984). Alfvén waves couple to relativistic electrons through the cyclotron resonance $\Omega_g = \omega - k_{||}v_{||} = k_{||}v_{||}$, where the subscript $\{||\}$ refers to the component resolved parallel to the magnetic field and Ω_g is the electron's (relativistic) gyrofrequency. The resonant waves have wavelengths comparable with the electron's Larmor radius, typically 10^{-9} times the wavelength at which it is postulated that the turbulence be generated. As Alfvén waves exist only below the ion gyrofrequency, there is a threshold energy $\sim m_p ac$ for relativistic electrons below which resonant Alfvén wave interaction cannot occur. An auxiliary acceleration mechanism must be invoked to inject relativistic electrons at this energy. Henriksen, Bridle, and Chan (1982) (and Eilek and Henriksen, 1984) propose that Alfvén waves be radiated by turbulent eddies in the Kolmogorov spectrum. Their periods will be comparable with the turnover time of the associated fluid eddy. They argue that monopole emission is appropriate and that the emitted power therefore scales as $P_k \propto k^{-3/2}$. This will produce an electron spectrum $N_E \propto E^{-5/2}$ if the electron acceleration is balanced by radiative losses.

As Alfvén waves have a momentum-to-energy ratio of v_A^{-1}, much larger than that of relativistic particles, they are far more efficient at pitch angle scattering than increasing the particle energy. For this reason, Henriksen and collaborators have advocated Fermi acceleration by longer-wavelength magnetosonic modes through the Landau resonance $\omega = k_{||}v_{||}$. (It is also necessary, in order that this type of Fermi acceleration operate, to invoke a level of Alfvén turbulence that will give the electrons a scattering mean free path somewhat longer than the wavelength of the accelerating waves.) Above threshold, the acceleration time is given roughly by $(\delta B/B)^{-2}\omega^{-1}$, independent of particle energy. Magnetosonic waves are also subject to competitive decay processes, especially Landau damping (both linear and nonlinear) on the background medium. Nevertheless, granted certain restrictions on the physical conditions within the source, this form of acceleration can be very efficient, with a large fraction of the turbulence energy ending up in the particles. One possible observational difficulty, however, is that if the turbulence is generated at the walls of the jet, then limb brightening should be seen. There is little evidence for this as yet, except possibly within hot spots (Eilek, 1982). However, the wave turbulence may lead to enhanced cross-field diffusion (Benford, Ferrari, and Trussoni, 1980).

There is a clear need also for *in situ* acceleration within the extended lobes and tails of some radio sources (e.g., Vallée and Wilson, 1976; Scott, 1977b; Jenkins and Scheuer, 1976; Burns, Owen, and Rudnick, 1978; Jaffe, 1980; Strom *et al.*, 1981; Simon, 1979; Andernach, 1982), unless relativistic electrons are able to propagate within these regions at super-Alfvénic and, in some cases, supersonic speeds (cf. Holman, Ionson, and Scott, 1979; Achterberg, 1980). These regions are probably high-beta plasmas in which the sound speed exceeds the Alfvén speed. Acceleration processes analogous to those described above have been proposed involving long-wavelength sound waves or weak shock waves. Moderate-amplitude waves excited by unsteady shear flows in the vicinity of the jet, the hot spot and the contact discontinuity separating shocked jet fluid from the shocked IGM, may propagate in to the lobes and be damped there, provided that the wave crossing time is sufficiently short compared with the cooling time of the electrons (see Hughes, 1980). If the effective mean free path of the particles in the background medium is short compared with the wavelength, the waves can be viewed as being damped by thermal conduction. However, if relativistic electrons have sufficiently long mean free paths, then they can absorb more of the wave energy than the thermal background can (Blandford, 1979). Weak shock waves can also preferentially heat relativistic electrons because the entropy gain by the first-order Fermi process is second order in the velocity amplitudes rather than third order as is the case for the background plasma.

Quite different types of acceleration process occur in the vicinity of neutral points. Most of our understanding of this comes from studies of the Earth's magnetotail (e.g., Krimigis, 1979). If the reconnection occurs rapidly, as in an explosive tearing mode instability, then large potential differences can be induced in the vicinity of the

neutral line by the rapidly changing magnetic field. We have argued that in the magnetized flow of jets, magnetic loops must be continually reconnecting, and provided that a significant fraction of the reduction in the magnetic energy is channeled into relativistic electrons by this process, this is also an attractive acceleration mechanism within extended jets. Again because of the large scales involved there is no problem of principle in accelerating particles to large energies. As an example, with a velocity gradient of 1000 km s^{-1} across 3 kpc and a field strength $\simeq 10^{-5}$ G (values appropriate to extended jets), potential differences $\simeq 10(l/\mathrm{kpc})^2$ GV are maintained across regions of size l. For comparison, the maximal potential drop across the terrestrial magnetosphere is only ~ 100 kV, and here particles with energies in excess of 1 MeV are regularly accelerated in substorms. Neutral points may also be sources of intense Langmuir turbulence which may provide an effective method of injecting relativistic electrons (Smith, 1976,1977).

So far, we have implicitly confined our attention to the acceleration of a power-law distribution of relativistic electrons. There is little evidence that power laws are required in compact sources, and indeed Cioffi and Jones (1980), Jones and Hardee (1979), Jones and O'Dell (1977a), and Wardle (1977) have considered the spectral implications of relativistic quasi-Maxwellian distribution functions. Such distributions may be generated with temperatures in the necessary $\simeq 10^{11}$–10^{12} K range if the particles are roughly thermalized behind a relativistic blast wave (Blandford and McKee, 1977; Jones and Tobin, 1977). There is, however, no reason to expect a precise Maxwellian, since true two-particle interactions are too slow to be competitive with electron cooling.

As we have remarked above, the mean surface brightness of observed extended radio jets decays with distance fairly slowly. Typically, $I_\nu \propto \nu^{-0.6} r^{-1.4}$; this is evidence for ongoing particle acceleration within jets (see Sec. II.C.6). Because of the inferior dynamic range of VLBI we know less about the brightness distributions in the small-scale jets associated with compact radio sources. These usually contain flat-spectrum, unresolved cores, and it has been proposed that they comprise a continuous superposition of self-absorbed, steep-spectrum sources (e.g., Condon and Dressel, 1973; de Bruyn 1976; Marscher, 1977; Cook and Spangler, 1980). There is no direct evidence that these cores are themselves jetlike, but if they are, the observed flux can be computed as a function of frequency (see Appendix A). For a uniformly expanding jet with $B \propto r^{-q}$, and assuming equipartition, $S_\nu \propto \nu^{[17(1-q)]/2(1-4q)}$ (Blandford and Königl, 1979b; Reynolds and McKee, 1980). For q in the range 0.8–1.0, as indicated by observations of extended jets, the spectral index α lies in the range 0–0.7, and it is possible to reproduce the observed spectral slope. If the jet speed is relativistic and constant, then the slope is unchanged, although for a jet of given size the flux is boosted and the brightness temperature can exceed the inverse Compton limit of $\sim 10^{12}$ K. Clearly an even richer variety of spectral behavior can be reproduced by allowing the jet width, the velocity, and the electron distribution function to vary independently. The optical, x-ray, and γ-ray fluxes produced by synchrotron and inverse Compton emission from a relativistic jet have been computed by Königl (1981), taking into account radiative losses. In flow models of compact radio sources, the observed spectrum should steepen at a frequency at which the radiative cooling time equals the outflow time. Typically, this lies in the millimeter or far-infrared part of the spectrum for "hot spots." In cocoons, or extended regions of lower surface brightness, the break moves down into the radio band.

8. Inhomogeneities

Although some jets have relatively smooth surface brightness variation, the majority show localized patches of relatively high intensity (hot spots, knots) along their lengths. Many jets also show a distinct suppression of radio emission in the innermost parts close to the nucleus, termed gaps.

Some knots (e.g., in M87) are of such high relative brightness that they are probably out of pressure equilibrium with the rest of the jet. Rees (1978a) identified the knots in M87 as internal shocks which develop from irregularities in the flow speed of the jet. If the velocity at the source varies by a fractional amount $\Delta v_j/v_j \gtrsim M_j^{-1}\gamma_j^{-2}$ on a time scale Δt, then the faster material will catch up with the slower material in a time $\sim v_j \Delta t/\Delta v_j$, and a strong shock traveling with speed v_j will form. The fraction of the jet kinetic energy dissipated in the shock is $\sim \gamma_j^2(\Delta v_j/v_j)^2$. The optical emission from the knots of M87 appears to be synchrotron radiation (e.g., Schmidt, Peterson, and Beaver, 1978), and the equipartition pressure is $\simeq 10^{-7}$ dyn cm^{-2}. The emitting electrons must be accelerated *in situ,* presumably at the shock front (see Sec. II.C.7), and can cool behind the shock, thus reducing the transverse expansion. If the M87 jet is mildly relativistic, "Doppler favoritism" (see Sec. II.A.4, Appendix C) can account for the fact that knots are seen only on one side. The necessary time scale $\Delta t \simeq 10^2$–10^3 yr might be related to the time between ingesting stars at the source of the jet (see Sec. III.C.1).

Internal shocks generated either as a consequence of fluctuations at the source or arising from the development of large-amplitude instabilities provide an attractive explanation of inhomogeneities in other jets, in particular the superluminally expanding features in some bright compact radio sources. A shock in an ultrarelativistic jet will move with a Lorentz factor of up to $\sim \gamma_j$, and the emitting material behind the shock will be subject to a large Doppler boost.

An alternative explanation for knots is that they represent obstacles (e.g., H I clouds) that have entered the jet (e.g., Blandford and Königl, 1979a). These clouds can be accelerated by the jet; under certain conditions they can attain the velocity of the jet itself, which again can be

relativistic. They will be followed by a strong shock, the site of nonthermal emission. Polarization properties of knots in relativistic motion have been considered by Blandford and Königl (1979b) and Bjornsson (1982). This is probably the explanation of the knots observed in Coma A (3C277.3), where both nonthermal and photoionized emission line optical radiation have been seen (Miley *et al.*, 1981). The knots have a low velocity of 200—300 $\mathrm{km\,s^{-1}}$, characteristic of galactic motion, and therefore must be sufficiently massive not to have been accelerated by the jet. The radio emission from accelerating clouds should show the steepest brightness gradient on the side closest to the nucleus, opposite to what is observed in 3C147 (Readhead and Wilkinson, 1980). This may be complicated, however, by the effects of Rayleigh-Taylor and Kelvin-Helmholtz instability (Blake, 1972).

One feature of the knots which is explained by neither of these models is the reported periodicity in the distribution of knots in some sources. Early reports of this effect in NGC 1265 have not been confirmed (Owen, Burns, and Rudnick, 1978), but the knots in M87, for example, show a fairly regular spacing (Laing, 1980a). This is consistent with the development of a Kelvin-Helmholtz instability (Stewart, 1971; Hardee, 1979), with the spacing determined by the fastest-growing mode. Apparent helical structure in the intensity and the magnetic field direction (Owen and Hardee, 1980; Laing, 1980a) is consistent with an $m=1$ (kink) rather than an $m=0$ (pinch) mode.

A variation on this idea is suggested by recent numerical simulations by Norman *et al.* (1982) and Norman, Winkler, and Smarr (1983), who follow (in two dimensions) the propagation of an axisymmetric jet into a quiescent medium. They find that under certain conditions the backflow in the cocoon becomes supersonic, and that Kelvin-Helmholtz instabilities in the cocoon can therefore drive strong shocks into the jet. It appears that the large pressure enhancements which occur in the simulations require strong focusing towards the jet axis, and therefore it is uncertain whether the effect will be as dramatic when the calculation is repeated in three dimensions. The pressure peaks (interspersed with deep rarefactions) are approximately periodic, and die out some distance upstream from the head of the jet.

Other possible causes of inhomogeneity include the generation of sound waves in the jet as a result of propagation through a rapidly changing pressure gradient (Königl, 1980; see Sec. II.C.3), projection effects in precessing jets (Icke, 1981; Linfield, 1981b), and Kelvin-Helmholtz instability of a nozzle (Norman *et al.*, 1981; Sec. III.D.1).

Gaps may reflect changing external conditions, and as such figure prominently in models by Chan and Henriksen (1980), who associate the onset of emission with the throat of a multikiloparsec-scale nozzle (see Sec. III.D.1). Alternatively, they may reflect the dissipation properties of the jet. In the phenomenological α^* model of Begelman (1982; see Sec. II.C.6), strong dissipation sets in only after the jet has been collimated to a cone angle $\theta\sim\alpha^*$ by the processes described in Secs. II.C.1—II.C.4.

D. Curved jets

1. Pressure bending

Many jets, particularly those of low power, show curvature. Prominent among these are the radio trails, also called head-tail sources (Miley *et al.*, 1972; Riley, 1973; Wellington, Miley, and van der Laan, 1973; Owen, Burns, and Rudnick, 1978; Rudnick and Burns, 1981; see Fig. 6). In high-resolution maps of these sources, jets can clearly be seen emerging from an unresolved nucleus and being bent through a large angle to feed a tail that extends for up to 1 Mpc behind the galaxy. In 3C129, the jet bends through more than a right angle without breaking up. There is also evidence for precession in the jets of 3C129, superposed on the trail (Rudnick and Burns, 1981; Icke, 1981; Sec. II.D.3). The generally accepted interpretation of these sources is that they are double sources which have been distorted by ram pressure due to the motion of the associated elliptical galaxy through a dense, intracluster medium. Indeed, clusters (or x-ray evidence of intracluster gas) have been found to be associated with most of the known radio trails. In the context of the jet model, this requires that continuous streams of gas be deflected through large angles by the intergalactic medium (see Jaffe and Perola, 1973). (The apparent continuity in the jet features makes it hard to reconcile the observations with models in which a sequence of "plasmoids" are ejected by the galactic nucleus into the intergalactic medium.) Further bending of the oldest, faintest parts of the tails, often over hundreds of kiloparsecs, may be due to buoyancy in the intracluster gas (Cowie and McKee, 1975; Harris, 1982).

If it is assumed that over most of their length, the jets remain in pressure balance with ram pressure $\rho_e v_g^2$ (where v_g is the galaxy velocity) of the intergalactic medium, then it is easy to obtain an estimate for the Mach number in the jet $M_j\sim(R/h)^{1/2}$ where R is the radius of curvature of the bend and h the transverse "scale height" in the jet. The external density ρ_e can be estimated using observations of cluster x-ray emission, and v_g from the cluster velocity dispersion and direct measurements of the radial velocity. For NGC 1265 the estimate for the ram pressure is $\simeq 5\times 10^{-11}$ $\mathrm{dyn\,cm^{-2}}$, which is similar to the equipartition pressure in the narrowest part of the jet. This implies that the radio-emitting part of the jet does not depart significantly from equipartition, and that there is not a much larger pressure in the thermal gas than in the relativistic particles. It also implies that the emission cannot be confined to a thin ribbonlike surface on the windward side of the jet (Begelman, Rees, and Blandford, 1979). The jet velocity is probably nonrelativistic, otherwise we would see substantial brightness variation along the length of the jet as its orientation with respect to the observer changes. The velocity can, in principle, be estimated with the aid of polarization observations, via measurements of p_j. However, such observations are not yet available.

In an alternative dynamical model (Jones and Owen, 1979), the jet is assumed to be roughly trans-sonic and bent by a thermal pressure gradient in the galaxy's interstellar medium; the same pressure gradient, it is argued, is driving a wind of hot gas out of the galaxy. (There is no nonradial pressure gradient in the absence of this wind because the gas would then be in hydrostatic equilibrium with respect to the galaxy, which is itself in free fall in the cluster.)

In an axisymmetric variant on this idea, Eichler (1982) has proposed that jets are focused by pressure bending to form the surprisingly compact hot spots seen in some sources. Outflowing gas from a central source is presumed to pass through a strong radiative shock whose distance from the source increases with latitude. The post-shock flow is parallel to the shock front, whose surface is fixed by balancing the ram pressure and centrifugal pressure of the shocked gas by the external gas pressure. It may be hard to produce this collimation in practice (cf. Sanders, 1983).

The most surprising feature of radio trails is the apparent stability of the jets whilst being bent through $\sim 90°$. This may support models with supersonic rather than trans-sonic flow (see Sec. II.C.5). Probably the best hope of further enlightenment rests with laboratory studies of high-Mach-number jets in cross flows.

Wide-angle tails appear to be morphologically intermediate between weak, two-sided straight sources and trails (Fig. 7). However, unlike radio trails, most wide-angle tail sources are associated with massive cD galaxies, which presumably do not have the high velocity with respect to the intracluster medium necessary to do the bending (Burns, 1981). A variety of mechanisms for bending these sources have been proposed (Burns, Eilek, and Owen, 1982), but it is not yet clear which, if any, is correct.

Bends are also a feature of compact radio sources. Readhead *et al.* (1979) have presented maps showing a systematic rotation of the jet's orientation as the angular scale increases, often tending to align with larger-scale radio structure. This bending may be caused by a pressure gradient, provided the flow is not highly supersonic (Smith and Norman, 1981; Allan, 1984). Inversion-symmetric sources like 3C293 may be produced when the jets are created at an angle to the major axis of an ellipsoidal gas distribution (Henriksen, Vallée, and Bridle, 1981).

It is possible that beams produced deep in a galactic nucleus could be destroyed by instabilities and then recollimated on a larger scale. In this case the orientation of the larger-scale beams would reflect the overall shape of the galaxy rather than its nucleus; characteristic differences between the radio morphologies of spirals and ellipticals could be a consequence of the different gaseous environments in these systems, the gas in the ellipticals having a larger scale height but less angular momentum than that in spirals (Sparke and Shu, 1980).

There is no direct evidence that collimation of large-scale jets is produced on the subparsec scale. A jet flow may, in principle, pass through a second nozzle located at a distance ~ 100 pc—3 kpc from the nucleus (Blandford and Rees, 1974; Chan and Henriksen, 1980), provided that the particles emerging from the nucleus have been randomized by passage through a strong shock (Smith *et al.*, 1981; Norman *et al.*, 1981). Recollimation occurs through a nozzle aligned with the minor axis of the ambient gas distribution. If the jet is reborn, then the alignment of a small- and a large-scale structure jet requires a coincidence between the angular momentum direction of the nucleus and the minor axis of the galaxy. In the majority of radio galaxies, the galaxy minor axes and the radio source axes of the large-scale structure are within 30° of each other (Bridle and Brandie, 1973; Guthrie, 1979; Palimaka *et al.*, 1979 and references therein; Shaver *et al.*, 1982). However, spectroscopic observations of five radio galaxies by Jenkins (1981) indicate that the radio source axes are unrelated to the galaxy rotation axes. If, as appears to be the case in most bright ellipticals, the observed flattening is not induced by rotation, but is rather an indication of the triaxiality of the galaxy's potential, then recollimation would still be expected to occur along the minor axis. However, it is not obvious that this minor axis would then be aligned with the spin axis of the central engine.

In order for a powerful radio jet to be recollimated on a kiloparsec scale, three conditions must be satisfied. First, the outflowing gas must not cool on the expansion time scale between the shock and the nozzle. This is generally easy to satisfy. Second, there must be a sufficient pressure drop, typically $\gtrsim 1000$ as calculated in Sec. II.C.1, between the nozzle and the observed jet, or magnetic collimation must be invoked. Third, the confining gas around the nozzle must not be so dense as to violate observational constraints on its mass, x-ray luminosity, and optical depth (Smith *et al.*, 1981).

2. Orbital motion

Many radio sources exhibit a high degree of reflection (*C*-type) symmetry (Harris, 1974). This symmetry is quite pronounced in at least eight sources that contain jet features. Prominent amongst these are 3C 31 and 3C 449 (Fig. 3). One explanation of this type of morphology is that we are looking at a subset of unstable jets that by chance appear mirror-symmetric. However, both 3C 31 and 3C 449, and indeed most of these sources, have close companions (Ekers, 1982; Shaver *et al.*, 1982; Rose, 1982). This suggests that the jet curvature results from acceleration of the parent galaxy by its companion (Jaffe and Perola, 1975; Blandford and Icke, 1978; Wirth, Smarr, and Gallagher, 1982). If this is the explanation, then the observation that the radius of curvature of the jet is comparable with the galaxy separation implies that the jet channel evolves at a speed that is comparable with the escape velocity from the binary, of order 300—500 km s^{-1}. If the density of the jet is comparable with or larger than that of the ambient medium, then the jet velocity itself

must lie in this range, and the jet, as well as its source, must be accelerated by the companion. However, a low-density jet may have a considerably larger velocity. [In an alternative scheme proposed by Vallée, Bridle, and Wilson (1981; cf. Valtonen and Byrd, 1980), for IC 708, the curvature of the jet is attributed to motion of the galaxy through an ambient medium (as in radio trails), rather than a "ballistic" effect. A jet speed of $\sim 10^4$ km s^{-1} is then possible.]

The shapes must be influenced by the interaction of the jet and the ambient medium. The ram pressure of the external gas can cause a curvature additional to that attributable to gravitational acceleration, which can be quite significant unless the Mach number is large. Furthermore, characterizing the orbit as simply Keplerian is probably an oversimplification because there are other galaxies in the field, and the interacting galaxies might be enveloped by a massive halo.

Such low jet speeds as ~ 300 km s^{-1} contrast strongly with the relativistic speeds proposed for more powerful sources (see Sec. II.A.4). They also are difficult to reconcile with the large total size of these sources unless the jet speed was much larger in the past. [Some increase in speed is possible if the orbital motion corresponds to a black hole orbiting the nucleus of the galaxy (Lupton and Gott, 1982).] We must await a careful analysis of a large sample of symmetric sources to see whether or not orbital motion is involved.

3. Precessional motion

Some extended sources display "inversion" (or 180° rotation) symmetry, also called *S*-type symmetry (Harris, 1974), which is suggestive of precession in the beams' orientation. Examples include the jets in NGC 326 (Ekers *et al.*, 1978) and 3C 315 (Willis *et al.*, 1981), the hot spots in the lobes of Cygnus A, and perhaps the spiral features in our galactic center (Lo and Claussen, 1983). It is possible to fit quite complex jets with simple kinematical models (e.g., Icke, 1981; Gower and Hutchings, 1982a,1982b; Gower *et al.*, 1982). Note that if the jet speed is relativistic, then distortions from strict inversion symmetry can be explained by light-travel-time effects. The source SS433, which has precessing jets, is perhaps a small-scale version of this phenomenon. Inversion symmetry in some radio galaxies may be a manifestation of complex nonaxisymmetric gas flow in the gravitational potential well of an elliptical galaxy, or the rotational dragging of material jets injected nearly in the disk plane of a spiral (e.g., NGC 4258; Van der Kruit, Oort, and Mathewson, 1972; Henriksen, Vallée, and Bridle, 1981; Oort, 1982). However, if the beams are collimated on a very small scale, near a massive black hole, changes in the hole's spin axis must be involved in the phenomenon.

One possibility is that a hole whose spin axis is misaligned with the angular momentum vector of infalling gas is gradually (on a time scale $\sim M/\dot{M}$) being swung into alignment (Rees, 1978b). However, in the case of NGC 326, the jets appear to have precessed rather than aligned. The only way a black hole could actually *precess* at a significant rate would be if it were orbited by another hole of comparable mass or by a disk of sufficient total angular momentum (Sarazin, Begelman, and Hatchett, 1980). Massive black hole binaries would form if two galaxies, each containing a black hole in its nucleus, were to merge. Mergers between galaxies appear to be frequent. cD galaxies in clusters and small groups were quite probably formed in this manner, and there is strong evidence that the nearby active galaxy Centaurus A is a merger product. If massive black holes are present in their nuclei—relics of earlier activity—then they will settle, under dynamical friction, in the core of a merged stellar system (Begelman, Blandford, and Rees, 1980; Roos, 1981). Many cD galaxies contain double or multiple cores that may have formed in this way. There are other scenarios for binary black hole formation. For instance, a rotating supermassive star may undergo bar-mode instability and fission into two components which both collapse (Begelman and Rees, 1978 and references therein).

Binaries involving black holes contract slowly and eventually coalesce. The longest-lived phases, in which such systems stand the biggest chance of being observed, correspond to separations such that r lies in the range 6×10^3–$2\times 10^5 r_g$ (corresponding to 10^{17}–3×10^{18} cm for masses $\sim 10^8 M_\odot$; see Appendix C). When the systems are more tightly bound than this, gravitational radiation causes rapid coalescence; for separations exceeding this range, dynamical friction is efficient. For a given binary, the orbital period varies as $r^{3/2}$ and the precession period as $r^{5/2}$. "Wide" binaries with precession periods $\sim 10^8$ yr may be responsible for the inversion-symmetric features in large-scale jets and double sources; closer binaries, with orbital periods ~ 30 yr and precession periods $\sim 10^4$ yr, may produce bending and misalignment in VLBI jets through the kinematic consequences of precession. Precession on somewhat shorter time scales could account for the apparent superluminal motion of the knots in VLBI sources (Linfield, 1981b). Bending on small length scales and short time scales may alternatively be caused by dynamical instabilities or jitter in the accretion flow pattern.

Some precession effects—particularly those cases where the precession or misalignment is observed on a scale $\lesssim 1$ kpc—are probably due to binary black holes. Alternatively, some could be due to precession effects, tidal torques, etc., involving an entire galaxy which has a close binary companion (Wirth, Smarr, and Gallagher, 1982). (This would require a collimation scheme along the lines discussed by Sparke and Shu, 1980). Observationally, it appears that inversion symmetry is more often associated with the presence of one nearby companion than with a high local density of galaxies (Shaver *et al.*, 1982). In SS433, where precession is indubitably occurring, there is again an uncertainty as to whether the axis is tied to a relativistic object, or whether the relevant dynamics are Newtonian (e.g., Sarazin *et al.*, 1980; van den Heuvel, Ostriker, and Petterson, 1980).

III. PHYSICS OF GALACTIC NUCLEI

We believe that radio sources are powered by massive black holes residing in the nuclei of galaxies. In this section we review current theoretical ideas on how this is brought about.

A. Nuclear radio sources

1. Overview

Radio sources used to be subdivided into *compact* (size $\lesssim 3$ kpc at 5 GHz) sources, usually distant quasars with a flat radio spectrum and often variable, and *extended* (size $\gtrsim 3$ kpc at 5 GHz) sources which are usually nearby and double, with a steep spectrum. As we remarked in Sec. I.C, it has become apparent that the majority of the compact sources are surrounded by irregular, low-frequency halos (e.g., Wardle, 1978; Weiler and Johnston, 1980; Perley, Fomalont, and Johnston, 1980; Wardle, Bridle, and Kesteven, 1981) and that the extended sources straddle fainter cores identified with the nucleus of the associated galaxy or quasar (e.g., Peckham, 1973; Miley, 1980).

Our view of these nuclear radio sources has been greatly modified by recent VLBI observations (summarized by Readhead, 1980; Pauliny-Toth, 1981; Kellermann and Pauliny-Toth, 1981; Kellermann and Setti, 1984). It appears that many of the brighter nuclear radio source exhibit a one-sided core-jet structure. Furthermore, the radio jets in the nuclei of extended sources tend to be well aligned with large-scale structure such as outer jets and hot spots, whereas in the compact components misalignment by angles $\sim 20°$—$40°$ tends to be the rule. When both nuclear and outer jets are one sided, they are extended on the same side of the core. Apparent superluminal expansion has been detected within the nuclei of seven powerful compact sources (Cohen and Unwin, 1984), but has not yet been observed within the nuclei of extended sources; neither have further examples been found amongst other powerful sources (Readhead, Pearson, and Unwin, 1984). The regions of low-surface-brightness emission from compact sources are physically smaller than those from extended sources.

These conclusions must be regarded as tentative, based as they are on a heterogeneous sample. However, they do suggest a powerful unifying theory of extragalactic radio sources (Blandford and Rees, 1978a; Readhead, Cohen, Pearson, and Wilkinson, 1978; Scheuer and Readhead, 1979; Blandford and Königl, 1979b; Orr and Browne, 1982; and Sec. II). This is that the majority of extragalactic radio sources are fueled by twin relativistic jets that emerge from the environs of a compact spinning object. These jets span a wide range of intrinsic powers. Jets that are pointed toward us are Doppler brightened and comprise the majority of the compact sources. Jets that are not aligned close to our line of sight comprise the extended sources in which most of the flux comes from the isotropically emitting double components. In this model most jets are intrinsically curved to some degree but the bending is exaggerated by projection effects in the compact sources. The halo emission associated with compact sources comes from a low-luminosity double component seen along the symmetry axis. Finally, superluminal expansion is caused by relative motion between the stationary optically thick regions in the innermost parts of the jet and inhomogeneities advected along with the outflowing material, both components being subject to strong Doppler boosting.

By contrast, until recently most phenomenological studies of nuclear radio sources have concentrated upon spherically symmetric models and might therefore appear to be inconsistent with the VLBI observations. However, we believe that they are still quite relevant for two reasons. First, we have as yet no direct evidence that the *cores* are not basically spherical, and second, the modifications required in going from a spherical to a jet geometry are often fairly minor. We therefore include them within our review.

2. Physical conditions

Radio emission from nuclear sources is generally attributed to the synchrotron process. There is scant direct evidence for this, although as we argue below it is broadly consistent with the observations of flux variability. In particular, the observed degrees of polarization in most sources are comparatively small ($\lesssim 10\%$) and are therefore not so strongly suggestive of the synchrotron mechanism as in the extended sources. The spectra of compact sources are generally bumpy although fairly flat on the average (i.e., $\alpha \sim 0$), in contrast to the smooth steeper spectra associated with extended components ($\alpha \sim 0.7$). Compact source spectra have generally been attributed to the superposition of several self-absorbed components whose individual flux densities rise with frequency up to a maximum flux and then fall at higher frequencies (e.g., Cotton *et al.*, 1980; Shaffer and Marscher, 1980). This means that most of the flux at a given frequency is coming from a region in which the optical depth is of order unity. As outlined in Appendix A, this assumption plus an estimate of the source's angular size (and therefore the brightness temperature T_b) enables us to derive a value for the magnetic field strength in this region. The energy of the emitting electrons is $\sim 3kT_b$, and B is proportional to $T_b^{-2}\nu$. VLBI maps are not yet available for the majority of compact sources, so we must rely on the flux variability to set a limit on the source angular size. If the source changes its flux significantly in a time $\sim t_{\rm var}$, then the light-travel-time constraint on causality suggests that the angular size should be less than $\sim 0.1 t_{\rm var}(1+z)/d_L$ mas, where d_L is the luminosity distance in Gpc (Appendix C Sec. 3). In this way, a lower bound can be set on the brightness temperature T_b, and thus an upper bound placed on B.

Now, there is a maximum possible brightness tempera-

ture for a radio source, insensitive to the frequency, that is set by the inverse Compton limit $T_b \lesssim 10^{12}$ K (see Appendix A Sec. 6 and Jones and Burbidge, 1973; Jones, O'Dell, and Stein, 1974a,1974b; Burbidge, Jones, and O'Dell, 1974 for detailed expressions). Brightness temperatures derived from variability exceed 10^{12} K by factors of up to 1000 for some of the stronger sources, particularly at low ($\sim$400 MHz) frequency (e.g., Hunstead, 1972; Condon *et al.*, 1979). A similar problem arises for the central components of some extended radio galaxies (Hine and Scheuer, 1980). Furthermore, the magnetic energy density inferred is well below the equipartition value, making it difficult for the source to be confined. These discrepancies can be removed if the source is expanding relativistically toward the observer (Rees, 1966,1967a). This is because the source's angular size can be increased over the variability size by a factor $\sim\gamma$, and the observed brightness temperature will be boosted over the temperature of the radiation in the comoving frame (Appendix C Sec. 1). The brightness temperature can be reduced from the value derived on the basis of variability by a factor $\sim\gamma^{-3}$. Thus a Lorentz factor $\gamma\sim 10$ for the bulk expansion velocity is adequate to meet the inverse Compton constraint when this is imposed in the comoving frame of the emitting plasma.

This essentially theoretical deduction is supported directly by observations of superluminal expansion and indirectly by the failure to detect Compton-scattered x rays in rapidly varying sources (e.g., Marscher and Broderick, 1982; Urry and Mushotzky, 1982; Marscher, 1983). The inferred magnetic field strength is highly sensitive to the assumed source size ($B\propto\theta^4$) and relativistic corrections. At this stage it is only possible to conclude that, in most powerful sources, the magnetic field strength ($B\approx 10^{-2}$ G) is roughly compatible with the equipartition value, and that the associated pressure is similar to that inferred within the roughly coextensive forbidden line region in quasars ($p\approx 10^{-6}$ dyn cm^{-2}).

Relativistic expansion is not the only means of avoiding the "inverse Compton catastrophe." The upper size limit based on the variability time may be relaxed in specially contrived geometries (e.g., Marscher, 1979). If the electrons are streaming outward along radial field lines with small pitch angles (O'Dell and Sartori, 1970; Epstein, 1973; Cocke, Giampapa, and Pacholczyk, 1979), then the inverse Compton scattering rate is reduced relative to the synchrotron emission rate (e.g., Woltjer, 1966; Sanders, 1974; Milgrom and Bahcall, 1978). However, in an expanding field the synchrotron emissivity $\propto B^2P_\perp^2\propto B^3$ (where $P_\perp$ is electron momentum resolved perpendicular to the field) falls dramatically with increasing radius r, and so most of the emission comes from a narrow range of radii.

With the confirmation of low-frequency variability, several authors have explored alternative emission processes to synchrotron radiation. Ripple radiation (essentially inverse Compton scattering of hydromagnetic waves) has been discussed by Cocke, Pacholczyk, and Hopf (1978). The possibility of coherent radio emission certainly cannot be ruled out. If the primary power source had dimensions comparable with the gravitational radius r_g of a massive black hole, it might possess field strengths as high as $\sim 10^4$ G (see Sec. III.D.5); the gyrofrequency can then be in the GHz band. Conditions may be similar to those found in the magnetospheres of radio pulsars. Thus coherent cyclotron-maser emission cannot be excluded.

But if the radiation were produced deep in the quasar core, it would be vulnerable to absorption (the inverse of incoherent emission) at larger radii. Moreover, the brightness temperature T_b would be so high that induced scattering [which swamps spontaneous scattering by a factor $(kT/m_ec^2)\times$ solid angle factors; Appendix A Sec. 6] could quench the radiation unless there were directions along which $\tau_{es}\ll 1$ or the electrons were all flowing out with high Lorentz factors, in which case relativistic corrections reduce the scattering. Thus, if the sub-GHz variations involve coherence, it is likely to be a mild degree of coherence within a region comparable in size to the radio components already resolved by VLBI, rather than pulsar-type emission from the central core. Drawing an analogy with pulsar models, Cocke and Pacholczyk (1975), Benford (1977), Cocke, Giampapa, and Pacholczyk (1979), and Kirk (1980), have suggested that bunches of electrons streaming out along curved field lines could radiate by the coherent curvature process. This proposal is not without difficulties. If the field lines have a radius of curvature $R\sim 10^{17}$ cm, then in order to radiate at a frequency $\nu\sim 300$ MHz, the bulk Lorentz factor must be $\gamma\sim(\nu R/c)^{1/3}\sim 10^5$. For high radiative efficiency, the number of particles in the bunch must approach $(c/\nu r_e)\sim 3\times 10^{14}$ (where $r_e=2.8\times 10^{-13}$ cm is the classical electron radius), all contained within a cubic wavelength (e.g., Jackson, 1977). The field would have to be greater than $\sim 10^5$ G, stronger than generally expected, in order to channel the outflowing bunches. A further difficulty is the absence of strong polarization in the observed radio emission.

A quite different explanation for low-frequency variability has been advanced by Rickett, Coles, and Bourgois (1984). They point out that refraction by large clouds moving in the interstellar medium can cause monthly variability of compact radio sources. Such an effect is commonly seen in pulsars. The extragalactic sources subtend too large an angular size to create a diffraction pattern and scintillate, like pulsars, in either the interstellar or the intergalactic media (Condon and Backer, 1975; Dennison and Condon, 1980). Interstellar refraction will not influence observations at frequencies $\gtrsim 5$ GHz, however, and does not greatly alter the angular sizes that are observed.

As we mentioned in Sec. II.A.3, internal Faraday rotation does not appear to be present in observed compact radio sources. This points to a lower density of nonrelativistic and mildly relativistic electrons within the emission region than of directly observed relativistic electrons (Jones and O'Dell, 1977a; Wardle, 1977). Again, this is compatible with the notion of relativistic expansion, as

the expansion will not be seriously impeded by the inertia of the thermal plasma and protons. For example, if, as indicated by the absence of Faraday rotation, most of the electrons have energies $\gtrsim 30$ MeV, then the sound speed in the plasma exceeds $\sim c/10$. [A still higher sound speed would be obtained if e^+-e^- pairs were present in addition to the electrons which neutralize the ions (Sec. III.D.6).]

Even in the absence of thermal plasma, the relativistic electrons can alter the polarization of the radiation as it propagates out of the source region (Sazanov, 1969; Zheleznyakov, 1969; Seaquist, 1972; Rosenberg, 1972; Pacholczyk, 1973; Pacholczyk and Swihart, 1970, 1971a,1971b,1973,1974,1975; Cheng and Fung, 1977a, 1977b; Jones and O'Dell, 1977b; Jones and O'Dell, 1978; Wilson, 1980; Hodge, 1982). The characteristic modes propagating through a relativistic plasma are elliptically polarized and differ from those that are emitted and absorbed by the synchrotron process. This means that in addition to Faraday rotation of the plane of linear polarization, which arises from the difference in phase velocities between these two modes, there will be a conversion of linear polarization into circular polarization. The degree of circular polarization in the radiation emerging from a self-absorbed source may be larger than that emitted directly by the relativistic electrons (cf. Appendix A Sec. 1; Sazanov, 1973a,1973b). In principle, circular polarization could be a powerful diagnostic of conditions within a radio source because it is predicted to change sign near the frequency at which the source becomes optically thin. Emission and propagation, as sources of circular polarization, could be distinguished from one another by the difference in the predicted frequency dependence of the degree of polarization ($\nu^{-1/2}$ and ν^{-1}, respectively). This is complicated, however, by strong indications that observed compact radio sources are spatially inhomogeneous. For example, they exhibit degrees of linear polarization typically of order 3%, much less than the maximum associated with the synchrotron emission ($\sim 70\%$), a fact which strongly supports inhomogeneity (Melrose, 1971a,1971b; Ryle and Brodie, 1981). This means that we should be pessimistic about learning much of value in the near future from circular polarization measurements (which are themselves quite controversial, e.g., Ryle, Waggett, and O'Dell, 1975).

These arguments do not limit the density of thermal gas in the region surrounding the compact source, because the magnetic field strength might be lower here. The best constraints are obtained from requiring that the free-free optical depth be less than unity and that induced Compton scattering (Sunyaev, 1971; Levich and Sunyaev, 1970; Wilson, 1982) not seriously distort the radio spectrum (see Appendix A). For a typical source observed at $\nu \sim 1$ GHz and of size $\sim l$ pc, these conditions translate into

$$n_e \lesssim \min[2\times 10^3 (T/10^4\ \mathrm{K})^{3/2} l^{-1/2}, 3\times 10^3 l^{-1}]\ \mathrm{cm}^{-3}\ , \tag{3.1}$$

where T is the external temperature and we have assumed that the gas density is uniform.

3. Radio source models

The earliest model for variability of a compact radio source was an adiabatically expanding sphere of magnetized relativistic electrons (Shklovsky, 1960; van der Laan, 1966; Kellermann and Pauliny-Toth, 1968). If the source radius R increases $\propto t$ and magnetic flux is conserved, then the optically thick flux density $S_\nu \propto \nu^{5/2} B^{-1/2} R^2$ increases $\propto t^3$ and the optically thin flux density $S_\nu \propto \nu^{-\alpha} B^{1+\alpha} R^{-2\alpha}$ decreases $\propto t^{-2(2\alpha+1)}$. The flux S_m and frequency ν_m at the maximum of the spectrum both decrease with time: $S_m \propto \nu_m^{(5+7a)/(5+4a)} \propto t^{(5+7a)/(5/2+a)}$. Despite some initial success (Kellermann and Pauliny-Toth, 1968), this model was found to be inconsistent with flux variations in the majority of sources that are regularly monitored (Altschuler and Wardle, 1977; Kellermann and Pauliny-Toth, 1981). Better agreement with the observations is obtained if the source is made inhomogeneous (Hirasawa and Tabara, 1970; Condon and Dressel, 1974; de Bruyn, 1976; Pacini and Salvati, 1974; Peterson and King, 1975; Marscher, 1977; Spangler, 1980; Pineault, 1984) and particles are continuously accelerated throughout the expansion (Simon, 1969; Shklovsky, 1971; Takaroda, 1970; Hirth, 1970; Kogure, 1971; De Young, 1971b; Walmsey, 1971; Peterson and Dent, 1973; Aller and Ledden, 1979). Jones and Hardee (1979) and Spangler (1980) considered models in which the electrons have a relativistic Maxwellian rather than power-law distribution function and also claimed improved agreement with the observations. It is perhaps not surprising that these models have sufficient freedom to fit flux variations from many sources.

However, as we have discussed, nonrelativistically expanding source models may encounter the inverse Compton problem, and this can be alleviated through relativistic expansion. The total flux observed from a relativistically expanding sphere has been calculated by Rees (1966,1967a), Rees and Simon (1968), van der Laan (1971), and Königl (1978). The observed appearance of the sphere depends sensitively on the assumed distribution of emissivity as a function of radius and the velocity field. Superluminal expansion can be observed only if the emission is confined to a thin shell or the expansion is collimated along one dimension (De Young, 1972; Kurilchik, 1972; Jones and Tobin, 1977; Vitello and Pacini, 1977,1978; Salvati, 1979). These models can be made dynamical by assuming that the expanding sphere is the bounding shock of a relativistic blast wave (Blandford and McKee, 1977; Shapiro, 1979a,1980). Relativistic particle acceleration and magnetic field amplification can be incorporated naturally into this type of model (see Sec. II.C.7).

These early models illustrated that rapid variability, as well as superluminal apparent transverse motions, can occur without violating the upper limit on the surface brightness temperature of incoherent synchrotron sources. However, the more recent VLBI evidence for jetlike structures in superluminal sources makes these models less relevant. Instead, attention has shifted towards calculat-

ing the spectrum and structural variability expected from jets. Blandford and Königl (1979b) and Königl (1980) calculated the synchrotron and Compton spectra from a steady relativistic jet, on the assumption that a power-law distribution of relativistic electrons is present, and that the magnetic field weakens as the jet moves out. The self-absorption turnover shifts to lower frequencies further out, and the net spectrum at low frequencies cuts off more gradually than $\propto \nu^{2.5}$.

The variations observed by VLBI show that the jets are not stationary. The outward-moving blobs of high surface brightness may be associated with shock fronts at which relativistic electrons can be freshly accelerated. This local acceleration is in any case necessary to overcome adiabatic losses in the expanding flow (see Secs. I.B.2, II.C.7, and II.C.8).

Various essentially kinematical models were previously proposed to account for superluminal flux variation and expansion. In an early forerunner of jet models, Ozernoi and Sazanov (1969) computed the radio flux to be expected from two expanding synchrotron-emitting spheres flying apart with relativistic speeds (cf. also Andrews, 1973; Seielstad, 1974; Ozernoi and Ulanovskii, 1974). Reynolds and McKee (1980) have applied some of these ideas to the radio source at the galactic center. Further suggestions (classified and discussed in the reviews of Blandford, McKee, and Rees, 1977, and Marscher and Scott, 1980) are due to Barnothy (1965), Morrison and Sartori (1968), Rees and Simon (1970), Cavaliere, Morrison, and Sartori (1971), Dent (1972), Blandford and Rees (1972), Sanders (1974), Cocke and Pacholczyk (1975), Richter (1976), Epstein and Geller (1977), Lynden-Bell (1977), Milgrom and Bahcall (1978), Marscher (1978a,1978b), Shapiro (1979a,1979b), Cohen *et al.* (1979), Segal (1979), Chitre and Narlikar (1979), Bahcall and Milgrom (1980), not to mention proposals invoking tachyonic motion and noncosmological redshifts. All of these models are in conflict with some existing observations, and we consider them no further.

B. Prime movers

The observations tell us that two characteristic properties of active galactic nuclei are (a) the production of nonthermal emission and (b) expulsion of energy in two oppositely directed beams. Nuclear activity manifests itself on many very different scales—up to several Mpc in the case of giant double sources. The simplest hypothesis, however, is that the central "prime mover" is qualitatively similar in all active nuclei. The primary energy may be reprocessed in different ways, depending on the details of the galactic (or extragalactic) environment.

It is still not proven that *all* quasars are located in galaxies, though this view is strongly supported by "continuity" arguments with lower-luminosity active nuclei. If we do accept this, it is natural to interpret all active nuclei in terms of some runaway process whereby gas and stars accumulate in the gravitational potential well at the center of a galaxy. Figure 15 (adapted from Rees, 1978c)

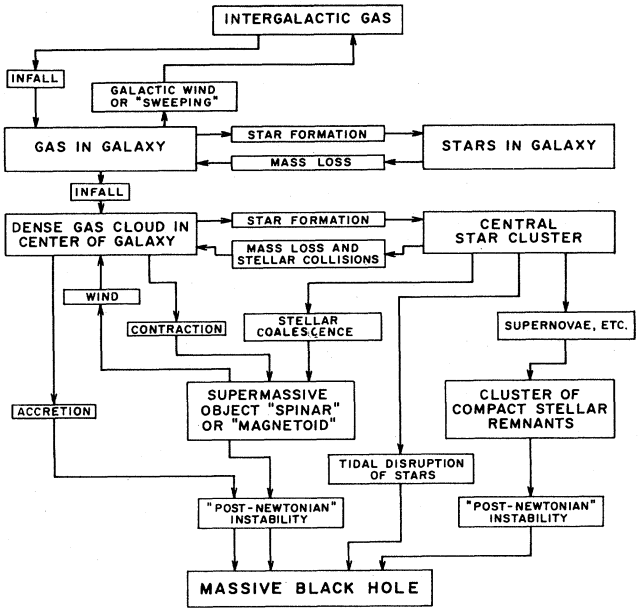

FIG. 15. Flow chart indicating the various processes whereby gas and stars may accumulate at the nucleus of a galaxy. The final result is likely to be the formation of a massive black hole, which may be the "prime mover" behind all types of active galactic phenomena (adapted from Rees, 1978c).

indicates schematically the various evolutionary pathways that may be involved in this type of runaway process. The important message of this diagram—the "bottom line"—is that the most likely end point of such a system will be the collapse of a large fraction of the mass involved to a massive black hole. Furthermore, as we discuss later, a black hole embedded in infalling matter offers a more efficient power source than any conceivable progenitor; it is our firm prejudice that quasars and strong radio galaxies are energized by mechanisms that involve black holes. The possible "precursor" phases may be observable, and perhaps can be associated with some classes of lower-level activity in galactic nuclei. For this reason—and in deference to the extensive earlier literature on "star cluster" or "supermassive star" models for quasars—we review all the options below.

1. Star clusters

Star densities in the nuclei of normal galaxies are known to be $\gtrsim 10^6$ pc^{-3}, and it has often been suggested that the power supply in active galaxies and quasars derives from a very dense stellar system. A cluster of $\sim 10^8$ *O* stars packed into a volume ~ 1 pc would satisfy the energetic (as well as compactness) requirements of some of the more luminous quasars, yet the integrated spectrum would hardly be quasarlike. In addition, since nuclear burning converts only $\sim 0.1\%$ of the mass into energy, the active phase of such an object would be rather short lived. To obtain higher efficiencies from a cluster

of ordinary stars, it is necessary to assume that the cluster is undergoing some kind of violent evolution, possibly involving star-star collisions and/or individual stellar explosions.

Such evolution is inevitable when the velocity dispersion of a cluster becomes sufficiently high. Clusters of low-velocity dispersion evolve toward higher specific binding energy through two-body gravitational encounters. However, when the velocity dispersion v_c exceeds the typical escape speed v_{esc} from a star (620 km s^{-1} for the sun), the cross section for physical collisions exceeds the mean cross section for gravitational scattering through 90°, and collisions begin to dominate the evolution. For a self-gravitating isothermal core containing $10^8 N_8$ main sequence stars within R_{pc} parsecs, this occurs when $R_{pc} \lesssim N_8$. General discussions of collisional evolution have been given by Peebles (1972) and Begelman and Rees (1978) (amongst others), while the details of star-star collisions have been discussed by Spitzer and Saslaw (1966), Colgate (1967), Sanders (1970), and Seidl and Cameron (1972). Star-star collisions are highly inelastic, and the outcome depends sensitively on the impact parameter and relative velocity $v_{rel} \sim \sqrt{2} v_c$ of the colliding stars. If v_{rel} exceeds v_{esc}, then the collision will be disruptive and liberate some fraction ζ of each star's mass. ζ has been estimated for off-center collisions (Spitzer and Saslaw, 1966) and computed more accurately for head-on collisions (Seidl and Cameron, 1972), and its ensemble average rises rapidly to $\sim O(1)$ with increasing v_{rel}. For smaller v_{rel}, the relative kinetic energy goes into heat, decreasing the internal binding energies of the stars involved but liberating little mass. In general, sufficient kinetic energy will be lost to cause the stars to coalesce (Colgate, 1967) or to cause the stars to become bound in a binary which rapidly decays due to tidal losses (Fabian, Pringle, and Rees, 1975).

Evolution of a star cluster in the coalescence regime was investigated by Colgate (1967) and Sanders (1970). As a typical star becomes increasingly massive through coalescence, its main sequence lifetime rapidly decreases. Sanders found that for clusters more massive than $10^8 M_\odot$, the time between successive collisions is longer than the main sequence lifetime of stars of mass ~ 10—$50 M_\odot$; hence these ultimately explode as supernovae. Sufficiently massive clusters passing through the "coalescence strip" of the density-velocity dispersion plane (Begelman and Rees, 1978) may therefore become transformed largely to clusters of compact objects—black holes and neutron stars—with up to $\sim 90\%$ of the total mass lost through the explosions. For clusters less massive than $\sim 10^8 M_\odot$, the collision time is shorter than the main sequence lifetimes of the coalesced stars, and Sanders concluded that the coalescence process can "run away" with the formation of a few supermassive stars. Colgate, however, argued that coalescence between massive stars and ordinary stars would saturate when the former reach 50—$100 M_\odot$, because they are then so diffuse that the latter pass straight through them without being captured. Unfortunately, the sensitivity of the coalescence process to details of the input physics has kept this controversy from being satisfactorily resolved.

Coalescing star clusters have been used in models of quasars and active galactic nuclei either as sources of energy directly through supernova explosions (Burbidge, 1961; Colgate, 1967) or as precursors to clusters of pulsars which provide the energy electromagnetically (Gunn and Ostriker, 1970; Arons, Kulsrud, and Ostriker, 1975; Kulsrud and Arons, 1975). In the former, the energy tapped is the kinetic energy of the supernova explosion, which is roughly 2 orders of magnitude larger than the energy output of the supernova's photosphere and may amount to more than 1% of the binding energy of a remnant neutron star. The remaining $\sim 99\%$ of the energy is released as neutrinos. In energy terms, supernovae are of comparable efficiency to nuclear burning. To turn this energy into heat and thence to radiation the ejecta must do work on a comparable mass of surrounding gas. The rate of supernovae explosions is governed by the coalescence rate, and is typically 5 to 10 a year. One drawback of such a model using ordinary supernovae is that the energy per explosion is at most a few times 10^{51} ergs, considerably smaller than the energy contained in the luminosity fluctuations of many quasars. To remedy this, Colgate and Petschek (1976) proposed that "hypernovae," releasing up to $\sim 10^{53}$ ergs in kinetic energy, could be triggered by the passage of neutron stars through the cores of massive stars (the result of multiple coalescences).

In the multiple pulsar model, the amount of energy made available through each explosion is comparable with that in the supernova model, but the energy contained in the rotation of the pulsars (up to $\sim \frac{1}{2}$) may be transformed into radiation in a considerably different fashion. Kulsrud and Arons (1975) and Arons, Kulsrud, and Ostriker (1975) proposed that the energy outputs of several pulsars could be stored in electromagnetic form in the nucleus of a quasar, until "dumped" into radiation as a result of nonlinear interactions between particles and the strong waves. This sudden dumping could occur in a light travel time across the region, resulting in luminosity fluctuations containing far more energy than could be supplied by a single pulsar or supernova explosion. Both the pulsar and supernova models share the flaw that they possess no intrinsic directionality which would naturally give rise to a jet. VLBI observations indicate that jetlike structure exists on scales as small as ~ 1 pc, which is in any event an upper limit to the cluster size consistent with variability time scales. If the pulsar or supernova model were correct, all collimation would have to occur in a rotationally flattened gas cloud bound to the cluster. While this cannot be ruled out for quasars, the lack of strong x-ray emission from the cores of some radio galaxies makes this unlikely for the latter objects (see Sec. III.D.1).

The net effect of the coalescent phase on the evolution of a cluster is far from certain. Coalescent star clusters should evolve toward higher binding energy per unit mass, even if most of the mass is lost through explosions (Begelman and Rees, 1978). When the cluster mass is $< 10^8 M_\odot$, so that the dynamical evolution time scale is

less than the stellar-evolution time scale (see Sanders, 1970), the cluster should pass through the "coalescence strip" and enter the disruptive regime well before all of its mass has been transformed into compact objects or lost through explosions.

The evolution of a star cluster in the disruptive regime has been discussed by Spitzer and Saslaw (1966), Spitzer and Stone (1967), Spitzer (1971), and Begelman and Rees (1978). At the outset of the regime, collisions liberate energy with a mass-to-energy conversion efficiency of only $(v_{\rm esc}/c)^2$ ($\sim 4\times 10^{-6}$ for the sun). The debris cools rapidly, but is prevented from falling to the center of the potential well by even a small amount of angular momentum. Spitzer and Saslaw (1966) concluded that the material would collect in a disk, the column density of which would steadily increase until it became vertically self-gravitating. They assumed that the debris would then fragment and form new stars, which could repeat the process of disruption at a somewhat higher binding energy. Spitzer and Stone (1967) realized that additional energy could be liberated if the gaseous debris formed a self-gravitating subsystem at the center of the cluster. Begelman and Rees (1978) carried the evolution further, and showed that star formation must cease when the density within a central region of radius r parsecs reaches $10^9 r^{-2/3} M_\odot$ pc^{-3}. At this point the stars lose their identities and a supermassive object forms which, in general, is expected to collapse to a black hole. Once the black hole forms, subsequent star-star collisions release gas which can power the source through accretion (see Sec. III.C.1). Before a black hole forms, only a fraction $\sim 3\times 10^{-4}\varepsilon^{13/9} N_8^{4/7}$ of the rest mass energy can have been converted into radiation, where ε^2 is the original rotational ellipticity of the core.

Because of the above limit on the recycling of stellar debris, it appears rather difficult to form self-gravitating star clusters with velocity dispersions much larger than a few times $v_{\rm esc}$. However, this is possible if part of the potential well is deepened by the presence of an additional mass, e.g., a preexisting central black hole. If a mass M is introduced on a time scale shorter than the evolution time of the cluster, then the cluster will develop a cusp of stars bound to the central mass with a density run $\propto r^{-7/4}$ for $GM/v_{\rm esc}^2 < r < GM/v_c^2$. For collision-dominated clusters, formation of a cusp steeper than $r^{-3/2}$ is hindered by the destructiveness of the encounters. The possibility of fueling quasars by tidally disrupting stars from a cluster surrounding a black hole is discussed in Sec. III.C.1.

The evolution of a star cluster may be altered considerably if the cluster is embedded in dense gas. Bisnovatyi-Kogan and Sunyaev (1972a,1972b) noted that the presence of stars would help to stabilize a supermassive gas cloud against the post-Newtonian stability (cf. Hoyle and Fowler, 1963a,1963b; Sec. III.B.2), but concluded that a tightly bound cluster of $\lesssim 10^9$ normal stars could not coexist with a comparable mass of gas: the ram pressure of stellar motions would generate a luminosity exceeding the Eddington limit (see Sec. III.C.2), which would drive the surplus gas away until the situation stabilized. For a cluster of black holes or nonmagnetized neutron stars, the luminosity generated by stellar motions is negligible by comparison, but accretion onto the individual compact objects (Weedman, 1983) could increase the total output by a factor $\sim 0.1(c/v_c)^2$. The mass in gas must generally exceed that in stars in order for the evolution to be affected. The only exception to this statement would be a cluster of *magnetized* compact objects (Begelman and Rees, 1978). In this case, the effective cross section for star-gas interaction may be increased over the geometric or gravitational cross section, because the ionized gas is unable to flow freely through the magnetosphere. The radius $r_{\rm mag}$ of the magnetosphere is obtained by balancing magnetic pressure at $r_{\rm mag}$ against the ram pressure $\sim \rho_{\rm gas} v_c^2$. Since the result depends on the magnetic moment of the compact object, the effect may be stronger for magnetized white dwarfs than for neutron stars, which typically have larger surface fields but smaller magnetic moments. Other star-gas interactions which have been discussed in the literature include ablation and evaporation of stellar material (Unno, 1971) and enhanced mass loss due to irradiation by an intense radiation field (Begelman and Rees, 1978; Edwards, 1980; Shull, 1983; Mathews, 1983).

2. Spinars and supermassive disks

In an alternative class of quasar models, massive uncollapsed spinning bodies are invoked to provide the power. When these bodies have not collapsed behind event horizons to form black holes, they are known as supermassive stars (e.g., Fowler, 1966), magnetoids (e.g., Ozernoi, cited in Ozernoi and Chertoprid, 1966), or spinars (e.g., Cavaliere, Morrison, and Pacini, 1970). A massive nonrotating gas mass should be supported primarily by radiation pressure and is expected to be in convective equilibrium. This means that the effective specific-heat ratio of the fluid $(\partial \ln p/\partial \ln \rho)_s$ is very close to $\frac{4}{3}$. From a Newtonian point of view, this in turn implies that such a supermassive star is only marginally stable, and when general relativistic corrections are incorporated it is found that the star is unstable unless its radius exceeds $\sim 10(GM/c^2)(p_{\rm rad}/p_{\rm gas})$ (e.g., Fowler, 1966; Weinberg, 1972). This in turn implies that the binding energy released by such a star is a very small fraction of the rest mass of the gas, and despite its initial promise (e.g., Hoyle and Fowler, 1963a,1963b) such an object does not constitute a credible quasar power source.

However, if a supermassive star is rotating, and it conserves angular momentum during its collapse, then it should slowly evolve into a supermassive rotating disk (e.g., Salpeter and Wagoner, 1971; Salpeter, 1971). The vertical support in such a disk must be due to radiation pressure, and the total luminosity will approach the Eddington value. Such a disk is unstable to local axisymmetric modes if it becomes thinner than ≈ 0.05 of its radius (Bardeen and Wagoner, 1971). A less stringent condition may be sufficient for instability to bar modes.

Fragmentation or other instability can be avoided if

sufficient internal viscous dissipation allows the disk to remain thick. Such "high-entropy" objects will slowly contract, radiating away their gravitational binding energy, and may ultimately be able to liberate a few percent of their rest mass (Ozernoi and Usov, 1973b).

Three important radiation channels have been considered. First, an object of $\sim 10^8 M_\odot$ must radiate $\sim 10^{46}$ ergs s^{-1} of ultraviolet radiation to ensure vertical pressure support. This means that spinars are extremely unlikely to power the majority of radio galaxies, from which such radiation is conspicuously absent. However, they are a quite plausible and perhaps necessary precursor to the black holes that we discuss below, and as such they may be found in the high-redshift quasars.

A second way that a spinar can liberate its binding energy is to develop a large-scale magnetic field and act as a giant pulsar (e.g., Morrison, 1969; Cavaliere, Pacini, and Setti, 1969; Flasar and Morrison, 1976), although it has been argued that this is not a strong analogy (Sturrock, 1971). (Evidence for periodicity in the light output of certain quasars, e.g., Morrison, 1969; Ozernoi and Chertoprid, 1966, which motivated this suggestion, is now discounted.) If there is an ordered field B, an angular velocity ω, and the size of the spinning object is R, then the magnetic dipole moment is $\sim BR^3$. General arguments (e.g., Goldreich, Pacini, and Rees, 1971) suggest that the nonthermal magnetic-dipole-like luminosity will be

$$L_{\rm em} \simeq \frac{B^2 R^6 \omega^4}{c^3} . \tag{3.2}$$

For illustrative purposes, set $\omega R \sim 0.1c$ and $R \sim 10^{15}$ cm. In this case, a field $B \sim 3\times 10^4$ G will suffice for the nonthermal luminosity to exceed the thermal luminosity, and the rotation period is ~ 1 yr. (The existence of a magnetic dipole moment as powerful as this is incompatible with differential rotation, and so spinars are argued to be uniformly rotating, e.g., Ozernoi and Usov, 1971.) The evolution of a magnetized spinar contrasts with that of a pulsar in that the luminosity increases with time until the spinar goes dynamically unstable and forms a black hole. Detailed evolutionary models of spinars have been presented by Ozernoi and Usov (1971), Woltjer (1971), Opher (1975), and Pacini and Salvati (1978). See also Sec. III.D.5 below.

The third channel is gravitational radiation, which will be emitted at twice the spin frequency if instability causes a spinar to depart from axisymmetry (e.g., by developing a bar mode or fragmenting). For a fractional difference ε in the two perpendicular moments of inertia, the quadrupole radiation rate is

$$L \sim \left[\frac{c^5}{G}\right]\varepsilon^2\left[\frac{GM}{Rc^2}\right]^5$$

$$\simeq 10^{59}\left[\frac{GM}{Rc^2}\right]^2\left[\frac{\omega R}{c}\right]^6\varepsilon^2 \text{ ergs s}^{-1} , \tag{3.3}$$

which may greatly exceed the magnetic dipole and thermal luminosities if strong asymmetry occurs. This is likely to be of particular importance in the final collapse to a black hole, when most of the binding energy will be released (see Smarr, 1978 for further discussion).

3. Black holes

The physics of dense star clusters and of supermassive objects is complex and poorly understood. In contrast, the final state of such a system—if indeed gravitational collapse occurs (see Fig. 15)—is comparatively simple, at least if we accept general relativity. According to the so-called "no hair" theorems, the end point of a gravitational collapse, however messy and asymmetric it may have been, is the formation of a black hole characterized by just two parameters—mass and spin—and described exactly by the Kerr metric. After a violent or sudden collapse, it takes several dynamical time scales for the black hole to settle down, during which gravitational waves are emitted. The final state is described by the Kerr solution, provided only that the material left behind outside the hole does not cause a strong perturbation. The characteristic size of a collapsed object is

$$r_g \equiv m = \frac{GM}{c^2} = 1.5\times 10^5 (M/M_\odot) \text{ cm} \tag{3.4}$$

and the spin angular momentum is J. We describe some of the standard properties of black holes in Appendix C Sec. 4.

Black holes can power nuclear activity only as long as they interact with gas. This gas will probably have sufficient angular momentum to orbit the hole. However, the orbits may not all lie in the same plane. Fortunately a spinning black hole causes the orbits to undergo differential Lense-Thirring precession (see Appendix C Sec. 4). Close to the hole, the precession time is $(r/r_g)^{3/2}(J/Mr_g c)^{-1/2}$ orbital periods, and can become shorter than the inflow time. Viscous torques will then cause the gas to sink into the equatorial plane of the hole (Rees, 1978b; but see Papaloizou and Pringle, 1984). The Lense-Thirring precession, an inherently relativistic effect, thus guarantees that a wide class of flow patterns near black holes will be axisymmetric—an important simplification of the problem.

It has been proposed in recent years that magnetic effects around black holes may have important astrophysical consequences (Blandford and Znajek, 1977; Macdonald and Thorne, 1982; Phinney, 1983a). The event horizon of a black hole behaves in many respects like a spinning conductor. For example, when a black hole forms out of collapsing magnetized material, the magnetic field outside the horizon decays in a time scale $\sim r_g/c$. This can be translated into an equivalent surface conductivity of $\sim 0.03\ \Omega^{-1}$ (Znajek, 1978). Similarly, when a black hole is embedded in a uniform vacuum magnetic field B, supported by external currents and parallel to its spin axis, then an electric field will be induced outside the hole just as if the event horizon supported a quadrupolar

surface charge distribution. For a slowly spinning hole, this is the same field pattern that would be found outside a conductor of radius r_+ spinning with angular velocity $J/4Mr_g^2$ (Phinney, 1983a) just as in a classical unipolar inductor a potential difference of magnitude $\sim aB$ will be supported between the pole and the equator. However, the hole will be surrounded by sufficient plasma to allow currents to flow to larger radii where an electron-positron jet may be accelerated (see Sec. III.D.5).

In later sections we shall discuss accretion onto black holes. It may be helpful at this stage to introduce some characteristic quantities, which give a feel for the orders of magnitude involved and for what approximations are justified.

A fiducial luminosity is the "Eddington limit" at which radiation pressure on free electrons balances gravity:

$$L_E=\frac{4\pi GMm_pc}{\sigma_T}=1.3\times10^{46}M_8\ \text{ergs s}^{-1}\ , \tag{3.5}$$

where M_8 is the mass in units of $10^8M_\odot$. The associated accretion rate is $M_E\times(\text{efficiency})^{-1}$, where $M_E=L_E/c^2$. The black body temperature if luminosity L_E emerges from a sphere of radius r_g is

$$T_E\simeq3\times10^5M_8^{-1/4}\ \text{K}\ . \tag{3.6}$$

Related to this is a characteristic time scale

$$t_E=\frac{\sigma_Tc}{4\pi Gm_p}\simeq4\times10^8\ \text{yr}\ . \tag{3.7}$$

This is the time it would take an object to radiate its entire rest mass if its luminosity were L_E. The time scale over which an accretion-driven source would double its mass is $\sim(L/L_E)^{-1}\times(\text{efficiency})^{-1}\times t_E$.

The dynamical and orbital time scales near black holes are modest multiples of $(r_g/c)=500M_8$ s; these time scales are therefore vastly shorter than t_E. It is primarily for this reason that the mass of material in any stationary flow pattern around the hole is generally negligible compared to the mass of the hole itself—this justifies our assuming an undistorted Kerr metric and neglecting the self-gravity of plasma around the hole. Radiation of the hole's rest mass on a time scale r_g/c would yield a luminosity $c^5/G=4\times10^{59}\ \text{ergs s}^{-1}$.

A fiducial particle density in the hole's environment is

$$n_E=\frac{c^2}{\sigma_TGM}\simeq10^{11}M_8^{-1}\ \text{cm}^{-3}\ . \tag{3.8}$$

This is the density at $r=r_g$ if a mass flux $\dot{M}_E$ is falling radially inward at speed c. A characteristic magnetic field strength is that for which $(B^2/8\pi)=n_Em_pc^2$:

$$B_E=\left[\frac{8\pi c^2m_p}{\sigma_TGM}\right]^{1/2}=2\times10^4M_8^{-1/2}\ \text{G}\ . \tag{3.9}$$

If a field B_E were applied to a black hole with $J\simeq J_{\max}$, the electromagnetic power extraction would be $\sim L_E$. In such a field, the gyro frequency is $\Omega_g=eB_E/m_ec=3\times10^{11}M_8^{-1/2}\ \text{rad s}^{-1}\ll r_g$. The maximum emf permitted by the unipolar inductor argument is then

$$(\Omega_gr_g/c)(J/J_{\max})m_ec^2\simeq10^{21}M_8(J/J_{\max})V\ . \tag{3.10}$$

This means that the density of charges required to "short out" the field is $\lesssim10^{-12}n_E$. It is unlikely that the charge density close to the event horizon could remain as low as this. In consequence, we expect that the plasma around a black hole is nearly neutral, and can be treated by the MHD approximation. (The bulk flow speeds, Alfvén speed, etc., will of course still be relativistic.) A related inference is that the *gravitational* effect of charges and magnetic fields is negligible; in practice one need never use the Kerr-Newman metric, the generalization of the Kerr metric that includes a contribution from electromagnetic mass-energy.

In the following section, we try to place massive black holes in a realistic astrophysical context.

C. Accretion flows

1. Gas supply

In principle, flow into a compact object can liberate gravitational potential energy at a rate approaching a few tenths of $\dot{M}c^2$, where $\dot{M}$ is the inflow rate. Even for such high efficiencies the mass requirements of the more luminous sources are rather high,

$$\dot{M}\sim1.5\left[\frac{0.1}{\varepsilon}\right]\left[\frac{L}{10^{46}\ \text{ergs s}^{-1}}\right]M_\odot\ \text{yr}^{-1}\ , \tag{3.11}$$

where ε is the efficiency (i.e., the fraction of the rest mass radiated). The most obvious source of fuel for an active galactic nucleus is the material of the galaxy itself. Stellar mass loss due to winds, planetary nebulae, supernovae, etc., in the typical population of an elliptical galaxy amounts to 10^{-11}–$10^{-12}M_\odot\ \text{yr}^{-1}$ per solar mass of galaxy, suggesting that moderately (but not extremely) strong sources could be fueled continuously only by giant ellipticals, and only if most of the gas released falls into the nucleus. Macdonald and Bailey (1981) have suggested that if the stellar velocity dispersion exceeds 300 km s^{-1}, then supernovae will be unable to prevent infall of the gas. In this way they are able to account for the association of nuclear activity with giant elliptical galaxies and cosmological evolution (see Secs. IV.B and IV.D below). Magnetic torques may be invoked to allow infall to proceed in the presence of angular momentum (Sparke, 1982b). The situation becomes considerably worse if one takes into account heating due to supernovae, which may drive much of the gas out of the galaxy (Mathews and Baker, 1971) and the possibility that gas may be stripped by ram pressure (Gott and Gunn, 1972; Gisler, 1976) or ablated thermally (evaporated; Cowie and Songaila, 1978; Balbus, 1982) as a result of the galaxy's motion through an intracluster medium.

Two ways around this problem have been proposed. First, the infalling gas could be locked up in dense neutral hydrogen clouds (or gas-rich dwarf galaxies) which orbit the galaxy coherently for considerable times. These

would gradually sink toward the nucleus as a result of dynamical friction and/or highly inelastic cloud-cloud collisions (Silk and Norman, 1979). H I clouds have been observed in several ellipticals (e.g., Knapp, Kerr, and Williams, 1978). Second, the inflow need not be continuous over the lifetime of the galaxy, merely over the lifetime of the source. Arguments based on radio source counts and the dimensions of extended sources generally require duty cycles of 10^7–10^8 yr, leaving periods of $\gtrsim 10^9$ yr over which gas could be accumulated, possibly cooling to form a centrifugally supported disk. Bailey and Clube (1978) and Bailey (1980) suggested that such a disk could grow quiescently at radii of several kpc until it became self-gravitating in the vertical direction. Then gravitational instabilities could trigger inflow by creating a turbulent viscosity.

A variation on the gaseous reservoir idea was suggested by Gunn (1978), who argued that the H I observed in certain radio ellipticals, possibly the source of fuel for the nucleus, was accreted from outside the galaxy. The strongest observational support for this hypothesis comes from observations of NGC 4278 (Knapp, Kerr, and Williams, 1978), where there appears to be a centrifugally supported disk of H I whose axis is inclined at an angle of 70° with respect to the rotation axis of the galaxy. NGC 4278 lies in a small group of galaxies, of the type in which isolated clouds of H I are known to exist (Mathewson, Cleary, and Murray, 1975) and where mergers of galaxies may be relatively more frequent than in rich clusters (e.g., Hausman and Ostriker, 1979). A misaligned H I cloud, once accreted, would undergo differential precession in the gravitational field of the galaxy, which would probably cause it to align after a few orbital times. Meanwhile, frictional interactions between the disk and the surrounding (hotter) interstellar medium (e.g., turbulent viscosity due to the Kelvin-Helmholtz instability) could cause inflow on a comparable or shorter time scale. Unfortunately, intergalactic H I appears to be fairly uncommon (Lo and Sargent, 1979). A reservoir of gas might also be supplied by the merger of a gas-rich spiral with an elliptical, as has been suggested for Cen A (Tubbs, 1981; but see van Albada, Kotanyi, and Schwarzschild, 1982).

Statistical studies support the idea that conditions outside the galaxy strongly affect the activity of the nucleus (see Sec. IV.D for details). In general, the probability of activity increases with membership in a group or cluster (Slingo, 1974b; Dressel, 1981; Hummel, 1981; Biermann *et al.*, 1981), or even with the presence of a single nearby galaxy (Hummel, 1981). Suggested interpretations of these correlations have generally concentrated on the increased availability of gas to the nucleus, through (a) tidal effects on the interstellar medium of the active galaxy, (b) tidal capture of gas from nearby galaxies, (c) mergers, and (d) capture of gas from an enhanced intergalactic medium. The nature and intensity of the observed activity does not appear to be strongly correlated with the concentration of nearby galaxies, but simply with their presence or absence. This suggests that the rate at which gas is processed through the central engine is regulated within the active galaxy, and is relatively insensitive to the rate at which gas is supplied, provided that the supply is more than adequate. Another possibility is that the formation of a central massive black hole is correlated with the presence of nearby galaxies. If this were the case, then holeless isolated galaxies would not produce radio sources, even if the fuel were available.

In many groups and clusters of galaxies, the dominant radio source is also the dominant galaxy, a giant elliptical or cD galaxy (Burns, White, and Hough, 1981; McHardy, 1979). Radio emission appears to be correlated with the presence of optical emission lines (Heckman, 1980) and x rays (Burns, Gregory, and Holman, 1981). Such galaxies, which lie virtually stationary at the bottom of the cluster or group potential, are widely believed to be the products of mergers (Hausman and Ostriker, 1979; Roos and Norman, 1979). The radio sources associated with cD's often have simple double or unresolved morphologies, believed to be characteristic of sources injected into a stationary, symmetric distribution of ambient gas. The insensitivity of source structure and intensity to the richness of the surrounding cluster or group, the high minimum pressures, and the limited spatial extent associated with these sources suggest that the gaseous environment is self-contained by the deep potential well of the galaxy (e.g., Heckman, 1980). Other cD's exhibit a wide-angle tail morphology (see Sec. I.C; Burns, Schwendeman, and White, 1983). This is also consistent with the jet's rising sub- or trans-sonically through a stationary, symmetry atmosphere bound to the cD. The extent of this atmosphere is delineated by the onset of the tail, whose shape reflects the pressure and velocity of the cluster gas relative to the cD.

For a comprehensive review of the relationship between active nuclei and their galactic hosts see Balick and Heckman (1982).

In an alternative class of models for fueling the central object, it is supposed that the source of gas is contained within the nuclear region. Consider a central black hole of mass $10^8 M_8 M_\odot$, surrounded by a star cluster. If the velocity dispersion v_c of the cluster exceeds the escape speed v_{esc} from a typical star, then the cluster will evolve principally by physical star-star collisions rather than by two-body gravitational encounters (see Sec. III.B.1). For velocity dispersions of $\lesssim v_{esc}$, the inelasticity of such collisions leads to coalescence, while for larger relative velocities the stars involved are partially or totally disrupted.

As noted in Sec. III.B.1, coalescent star clusters have been invoked chiefly as direct sources of energy or as progenitors to clusters of compact objects. However, they may also figure in accretion models, in several ways. First, if coalescence "runs away" in the manner described by Sanders (1970), the process may rapidly lead to the formation of a central compact object, even if none exists to begin with (Begelman and Rees, 1978). If a central black hole already exists, tidal disruption of the low-density supermassive stars (which rapidly sink toward the center due to dynamical friction) by the black hole could provide

a source of accreted mass. Second, the supernovae themselves may act as sources of mass, to be accreted by a central black hole, with a tenfold increase in efficiency over the energy released in the explosion. Preconditions for accretion rather than escape of the ejecta are (1) a sufficiently deep potential well at the site of the explosion or (2) significant cooling and deceleration of the ejecta by interaction with other ejecta or an ambient medium. Finally, the coalescence phase may be the precursor to the disruptive regime, which may also lead to the formation of a massive compact object (see Begelman and Rees, 1978; Sec. III.B.1) as well as supplying mass for accretion.

A novel version of the stellar disruption-accretion scenario was proposed by Hills (1975,1978), who pointed out that stars coming too near the black hole could be disrupted tidally, and the debris subsequently accreted to provide the energy. In order for a star to be disrupted outside the event horizon, the Schwarzschild radius must be smaller than the Roche radius $r_T \sim 10^{11}(M/M_\odot)^{1/3}$ cm for normal stars. The mass at which these two radii coincide for a solar-type star is $\sim 3\times 10^8 M_\odot$, a value which Hills associated with the maximum mass (and, through the Eddington limit, the maximum luminosity) of a quasar, as a star swallowed whole would not release much energy. Considerable work has gone into determining the rate at which stars would be swallowed by a black hole of given mass, embedded in a cluster of given density and velocity dispersion (e.g., Young, Shields, and Wheeler, 1977; Shields and Wheeler, 1978; Gurzadyan and Ozernoi, 1982). The main theoretical subtleties involve the strongly non-Maxwellian character of the cusplike distribution of stars bound to the black hole (Peebles, 1972) and the diffusion process which governs the depletion and resupply of "loss-cone" orbits, i.e., orbits of low angular momentum which bring stars within the Roche radius (Frank and Rees, 1976; Lightman and Shapiro, 1977; Bahcall and Wolf, 1976; Young, 1977; Cohn and Kulsrud, 1978). Triaxility of the central star cluster (Norman and Silk, 1983) or the presence of a black hole binary companion (Begelman, Blandford, and Rees, 1980) may enhance the diffusion rate into the loss cone. However, more quantitative analyses of the parameter space (Hills, 1975; Frank, 1978) have shown that for mass injection rates appropriate to quasars, stars are captured primarily from outside the cusp (i.e., not bound to the black hole), and that the swallowing rate is generally exceeded by the disruptive rate due to star-star collisions. Thus tidal disruption by the black hole in an isolated galaxy is probably a relevant process only in weak sources, if it is important at all. Roos (1981), however, has pointed out that tidal effects during a merger may increase the rate at which loss-cone orbits are repopulated, and hence the disruption rate.

2. Quasispherical accretion

The way in which gas flows into an accreting object depends largely on the conditions where it is injected. If the gas has no angular momentum, it can flow in radially (assuming that it is not channeled by an anchored magnetic field, as in accretion onto a magnetized neutron star). The simplest spherical accretion problem, assuming adiabatic flow, was solved for a Newtonian point mass by Bondi (1952). If the gas at infinity is stationary and uniform, with specified density ρ_∞ and sound speed c_∞, then there is a unique trans-sonic flow for adiabatic index $\Gamma < \frac{5}{3}$, with an accretion rate

$$\dot{M} = 4\pi\eta\rho_\infty (GM)^2 c_\infty^{-3} , \tag{3.12}$$

where η is a constant of order unity depending on Γ. This result is essentially unchanged if the problem is done general-relativistically in the Schwarzschild metric (Michel, 1972; Begelman, 1978b), but for $\Gamma > \frac{5}{3}$ a relativistic critical (trans-sonic) point appears outside the event horizon.

If the gas radiates as it falls, but is heated adiabatically with $\Gamma < \frac{5}{3}$, then the radiative efficiency is low (Shapiro, 1973a), because the internal energy (and hence the "pdV work") is small compared with the free-free kinetic energy. However, if a flow is heated during infall with an *effective* $\Gamma > \frac{5}{3}$, but is simultaneously able to cool, then it may both be trans-sonic and radiate gravitational energy efficiently. The large effective adiabatic index could be the result of a tangled magnetic field (effective $\Gamma = 2$) or turbulence (Mészáros, 1975).

The question of whether infalling gas can dissipate its binding energy efficiently is distinct from the question of how much of the radiation thus produced escapes to infinity. Outflowing radiation exerts an outward force on the gas. Since the gas is likely to be ionized, the interaction cross section per electron is at least the Thomson cross section σ_T, and if the flux of radiation exceeds the Eddington limit, L_E (see Sec. III.B.3), then the gravitational force is canceled by radiation pressure. Since steady accretion onto a neutron star or white dwarf of radius r_* always liberates $\dot{M}(GM/r_*)$, the Eddington limit places an upper limit on the accretion rate. Black holes, not having hard surfaces, do not impose this constraint; arbitrary amounts of radiation as well as mass may be swallowed. In fact, despite some early controversy (Kafka and Mészáros, 1977) it is now plain that radiation pressure exerted through Thomson scattering cannot halt spherical accretion into a black hole (Begelman, 1978a,1979; Gilden and Wheeler, 1980; Flammang, 1982). One can easily understand the result, since the maximum emissivity, integrated from infinity to some radius r, cannot exceed L_E until the gas has crosssed the "trapping radius,"

$$r_{\rm tr} = (\dot{M}/\dot{M}_E) r_g , \tag{3.13}$$

where $\dot{M}_E = L_E/c^2$ is the "critical" accretion rate associated with the Eddington limit. Below $r_{\rm tr}$, however, the flow speed of the gas inward always exceeds the diffusion speed outward of the radiation $\sim c/\tau$, where $\tau = \rho\sigma_T r/m_p$ is the characteristic electron scattering optical depth at r. Thus most of the radiation produced below $r_{\rm tr}$ is trapped and dragged into the hole, while the luminosity escaping

to infinity saturates at some fraction of L_E.

Although radiation pressure cannot *halt* spherical accretion into a black hole, heating by the outflowing radiation may modulate the inflow. Using a simple model which pits Compton heating against bremsstrahlung cooling, and a power-law approximation to line cooling, Ostriker *et al.* (1976) and Cowie, Ostriker, and Stark (1978) argued that steady flows with Bondi-type boundary conditions at infinity were impossible for sufficiently hard spectra and luminosities exceeding only a small fraction (typically $\sim 10^{-3}$) of L_E. Bisnovatyi-Kogan and Blinnikov (1980) have argued that other equilibrium flows may exist; however, Krolik and London (1983) argue that these alternative flows are themselves unstable. Finally, we note that flows in which preheating is important are particularly prone to thermal instabilities. If the inflowing gas breaks up into two phases (Krolik, McKee, and Tarter, 1981; Krolik and London, 1983), then quasisteady inflow of the inhomogeneous gas may be established.

3. Accretion with angular momentum

The flow pattern changes dramatically if the inflowing gas has a small amount of angular momentum. The quasispherical approximation breaks down when $r \lesssim l^2/GM$, where l is the specific angular momentum per unit mass. If the inflowing gas is injected more or less isotropically from large r, but has angular momentum such that $l^2/GM \gg r_g$, then if it is unable to cool, it will form an evacuated funnel about the rotation axis (Cassen and Pettibone, 1976; Sparke and Shu, 1980); if it can cool, it will form a thin accretion disk, familiar to astrophysicists from its application to galactic x-ray sources (see, for example, Pringle, 1981, and references therein). The idea that active galactic nuclei could be powered by accretion disks originated in the work of Zel'dovich and Novikov (1964), Salpeter (1964), and Lynden-Bell (1969).

a. Thin disks

In the standard thin-disk model, it is assumed that the gas at each radius is nearly in Keplerian orbit about the central object. Slow radial inflow occurs if there is a viscous stress $t_{\varphi r}$ which transfers angular momentum outward. The energy dissipated by the viscous stress is assumed to be radiated locally, at a rate three times the local rate at which gravitational energy is liberated ($GM\dot{M}\,dr/r^2$ between r and $r+dr$). The factor of 3 occurs because the viscous stress transports energy as well as angular momentum outward. This local imbalance is globally rectified in the innermost region of the disk, where the local release of binding energy exceeds the dissipation. For thin disks around a Schwarzschild black hole, slow inflow can be maintained down to the innermost stable orbit, located at $6r_g$ (Appendix C Sec. 4).

A thin disk has a geometrically small but finite scale height normal to the orbital plane, determined by balancing pressure against the vertical component of gravity. Roughly, the scale height h is given by $h/r \sim c_s/v_{\rm Kep}$, where c_s is the sound speed in the orbital plane and $v_{\rm Kep}$ is the orbital speed. Generally, for disks with low accretion rates and low central masses, and at large distances from the central object, the vertical support is provided by gas pressure. At small distances, and for disks with high accretion rates around relatively massive objects (the case usually relevant to active galactic nuclei), disks are radiation-pressure dominated (Pringle and Rees, 1972; Shakura and Sunyaev, 1973; Novikov and Thorne, 1973; Page and Thorne, 1974; Thorne, 1974). In the latter case, where Thomson scattering is the dominant opacity, it is easily shown that h is approximately equal to half the trapping radius (Sec. III.C.2).

The weak point in the modeling of thin disks is the specification of a viscosity law. As is the case for jets (Sec. II.C.6), ordinary molecular viscosity is almost certainly irrelevant, and one must appeal to magnetic or turbulent viscosity, the nature of which is not well understood. Although the radial dependence of the viscosity law will not change the energetics for a disk with given $\dot{M}$, it *will* affect the column density through the disk and may change the emitted spectrum. In lieu of a detailed theory, the most widespread convention is to dispense with a coefficient of viscosity and stress-strain relation altogether, and to suppose that the viscous stress has the form

$$t_{\varphi r} = \alpha^* p \ , \tag{3.14}$$

where p is the pressure in the equatorial plane (Shakura and Sunyaev, 1973; Callahan, 1977). This prescription has some basis in phenomenological models of turbulent (Lynden-Bell and Pringle, 1974) and magnetic (Lynden-Bell, 1969; Eardley and Lightman, 1975; Takahara, 1979; Coroniti, 1981; Sakimoto and Coroniti, 1981; Pudritz, 1981) viscosities, which "predict" values of α^* in the range $\sim(10^{-3}$–$0.1)$. If $\alpha^* < 1$ then the inflow is subsonic with respect to the gas in the disk, and the approximation of hydrostatic equilibrium normal to the disk plane is valid.

Thin disks are subject to a variety of instabilities. Some of these arise from the form of the viscosity model (Lightman and Eardley, 1974), while others are related to the processes by which thin disks cool, and are particularly dangerous for disks supported vertically by radiation pressure (Pringle, Rees, and Pacholczyk, 1973; Pringle, 1981; Shakura and Sunyaev, 1976; Piran, 1978). The above instabilities are secular, i.e., they grow over times considerably longer than the orbital time; their general effect is to cause the disk to break up into rings. Other instabilities operate on a dynamical time (although the unstable conditions evolve over an inflow time), e.g., convective instabilities (particularly for radiation-dominated disks: Cunningham, 1973; Shakura and Sunyaev, 1976) and Parker-type instabilities involving the escape of buoyant loops of magnetic field. These may result in much of the dissipated energy's reaching the disk surfaces as macroscopic motions rather than radiation, and could lead to the formation of a hot corona surrounding the disk

(Galeev, Rosner, and Vaiana, 1979). These instabilities can be avoided if the viscous stress scales as the gas pressure rather than the radiation pressure (Sakimoto and Coroniti, 1981; Meier, 1979). Finally, certain dynamical instabilities have been suggested as the basis of the angular momentum transport, e.g., the Kelvin-Helmholtz instability leading to inflow in the Gunn (1978) model for NGC 4278 (Sec. III.C.1) and the weak Jeans instability in a disk which is marginally self-gravitating in the vertical direction (Paczyński, 1977a; Bailey and Clube, 1978).

One area that remains problematic for accretion disks in active galactic nuclei is the nature of the sink for angular momentum which is carried outward by viscous stresses. In binaries undergoing mass transfer, it is widely believed that tidal stresses due to the companion star both truncate the disk and absorb the excess angular momentum, returning it to the binary orbit (e.g., Smak, 1976; Paczyński, 1977b). In lieu of such a mechanism, which presumably does not operate in active galactic nuclei, the outer parts of the disk would continue to spread until some other agent removed the excess angular momentum. A number of schemes have been proposed to accomplish this (any of which may also operate in binaries). These include

(1) Gunn's (1978) Kelvin-Helmholtz mechanism (Sec. III.C.1) for NGC 4278, in which the angular momentum is transferred to hot ambient gas or a hot corona which is not corotating with the disk.

(2) Hydromagnetic winds (see Sec. III.D.5). If the disk is threaded by open magnetic field lines then a centrifugally driven wind may be established, which can carry away the excess angular momentum. As is the case with the Kelvin-Helmholtz model, the hydromagnetic wind can operate at every radius within the disk and account for *all* of the "viscous" transfer of angular momentum (Blandford and Payne, 1982).

(3) Compton-heated winds (Begelman, McKee, and Shields, 1983; Begelman and McKee, 1983). These operate effectively when the surface of the outer disk is irradiated by hard x rays, presumably from the central engine but possibly also from the jet iself.

(4) Dynamical friction against a nonrotating cluster of stars (Ostriker, 1983). This will operate on the dynamical relaxation time scale of the cluster.

b. Tori

If gas passing through a thin disk reaches a radius within which the internal pressure builds up—either because it is unable to cool in an inflow time or because the radiation-pressure force is competitive with gravity—the disk will become geometrically thick ($h \sim r$). In a thick disk or torus the pressure provides substantial support in the radial as well as the vertical direction, and the angular momentum distribution (now a function of z as well as r) may be far from Keplerian. Nevertheless, the analogy with thin accretion disks still applies if slow inflow occurs as a result of the viscous transfer of angular momentum.

Tori may be supported by either radiation pressure or gas pressure. A radiation-pressure-supported thin disk has a constant thickness $\sim r_{\rm tr}$, the trapping radius defined in Sec. III.C.2; hence it becomes geometrically thick at $4r_g < r \lesssim r_{\rm tr}$, when the accretion rate exceeds the critical value $\dot{M}_E$. A gas-pressure-dominated disk would become thick in the opposite limit, that of low accretion rate, because the cooling time varies inversely with $\dot{M}$, while the infall time $\sim \alpha_*^{-1} t_{\rm Kep}$ should be insensitive to $\dot{M}$ for a turbulent or magnetic viscosity (Rees, Begelman, Blandford, and Phinney, 1982). Most work to date has focused on the radiation-dominated case; hence we shall couch the following discussion in terms of supercritical accretion. However, virtually all of the arguments in this section can be modified to apply to gas-supported tori. We discuss the differences between radiation-dominated and ion-supported tori in Sec. III.C.4.

As was the case in early work on spherical supercritical accretion (Sec. III.C.2), there has been considerable controversy over whether thick supercritical disks can indeed exist. Shakura and Sunyaev (1973) conjectured that a strong wind would emerge from the region within $r_{\rm tr}$, driven by the energy dissipated in excess of L_E. As a result the residual inflow rate would decrease linearly with r, and the disk would hover at its "trapping radius" all the way into the hole. Meier (1979,1982b,1982c) has worked out detailed models of winds from such disks, assuming quasispherical symmetry, and Frank (1979) has considered the toroidal case (cf. also Bisnovatyi-Kogan and Blinnikov, 1977).

An alternate approach is to suppose that the disk suffers little mass loss and (except in a cusplike region near the black hole) lies close to static equilibrium, with radiation pressure and centrifugal force nearly balancing gravity. Such a flow is possible in principle for two reasons. First, as in spherical supercritical accretion, radiation is trapped in the interior of the disk; diffusion is important only in a narrow surface layer. Unless the energy dissipated in the disk interior is convected into this surface layer or released in the cusp region near r_g, it will be dragged into the hole, and the luminosity reaching infinity will not exceed the critical (Eddington) value for the disk. Second, although the accreting gas must lose most of its angular momentum in drifting from $r_{\rm tr}$ into the hole, the rate of energy dissipation is not related to the angular momentum transfer as simply as it is in a thin disk. Abramowicz and collaborators, extending earlier work by Maraschi, Reina, and Treves (1976), Fishbone and Moncrief (1976), and Lynden-Bell (1978), have shown that inward-directed pressure gradients at several Schwarzschild radii can push the inner edge of the quasistatic region inside the marginally stable circular orbit ($6r_g$ for a Schwarzschild black hole), toward the orbit of zero binding energy ($4r_g$; Kozlowski, Jaroszyński, and Abramowicz, 1978; Abramowicz, Jaroszyński, and Sikora, 1978; Jaroszyński, Abramowicz, and Paczyński, 1980; Appendix B Sec. 5). Since the pressure force points outward at radii $\lesssim r_{\rm tr}$, there must be a pressure maximum at some point on the equator. As a result of the (general-relativistic) inner boundary conditions, the specific bind-

ing energy of the inner region of the disk may be small compared with GM/r, and the total dissipation rate much smaller than the $\sim 0.057\dot{M}c^2$ predicted by the theory of thin disks around Schwarzschild holes. Qualitatively similar arguments apply for a Kerr hole.

Whether such low-binding-energy inner regions can be maintained depends on the magnitude of the viscosity. Such a region would have a nearly uniform distribution of angular momentum. It therefore requires very little viscosity to drive the inflow through the cusplike inner edge and into free fall. In fact, inflow could be driven primarily by slight violations of hydrostatic equilibrium, in much the same way as material streams through the Lagrangian point in an x-ray binary (Paczyński, 1977b). If the viscosity is too large, gas will be driven through the cusp at a high rate, and heat will be generated within the torus so rapidly that the torus will become unbound. The *maximum* viscosity consistent with a low-binding-energy cusp is not much larger than the viscosity due to the radiation alone (Weinberg, 1972; Blandford, Jaroszyński, and Kumar, 1984), which is a *lower limit* on the total viscosity present.

As is true of thin accretion disks, the largest uncertainty in constructing a model of a thick disk is the nature of the viscosity. This uncertainty is not crucial to many of the qualitative features of thin-disk theory (e.g., the energetics), where only one component of the viscous stress tensor is important. However, in a thick disk one must deal explicitly with shear stresses in two directions. The stresses determine the distributions of both angular momentum and enthalpy, and therefore the shape of the isobars inside the disk. The isobars at the disk surface, however, depend only on the surface distribution of specific angular momentum. This fact has enabled Paczyński and Wiita (1980), Jaroszyński, Abramowicz, and Paczyński (1980), Abramowicz, Calvani, and Nobili (1980), and Wiita (1982) to construct global models of thick disks without reference to the viscosity. They specify, *a priori,* the angular momentum distribution along the surface of the disk in such a way that it smoothly connects a cusp solution near the hole with a thin disk at sufficiently large radii. Although self-consistency and stability considerations do somewhat constrain the acceptable forms of the angular momentum distribution (Abramowicz, Calvani, and Nobili, 1980), they nevertheless allow one considerable freedom to specify the shape of the surface arbitrarily, and yield virtually no information about the interior.

To determine the precise disk shape and, more importantly, to discover whether quiescent supercritical disks can exist at all [as opposed to the wind-dominated flows proposed by Shakura and Sunyaev (1973)], it is necessary to deal with the two-dimensional structure of the viscous disk interior. Since the true viscosity is unknown, the best one can hope to do at present is to explore the consequences of assuming different viscosity prescriptions. Even with a well-defined local viscosity law, the problems of computing two-dimensional hydrodynamic solutions are considerable (see Appendix B Sec. 5). Some simplification occurs if one is able to specify the surfaces of constant angular velocity *a priori,* as when the disk is barytropic (pressure a function only of density) and von Zeipel's theorem requires that the fluid rotate on cylinders. For laminar viscous flow, such a specification is generally invalid. Although instabilities exist which tend to drive differentially rotating flows toward barytropicity (Goldreich and Schubert, 1967; Seguin, 1975), these may be too slow, compared with the inflow time, to complete the necessary redistribution of enthalpy and angular momentum (Begelman and Meier, 1982). More drastic simplification occurs if a portion of the disk is assumed to be self-similar in radius. The self-similarity approximation is self-consistent in the radius range $r_g \ll r \ll r_{tr}$ (i.e., for *very* supercritical flows), provided the viscosity can be expressed in a suitably scale-free manner. Begelman and Meier (1982) generated a family of laminar self-similar models, and examined their internal structure and stability. They found no models which were convectively stable at all latitudes. Instability occurs because radiation is trapped in the inflowing gas ($r \ll r_{tr}$), the specific entropy of which therefore increases with decreasing radius. The stabilizing influence of the angular momentum distribution is apparently unable to counteract the destabilizing effect of the entropy gradient. Convection, which may take the form of turbulence or slow circulation, should be able to keep an otherwise unstable interior region of a disk near marginal stability, largely by transporting heat toward the disk surface (Paczyński and Abramowicz, 1982). Near the surface, however, convection becomes inefficient, and much of the burden of transporting energy may be returned to radiative diffusion. If this occurs, the supercritical luminosity will drive a strong wind, and the flow will resemble the Shakura-Sunyaev picture; if not, then quiescent tori as described above may indeed exist. The resolution of many of these uncertainties may be aided by numerical hydrodynamical simulations; first steps in this direction have been taken by Hawley, Smarr, and Wilson (1984a,1984b; Fig. 16).

Radiation tori are similar in many respects to the massive objects originally postulated by Hoyle and Fowler (1963a) and may suffer the same fate—i.e., be shown to be dynamically unstable. There are possible axisymmetric local instabilities caused by unfavorable entropy and angular momentum gradients (e.g., Seguin, 1975; Kandrup, 1982). These presumably evolve to create marginally stable convection zones just as in a star. More threatening are nonaxisymmetric instabilities. Papaloizou and Pringle (1984) have recently demonstrated that a toroidal configuration known to be marginally stable to axisymmetric disturbances possesses global, nonaxisymmetric dynamical instabilities. It will apparently destroy itself in a few orbital periods unless nonlinear terms can saturate the instability at a low amplitude. It is not yet known if this is a general property of these tori. Furthermore, it is not at all clear that tori can evolve towards stable or marginally stable states even if they exist, nor that the rate of internal energy generation through viscous dissipation can always be balanced by the transport.

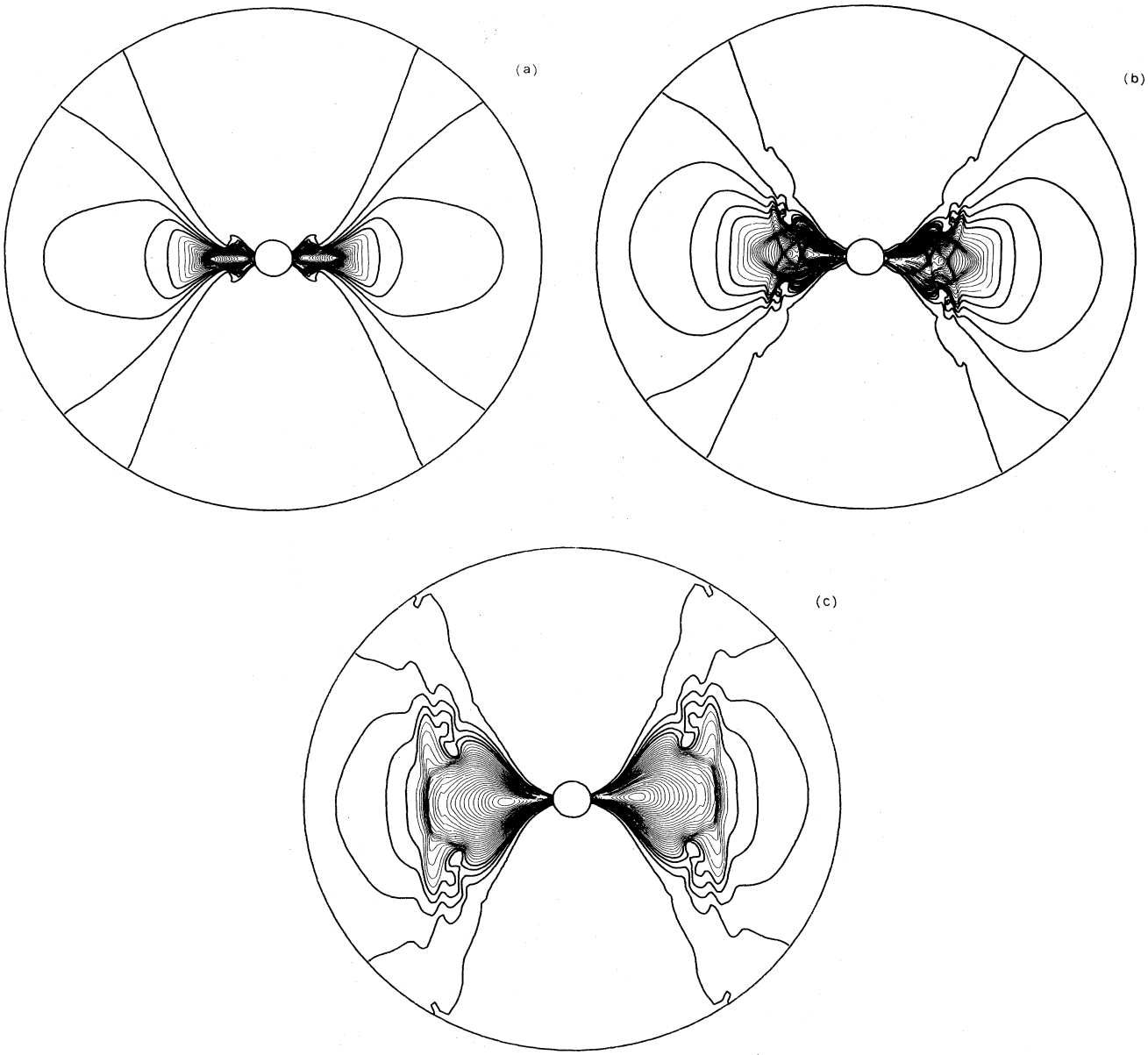

FIG. 16. Three snapshots of density contours from a two-dimensional numerical simulation by Hawley and Smarr (1984), depicting the infall of hot fluid towards a black hole and the subsequent formation of a thick disk. Initially, material is introduced at the outer (circular) boundary of the 120×160 polar grid, with angular momentum slightly less than the marginally bound value. The infalling material flows almost radially to a point just inside two Schwarzschild radii, where two oblique shocks form, turning the flow towards the hole. These shocks move outward, and the post-shock fluid flows inward. It encounters the centrifugal wall which defines the "funnel," the region along the orbital axis kept evacuated by centrifugal accelerations. Fluid encountering this boundary slows and stops (a); material begins to pile up from behind, and two curved shocks form, moving outward from the centrifugal barrier. Behind the shocks, much of the fluid has turned in its trajectory and is moving outward. This outflow runs into the inflowing disk, and another shock occurs; the outflow is redirected up along the surface of the inflow. These shocks are clearly seen in (b). Along the leading edge of the backflow, shear instabilities produce a vortex. By the end of the calculation (c), the three pairs of shocks have run together, and the flow is relaxing towards a hot, pressure-supported, thick disk.

Most work on tori has been based on the assumption that a strict stationary state prevails. But this may be overrestrictive: material could be periodically "dumped" onto a black hole and then drain away (Sec. III.C.1), or a massive torus may be left behind after a supermassive spinning object collapses to a black hole, and the torus could still resemble those discussed above.

4. Physical parameters

The inner regions of disks with mass fluxes close to $\dot{M}_E$ are generally able to cool by radiation on time scales shorter than the inflow time and may have luminosities approaching L_E. If $\dot{m}\equiv\dot{M}/\dot{M}_E\lesssim1$, then the bulk of the

radiation comes from a region only a few gravitational radii in size, and the physical conditions can be scaled in terms of the "Eddington quantities" defined in Sec. III.B.3. The main extra parameter is $v_{\rm inflow}/v_{\rm freefall}$. The inward drift speed $v_{\rm inflow}$ would be of order $v_{\rm freefall}$ for radial accretion; when angular momentum is important, this value depends on viscosity. Suppose that the accretion rate yields a luminosity L with an efficiency 0.1. Then characteristic quantities at distances r from the hole are

(a) Optical depth to electron scattering:

$$\tau_e \sim \dot{m}(r/r_g)^{-1/2}(v_{\rm freefall}/v_{\rm inflow}) . \tag{3.15}$$

(b) Particle density:

$$n \sim \dot{m}(r/r_g)^{-3/2}(v_{\rm freefall}/v_{\rm inflow})n_E . \tag{3.16}$$

The maximum magnetic field, corresponding to equipartition with the bulk kinetic energy, would be

$$B_{\rm eq} \sim \dot{m}^{1/2}(r/r_g)^{-5/4}(v_{\rm freefall}/v_{\rm inflow})^{1/2}B_E \tag{3.17}$$

[see Eqs. (3.5), (3.8), and (3.9)]. Any thermalized radiation emerging directly from the central "core" would tend to be in the far ultraviolet or soft x-ray parts of the spectrum [$T \lesssim T_E$; Eq. (3.6)]. Note that kT_E is far below the "virial temperature" $kT_{\rm virial} \simeq m_p c^2(r_g/r)$; gas that has cooled down to thermal equilibrium at a temperature $\sim T_E$ can therefore only be supported against gravity if radiation pressure exceeds gas pressure by a large factor $\sim(T_{\rm virial}/T_E)$. Deep inside a very optically thick disk, the temperature will exceed T_E by a factor $\sim\tau_e^{1/4}$, but even when this factor is included, radiation pressure is strongly dominant (just as it is in supermassive stars).

In an optically thick disk the interior conditions resemble those beneath the photosphere of an O star; a disk supported by gas pressure (requiring ion kinetic temperatures $\sim$100 MeV) is very different. Since the random velocities are comparable with c, conditions are exceptionally favorable for the acceleration of ultrarelativistic particles. Indeed, the distinction between "thermal" and "nonthermal" particles becomes rather blurred under these extreme conditions. The energy available for each "thermal" ion is $\sim$100 MeV, and at kinetic temperatures corresponding to this we cannot assume that the electron temperature (T_e) and the ion temperature (T_i) are equal, nor that there is any well-defined component of the plasma with a Maxwellian velocity distribution. In general, it is likely that $T_e < T_i$, the electrons being efficiently cooled and maintained at energies $\lesssim 1$ MeV by synchrotron or Compton emission (except for the small proportion that may have just passed through a shock, or a region of magnetic reconnection, where the coupling between electrons and ions is more efficient than that due to ordinary Coulomb encounters). It is therefore the ions, rather than the electrons, which provide the dominant kinetic pressure in thick disks.

At radii of $\lesssim$1000 Schwarzschild radii, where the ion virial temperature exceeds the electron rest mass, cooling will always be efficient if the ions channel their energy to the electrons on a time scale shorter than the inflow time. However, this cannot occur by the usual process of Coulomb interactions for $\dot{m} < 50(v_{\rm infall}/v_{\rm freefall})^2$ (Rees *et al.*, 1982). Unless collective effects step in to couple the electrons and ions, the flow will be unable to cool, resulting in the formation of a thick disk. For a thick disk, the factor $(v_{\rm infall}/v_{\rm freefall})$ is of order the viscosity parameter α^*. The dominant viscosity is probably magnetic, and estimates (e.g., Eardley and Lightman, 1975) suggest that α^* lies in the range $10^{-2} \lesssim \alpha^* \lesssim 10^{-1}$. Since there is no reason why α^* should diminish as $\dot{m}$ falls, one may conclude that the regime of inefficient cooling would definitely be attained for sufficiently low $\dot{m}$. The only perceptible radiation emitted from such a flow would be due to a nonthermal tail of electrons (accelerated behind shocks, or by processes related to the magnetic reconnection and viscosity). The pressure distribution of the hot thermal plasma (in which $T_i > T_e$)—apart from a "funnel" along the rotation axis—would be approximately of the form $p \propto r^{-5/2}$ at large distances from the hole. This cloud may be responsible for the collimation of jets and beams from such systems. The high-entropy plasma escaping in the beam could be produced by exotic processes which extract rotational energy from the hole [maybe involving Blandford-Znajek (1977) electromagnetic effects], and thus need not rely on the release of gravitational energy by infalling material (see Secs. III.D.5 and III.D.6).

The objects M87 and Cygnus A may be examples of active galactic nuclei with $\dot{M} \ll \dot{M}_E$, whose gas-pressure-supported inner accretion disks are unable to cool. The nuclei of both are extremely underluminous compared with the energy outputs (presumably in kinetic energy of jet motion) inferred from observations of the extended radio structure. In addition, if M87 indeed contains a black hole of $5\times10^9 M_\odot$, as has been claimed (Young *et al.*, 1978), then the level of activity in the nucleus yields a luminosity of only $10^{-4}L_E$. This nucleus certainly cannot contain a radiation torus emitting at the Eddington luminosity; on the other hand, provided the magnetic viscosity yields $\alpha^* \gtrsim 10^{-2}$, the cooling time scale for thermal plasma accreted onto it could still be longer than the inward drift time scale, allowing the possibility of a cloud supported by ion pressure.

5. Scaling laws

The flow pattern when accretion occurs is determined by the values of the parameters L/L_E (which determine the relative importance of radiation pressure and gravity) and the ratio $t_{\rm cool}/t_{\rm dynamical}$ (which fixes the temperature if a stationary flow pattern is set up). Suppose we have an object with given values of M and L, where the flow pattern is axisymmetric and characterized by a velocity $v(r,\theta)$, θ being the angle made with the symmetry axis; we can then inquire about the properties of a scaled-down object with mass $M'=xM$. If we scale $L'=xL$, then the scaled version has the same value of L/L_E. The gravitational radius r_g scales as M. If the flow pattern is similar

in the scaled version (which is equivalent to requiring similar viscosity parameters), then $v'(xr,\theta)=v(r,\theta)$, and the dynamical time scales then scale as $t'_{\rm dynamical}=xt_{\rm dynamical}$. If the objects are fueled by accretion, and the efficiencies are the same in both cases, then $\dot{M}'=x\dot{M}$. The characteristic densities then scale as $\rho'(xr,\theta)=x^{-1}\rho(r,\theta)$. Now, in general, $t_{\rm cool}\propto\rho^{-1}\times$(function of T): the ρ^{-1} dependence applies not only to two-body cooling processes, but also to cyclotron-synchrotron cooling if B^2 scales with ρ^{-1}, which will be the case if the magnetic stresses are an M-independent fraction of the total pressure. If $T'(xr,\theta)\sim T(r,\theta)$ (or more generally if the cooling time depends weakly on T), we then have $t'_{\rm cool}\simeq xt_{\rm cool}$—in other words, the ratio $t_{\rm cool}/t_{\rm dynamical}$ is the same in the "scaled" flow pattern, given that L is scaled with M.

Thus the apparent analogy between stellar-scale phenomena (SS433, Sco X1, etc.) and active galactic nuclei may indeed reflect a close physical similarity. There are probably miniquasars (Seyfert nuclei) and nanoquasars (SS433, etc.). The relevant parameter is $\dot{m}=\dot{M}/\dot{M}_E$ ($\propto L/L_E$ for a given efficiency).

Just as M87 and similar low-luminosity active nuclei may display the "purest" nonthermal emission (because the cooling time for nonrelativistic gas is so long), these objects may have small-scale counterparts in our galaxy, detectable only in the radio (and maybe also the gamma-ray) band. In Sec. V.A.2 we discuss a possible "unified" scheme for active nuclei, which makes use of these scaling relationships.

The preceding discussions of black holes and accretion flows provide a basis for general models of active galactic nuclei, aimed at interpreting the data in all wavebands. This topic lies beyond the scope of our review; we therefore now concentrate specifically on the origins of the jets which provide power to cosmic radio sources.

D. Production of jets

Two ingredients are necessary for the production of jets. First, there must be a source of material with sufficient free energy to escape the gravitational field of the prime mover. Second, there must be a way of imparting some directionality to the escaping flow. This directionality need not involve initial collimation to better than ~ 1 rad. Once the flow has become supersonic, the collimation processes discussed in Sec. II can provide additional focusing further out. However, some degree of asphericity is necessary in the trans-sonic region of the flow.

Our eventual aim must be to understand the overall flow pattern around a central compact object, involving accretion, rotation, and directional outflow, but we are still far from achieving this. Most authors who have discussed outflow and collimation have simply invoked some central supply of energy and material. For instance, Blandford and Rees (1974) postulated a point source of high-entropy gas in the center of a stationary flattened gas cloud; they showed, by a gas-dynamical treatment, that this gas could squirt out in collimated jets (with terminal velocity depending on the specific enthalpy of the injected material), but did not consider the induced motions in the cloud, nor how the power and mass flux might be supplied.

A self-consistent model incorporating inflow and outflow must explain how some fraction of the matter can acquire more than its share of energy (i.e., a high enthalpy or p/ρ). Possible flows of this type were suggested by Shakura and Sunyaev (1973) in the context of a thick supercritical accretion disk which exhibited inflow along the equator and outflow near the poles. Whether these flows can be realized depends on the details of the viscosity (see Sec. III.C.3). If the radiation-supported gas adopts a hydrostatic toroidal configuration, then a pair of funnels will be defined which, as Lynden-Bell (1978) argued, could be responsible for the production of jets. The jets in these funnels will be driven by radiation pressure. Relativistic outflows with modest Lorentz factors can be achieved, especially if there is an electron-positron plasma in the funnel. However, this mechanism cannot convert a high fraction of the overall luminosity into a relativistic jet, for reasons discussed in Sec. III.D.2 below. Radiation can be used much more efficiently to power jets if it is trapped within the gas during the acceleration phase. The gas (plus trapped radiation) then behaves as a fluid with very high entropy—indeed, it is possible that $p_{\rm rad}/c^2$ may exceed the *rest* mass density of the matter. Begelman and Rees (1984) have considered models in which an optically thick radiation-supported cloud surrounds a central energy source capable of releasing $L\gg L_E$. If this extra energy goes into only a small fraction of the gas in a central "cauldron," the resulting high-entropy material can escape relativistically through nozzles. The cauldron idea can be generalized to include precollimation by funnels or magnetic stresses, and acceleration due to forces other than radiation pressure. However, because it relies on the hypothesis that some turbulent process mixes energy into a fraction of the matter, the detailed physics of cauldrons may not be understood for some time.

Jets may also be produced electromagnetically. The potential difference across a disk threaded by open magnetic field lines can exceed 10^{20} V (Lovelace, 1976; Blandford, 1976), and this is available for accelerating high-energy particles which will produce an electron-positron cascade and ultimately a relativistic jet that carries away the binding energy and angular momentum of the accreting gas. Blandford and Znajek (1977) extended this idea to black holes and showed how the spin energy of the hole could likewise be extracted. A hydromagnetic description of this mechanism is more likely to be appropriate (Blandford and Payne, 1982; Phinney, 1983b).

1. Nozzles

Trans-sonic flow through a nozzle (Blandford and Rees, 1974,1978b; Rees, 1976) is capable of providing

precollimation under a wide variety of conditions. The only requirement is that buoyant material be injected at the center of a cloud of cooler (denser) gas, which is gravitationally bound in the central potential well of the galaxy. The interface between the two fluids is subject to Rayleigh-Taylor instability, which would result in parcels of buoyant fluid percolating through the cloud in an absolutely spherical system. However, if the isobaric surfaces in the cloud are slightly oblate, as they would be if the cloud were rotating or situated in an oblate gravitational potential, then the buoyant gas would emerge along the minor axis.

If a steady flow pattern is established, its form is calculable provided that an equation of state (or energy equation) is known for the buoyant fluid, and the pressure run $p(r)$ is known for the cloud. In the one-dimensional approximation with adiabatic flow (Appendix B Sec. 3), the problem is equivalent to the steady discharge of gas through a channel of variable cross section, except that here the external pressure rather than the cross-sectional area of the flow is specified as a function of position. The cross section adjusts to maintain pressure balance across the walls and forms a de Laval nozzle where the external pressure drops to about half the stagnation pressure (Blandford and Rees, 1974). A critical (trans-sonic) point occurs at the nozzle; further out, the flow is supersonic and the channel slowly broadens as the external pressure drops off. The channel cross section is proportional to the energy flux carried by the jets, and varies inversely with the pressure in the cloud. One may straightforwardly take into account heating or cooling of the buoyant fluid in these calculations. In the subsonic region, the effect of heating is to increase the Mach number of the gas over what it would have been in the adiabatic case, while that of cooling is to decrease the Mach number M_j. The effects are reversed in the supersonic regime. Clearly the extent to which heating or cooling affects the flow depends on their competition with the pressure gradient, which always tends to increase M_j. If the buoyant gas is injected with enthalpy not much greater than the escape enthalpy, then gravity will be important in determining the position of the nozzle and the jet's terminal velocity. As in the case of a spherical wind, a larger gravitational field at the stagnation point brings the nozzle in closer but decreases the terminal velocity.

Even if equilibrium flow patterns exist that can give rise to jets, they may be subject to serious instabilities. Given the difficulty of predicting the stability of terrestrial and laboratory fluid flows, one should be cautious about attaching too much weight to such calculations when they are applied to the flow of magnetized (possibly relativistic) plasma flowing through a medium of uncertain properties. Kelvin-Helmholtz instabilities can occur anywhere along the beam's path (see Sec. II.C.5); but even more serious is the possibility that the setting up of the collimated flow may be completely prevented by Kelvin-Helmholtz and Rayleigh-Taylor instabilities, both of which could in principle occur in the nozzle region.

Several authors (Wiita, 1978a,1978b; Norman *et al.*, 1981) have attempted two-dimensional numerical calculations of how the trans-sonic flow pattern might be set up. A gravitationally bound cloud is taken to be already established in a flat-bottomed potential well; the central source of "hot" plasma is then switched on; it inflates a bubble, which finally breaks out along the minor axis. In some cases, a quasisteady flow pattern may then be set up, similar to that predicted by the one-dimensional analysis. The most recent calculations along these lines are those of Norman *et al.* (1981,1983; see Fig. 17). They find that the twin-exhaust pattern seems stable only if the width of the nozzle is comparable with the scale height—i.e., for a limited range of energy fluxes (the external pressure being given). At too high a flux the flow pattern is disrupted by violent Kelvin-Helmholtz instabilities, while at too low a flux the channel quasiperiodically pinches off, due to Rayleigh-Taylor instability. The resulting flow, in the latter case, resembles a string of bubbles rather than a continuous jet, as was proposed by Gull and Northover (1973) in their model for Cygnus A. While these calculations are the best we yet have, they contain several simplifying features which could render the results unrealistic. First, they are based on assuming simple equations of state for each fluid. Second, they ignore the effects on stability of strong turbulence or large-scale cir-

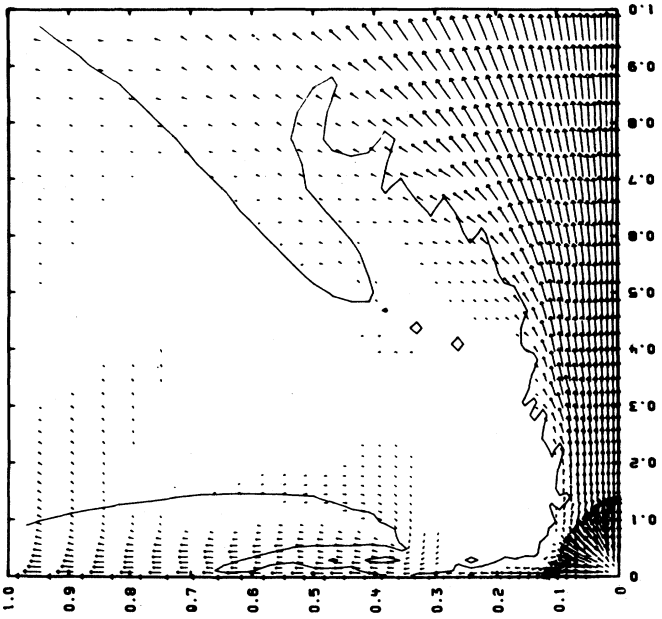

FIG. 17. Snapshot from a two-dimensional hydrodynamic calculation by Norman *et al.* (1981), showing the formation of a de Laval nozzle when hot gas is injected at the center of a flattened gas cloud. The solid line marks the boundary between high-entropy jet gas and the low-entropy confining cloud, and arrows indicate the velocity field. Note the central acceleration zone ending in a spherical shock (lower right-hand corner), and the nozzle located at ordinate ≈ 0.2. A torus of buoyant gas has also escaped along the equatorial plane. Reproduced, with permission, from Norman *et al.* (1981), © 1981 by the American Astronomical Society.

culation. In some models (e.g., the "cauldron" model of Begelman and Rees, 1984) such mixing processes play a dominant role. Furthermore, they use a two-dimensional code rather than full three-dimensional hydrodynamics. Thus the "instabilities" are due to ring-shaped protuberances around the flow boundary. It is not obvious whether this underestimates the instability—these axisymmetric perturbations are harder to excite than a localized perturbation; on the other hand, once they are formed, their effect on the flow is more drastic. (Norman and his collaborators have recently carried out some calculations—again in two dimensions—but for slab rather than axisymmetric geometry. These calculations can reveal "firehose"-type instabilities, and yield information complementary to that provided by the previous studies.)

Numerical simulations may also prove useful in examining how asymmetries affect the flow. If both the confining cloud and the source of buoyant fluid are symmetric about the equatorial plane, as is assumed in most calculations, then the flow should form a pair of identical jets pointing in opposite directions, termed a "twin exhaust" by Blandford and Rees (1974). This provides a natural explanation for the high degree of symmetry found in many extended double sources, both in the placement and luminosity of the lobes and hot spots (stronger sources) and in the symmetry of the luminous jetlike structures in weaker sources. Alternatively, *asymmetry* about the equator may account for the one-sidedness which is a common feature in many sources of moderate luminosity. For example, a jet may emerge on one side only if the source of buoyant gas is offset from the equatorial plane, as has been verified in simulations by Wiita and Siah (1981), Siah and Wiita (1983), Gull (1974), and Rayburn (1977). The jet would presumably reverse on the oscillation period of its source. Another possibility is a time-dependent flip-flop behavior, setting the surrounding gas into meridional circulation by friction with the jet (Icke, 1983). In either case, the presence of symmetric double radio lobes, even in sources with a one-sided jet, means that the jets must have squirted for comparable times in each direction, averaged over the source lifetime. Moreover, the last injection on the now-defunct side must have been sufficiently recent to generate the highest-energy electrons still radiating. But when jets are as long as in NGC 6251, each jet must squirt for $\gtrsim 10^8 (v_j/c)^{-1}$ yr between reversals. It is surprising that this interval should be so long. Only a small range of time scales can be squeezed between the two constraints.

The cloud which confines and collimates the jets must be gravitationally bound in a potential well, but its pressure must be sufficient to prevent it from collapsing into the center (or into a thin disk if it is rotating). Consequently, the value of (p/ρ) for the cloud material must be of the same order as the specific gravitational binding energy. As noted earlier, the nozzle is situated roughly where the pressure drops to half its stagnation value. This result is relatively insensitive to the steepness of the run of external pressure and to the equation of state in the jet material. Blandford and Rees (1974) envisaged that the cloud was confined within a flat-bottomed potential well due to the stars in the inner region of the galaxy, and supported by gas pressure. This required temperatures in the keV range, implying that the cloud itself would be a source of x rays. Observations by the Einstein observatory have placed constraints on this model for some sources, e.g., for Cyg A, Cen A, and M87.

If the confining cloud were much more compact, and in a deeper potential well, a higher value of p/ρ would be needed to support it. For clouds around massive black holes, where p/ρ may exceed $(m_e/m_p)c^2$, it becomes implausible to suppose that the pressure comes from an electron-ion plasma with $T_i = T_e$; the electrons would then need to be relativistic, and their cooling (via synchrotron and Compton processes) would be very rapid. There are two classes of model for a pressure-supported torus in a relativistically deep potential well. These are discussed in more detail in Secs. III.C.3 and III.C.4.

(1) The cloud may be supported by ion pressure, the electrons being cooled by radiative losses to $\lesssim 1$ MeV. (This option is plausible only when the density is low, so that the electron-ion coupling time is sufficiently long to prevent all the ion energy from being drained away too rapidly.)

(2) The cloud is supported primarily by radiation pressure. The gas temperature can then be lower than the virial temperature by the same factor by which radiation pressure exceeds gas pressure. If the cloud is sufficiently dense and opaque, the radiation will acquire a blackbody spectrum at temperature $T_{\rm rad}$, and the gas kinetic temperature will also be $T_{\rm rad}$. If radiation pressure provides the primary support, the leakage of energy must correspond to the "Eddington luminosity" for the central mass.

If the nozzle occurs close to a massive black hole—especially if it occurs in the domain where Lense-Thirring precession can enforce axisymmetry (Secs. III.D.8 and III.B.3)—the confining cloud lies in a potential well which is approximately of the form r^{-1}, rather than being flat bottomed. As Blandford and Rees (1974) already recognized, this may make it harder to establish a stable twin-exhaust geometry. The pressure in the cloud would fall off as $\sim r^{-4}$ (if supported by radiation pressure) or as $\sim r^{-5/2}$ (if supported by ion pressure); in either case, this falloff is so steep that a *homologous* perturbation of an equilibrium flow (e.g., expansion or contraction of the central cavity) may lead to instability. If, however, the confining cloud possesses some angular momentum, so that its pressure distribution has the form expected in the "donut" configuration, the prospects for stability are much improved. This is because the pressure can in principle rise by several orders of magnitude as one moves cylindrically out from the rotation axis. The effective "pressure" associated with rotation obeys a relatively hard "equation of state," with exponent $\beta = 2$ (see Sec. II.C.1). Thus even a drastic increase in the power of the central source need cause only a small enlargement of the channel. In computing such flow patterns, one should also take into account rotational effects in the jet material it-

self.

Finally, if the collimation is established on scales $\lesssim 10^2 r_g$, it ceases to be realistic to regard the confining cloud and the expelled jet material as separate entities: each is part of a rotational flow pattern in the gravitational potential well of a relativistic central body. Conditions in the cloud can change on the same time scale as the jet flow itself; the flow may involve continuous gradations in (p/ρ) rather than two distinct components.

Two features may make the nozzle mechanism applicable in a wide variety of situations. First, it works independently of the source of free energy or buoyant gas. Thus the precollimation and gas injection need not be considered as a single process, even in the context of a cauldron scenario (Begelman and Rees, 1984); and precollimation by a bound gas cloud may enhance or overrule other processes described in the following subsections. Gas injected preferentially along one axis may be redirected along the axis of the confining cloud, which may be different. Indeed, the energy in an already supersonic flow—either partially collimated or isotropic—may be randomized in a shock, then redirected through a second trans-sonic surface. The possibility of such "born-again" jets was discussed in Sec. II.C.1. Second, a nozzle may develop on any scale, and its qualitative features are scale independent. Thus precollimation may occur at a few hundred Schwarzschild radii if the cloud is bound to the central black hole, at tens to hundreds of parsecs if it is bound to the nuclear star cluster, and on scales of kiloparsecs if the cloud is of galactic scale. Chan and Henriksen (1980) have suggested that subsonic, uncollimated flow out to several kiloparsecs may be responsible for the gaps observed in many sources (see Sec. II.C.8) and have sought to associate the "turn-on" radius with position of the nozzle.

2. Funnels

Whereas nozzles are established by the dynamical interaction of an aspherical gas cloud with a stream of buoyant gas, funnels are better described as preexisting channels with rigid walls. The shape of the funnel is determined by the balance of pressure and centrifugal force in the external medium.

Two effects can give rise to funnels. In the first case, we might describe the funnel as the region of an accretion flow from which material is excluded by centrifugal force (see Sec. III.C.3). This has been discussed in the context of accretion from a nearly isotropic medium by Cassen and Pettibone (1976), Cassen (1978), and Sparke and Shu (1980), and in the context of thick-disk accretion by Paczyński and Wiita (1980), Jaroszyński, Abramowicz, and Paczyński (1980), Abramowicz, Calvani, and Nobili (1980), Begelman and Meier (1982), and Scott and Lovelace (1981). The shape of such a funnel depends on the distribution of specific angular momentum along its walls. For gas infalling from a nearly isotropic medium, this may reflect the original angular momentum distribution of the gas at large distances. In the disk case, it is more likely to be a function mainly of the viscosity and the equation of state. As a rule, the degree of collimation varies inversely with the magnitude of the specific angular momentum. Exploiting this fact, Sparke and Shu (1980) have suggested that double radio structure is associated with elliptical rather than spiral galaxies because of the former's slow rotation.

In a more detailed model (Sparke, 1982a) it is shown that in the weaker sources relativistic plasma produced in the nucleus can be recollimated along the spin axis of the infalling interstellar gas in the inner parts of the galaxy. This inflow may be assisted by magnetic braking (Sparke, 1982b). Stellar mass loss in the outer parts drives a radial wind. Radio source axes should be aligned with galaxy rotation axes, and inversion-symmetric jets can be attributed to precessional motion of the interstellar gas.

The second type of funnel occurs only in the innermost regions of thick accretion disks around black holes, and arises from purely relativistic properties of the potential well. It represents a "region of nonstationarity," within which no combination of pressure gradients and centrifugal force can support a stationary axisymmetric flow. All material within this region must either have positive energy (in which case it will escape) or else have so little specific angular momentum that it falls freely into the hole. On orbits bounding this roughly paraboloidal region, the specific angular momentum is nearly constant and marginally above the specific angular momentum of a zero-binding-energy orbit (which is located at $r=4r_g$ for a Schwarzschild hole; see Sec. III.B.3 and Appendix C Sec. 4). Thus the region of nonstationarity is bounded by circular orbits of zero binding energy, and a torus whose funnel coincides with this region displays the limiting behavior of the low-binding-energy disks discussed in Sec. III.C.3. Numerical simulations showing the establishment of such a funnel have been carried out by Hawley and Smarr (1984; Fig. 16).

As was the case for nozzles (Sec. III.D.1), funnels are compatible with any process which supplies hot gas near the base. Alternatively, material may be stripped from the walls of the funnel and subsequently accelerated. In either case, if the material expands to fill the channel laterally, then the degree of collimation is simply determined by the geometry of the funnel. To produce a supersonic jet, the trans-sonic surface should be located near the base of the funnel, since the monotonically diverging walls of the outer parts can increase the Mach number only if the flow is already supersonic (see Sec. III.D.1). Indeed, if the isobars outlining the funnel "turn over" at some characteristic radius, as they must do in a thick disk, then the emergent jet should be sufficiently supersonic to avoid sudden decollimation (see Sec. II.C.3) at the mouth of the funnel.

Acceleration within a funnel has been extensively studied only in the context of radiation-pressure-supported thick disks. The funnel shape depends on the angular momentum distribution within the torus. The narrowest funnels, roughly paraboloidal in shape, correspond to tori

where the angular momentum is independent of r, and where the surface binding energy is everywhere small (or the efficiency is low). Other angular momentum laws (less vulnerable to instability) tend to give broader and more conical funnels. If no mass were present inside the funnel, the total luminosity emerging from the funnel would exceed the Eddington limit by a factor of $\sim \ln(h/r_g)$, where h is the height at which the funnel "turns over," typically of order r_{tr}, the "trapping radius" (see Secs. III.C.2 and III.C.3). At least half of this luminosity, however, is concentrated in the solid angle subtended by the mean opening angle of the funnel, typically $\ll 1$ rad (Sikora, 1980a,1980b,1981). Thus the flux density perceived by a test particle placed at radius r within this solid angle would exceed the Eddington flux density for that radius by a factor of up to $\sim (h/r_g)\ln(h/r_g)$ (for the paraboloid, which is the most highly collimated configuration).

Most calculations to date have dealt with the radiative acceleration of a single particle placed within an otherwise empty funnel of specified configuration (Abramowicz and Piran, 1980; Sikora and Wilson, 1981). The radiation acts on electrons rather than ions, but the two species are strongly coupled electrostatically. Subtleties arise because the "reflection effect" (Sikora, 1981), i.e., photons bouncing off the walls of the funnel many times before escaping, may cause the mean intensity of radiation deep within the funnel to become many times larger than the flux density. As a result, radiation drag can prevent electrons from being accelerated to high velocities while inside the funnel. The drag becomes worse as the collimation of the funnel increases, in such a way that it roughly cancels the enhancement in flux density caused by narrowing the channel. Regardless of the funnel's geometry, if most of the radiation is multiply reflected, then the velocity of the outward-bound test particle *decelerates* as r increases, being everywhere some fraction of the local escape speed $(GM/r)^{1/2}$ (Sikora and Wilson, 1981).

However, not all photons are multiply scattered as they traverse the funnel. Since a funnel is open ended, each photon has a finite probability of being scattered into the "loss cone" with each scattering. This probability is proportional to the solid angle subtended by the open end, viewed from the place of scattering, and increases as the mouth of the funnel is approached. Thus the ratio of loss-cone intensity to "diffusive" (multiply reflected) intensity increases with radius, and approaches unity at some point within the funnel. Once this point is passed, particles begin to accelerate as they move out.

The final velocity and degree of collimation of an optically thin jet of radiatively accelerated particles depend on the shape of the funnel. In a conical funnel, the loss-cone intensity begins to dominate at a much smaller height than in a paraboloidal funnel of comparable mean opening angle ($\sim$diameter of funnel mouth$/h$), because the number of scatterings required for a photon to diffuse a given distance is larger inside the cone than inside the paraboloid, while the escape probabilities per scattering are the same for both. Although detailed calculations for funnels of various slopes (Abramowicz and Piran, 1980; Sikora and Wilson, 1981; Abramowicz and Sharp, 1983) indicate that accelerations to moderately large Lorentz factors with adequately high degrees of collimation are possible in principle, physical constraints on the stability of the funnel may limit the terminal velocity to $\gamma_j < 1.5$ (Piran, 1982). The maximum Lorentz factor may be larger if the accelerated gas consists of electrons and positrons rather than electrons and protons (see Sec. III.D.6), although the maximum degree of collimation is diminished.

The above models for acceleration and collimation become invalid when optical depth effects become important in the accelerated material (Sikora and Wilson, 1981). Thomson optical depths can become significant at rather modest flow rates, of order $(r_g/h)^{1/2}\dot{M}_E$ for a jet accelerated by loss-cone radiation and $\sim\dot{M}_E$ for a jet accelerated by multiply reflected photons in a paraboloidal funnel of height $\sim r_{tr}$. As the mass flux increases, both the degree of collimation and the rate of acceleration decrease. As Nityanda and Narayan (1982) point out, a mass flux of order $\dot{M}_E$ is virtually certain to be stripped off the walls of the funnel, since the radiation flux densities required to support the optically thick interior of a torus are incompatible with support of the optically thin funnel walls in centrifugal equilibrium (see also Narayan, Nityanda, and Wiita, 1983).

In addition to the inverse correlation between mass flowrate and acceleration/collimation, radiatively accelerated jets of low to moderate optical depth are unattractive because of their inefficiency in utilizing available energy. Two factors contribute to this inefficiency. First, for radiation pressure to support funnel walls of height $h \gg r_g$, the overall efficiency is probably lower than that of a thin disk. Second, a flow which is optically thin along the funnel cannot utilize the available radiation effectively, since most photons escape without suffering even a single scattering. Flows of moderate optical depth make greater use of the radiation energy, but pay for their increased efficiency by worsening collimation.

All of these difficulties can be avoided if the radiation is somehow injected into the gas mechanically rather than by diffusion, and if the gas is so optically thick that the radiation is trapped during the acceleration phase (see introduction to Sec. III.D). As long as the radiation remains trapped, the radiation-gas mixture behaves as an adiabatic, $\gamma = \frac{4}{3}$ polytrope. Fukue (1982) has considered isentropic outflow through a funnel, and has shown that relativistic terminal velocities can be achieved if the sonic point is sufficiently close to the hole. The perfect hydromagnetic generalization (without angular momentum) is considered by Fukue (1983). Mathematically, the gravitational field plays the role of a nozzle in the equations of motion, so that transonic flow is possible even in a steadily widening channel.

The degree of collimation with which an optically thick jet emerges from a funnel depends both on the power in

the jet and on the properties of the funnel. For example, consider a torus with a maximum pressure $p_{\max}$ and a paraboloidal funnel which turns over at a height h. If the stagnation pressure at the base of the jet is p_0 (related to the jet power by $L_j \sim p_0 v_j r_g^2$), then the jet will suffer poor collimation for the two extremes of high and low $p_0/p_{\max}$: (i) For $p_0/p_{\max} \ll (h/r_g)^{-2}$, the jet does not reach a very high Mach number before it exits the funnel, and as a result it diverges dramatically at the mouth of the funnel. (ii) For $p_0/p_{\max} \gg (h/r_g)^{-2}$, the jet exerts sufficient pressure on the walls of the funnel to widen it into a conical shape. The jet therefore diverges even *within* the funnel. In between the two extremes, when $p_0/p_{\max} \sim (h/r_g)^{-2}$, the jet can be maximally collimated to an open angle

$$\theta_{\min} \sim \left[\frac{h}{r_g}\right]^{-1/4} \tag{3.18}$$

which is larger than the geometric opening angle of the empty funnel, by a factor $(h/r_g)^{1/4}$.

A radiation-dominated jet interacts with surrounding gas in other ways which are calculable, but which have not yet been widely explored in the literature. Potentially important effects include the sideways leakage of radiation from a jet, which must accompany decollimation (because radiation flow provides the centripetal force necessary to accelerate the gas along a curved trajectory), and the effect of radiation viscosity (the optically thick analog of Compton drag) on the shear layer between the jet and its channel.

3. Winds

Many types of outflow, any of which might occur in the nuclei of radio sources, may be lumped together under the heading "winds." All that is required for a wind to be established is a source of fluid and some means of injecting the fluid with sufficient energy to escape. The types of winds most commonly discussed in astrophysics are quasispherical, and involve either the distributed injection of mass and energy over a sizable region, as in the galactic winds studied by Mathews and Baker (1971), or the injection of energy into the base of a hot corona which overlies a denser substrate, as in the solar wind. In active galactic nuclei, either description may apply, depending on the nature of the "prime mover" (see Sec. III.B). For multiple supernova (Colgate, 1967) or pulsar (Arons, Kulsrud, and Ostriker, 1975) models, the outflow may be essentially a compact version of a Mathews-and-Baker-type wind. Alternatively, a "distributed" wind may be driven by pressure or heating due to the absorption of energy and momentum by the gas, including Compton scattering, free-free absorption (Krolik, McKee, and Tarter, 1981), and resonance line absorption and scattering (e.g., Dyson, Falle, and Perry, 1980). The "coronal" type of wind would be associated with the surface of an accretion disk, the geometry of which may be quasispherical or roughly planar. Several mechanisms for heating the corona have been proposed, including acoustic waves due to convection (e.g., Shakura, Sunyaev, and Zilitinkovich, 1978) and hydromagnetic instabilities (Galeev, Rosner, and Vaiana, 1979). These tap the energy released within the disk as a result of accretion. Compton heating may also drive a wind from the surface of a disk, if there is an external source of sufficiently hard radiation (Begelman, McKee, and Shields, 1983; Begelman and McKee, 1983). Alternatively, the wind may be driven by radiation pressure, probably by Thomson scattering of radiation from within the disk or from a central source (Icke, 1977,1980; Bisnovatyi-Kogan and Blinnikov, 1977; Shakura and Sunyaev, 1973; Meier, 1979; Frank, 1979).

Winds driven by radiation pressure have been the best studied to date. If the coupling between gas and radiation is through resonance line absorption, then the cross section per ground-state particle is many orders of magnitude larger than the Thomson cross section per electron. Effective acceleration is then possible even for very sub-Eddington luminosities if the ionization state of the outflowing gas can be kept sufficiently low, i.e., if the kinetic temperature of the gas is $\sim 10^4$ K for hydrogen lines and $\lesssim 10^6$ K for x-ray resonance lines of oxygen and iron. For luminosities typical of quasars, this means acceleration starting at radii $\gtrsim 10^{16}$–10^{17} cm, with terminal velocities limited to $\lesssim 3\times 10^4$ km s^{-1} because of the divergence of the photon flux from the central source. Resonance line acceleration has been proposed mainly for inhomogeneous flows, e.g., to account for the high velocities of quasar emission line clouds (Blumenthal and Mathews, 1975) and some quasar absorption line systems, and is less suited to the acceleration of a relatively uniform wind. On scales where extragalactic jets are visible, there is no evidence for clumps of line-emitting gas comprising the jets themselves. However, in one Galactic jet, SS433, there is definite evidence that much of the mass is in cold clouds (Begelman *et al.*, 1980). Milgrom (1979) has suggested that line locking of the redshifted Lyman edge to the Lyman α line could explain the steady velocity of $0.27c$ in the outflowing gas; however, later work shows that it is very difficult to make line locking work in a realistic model for SS433 (Shapiro, Milgrom, and Rees, 1982).

Winds driven by Thomson scattering, mainly of radiation produced by the underlying disk, have been studied in both optically thin and optically thick limits. Bisnovatyi-Kogan and Blinnikov (1977) and Icke (1977,1980) calculated orbits of individual electrons in the radiation field of a radiation-pressure-supported thin disk. Both noted the disruptive effect of total disk luminosities in excess of $\sim 0.4 L_E$, and Icke pointed out a tendency for the trajectories of expelled particles to be somewhat collimated parallel to the disk axis, provided that the luminosity is not too large. Icke's investigation did not take into account the initial angular momentum of particles, which would tend to decollimate the orbits but make it easier for the particles to escape.

As noted in Sec. III.D.2, acceleration of optically thin gas by Thomson scattering is intrinsically inefficient, be-

cause only a fraction τ of the photons give up their momenta to the electrons, where $\tau \ll 1$ is the optical depth along a typical photon path. In addition, the maximum velocity attainable, while possibly relativistic, is limited to bulk Lorentz factors γ_j of $\lesssim 2$—5 for an electron-proton plasma being accelerated by a source whose total luminosity does not much exceed L_E. Acceleration is limited by two effects, the first being radiation drag due to a nearly isotropic component of intensity (in the electron's frame) when the distance from the source is $\lesssim \gamma_j$ times the extent of the source. At larger distances the $1/r^2$ decline in radiation density limits acceleration. These are the same effects that limit radiative acceleration in funnels (Sec. III.D.2), where the flux density may greatly exceed the Eddington limit but where the narrowness of the funnel increases the drag correspondingly. If a source could possess quasispherical geometry and nevertheless have $L \gg L_E$, then the terminal Lorentz factor would increase $\propto L^{1/4}$ (see Sec. III.D.6). Note that all of the above effects are still important in an electron-positron plasma, although terminal Lorentz factors are scaled up by a factor $(m_p/m_e)^{1/4} \sim 6.5$ as a consequence of the lower inertia per unit cross section.

Optimal use is made of the radiation momentum if the optical depth of the accelerated gas approaches unity. However, one may obtain much higher energy input into the wind by tapping the energy flux of the radiation. The latter requires $\tau \gg 1$ by an amount which depends on the temperature of the electrons as well as the spectral properties of the radiation. As the energy use becomes more efficient, however, the terminal velocity decreases and may become mildly relativistic or subrelativistic. In the limiting case the radiation is initially trapped in the outflowing wind, and the radiation-gas combination behaves like a fluid with an adiabatic index of $\frac{4}{3}$. An extensive array of idealized wind models, spanning a wide parameter space, have been constructed by Meier (1979, 1982a,1982b,1982c), who also included the angular momentum of the wind, viscous effects, and the possibility of heat deposition by convective fluxes. In the limiting case of a fully trapped flow, radiative transfer effects may be neglected, and it is feasible to draw parallels between radiation-dominated flows and hydrodynamic flow with different equations of state. Bardeen (1978) and Bardeen and Berger (1978) have constructed self-similar gas-pressure-dominated flows, including simple models for local heating due to convection or viscosity. Both sets of models show tendencies to form winds, which in some cases appear to be rather well collimated.

A somewhat different approach to radiatively driven winds has been explored by O'Dell (1981) and Cheng and O'Dell (1981), who note that the relativistic radiation reaction force on an electron in inverse Compton scattering is proportional to $\gamma^2(1-\beta\cos\theta)^2$ (see Appendix A Sec. 6). This implies that an isotropic cloud of relativistic electrons will move like a rocket when the radiation field is anisotropic. Relativistic speeds can be achieved, although this process appears to result in unreasonably large heating rates if the electrons are to explain observed sources (Phinney, 1982).

Winds may also be driven by Alfvén waves (Yokosawa and Sakashita, 1980). The idea here is that outflowing particles transform their momentum density into resonant Alfvén waves (see Sec. II.C.7), which propagate parallel to an ordered magnetic field. Half of the momentum density is deposited in the background medium, which is therefore driven outwards. It is therefore possible in principle to drive a cold outflow. In practice the Alfvén wave amplitude is likely to be sufficiently nonlinear that the waves will be damped by the gas, which will then be heated.

From the variety of examples mentioned, it should be clear that the "wind" idea holds promise for producing at least the hot gas of which jets are made. It is less clear that it can provide the necessary "precollimation." The planar geometry of a thin disk provides directionality, and associated winds may show substantial collimation if they pass through a critical point sufficiently close to the surface (Katz, 1980). However, angular momentum in the accelerated gas works against such collimation, and simple models involving radiation pressure, both optically thick and thin, have not yielded encouraging results. Likewise, with a few exceptions, the self-similar hydrodynamic models do not produce an exceptionally high degree of collimation. Thus one probably should not expect precollimation into less than ~ 1 rad from any wind flow. More encouraging is the immense variety of flows which may be engendered as winds, from the ultrarelativistic flows resulting from electromagnetic processes (Sec. III.D.6) through the somewhat relativistic flows of low optical depth driven by radiation pressure, to the mildly relativistic and subrelativistic flows characterized by hydrodynamic processes (and hydromagnetic effects, which we consider separately in Sec. III.D.5).

4. Plasmoids

In the early days of radio source studies, theorists commonly attempted to model the components of double sources by envisaging two blobs of magnetized plasma ("plasmoids") which were ejected from the parent galaxy and plowed their way out through the external medium. If they were advancing supersonically, and were confined by the ram pressure of the external medium, then the relationship between v, the external density, and the internal pressure would be the same as for the beam model (De Young and Axford, 1967). However, the momentum would have to be provided by the inertia of the "plasmoid"—implying that it must contain thermal material—instead of by the continuing thrust of a beam.

It now seems clear that the energy content of extended radio sources is not supplied impulsively. Even so, jets could be created out of many small plasmoids that merge to form a jet by the time that they have traveled several parsecs, the scale of the compact radio sources (see Christiansen, 1971). This inhomogeneity on the shortest scales is apparent in optical and radio observations of SS433 (Margon, 1982; Hjellming and Johnston, 1981).

Two mechanisms for creating these small-scale projectiles have been discussed. If an explosion occurs in an exponential atmosphere (e.g., Kompaneets, 1960), most of the energy can be channeled into a very small solid angle (Sanders, 1976; Mollenhoff, 1976; Shapiro, 1979a,1980). Alternatively, an expanding blast wave may be subject to dynamical instabilities which cause the post-shock flow to break up into several dense clouds, the trajectories of which will subsequently be focused down the density gradient by aerodynamic forces, as advocated by Christiansen, Scott, and Vestrand (1978).

5. Hydromagnetic jets

Magnetic fields have long figured prominently in models designed to account for the double nature of extragalactic radio sources. Magnetic fields can operate in two different ways, *passively* in defining a channel along which a stream of high-energy particles can flow, and *actively* if the field itself carries a major component of the power leaving the nucleus.

In passive models (e.g., Levy, 1971; Kurilchik, 1972; Ozernoi and Ulanovskii, 1974; Sanders, 1974; Jaffe and Perola, 1973), the magnetic field lines must be anchored within a massive object. If, for example, we assume that the field in a compact radio source is unidirectional, of strength $B \sim 0.1$ G, and the source size is $d \approx 3$ pc, then the flux is $\Phi \sim Bd^2 \approx 10^{37}$ G cm^2. If this flux emerges from a self-gravitating object of mass M and size R, then the virial theorem tells us that $B^2/8\pi \times R^3 \lesssim GM^2/R$, i.e., the mass M must exceed $10^3(\Phi/\text{G cm}^2)$ g $\approx 10^7 M_\odot$ (Sturrock, 1965; Sturrock and Feldman, 1968). In fact, this is a lower limit because it is likely that only a small fraction of the flux threading the massive object connects with the radio source. If the field is dipolar and $M \lesssim 10^9 M_\odot$, then $R \gtrsim 10^{17}$ cm.

The field strength in the vicinity of the compact object is undoubtedly strong enough to cause relativistic electrons to radiate away all their transverse gyrational energy on an outflow time scale. (In fact, for a dipolar field, the radiation rate for outflowing electrons conserving their first adiabatic invariant decreases with increasing radius r in proportion to r^{-9}.) The situation is somewhat similar to that encountered in pulsars, and electrons would presumably stream outward almost parallel to the field until they were scattered in pitch angle, within the radio components. For protons of similar energy, the synchrotron cooling times are a factor $\sim (m_p/m_e)^3 \sim 10^{10}$ longer, and synchrotron losses are unimportant.

These constraints are considerably ameliorated if, as in most models, rotation of the source of field is important. The field lines will be frozen into the expanding plasma and, as discussed in Sec. II.C.4, they will soon become predominantly toroidal. If the fluid velocity v is roughly constant, then the field strength will vary as d^{-1} where d is the transverse size of the outflowing jet. That is to say, instead of having to invoke a field strength of $\simeq 10^5$ G at $r = 10^{17}$ cm, we can instead infer a field strength of $\sim 10^4$ G at $\approx 10^{14}$ cm, comparable with the Eddington "equipartition" field near the Schwarzschild radius of a black hole of $10^8 M_\odot$ [see Eq. (3.9)].

The presence of toroidal field B_φ has three further general consequences. First, as discussed in Sec. II.C.4, there can be a magnetic tension associated with it that is large enough to collimate the outflow. Second, there will be an associated Poynting flux of energy $\sim (B_\varphi^2/4\pi)v_j$. This energy flux is in a form suitable for driving particle acceleration at large distances from the central source, in particular within the radio components. Third, as the magnetic field is not entirely toroidal but retains a poloidal component B_p that decays with distance as d^{-2}, there is also a flux of electromagnetic angular momentum associated with the outflow $\sim B_p B_\varphi d/4\pi$.

This last property is particularly important because spinars, magnetoids, and accretion disks are generally envisaged as supported against collapse by centrifugal forces (see Sec. III.B.2). Therefore, for every erg of energy lost by the gas, $\sim(\omega/1 \text{ rad s}^{-1})^{-1}$ g cm^2 s^{-1} of angular momentum must be lost, where ω is the angular velocity of rotation. In conventional accretion disks in binary x-ray sources, the orbit is the natural repository of this liberated angular momentum. As there is no simple counterpart to a binary companion in the case of a single spinning object in a galactic nucleus, magnetic torques provide a particularly attractive method for extracting the excess angular momentum. (This is basically the mechanism that is believed to operate in the sun, which has been decelerated to its present spin period over its lifetime by the action of magnetic fields frozen into the outflowing solar wind.) Note that in order to ensure dynamical stability in a spinning object, the specific angular momentum must increase outward (Rayleigh's criterion). If the object is supposed to liberate most of its energy through slow collapse or gravitational inflow, this means that most of the angular momentum is liberated at large radii, whereas most of the energy is liberated at small radii (near the event horizon in the case of black hole models). The associated jet may well comprise a core carrying most of the energy surrounded by a sheath carrying off most of the angular momentum.

These general considerations have motivated the development of several models in which the power is extracted electro- or hydromagnetically. As we described in Sec. III.B.2, it had been proposed that magnetic dipole radiation emitted by a spinar or magnetoid (in direct analogy to pulsars) could be self-focused into a jet by the nonlinear refractive index in an extremely tenuous plasma (e.g., Ginzburg and Ozernoi, 1967; Ozernoi and Chertoprid, 1969; Ozernoi and Usov, 1971; Morrison, 1969; Morrison and Cavaliere, 1971; Sturrock, 1971; Woltjer, 1971). However, the frequencies of these waves are very low (typically $\sim 10^{-6}$–10^{-8} Hz), and in the presence of a very low plasma density (typically $n_e \gtrsim 10^{-4}$ cm^{-3}) the displacement current is shorted out by the conduction current and a hydromagnetic description becomes more appropriate. Alfvén rather than electromagnetic waves are radiated.

Piddington (1970,1981) proposed that the spinning massive object contain a magnetic moment aligned perpendicular to the spin axis and that loops of magnetic field be twisted around the spin axis. These loops would reconnect, and the associated dissipation of magnetic energy would fuel the radio source.

In the case of a differentially rotating accretion disk (or possibly a spinar), it is the parallel component of the magnetic moment that is relevant. In the limit of strict axisymmetry, there are no waves radiated, but energy and angular momentum can be still be extracted. This is because the magnetic field lines will be frozen into the spinning gas (Appendix B Sec. 5). In the nonrotating frame there will be an electric field of magnitude $E \sim (v_{\rm Kep}/c)B$. As ionized plasma is freely available on the surface of the disk, any component of electric field parallel to the magnetic field will rapidly be shorted out, and so the "magnetosphere" above the disk must contain a charge density $\sim \omega_{\rm Kep} B/4\pi c$. Associated with this charge will be a poloidal current which supports a toroidal magnetic field and which, when combined with the electric field, furnishes an outflowing Poynting flux of electromagnetic energy and angular momentum.

The electromagnetic structure of the magnetosphere is undoubtedly highly complex. In one simple limiting physical description (Lovelace, 1976; Blandford, 1976) the magnetic field is assumed to be axisymmetric and force free. This last assumption implies that we are ignoring gravitational forces and the inertia of the plasma, and so $\rho\mathbf{E}+(\mathbf{j}\times\mathbf{B})/c=0$, where ρ is the charge density and $\mathbf{j}$ is the current density. The field lines that are frozen into the disk can be thought of as spinning about the symmetry axis with the angular velocity ω of the disk (Ferraro's law); they are bent backwards in the toroidal direction when the light surface (where $|\boldsymbol{\omega}\times\mathbf{r}|=c$) is reached, just as in the Goldreich and Julian (1969) model of an axisymmetric pulsar. The particles that are responsible for carrying the current need not carry much of the binding energy liberated by the disk. However, a comparatively small component of electric field resolved parallel to the magnetic field is adequate to produce ultrarelativistic electrons and ultimately γ rays and positrons (M. L. Burns, 1981 and Sec. III.D.6).

Plasma can easily flow from the disk into the magnetosphere, and a hydromagnetic description is probably more appropriate than the force-free approximation (Blandford and Payne, 1982). Consider, for example, a poloidal field line emerging from the disk and making an angle θ with the outward radial direction. Plasma that is attached to this field line will behave somewhat like a bead on a wire, and it is straightforward to show that if the disk is in Keplerian orbit and $\theta \lesssim 60°$, then centrifugal force will exceed gravity and gas will flow away from the disk surface. The natural assumption to make in this case is that the particle stresses ρv^2 are in rough equipartition with the magnetic and gravitational stresses. That is to say, the plasma in the magnetosphere is streaming outward at roughly the Alfvén speed $B(4\pi\rho)^{-1/2} \sim (GM/r)^{1/2}$ rather than the speed of light, as was the case with the force-free assumption.

The assumption of axisymmetry, although vital to analytical models, is unlikely to be realized in practice. Again we can turn for guidance to the sun, where only a fraction of the surface is covered by open field lines that connect with the solar wind. Small-scale loops of magnetic field will probably connect the disk with a hot corona above and below the disk. Reconnection of magnetic field lines will allow the material in the disk to flow inward, probably causing flares that will heat the magnetosphere and perhaps lead to observable variability (Shields and Wheeler, 1976; Galeev, Rosner, and Vaiana, 1979; Pudritz and Fahlman, 1982; Belvedere and Molteni, 1982).

We have described an efficient mechanism that can convert the binding energy of the gaseous disk into ordered electromagnetic energy and bulk kinetic energy. An important question is, can the same mechanism also extract the spin energy of the central black hole? To answer this, we must consider the dielectric and conductive properties of a black hole. If a Schwarzschild black hole is immersed in an electric field, then after the transients have decayed, a modified field distribution will be established in which the field appears to cross the horizon normally. That is to say, the hole's event horizon is an equipotential surface, and the hole is behaving like a conductor (Sec. III.B.3). Similar behavior is observed when the hole is immersed in a magnetostatic field. This behavior of the event horizon as a conductor is quite general. The black hole does not have perfect conductivity, however. If it did, the magnetic flux would never be able to penetrate the horizon. We know that electromagnetic transients decay in a time $\sim GM/c^3$ in the vicinity of the horizon, which must be compared with a time $\sim R^2/4\pi\sigma$ for field decay in a conducting sphere of radius R. We can then associate a surface conductivity of $(120\pi)^{-1}\ \Omega^{-1}$ with the horizon. (This analogy can be put on a rigorous basis: Znajek, 1978; Damour, 1978; Carter, 1979; Thorne and Macdonald, 1982; Macdonald and Thorne, 1982; Thorne and Blandford, 1982; Macdonald, 1984; Coroniti, 1983.) The average "internal resistance" of the black hole is then $\approx 100\ \Omega$.

The efficiency of the energy extraction from a spinning hole depends on how well the resistance of the external part of the circuit is "matched" to that of the black hole. If the matching is good, then the energy dissipated, L_{EM} (in the form of Poynting flux, particle acceleration, etc.) can be of order $B^2 r_g^2 c$.

Magnetic field lines supported by external toroidal currents (Chitre and Vishveshwara, 1975; King, Lasota, and Kundt, 1976) are therefore partly dragged by the hole and can be responsible for the extraction of some of the spin energy of a Kerr hole (see Sec. III.B.3), provided that currents can flow through the magnetosphere above the horizon (Damour, 1976; Wilson, 1976; Blandford and Znajek, 1977). This causes a difficulty because current-carrying particles must move inward across the horizon, but presumably travel outward at a large distance from the hole. This means that they must be continually creat-

ed within the magnetosphere, presumably as electrons and positrons. The most efficient mechanisms for achieving this near a $\sim 10^8 M_\odot$ black hole involve γ rays. For instance, if there is a small residual component of electric field parallel to the magnetic field, a stray electron will be accelerated until it can inverse Compton scatter an ambient x-ray (or uv) photon as a γ ray. This γ ray can then, in turn, create an electron-positron pair by colliding with a second soft photon. The vacuum will break down and a current will flow as this cycle repeats many times. Necessary conditions for this type of discharge are that the Compton optical depth in photons of some given frequency $\sim\nu$ exceed unity and that the electrons can be accelerated to the pair-production threshold energy $\sim(m_e c^2)^2/h\nu$ by the field-parallel electric field. Alternatively, if there is a thick, pressure-supported disk surrounding the hole (Secs. III.D.1 and III.C.3), then γ rays radiated by the hot plasma should be adequate to produce pairs within the magnetosphere.

The Blandford-Znajek (1977) energy-extraction mechanism is of particular interest in the case where $\dot{M}$ is low and the accretion itself is inefficient because an ion-supported torus forms in which $t_{\rm cool} > t_{\rm inflow}$. (The main radiation from the torus may then be bremsstrahlung γ rays.) If the hole is spinning at a rate close to the maximum for a Kerr metric ($a \approx m$), and β_p, the ratio of the ion pressure in the torus to the poloidal magnetic stress, is ~ 1, then the electromagnetically extracted power can exceed by α^{*-1} the maximum rate at which binding energy is liberated by the accreting matter. α^* is the dimensionless parameter which measures the ratio of the shear stress to the pressure (see Secs. III.B.3 and III.C.3). The torus will confine and begin to collimate the extracted power.

To extract more power from the hole than is released by accretion, we must have $\beta_p \approx 1$ and $\alpha^* \ll 1$. Is this consistent with a physically attainable disk structure? One might naively suppose that the poloidal field could be generated by currents distributed through the torus, and thus be an extension of an ordered field structure within it. But if this were the case, the internal fields would transport energy and angular momentum outwards so efficiently that $\alpha^* \approx 1$ and L_{EM} would be $\approx \dot{M}c^2$. Furthermore, in the presence of a magnetosphere any current loop in Keplerian rotation around a central mass loses vacuum energy from its outer light cylinder at a rate $(J/J_{\rm max})^{-2}$ times the rate at which it could extract power were the central mass a black hole of angular momentum J. If the current loop runs in an accretion disk, the missing power must be provided by the liberation of binding energy, which again implies $L_{EM} \approx \dot{M}c^2$ [compare with the thin-disk solution of Blandford and Znajek (1977) in which $L_{EM} \approx 0.3(J/J_{\rm max})^2 L_{\rm disk}$].

To understand how a torus could avoid all this energy transport and loss, it is helpful to consider the time evolution of a perfectly conducting torus with a very weak ($\beta_p \gg 1$) magnetic field piercing it at large radii. (It may also have internally closed field loops of arbitrary strength.) This weak field is advected inwards with the flow, and by applying Faraday's law to a sufficiently large loop encircling the rotation axis, we find that the magnetic flux through the funnel increases as we carry field in, even though the field lines are causally disconnected from the matter in which they were frozen after the matter has crossed the event horizon (Macdonald and Thorne, 1982). If the torus behaves like a perfect conductor, it will exclude this increasing external flux by developing surface currents. The field and surface currents will increase (perhaps shutting off the accretion altogether) until either some large-scale plasma-field interchange instability leads to an explosive energy release or, more likely, dissipation in the surface layer destroys the piercing field as fast as it is advected in. The structure of such a torus is rather different from that of the field-free torus: the $j_\varphi \times B_p$ force across the surface layer (funnel boundary) must be balanced by a gradient of gas pressure, so that at its base $p_{\rm gas} \approx B_p^2/8\pi$. If we want $\beta_p \approx 1$, most of the drop of gas pressure must occur in the surface layer, the inner parts of the torus being at roughly constant pressure.

We can imagine the following self-consistent solution for a torus with a jet: toroidal currents in the thin surface layer of the vortex funnel produce a poloidal field which is torqued by the hole, driving an outgoing Poynting flux. This will soon become plasma loaded; toroidal fields will begin to dominate, causing self-collimation (Blandford, 1976; Blandford and Payne, 1982; Chan and Henriksen, 1980). The return poloidal current must also flow in the thin surface layer, pulling material from it into the funnel, but leaving the bulk of the torus unaffected. The only forces from the jet transmitted to the body of the torus are those due to the poloidal field (transmitted by the gas pressure in the subcutis), the pressure of which drops as (area of funnel)$^{-2}$ and which thus has less effect on the structure of the torus the further out we go. Simple solutions ignoring the jet can therefore correctly model the torus, while the jet may collimate itself on the paraboloidal field lines thus defined without exerting much modifying force on the torus.

The above discussion shows how a torus supported by ion pressure, with a low accretion rate $\dot{M}$, can catalyze the extraction of a hole's spin energy at a rate exceeding $\dot{M}c^2$. Moreover (see the discussion of ion-supported tori in Sec. III.C.3), the luminosity from the torus itself may be $\ll \dot{M}c^2$. Thus, if the meager losses from the torus can be replaced by energy and angular momentum extracted from the hole, there need be no accretion: only the inertia of the torus, and the currents in it, are needed to confine the magnetic fields that tap the hole's energy.

The torus will generally be optically thin to Thomson scattering, with a total optical depth along a line of sight in the equatorial plane, from the hole to infinity, of $\sim(\dot{M}/\dot{M}_E)\alpha^{*-1}$. Incoherent cyclotron and synchrotron radiation will be self-absorbed. [The conditions envisaged resemble those of a so-called "plasma turbulent reactor" (Norman and ter Haar, 1975), so that a power-law spectrum may be set up.] The torus will, however, be optical-

ly thin to γ radiation produced by relativistic electron bremsstrahlung, and to inverse Compton radiation at $\gtrsim 10^{13}$ Hz.

The γ-ray flux from the inner regions of the torus (which may include a redshifted positron annihilation feature) would have only a small probability of being reabsorbed near the hole. Nevertheless, the small number of interactions that will occur can produce sufficient electron-positron pairs within the funnel to complete the circuit and allow electric current to flow through the hole. For example, to support an electromagnetic power of 10^{44} ergs s^{-1} in the funnel, a current of 3×10^{17} A must flow, which requires a minimum pair creation rate of $\sim10^{36}$ s^{-1}. This can be maintained by γ rays from the torus.

The maximum power that can be extracted self-consistently from a black hole by a thick ion-supported torus, $\dot{M}$ being given, is achieved when α^* has the lowest value consistent with the electron-ion decoupling condition $\dot{M}/\dot{M}_E \lesssim 50(\alpha^*)^2$. Even if $\dot{M}$ is a free parameter, the maximum power extractable by an ion torus is $\sim 10^{45}\alpha^*_{-2}M_8$ ergs s^{-1}. [However, if strong magnetic fields are anchored in a dense radiation-pressure-supported torus, whose thermal luminosity is L_E, there is no clear-cut reason why the power extracted electromagnetically from the hole should not be orders of magnitude larger. A "cauldron" model along these lines (Begelman and Rees, 1984) may be relevant to objects such as 3C273 where, in contrast to the radio galaxies, there is a nuclear thermal luminosity $\sim L_E$, but where there is evidence also for a powerful relativistic jet.]

As already mentioned, the energy extraction approaches maximal efficiency only if the proper "impedance match" is achieved. When the power emerges as a magnetized e^+-e^- wind, one would like to know whether anything resembling this optimal situation can be set up. Phinney (1983b) has considered wind solutions relevant to this model (Fig. 18). He supposes that e^+-e^- plasma, created in some region outside (but close to) the hole, flows inward (into the hole) and outward; he considers the critical points for each flow. If MHD can be applied (even though the rest mass density of the particles is negligible compared with the magnetic energy density), then the ratio of the effective external resistance to that of the hole is $\Omega^F/(\Omega^H-\Omega^F)$, where Ω^H is the hole's angular velocity and Ω^F the angular velocity of the field lines. Phinney finds that there are consistent wind solutions where Ω^F is as large as $0.18\Omega^H$, corresponding to an efficiency 62% of the maximum.

Rees *et al.* (1982) argue that electromagnetic extraction of energy from holes surrounded by (low-$\dot{M}$) ion-supported tori is the dominant power source in strong double radio galaxies. These radio galaxies almost cer-

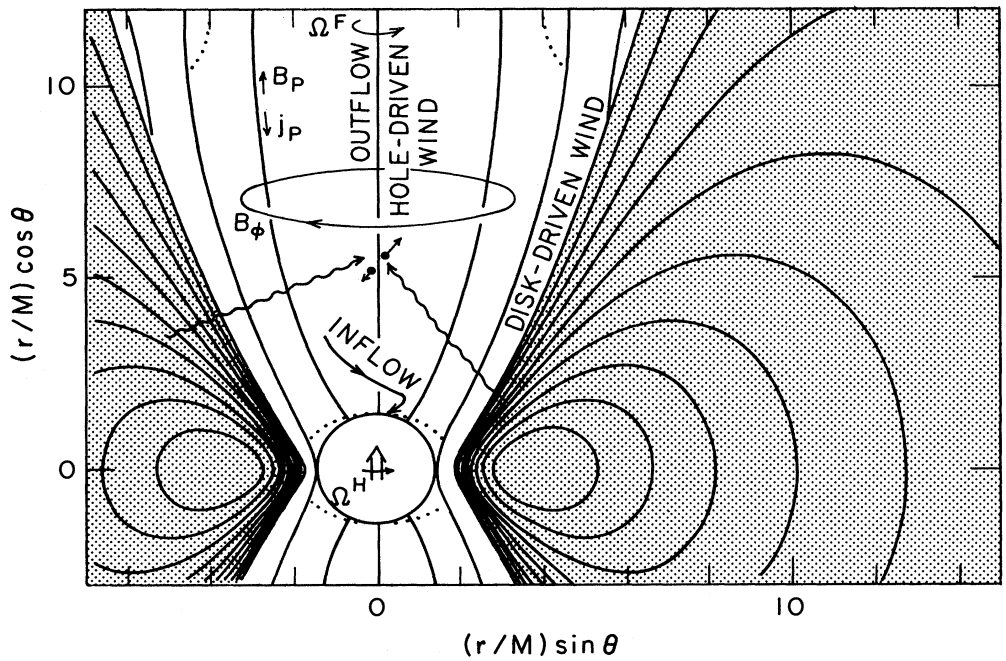

FIG. 18. Cartoon illustrating the features of a hydromagnetic wind driven by a Kerr black hole with a large angular momentum parameter $a/M=0(1)$. *Stippled:* external matter confining a poloidal magnetic field B_p to the hole. The precise geometry is unimportant; that shown is appropriate for a pressure-supported torus with constant specific angular momentum. *Wavy lines:* γ rays generated in the external matter create pairs in the otherwise empty "zone of nonstationarity" from which accreting material is excluded. On field lines which cross the event horizon, these pairs carry the current j_p which extracts rotational energy from the hole in the form of a direct-current Poynting flux. *Dotted lines:* the light surfaces for a simple MHD wind solution. The fast magnetosonic point is off the scale of the picture. Figure supplied by E. S. Phinney from Phinney (1983a).

tainly do have low fueling rates. Low-luminosity double-jet radio sources of the sort being mapped with the VLA generally have no detectable nuclear emission in the optical or x-ray bands; of the more powerful double-hot-spot radio sources, only a few (such as 3C390.3 with $\sim 2\times 10^{44}$ ergs s^{-1} in both optical and x-ray bands, and Cygnus A with $\sim 2\times 10^{43}$ ergs s^{-1} in the optical continuum) have nuclear luminosities above 10^{42} ergs s$^{-1}=10^{-4}M_8^{-1}L_E$. They cannot be produced by any process requiring super-Eddington luminosity, unless the mass of the hole is very small. This it cannot be, because some low-luminosity radio sources have giant ($\sim$Mpc) extensions with minimum energies of up to 2×10^{60} ergs$=10^6 M_\odot c^2$. Even if we make optimistic estimates of the efficiency of the central "engine" and of the likely efficiency with which power emitted from the nucleus can accelerate relativistic electrons in the radio lobes, we must conclude that a mass of at least 10^7–$10^8 M_\odot$ is involved.

The jets which power extragalactic sources are collimated on scales smaller than 1 pc. VLBI observations reveal small-scale structure, which is generally aligned with larger-scale structure. Misalignments of up to $\sim 45°$, which have been found in the core-dominated superluminal sources, are probably caused by viewing a slightly curved jet along an almost parallel line of sight. In the case of the cores of extended radio sources, however, the alignment is fairly good. Any mechanism which purports to explain them must, therefore, be capable of producing collimated jets of at least transrelativistic velocities while radiating as waste heat much less than an Eddington luminosity. Furthermore, in some sources, the mechanism must put orders-of-magnitude more power into the jet than escapes as (detectable) radiation directly from the nucleus. These constraints preclude the presence of radiation-pressure-supported tori in the nuclei of powerful radio galaxies.

6. Electron-positron jets

In recent years, it has been recognized that electron-positron-pair plasmas may play an important role in creating and processing the nonthermal photons that we observe from active nuclei. Thermal plasmas where kT_e attains values $\gtrsim 1$ Mev will create e^+-e^- pairs as well as bremsstrahlung photons. The fundamental collisional processes involved in these ultrahot plasmas have been discussed and reviewed by Gould (1981,1982a,1982b), Lightman (1982), and Svensson (1982a,1982b,1984). Moreover, in any compact source which contains a high concentration of photons with $h\nu > 0.5$ Mev (produced either thermally or nonthermally), pairs will be produced by $\gamma+\gamma\rightarrow e^+ + e^-$. The discovery of a positron annihilation line from the nucleus of our galaxy has further motivated research on these possibilities (Riegler and Blandford, 1982).

A pair-dominated plasma, with only ~ 1 Mev of rest mass energy per electron, offers an enhanced possibility of attaining bulk Lorentz factors $\gamma_j \gtrsim 5$, as required in the superluminal sources, and produces zero Faraday rotation and depolarization. However, the processes for generating pairs are likely to occur only rather close to a black hole. We must therefore consider acceleration processes near a black hole, and also whether this type of plasma—however it is generated—can be collimated, and can propagate out to $\gtrsim 1$ pc distances without catastrophic annihilation having occurred. The collimation is presumed to take place at smaller r, either via gas-dynamical processes or via electromagnetic effects.

a. Radiative acceleration

If e^+-e^- pairs are produced by electrodynamic activity near the event horizon of a black hole (see Sec. III.D.5), they are likely to be accelerated to high energy by electrodynamic or MHD effects. However, it is interesting to consider whether any pair plasma produced by (for instance) $\gamma+\gamma\rightarrow e^+ + e^-$ is automatically likely to attain a high γ because of radiation-pressure effects. It turns out that for a realistic radiation source, radiation pressure has significant limitations as a means of acceleration, even for a low-inertia plasma composed only of pairs.

Consider a test particle with cross section σ_T and an associated mass $\chi m_p c^2$ ($\chi=1$ for ordinary plasma; $\chi=m_e/m_p$ for e^+-e^- plasma). The terminal Lorentz factor can be estimated as follows, in the simple case where the source is a sphere of effective radius Kr_g and luminosity L. In the limit of zero inertia, the Lorentz factor saturates due to aberration into the forward hemisphere as seen from the moving particle (Noerdlinger, 1978), for

$$\gamma_{\rm sat}\simeq\left[\frac{r}{Kr_g}\right]. \tag{3.19}$$

However, in the absence of saturation (i.e., if the radiation effectively comes from a central point) but with finite inertia, the value of γ attained moving from r to $2r$ is

$$\gamma_{\rm acc}\simeq\left[\frac{L}{L_E}\right]^{1/3}\left[\frac{r}{r_g}\right]^{-1/3}\chi^{-1/3} \tag{3.20}$$

(this formula only applies when $\gamma_{\rm acc}\gg 1$). The terminal Lorentz factor is then that corresponding to the radius r at which $\gamma_{\rm acc}=\gamma_{\rm sat}$. Its value is

$$\gamma_{\rm terminal}\simeq\left[\frac{L}{\chi K L_E}\right]^{1/4}. \tag{3.21}$$

This illustrates the difficulty of obtaining a Lorentz factor larger than ~ 10, even for cold e^+-e^- beams, via radiation pressure. For nonspherical geometry the effects of radiation pressure are sensitive to details, but radiation can be important as an accelerator or as a cause of viscous drag, provided that the optical depths are $\lesssim 1$.

If the electrons form a plasma wind with random Lorentz factors $\gamma_r \gg 1$, but the radiation is from one side, then O'Dell (1981) and Cheng and O'Dell (1981) have shown that the energy released by inverse Compton cooling can go into directed motion (i.e., there is the possibili-

ty of boosting γ_j by a factor equal to the initial γ_r, just as in the case of adiabatic expansion). The terminal γ in this case, however, is still limited by $\gamma_{\rm sat}$. Phinney (1982) has given a detailed analysis of radiation-pressure acceleration, taking into account the "rocket" effect. The net result is that it is generally impossible to convert a large fraction of the radiative flux into kinetic energy of relativistic outflow.

Even if a jet can be accelerated to high γ_j (either by electromagnetic effects or by radiation pressure from a central source with $r \simeq r_g$), there is the possibility that it can be *decelerated* if it passes through an isotropic radiation field at much larger radii. This is an important constraint in quasarlike galactic nuclei which have a high radiative output in optical emission lines, since this line emission must come from radiation which is absorbed, and reemitted isotropically, at radii $r \gg r_g$. A jet would be vulnerable to Compton drag on passing through such a region. If we denote by $L(r)$ the luminosity emitted isotropically from shells of radii in the range r to $2r$, then the Compton drag on a jet moving from r to $2r$ will reduce its bulk Lorentz factor to

$$(\gamma_j - 1) \lesssim \left[\frac{L(r)}{L_E}\right]^{-1} \left[\frac{r}{r_g}\right] \chi \ . \tag{3.22}$$

This is a serious constraint, particularly on the velocities of relativistic e^+-e^- jets from quasar-type galactic nuclei. A more precise estimate of the emergent γ_j could be made only if the functional form of $L(r)$ were known—or, equivalently, the angular distribution of the radiative intensity at all values of r.

b. Annihilation and radiative losses

Consider an e^+-e^- jet which fills a solid angle Ω and carries an energy flux L_j. Then the pair density (measured in the moving frame) is

$$n_+ \simeq \left[\frac{L_j}{L_E}\right]\left[\frac{m_p}{m_e}\right]\left[\frac{r}{r_g}\right]^{-2}\left[\frac{\Omega}{4\pi}\right]^{-1} \gamma_r^{-1}\gamma_j^{-2} n_E \ . \tag{3.23}$$

The annihilation cross section for relativistic pairs is

$$\sigma_{\rm ann} \simeq \frac{3}{16}\sigma_T \frac{\ln\gamma_r^2}{\gamma_r^2} \ . \tag{3.24}$$

Since $n_E \sigma_T r_g \simeq 1$, this means that unless γ_j and/or γ_r were greatly to exceed unity, e^+-e^- jet luminosities would be limited to $\sim (m_e/m_p)(\Omega/4\pi) L_E (r/r_g)$. At first sight it must seem that annihilation would be suppressed in a jet with higher L_j if γ_r were $\gg 1$. However, the synchrotron cooling time would be less than the outflow time if the jet carried a field comparable with equipartition (unless these losses were suppressed by reabsorption). However, the main process that limits γ_r is inverse Compton scattering: this is quite catastrophic whenever the optical depth across the jet exceeds γ_r^{-2}. The losses due to Compton scattering of low-energy photons then vary not just as γ_r^2 but as a much higher power of γ_r (Rees, 1967b). Consequently an e^+-e^- jet with high L_j cannot retain a high γ_r and thereby reduce the annihilation rate. Vestrand *et al.* (1981) considered bremsstrahlung cooling and related processes for reducing a high γ_r, but they neglected the—generally much more important—synchrotron and Compton processes.

The only solution in which an e^+-e^- jet with $L_j \simeq L_E$ could emerge from a region of dimensions $r \simeq r_g$ without annihilating would be one in which the jet starts off with a bulk Lorentz factor $\gamma_j \gg 1$. If it started off with a high γ_r, then the random motions would not be converted into bulk motions as the jet expanded (according to the adiabatic law $\gamma_r \gamma_j \simeq$ const); instead, γ_r would be reduced by radiative cooling on less than the outflow time scale. Jets with high γ_j are, however, subject to Compton drag as they move through isotropic radiation in a galactic nucleus, so the resultant Lorentz factor would be limited by Eq. (3.22).

If annihilation occurs, the resultant γ-ray beam of characteristic photon energy $h\nu_\gamma$ could be reconverted into pairs at larger radii by interaction with x-ray photons of energy exceeding $(m_e c^2)^2/h\nu_\gamma$. This is an efficient loss-free method of channeling energy out of a region of strong magnetic field: it could be reconverted *in situ* into relativistic pairs, at the VLBI components.

Note that even if e^+-e^- plasma is involved in compact radio sources, searches for the 0.511-Mev annihilation line are not a promising diagnostic technique. It is true that the annihilation may occur after $(\gamma_r - 1)$ has been reduced to $\ll 1$ (especially if synchrotron or Compton cooling is efficient), but even then the bulk γ_j may be so large that the feature is smeared out. If the plasma initially has $(\gamma_r, \gamma_j) \gg 1$, any narrow unshifted line can represent only a very small fraction of the beam's total power output.

7. Can ultrarelativistic jets be generated?

There is no fundamental problem with generating jets with high γ_j (either of ordinary plasma or of e^+-e^- pairs) in cases when $L_j \ll L_E$, and where the photon luminosity of the galactic nucleus is too low to create serious Compton drag. Such jets could be produced through MHD-type processes, either off a disk or via a wind energized by a spinning black hole. Burns and Lovelace (1982) have proposed a cascade model of the equilibrium between electrons, positrons, and γ rays produced by a high-energy electron beam accelerated above a magnetized accretion disk. They find that a power-law electron distribution function may emerge. Their results, however, depend sensitively on the density and angular distribution of soft photons within the source, and on the importance of synchrotron losses.

Our foregoing discussion shows that a high photon density is surprisingly ineffective in producing high γ_j via radiation-pressure acceleration—indeed the Compton drag effect may *reduce* a high γ_j achieved in some other way. One might envisage that radiation pressure could be more efficient if the effective cross section were much

larger than σ_T. This would be the case if the relevant radiation were at frequencies lower than $\gamma_r^2 \nu_L$, where ν_L is the Larmor frequency, because synchrotron reabsorption would then occur. The reabsorption would also inhibit the synchrotron radiation losses, allowing the electrons and positrons to retain a high γ_r for the outflow time scale, even if the synchrotron cooling time scale (neglecting reabsorption) were much shorter. However, the inverse Compton losses will not be inhibited in the same way.

There are very severe constraints on possible mechanisms for producing intense ($L_j \simeq L_E$) ultrarelativistic jets near black holes in high-luminosity galactic nuclei. While annihilation in an e^+-e^- jet can be suppressed for given r and L_j if γ_j is made sufficiently large, the Compton drag effect precludes this possibility in a quasar-type environment. Even for an electron-ion plasma, Compton drag makes it very difficult to attain $\gamma_j \simeq 10$. This leads us to favor the view that in the observed "superluminal" quasars the energy emerges from $r \simeq r_g$ primarily as Poynting flux, only a small fraction of L_j being contributed by particle kinetic energy. An ultrarelativistic wind of the type discussed by Phinney (1983b) automatically has this property. The Poynting flux may not be converted into particle energy until it reaches distances of 1—10 pc, where radio emission is usually observed.

8. Jet axis

Most models for jet formation have in common the feature that the direction of the jet coincides with the instantaneous rotation axis of the material responsible for collimation. Since alignment (or gradual misalignment) is observed in some sources over many orders of magnitude in scale, and since extended structure may require $\gtrsim 10^8$ yr to be established, it is important to estimate the temporal stability of the jet axis in the various models.

If collimation occurs on kiloparsec scales, then the minimum time scale for changing the direction of the jet axis is the dynamical time $\sim 10^8$ yr for a typical galaxy. For an "isolated" galaxy in or outside a cluster, the net angular momentum of the stars plus interstellar medium should remain fixed for times exceeding $\sim 10^9$ yr, and the jet structure on all scales $\gtrsim 1$ kpc should be well aligned. (Any jets on smaller scales would have been collimated by a completely different mechanism in this case, and need not be aligned with the large-scale structure.) A number of events or conditions may lead to changes in the jet axis, including

(a) the interaction of the galaxy with a binary companion. Orbital motion may result in reflection ("*C*-type") symmetry (e.g., 3C31, 3C449; see Sec. II.D.2) and/or inversion symmetry (if tidal torques induce precession of the galaxy).

(b) accretion of an intergalactic H I cloud (see Sec. III.C.1). This would have a similar effect to a merger.

(c) any change in the rotation axis of the cloud that provides collimation and/or supplies mass for the jet. If the angular momentum of the cloud were misaligned with a symmetry axis of the galaxy's gravitational field, the cloud might precess on a time scale $\gtrsim 10^8$ yr. This could eventually bring the cloud and galaxy into alignment, and the wiggles in the jet trajectory would damp out.

If collimation occurs through a gas cloud or funnel associated with the stellar component of the galactic nucleus (scales ~ 1—100 pc), then the alignment of the jet axis depends both on the source of the gas and the shape of the potential well. Gas supplied by the body of the galaxy or captured from outside will generally retain its original axis, if the core is quasispherical and the gas passes through it sufficiently rapidly. However, if the gravitational potential is substantially flattened and the gas is retained for many dynamical times ($\sim 10^3$—10^5 yr), then it is likely to realign itself with the nucleus. Such realignment would tend to stabilize the jet axis against fluctuations due to the accretion of intergalactic clouds or tidal encounters with other galaxies, or precession due to binarism (the relatively compact nucleus would be less susceptible to tides and precession than the galaxy as a whole), but would have little effect on reflection symmetry due to orbital motion. Furthermore, changes in the jet axis occurring as a result of mergers might be *more* pronounced in this case, since the nuclei of the merging galaxies would rapidly spiral together under the action of dynamical friction. It should be noted, however, that there is a distinct preference for jets to be aligned roughly with the optical minor axis of the galaxy (Guthrie, 1979; Palimaka *et al.*, 1979; Shaver *et al.*, 1982), although it seems that this does *not* necessarily correspond to a galactic rotation axis in bright ellipticals. Of more direct relevance is the discovery by Kotanyi and Ekers (1979) that radio sources tend to be perpendicular to the central dust lanes when these are present.

A third possibility is that the jet alignment reflects the spin of a central massive object. Evidence for collimation on this small a scale is furnished by the observed correlation of the optical polarization direction with the large-scale radio source axis in quasistellar radio sources (Stockman, Angel, and Miley, 1979). Near a spinning black hole the Lense-Thirring dragging of inertial frames (see Sec. III.B.3) can enforce axisymmetry with respect to the hole's rotation axis, even if the inflowing material possesses angular momentum in an oblique direction. Thus, if the beams are collimated closer than the Bardeen-Petterson (1975) radius r_{BP} (see Appendix C Sec. 4), their orientation is, in effect, controlled by the "gyroscopic" effect of the hole: they are then impervious to jitter resulting from small-scale fluctuations in the flow pattern of the surrounding gas, and can swing or precess only in response to changes in the *hole's* spin axis. This stabilization is particularly important for jets collimated by "donuts" resulting from the tidal capture of individual stars [cf. Sec. III.C.1 and Frank (1979)]. Inversion symmetry of a pair of jets would result if the spin axis of the hole were slowly swung into alignment with the angular momentum of material being accreted or if the hole had a massive binary companion which caused it to precess (see Sec. II.D.3, and references therein).

IV. STATISTICS OF RADIO SOURCES

In this section we review the statistical properties of extragalactic radio sources and describe existing attempts to place them within an interpretive framework.

A. Taxonomy of extragalactic objects

The classification of active extragalactic radio objects has unfortunately not yet been standardized. This is partly for historical reasons, partly because of the conflicting perspectives of observers in different regions of the electromagnetic spectrum, but probably mostly because activity in the nuclei of galaxies is controlled by many more independent parameters than, for example, is the case for stars, where the observables luminosity and temperature are determined mainly by the physical quantities mass and age.

Quasars are defined by their optical properties (Ulfbeck, 1978; Hazard and Mitton, 1979). They are mostly starlike, although some show faint nebulosity (e.g., Wyckoff, Wehinger, and Gehren, 1981), and are more luminous than normal galaxies. Quasars are mostly found at large redshifts, $z \gtrsim 1$, although none are known with $z \gtrsim 4$. They are usually recognized by their broad emission lines ($\Delta z \gtrsim 0.03$). Roughly 10% of quasars are *radio loud.* The remainder are designated *radio quiet* (though not necessarily silent). Most of the compact radio sources (Sec. III.A.1) are quasars, although many radio-loud quasars are extended, having either symmetric double or highly asymmetric ("*D2*") structure (Miley, 1980; Perley, Fomalont, and Johnston, 1982). Radio properties of quasars appear to be correlated with their optical spectra. Extended radio sources tend to have broad and irregular emission lines, whereas the compact sources tend to exhibit narrower emission lines with smooth profiles (Miley and Miller, 1979). The majority of radio-loud and an uncertain fraction of radio-quiet quasars appear to be x-ray sources with a 1—3-keV x-ray luminosity which is typically a few percent of the optical luminosity (e.g., Feigelson, Maccacaro, and Zamorani, 1982).

The optical continuum radiation from quasars is often observed to vary, and roughly 10% of radio-loud quasars are designated *optically violently variable* (OVV) and can change their optical fluxes by a factor of ~ 2 in less than a week. OVV quasars can display high ($\sim 10\%$) linear polarization, which on occasion can vary even more rapidly (Angel and Stockman, 1980). Most of the other quasars show less than 1% polarization. Those low-polarization quasars that also possess double radio lobes exhibit a correlation between the optical polarization direction and the radio source axis (Stockman, Angel, and Miley, 1979; Angel and Stockman, 1980). Rapid variation (on times scales ~ 1 day) and high optical polarization (often exhibiting a preferred position angle) are also characteristics of another class of objects called *BL Lac objects* after the eponymous variable "star" *BL Lacertae* (Wolfe, 1978). These objects, which are also variable compact radio sources, are further distinguished by possessing weak or undetectable emission lines. It was E. Spiegel's prime contribution to this subject to coin the term "blazars" to describe the central continuum source in *BL Lac*'s and OVV's (Wolfe, 1978). Several low-redshift *BL Lac* objects are surrounded by a faint optical nebulosity which appears to be an elliptical galaxy.

By contrast, *Seyfert galaxies* are associated with spiral galaxies. Their bright, quasistellar nuclei have a luminosity function which joins smoothly with that of the low-luminosity quasars (Weedman, 1977). Seyfert galaxies are divided into two types. Type-1 Seyferts show broad permitted lines and relatively narrow forbidden lines similar to quasars, whereas Type-2 Seyferts show only the narrow lines. The radio luminosity of a Seyfert galaxy is typically $\sim 10^{39}$—10^{41} ergs s^{-1} (de Bruyn and Wilson, 1978; Wilson and Willis, 1980; A. S. Wilson, 1982), weaker than radio galaxies. A few Seyferts have nevertheless been shown to contain jetlike features in their nuclei up to several kpc in length (Wilson and Ulvestad, 1982). Most Seyferts are also powerful x-ray sources (Mushotzky, 1983). Seyferts show some similarities with the radio-quiet quasars. In particular, Fe II emission lines are prominent in both classes but not in the radio-loud quasars (Peterson, Foltz, and Byard, 1981).

Type-1 and Type-2 Seyferts have a parallel amongst the elliptical galaxies associated with strong radio sources, which are divided into *broad-line* and *narrow-line radio galaxies* (Osterbrock, 1978). Note, however, that many powerful radio galaxies show no evidence for any line emission.

Low levels of activity, including narrow emission lines, may be present in the nuclei of all normal galaxies (Dressel, 1981; Keel, 1983; Heckman, 1980; Balick and Heckman, 1982). The best studied example is, of course, our own. There is an unusual compact radio source within the galactic center, located in the middle of a powerful infrared source and identified with a powerful hard x-ray object. A strong, narrow, variable positron annihilation line is also observed (Riegler and Blandford, 1982). There is no reason to believe that our galactic center is atypical of spirals.

B. Radio luminosity functions

1. Source counts and the $\langle V/V_m \rangle$ test

Historically, the study of the disposition of radio sources and quasars in the universe had an immediate impact upon cosmology by effectively ruling out the steady-state theory. However, once it is admitted that sources may evolve, it turns out that evolutionary effects are observationally more important than the purely cosmographic differences between alternative world models. Therefore, the statistical properties of radio sources are significant primarily because they contain important clues as to what conditions are propitious for the formation of a powerful radio source within a galaxy, and how the

development of this source is controlled by its environment.

Two techniques are prominent in the statistical study of radio sources: source counts and the V/V_m test (e.g., Jauncey, 1977; Longair, 1978; Wall, 1979). Counts of radio sources in a given area of sky at a given frequency can be used to estimate the number $N(S)$ of sources of flux density exceeding S. If we lived in an unchanging Euclidean universe, we would find that $N \propto S^{-1.5}$. If we allow the universe to be Friedmannian but do not allow the sources to evolve with cosmic time, then there should be relatively fewer of the fainter sources than in a static universe. What is observed is that fainter sources are relatively more common than in a Euclidean universe, which implies that the comoving space density of powerful radio sources was far greater in the past than it is now (see Appendix C Sec. 3).

The $\langle V/V_m \rangle$ test can be used when the redshifts are known for a flux-limited sample of extragalactic objects. V is the total comoving volume out to the redshift of the source, and V_m is the comoving volume out to the maximum distance at which the source would still be included within the sample. The quantity $\langle V/V_m \rangle$ computed for a sample of strong extended radio sources lies typically in the range 0.6—0.7, again indicating strong evolution.

2. Space density of extragalactic objects

The results of these two tests can be used to estimate the space densities of different classes of extragalactic objects. This is conveniently expressed as Υ, the number per unit comoving cubic Hubble radius. Υ is a rough measure of the number of such objects in the accessible universe at the same cosmic time.

a. Galaxies

The luminosity function for galaxies of optical luminosity L_0 is roughly $L_0(d\Upsilon/dL_0) \simeq 5\times 10^8 e^{-(L_0/L^*)}$ (Kirshner, Oemler, and Schechter, 1979), where $L^* \simeq 10^{10} h^{-2} L_\odot$ is the characteristic luminosity of bright galaxies and the Hubble constant is $100h$ km s^{-1} Mpc^{-1} (see Appendix C Sec. 3). Roughly a third of bright galaxies with $L \sim L^*$ are ellipticals and two-thirds are spirals. Roughly 5% of ellipticals are radio sources (Auriemma *et al.*, 1977). The space density of giant ellipticals ($L \gtrsim 5L^*$) is $\Upsilon \sim 3\times 10^6$, of which about 10% are strong radio sources. cD galaxies are giant galaxies possessing extensive envelopes with $3L^* \lesssim L \lesssim 30L^*$, and have $\Upsilon \approx 10^4$. They are usually found in rich clusters and occur in about 5% of these. About half of the cD galaxies are strong radio sources (Burns, White, and Hough, 1981), and they figure prominently in catalogs of bright objects.

b. Quasars

(i) Radio-quiet quasars

The local density of quasars with $L_0 \gtrsim 3\times 10^{45} h^{-2}$ ergs s^{-1} is $\Upsilon \approx 10^4$. However, only a few percent of these have $L_0 \gtrsim 3\times 10^{46} h^{-2}$ ergs s^{-1}. At a redshift $z \approx 3$, Υ appears to be $\approx 10^6$. The brightest quasars in the universe have $L_0 \approx 10^{48} h^{-2}$ ergs s^{-1} if they are radiating isotropically. The local density of dead quasars depends on their assumed lifetimes, or equivalently on the total energies radiated. If each quasar radiates an energy Eh^{-3}, then Υ for dead quasars is $\sim 3\times 10^7\ (E/10^{61}\ \text{ergs})^{-1}$ (Schmidt, 1978; Green and Schmidt, 1978; Schmidt and Green, 1983).

(ii) Radio-loud quasars

The fraction of quasars which are radio loud ranges from ≈ 0.4 of the brightest (Condon *et al.*, 1981b) to only a few percent of the faintest. The radio and optical luminosities appear to be correlated (Schmidt, 1978). A few percent are OVV. Compact (flat-spectrum) quasars dominate high-frequency radio surveys. However, they do not appear to display as strong an evolution as the extended sources (Schmidt, 1978; Wall, Pearson, and Longair, 1981), except possibly at the highest luminosities (Peacock and Gull, 1981).

c. Seyfert galaxies

Roughly 1% of spiral galaxies are Seyferts with $10^{44} \lesssim L_o h^2 \lesssim 10^{45}$ ergs s^{-1} (Weedman, 1977), (i.e., $\Upsilon \sim 3\times 10^5$).

d. Blazars

The local density of OVV quasars is $\Upsilon \approx 60$ (Angel and Stockman, 1980). The density of *BL Lac* objects is very uncertain. Estimates range from $\Upsilon \approx 100$ to $\Upsilon \approx 10^4$ (Schmidt, 1978; Setti, 1978; Schwarz and Ku, 1983; Browne, 1983).

e. Radio galaxies

The local luminosity function of extended radio galaxies is given by

$$L_r \frac{d\Upsilon}{dL_r} \sim 2\times 10^5 \left[\frac{L_r}{L_r^*}\right]^{-1}, \quad 10^{40}\ \text{ergs s}^{-1} \lesssim L_r \lesssim L_r^* \approx 10^{42} h^{-2}\ \text{ergs s}^{-1}$$

$$\sim 2\times 10^5 \left[\frac{L_r}{L_r^*}\right]^{-2.5} \quad L_r^* \lesssim L_r \lesssim 10^{45} h^{-2}\ \text{ergs s}^{-1} \tag{4.1}$$

(Longair, 1978). Note that the luminosity L_r^* at which the luminosity function changes slope is roughly that which separates edge-darkened from edge-brightened radio galaxies (Fanaroff and Riley, 1974; Sec. I.C). At a redshift $z \approx 2$, the comoving density of the most luminous galaxies is ≈ 1000 times larger than locally. Weak radio galaxies evolve substantially less rapidly than this, if at all.

Extended radio sources are more often associated with galaxies than with quasars, in contrast to compact radio sources.

We are still not certain that quasars are associated with otherwise normal galaxies. The most reasonable conjecture has long seemed to be that the radio quasars are elliptical galaxies and that the optically selected radio-quiet quasars are powerful Seyferts associated with spirals. Studies of the nebulosity surrounding a few examples of both classes are consistent with this conjecture (Wyckoff, Wehinger, and Gehren, 1981; Boroson, Oke, and Green, 1982). Also, spectroscopic studies have shown that the Fe II lines are similar in radio-quiet quasars and Seyferts. We are confident that the quasar phenomenon is not confined to cD galaxies and giant ellipticals because these would already have been seen surrounding the nearest quasars.

Even though we do not yet understand the power source of active quasars in detail, it is hard to escape the conclusion that *dead* quasars would be massive black holes. These holes may lurk in the centers of many galaxies; they would be inconspicuous if they were now "starved" of fuel owing to the depletion of gas around them. Estimates of how many "dead" quasars exist are bedeviled by uncertainty about the lifetimes of individual quasars and the evolutionary properties of the quasar population.

An interesting argument bypassing the uncertainty in quasar lifetimes was recently presented by Soltan (1982). He points out that quasars contribute integrated background light amounting to 8×10^{66} ergs Gpc^{-3}. This is a lower limit: the actual value would be higher because of the contribution from faint quasars (Soltan assumed 200 quasars per square degree down to magnitude 22.5); also, there may be more luminosity in x rays than in the optical band. A lower limit of $8\times10^{13}(\varepsilon_e/0.1)^{-1}M_\odot$ Gpc^{-3} can then be placed on the total mass of the remnants, where ε_e is the overall efficiency with which rest mass is converted into electromagnetic energy over a typical quasar's active lifetime. This limit is independent of the individual quasar lifetime—it makes no difference whether 10 or 10^3 generations of quasars are born during a Hubble time. It does, however, imply the following:

(1) If the remnant masses were 10^8–$10^9 M_\odot$, there would be 10^5–10^6 of them per Gpc^3.

(2) If all bright galaxies ($M_B < -21.3$) (the space density of which is known) were at some epoch associated with quasars, the mean hole mass would be $>2\times10^7(\varepsilon_e/0.1)^{-1}M_\odot$. There may even be a dead quasar within the local group, and our galaxy may once have been a Seyfert galaxy and have a $\approx 10^6 M_\odot$ black hole at its nucleus (Bailey and Clube, 1978; Riegler and Blandford, 1982). Both Seyfert galaxies and radio-quiet quasars may be powered by supercritically accreting massive black holes with $L \approx L_E \approx 3\times10^{46}(M/10^8 M_\odot)$ ergs s^{-1}. Powerful radio emission would then be mostly associated with subcritically accreting black holes in which a higher fraction of the total emitted power is channeled into a relativistic electromagnetic or hydromagnetic wind. The association of source type with galaxy type then follows if large black holes are more likely to form in elliptical rather than spiral galaxies.

C. Angular size—redshift relations

The angular sizes of the largest extragalactic radio sources are observed to decrease inversely with increasing redshift z, just as one would expect in a Euclidean universe (Miley, 1971). However, in a Friedmannian universe, the angular size of a rod of fixed length z is given by z/d_A [see Eq. (C9)], and this generally has a minimum at redshift $z_{\min}$ dependent upon the density parameter Ω. (For $\Omega=1$, $z_{\min}=1.25$.) The main explanation of this difference is believed to be found in the luminosity-size relation for radio sources (Hooley, Longair, and Riley, 1978; Saikia and Kulkarni, 1979; see Sec. I.C). In a flux-limited sample, the more distant sources will be intrinsically more luminous and preferentially contain the 100–300 kpc edge-brightened double sources. Closer-by sources will be weaker, and on average larger. This selection effect can probably account for the observed $\theta(z)$ relation and almost certainly obscures the cosmological information contained within this distribution. A possible competing effect occurs because the mean density of the intergalactic medium (though not necessarily in clusters) was presumably greater in the past, which may have diminished the expansion of the radio components. However, the failure to see convincing evidence of this effect in comparing radio sources within and outside rich clusters (Sec. IV.D below) suggests that it is not very important. A third factor influencing the $\theta(z)$ relation is that the microwave background had a larger energy density [$\propto(1+z)^4$] in the past. Relativistic electrons within weak radio sources will have cooled more quickly than at present through inverse Compton scattering of the microwave background (Rees and Setti, 1968). This could have led to the premature death of large, weak radio sources at high redshift and thus could have skewed the observed $\theta(z)$ distribution. It is still not known whether or not there is genuine evolution of the sizes of extragalactic radio sources; hence we cannot learn anything useful about environmental influences on their structure from these studies (Downes, 1982; Kapahi and Subramanya, 1982; Onuora and Okoye, 1983).

D. Clusters and associations

Positional autocorrelation analyses of radio source surveys (Seldner and Peebles, 1978) reveal little if any clus-

tering. Since most of the sources in faint radio surveys are believed to lie at cosmological distances ($z \sim 1$—3), this result is taken to indicate isotropy on scales exceeding 100 Mpc. It tells us nothing about clustering on smaller scales because of the scarcity of sources on the sky. Cross correlations of galaxies (e.g., from the Lick and Zwicky catalogs) with radio sources indicate that the galaxies are clustered about radio sources much as they are about one another, i.e., with an overall cross-correlation function of the form $\omega(\theta) \propto \theta^{-0.77}$ (Seldner and Peebles, 1978). However, cross correlating galaxies with subsets of the radio data reveals that the amplitude of the clustering depends on intrinsic radio power and morphology. Longair and Seldner (1979) found that the weakest radio sources show no tendency to lie in clusters or groups. In contrast, extended powerful sources lie in regions which are 4—5 times as overdense as those surrounding typical galaxies, while the cross correlation between galaxies and classical doubles whose nuclei show strong emission lines is roughly the same as the galaxy-galaxy correlation.

Other correlations of radio activity with galaxy clustering have generally utilized smaller, more nearby radio samples in which the radio galaxies could be classified according to type. Gioia *et al.* (1981) examined a sample of radio sources associated with spirals and ellipticals, and found that galaxies in groups have a lower probability of being radio sources than do field galaxies. This appears to concur with Longair and Seldner's result for very weak sources, but most of the other surveys along these lines find a strong positive correlation between radio emission and the presence of neighboring galaxies. Stocke, Tifft, and Kaftan-Kassim (1978) found that isolated close pairs of galaxies are twice as likely to contain a radio source as wide pairs. Stocke (1978) generalized this conclusion to groups of galaxies, and argued that it applies equally well for ellipticals and spirals. Dressel (1981) found that ellipticals are more likely to be radio sources if they belong to a Zwicky cluster, and that this probability is increased further if the galaxy lies in a subgroup within the cluster; however, neither correlation holds for SO galaxies. Spirals with compact nuclear sources, however, do tend to be in pairs (Condon and Dressel, 1978; Hummel, 1981).

The consensus of these various studies seems to be that the presence of nearby neighbors enhances the probability of a galaxy's being a radio source. The two most common hypothetical explanations for this correlation are both related to the gas supply (Sec. III.C.1). They are (1) the increased likelihood of mass transfer between galaxies and (2) the possible triggering of mass inflow in the radio galaxy by tidal disturbances. It is interesting to note that the strongest correlations seem to involve the presence of *one* nearby neighbor, rather than membership in a group or cluster. Indeed, there are indications that properties of weak radio galaxies are insensitive to the richness of the surrounding galaxian environment, and that radio emission from normal galaxies may be *suppressed* in rich clusters, perhaps because the fuel supply is more easily stripped from the galaxy by its motion through the intergalactic medium (Gisler, 1976) or by thermal evaporation (Cowie and Songaila, 1978).

Studies of clustering around strong radio sources have concentrated on the role of giant elliptical and central dominant (cD) galaxies. Clusters containing such prominent galaxies have been labeled Types II and I, respectively, by Bautz and Morgan (1970), while clusters without a single dominant galaxy belong to Type III. There is apparently no correlation between cluster richness and Bautz-Morgan type. However, Longair and Seldner (1979) pointed out that when strong extended radio sources are found in rich clusters, the clusters are generally of Bautz-Morgan Type III. The parent galaxy in this case does not show strong emission lines, nor does the radio source exhibit strong double morphology. On the other hand, strong doubles tend to emanate from giant ellipticals or cD's, and show no preference for rich clusters. Longair and Seldner suggested that a precondition for the formation of a well-collimated double is a massive parent galaxy sitting near the bottom of the cluster potential, which can retain an extensive gaseous halo that confines the radio source lobes (cf. Norman and Silk, 1979). The hypothesis that the source environment is self-contained finds support in observational studies of cD sources (McHardy, 1979; Burns, White, and Hough, 1981) which show that (1) the probability of radio emission is independent of cluster richness and (2) properties of the radio source, such as spectral index and minimum pressure, are independent of cluster richness. Furthermore, x-ray and optical studies of dominant ellipticals have revealed extensive gaseous envelopes which in some cases (e.g., NGC 1275) appear to be in the process of being slowly accreted by the galaxy (Mathews and Bregman, 1978; Fabian *et al.* 1981; Burns, Gregory, and Holman, 1981). The infall, with concurrent thermal instabilities, could constitute one source of gas to fuel the activity in the nucleus. Other possible sources are discussed in Sec. III.C.1.

E. Beaming

As we have argued in Sec. II.A.4, there is evidence for directed relativistic motion in the superluminal sources. If this is true generally in compact sources, then the emission must be highly anisotropic and our perception of these sources must be largely governed by their orientations relative to us. If the opening angle of the directed outflow is smaller than $\sim \gamma_j^{-1}$, then we will see only the fraction $\sim \gamma_j^{-2}$ of sources which are aimed sufficiently close to our line of sight. Kinematic models of the superluminal sources suggest that γ_j lies in the range 5—10. In the very simplest type of model in which the radio core is the self-absorbed inner part of a conically expanding relativistic jet (Blandford and Königl, 1979b), the observed flux density is roughly

$$S_\nu \propto (1-\beta_j \cos\theta)^{-2} \propto (1+\gamma_j^2\theta^2)^{-2} \tag{4.2}$$

in the small-angle approximation (see Sec. II.A.4 and Appendix C Sec. 2); alternative but equally plausible geometrical assumptions lead to different exponents). For an ensemble of jets with the same intrinsic properties and

moving with the same speed, the source counts should satisfy $\Upsilon \propto \theta^2 \propto S^{-0.5}$ (Scheuer and Readhead, 1979). Scheuer and Readhead (1979) proposed that the unbeamed flux be measured by the optical luminosity and that the compact radio sources that are beamed away from us be identified with the radio-quiet quasars. As there are ~ 50 times as many radio-quiet as radio-loud objects, the Lorentz factor of the jets must be $\gamma_j \sim 7$, in rough agreement with the simple kinematic models of superluminal sources. In fact, there is probably a distribution of Lorentz factors, and a sample of sources selected without regard to orientation (e.g., on the basis of their extended emission) would be dominated by those of modest Lorentz factor $\gamma_j \sim 2$ (see Hine and Scheuer, 1980). Initially, this proposal appeared to be incompatible with studies of the brightest optically selected quasars (Strittmatter *et al.*, 1980; Condon *et al.*, 1981a,1981b; Smith and Wright, 1980), which found relatively few faint radio sources and therefore supported the view that the radio-quiet quasars constitute a separate population. However, a more sensitive survey by Kellermann *et al.* (1983) has detected two-thirds of the optical quasars, and indeed $\Upsilon \propto S^{-0.5}$. It remains to be seen whether this is due to relativistic beaming or whether the radio-quiet quasars have properties resembling the more nearby Seyferts. A further difficulty with the beaming hypothesis is that the halos found around many of the compact radio quasars, and which ought to be radiating isotropically, are not found around radio-quiet quasars (Browne *et al.*, 1982).

An alternative proposal (Blandford and Königl, 1979b; Browne *et al.*, 1982) is that the unbeamed sources be associated with the extended steep-spectrum radio sources and that the radio flux from the lobes be used as a measure of the intrinsic luminosity of the source. If this is the case, then the compact sources ought to be surrounded by low-surface-brightness, steep-spectrum halos, as indeed they often are (Perley, Fomalont, and Johnston, 1982; Moore *et al.*, 1981). Orr and Browne (1982) estimate the number/flux density counts of flat-spectrum quasars from those of steep-spectrum quasars by assuming a Lorentz factor ≈ 5 and random orientation, and find that unification of these objects by a beaming model is statistically consistent with the data. However, this simple model appears to fail quantitatively when we select quasars on the basis of their (presumably unbeamed) optical line emission rather than on the basis of their radio emission, because there are too few extended quasars to account for the unbeamed compact quasars.

There are further indications from individual sources that these simple kinematic models are inadequate (see also Sec. II.A.4):

(a) 3C179, so far the only radio source selected on the basis of its extended emission to be monitored with VLBI, shows superluminal expansion (Porcas, 1981). Furthermore, several cores of extended sources are known to exhibit superluminal flux variation consistent with $\gamma_j \approx 2$ (Hine and Scheuer, 1980).

(b) 4C39.25 is an extremely luminous compact source and yet shows no evidence for superluminal expansion.

(c) 3C345 has a compact component which appears to accelerate along a direction which does not pass through the core (Moore, Readhead, and Baåth, 1983; Biretta *et al.*, 1983).

From a theoretical standpoint, it is not surprising that simple kinematical models have to be rejected. We already have evidence that real jets are both more complex individually and more heterogeneous collectively than this. Some factors which ought to be included within realistic models are the following:

(i) Jets probably do not have a single outflow velocity. They probably contain more slowly moving material within shear layers and behind obstacles. Consequently the observed radio powers of the central cores of extended sources may not be $\approx \gamma_j^{-4}$ times the observed powers of compact sources. Furthermore, radio-emitting electrons cannot cool on the outflow time scale, and so jets could be surrounded by a sheath of isotropically emitting plasma. This may be relevant to the case of M87, which has a one-sided (kpc) optical and (pc) VLBI jet but a two-sided radio jet on kiloparsec scales (Rees, 1978b).

(ii) Extended radio sources may be ultimately collimated on length scales much larger than those probed by VLBI. In this case, the beamwidth of the emitted radio intensity may greatly exceed γ_j^{-1}. In the case of 3C273, where the radio power is lower relative to the optical than in other superluminal sources, the observed superluminal effects may be associated with peripheral emission (Rees, 1980).

(iii) The emitting plasma from the hot spots of the extended components may be moving mildly relativistically. Post-shock speeds $\sim c/3$ may occur if the beam speed is relativistic (even if the working surface itself advances slowly) and this may bias the statistics.

BL Lac's and OVV quasars can also be incorporated within this scheme. *BL Lac* objects may be relatively low-power radio galaxies beamed toward us and may also produce beamed optical continua that are sufficient to swamp the emission lines from the nucleus. Browne (1983) compares the space density of *BL Lac* objects ($\Upsilon \sim 5000$ down to a radio limit) with the space density of radio galaxies with extended components of similar radio power ($\Upsilon \sim 3 \times 10^5$) and finds that the *BL Lac* objects could indeed be beamed radio galaxies. OVV quasars would be versions of this phenomenon in which the emission lines are relatively stronger.

Optical and x-ray emission can be interpreted as Doppler-boosted synchrotron or inverse Compton radiation. Detailed models have been calculated by Königl (1981), Marscher (1980a), and Reynolds (1982a,1982b). In particular, several authors have argued for relativistic expansion on the grounds that without it inverse Compton scattering would produce more x rays than are observed (see Sec. III.A.2).

Of course, relativistic effects are not the only possible causes of beaming. Both free-free and synchrotron absorption could play a role in delineating the radiation

beam. However, the failure to detect a larger fraction of the optically selected quasars at radio wavelengths as the observing frequency is raised, together with the extreme physical conditions such absorption requires, makes this explanation seem rather implausible (Condon *et al.*, 1981a).

V. SUMMARY AND FUTURE PROSPECTS

In this final section we present a short summary of what we have learned so far about the physics of extragalactic radio sources. We comment upon the relationship of the radio emission to the general phenomenon of active galactic nuclei, and outline a unified model for the latter. We also describe what observational and theoretical progress can be expected in the near future.

A. Summary

1. Faith

In this review, we have tried to present a coherent theoretical interpretation of recent observational discoveries about extragalactic radio sources. This interpretation is based upon the physical notion of a jet—a continuous flow of fluid emanating from the nucleus of a galaxy and supplying the extended radio components with mass, momentum, energy, and magnetic flux. We contend that jets, whose existence was postulated before any good examples were discovered at radio frequencies, are an observational reality and must form the basis of any serious discussion of extragalactic radio sources. Alternative physical descriptions persist in the literature but, as we have discussed, these either conflict seriously with the observations or are similar to jets in most essential properties.

The jet description allows an immediate and appealing interpretation of many of the striking morphological features seen on maps of extended sources. The powerful edge-brightened double sources are relatively young objects aged $<10^7$ years in which the jets have so far penetrated only a few hundred kpc into the circumgalactic medium. The jets maintain their integrity, terminate at a strong shock within a hot spot, and have a fairly low radiative efficiency. In the weaker, edge-darkened sources, the jets are more susceptible to instability and sensitive to motion of their sources and the surrounding gas. Consequently they radiate away a larger fraction of their bulk kinetic energy, and the associated radio lobes have more complex shapes. Radio trails, which provide the most direct evidence for continuity of the jet flows, are extreme and striking examples of the interaction between a jet and its surroundings.

The energetics of radio sources inferred from radio observations are also consistent with estimates derived by independent means. Provided that the emission mechanism is synchrotron radiation and that the equipartition estimates are good to an order of magnitude, the pressures within the hot spots of the most powerful double sources are $\sim 10^{-8}$ dyn cm^{-2}. This is consistent with x-ray observations of circumgalactic gas which indicate that the gas density is $10^{-28}-10^{-27}$ g cm^{-3} and the temperature is 10^7-10^8 K, if the hot spots are confined by ram pressure. The associated static pressure appears to be sufficient to confine the lobes of the strongest sources. If we balance the hot spot pressure against the ram pressure of the surrounding gas, we conclude that the strongest sources must expand with speeds $\sim 0.1c$ and have ages ~ 3 million years. These jets must supply a power in excess of 10^{45} ergs s^{-1}, with a speed greater than $\sim 0.1c$; evidence of "Doppler favoritism" through one-sidedness in some sources indicates that the speed is probably relativistic. This power is within an order of magnitude of that associated with nonthermal activity in bright quasars. However, it is far smaller than that which would have to be invoked if the radio sources had been created impulsively, as was once thought to be the case. Larger jets appear to move more slowly than $\sim 0.1c$, and these are probably over 10^8 yr old. The total internal energies of these large sources can exceed 10^{61} ergs, although the associated pressures are typically only $\sim 10^{-13}$ dyn cm^{-2} and can probably be balanced by the pressure of the intergalactic medium.

The discovery of small-scale core-jet structure in the compact radio sources and the central components of extended sources indicates that jets are formed within regions much smaller than a parsec, although it does not preclude the possibility of additional collimation on larger scales. Apparent superluminal expansion is present in the brightest compact sources. Again, this has a natural interpretation in a jet model if the outflow speeds are relativistic. Radio-emitting material moving with Lorentz factor γ_j along a direction that makes a small angle $\sim\gamma_j^{-1}$ with the line of sight can appear to move transversely with a speed $\sim\gamma_j c$ and will be brighter by a factor $\sim\gamma_j^2-\gamma_j^3$.

2. Hope

We believe that the above summary reflects the opinions of the majority of astronomers interested in extragalactic radio sources. However, there are many more issues on which this consensus is currently replaced by lively debate. In the preceding sections, we have tried to represent many of the conflicting opinions to be found in the literature. Here we shall set down our personal prejudices and outline in qualitative terms a unified model of active galactic nuclei.

We propose that massive black holes form in the nuclei of most galaxies. This probably occurs soon after the galaxies themselves form. Black holes associated with elliptical galaxies have masses M in the range $10^7 \lesssim M \lesssim 10^{10} M_\odot$ and are $10-100$ times more massive

than those associated with spiral galaxies. Either the hole grows gradually or forms in a single catastrophic collapse, with a comparable mass of gas left over after its formation. Either way, the gas surrounding the hole will probably have sufficient angular momentum to be accreted through a disk, the spin axis of which will become aligned with that of the hole, at least in its inner parts.

The scaling argument of Sec. III.C.5 implies that the ratio $\dot{M}/M$, rather than $\dot{M}$ alone, determines the physical state of the accreting flow. If the accretion rate exceeds the rate associated with the Eddington limit, i.e., $\dot{M} \gtrsim \dot{M}_E \equiv L_E/c^2 \sim 10 M_8 M_\odot$ yr^{-1}, then the inner parts of the disk will thicken to form a radiation-supported torus. Internal dissipation then releases several times the Eddington limit in radiation, with effective temperatures in the uv range. In the case of very rapid accretion, $\dot{M} \gg 10 M_8 M_\odot$ yr^{-1}, the hole will be smothered by the infalling gas and most of the gas will probably be expelled through a wind or a jet. If gas is supplied at a relatively low, sub-Eddington rate, $\dot{M} \lesssim 0.1 M_8 M_\odot$ yr^{-1}, a torus can also be formed, this time supported by ion pressure. In the intermediate regime, $0.1 M_8 \lesssim \dot{M} \lesssim 10 M_8 M_\odot$ yr^{-1}, a thin radiative disk probably coexists with an active corona. Massive black holes are probably formed out of gas that is rotationally supported; hence they should have spin energies approaching the maximum possible for a Kerr hole (29% of the mass-energy). Magnetic torques can extract the spin energy of the hole, as well as some of the binding energy of the disk, at a rate that will be controlled by the inertia of the disk as well as the mass supply, and which may be much larger than the power released through accretion alone. The power extracted by this mechanism may be directed into two antiparallel jets collimated into an angle $\sim 30°$ by the pinching action of toroidal magnetic field. At this stage, jets contain mainly electromagnetic fields and ultrarelativistic plasma, predominantly positrons and electrons accelerated by the enormous potential differences (up to 10^{20} V) induced near the horizon of the hole.

We suggest that these magnetic torques lead to powerful jets only when there is an ion-supported torus or a very hot corona. The presence of a powerful thermal radiation field will inhibit nonthermal acceleration and emission processes. Furthermore, when there is a radiation-supported torus the magnetic pressure in the surface layers may be limited by the gas pressure, which is many orders of magnitude smaller than the radiation pressure. By contrast, gas pressure dominates in an ion-supported torus, and most of the energy released should be liberated nonthermally.

The jets produced by the black holes are probably not very well collimated. However the ratio of the pressure in the vicinity of a black hole to that in a compact radio source can be as large as $\sim 10^{10}$. This may allow the opening angle to decrease to $\sim 5°$ and produce a narrow jet through the mechanisms described in Secs. II.C.1—II.C.4.

Most compact sources comprise a core and a jet. The core we associate with the optically thick parts of the jet from which the radiation is beamed in our direction. The average position of the core on the sky should be fixed. We associate the outward moving features within the jets with transient shocks where fresh particle acceleration and field amplification are occurring.

As a jet climbs out of the gravitational potential well associated with the galactic nucleus, it will interact with its surroundings and be decelerated by entraining surrounding gas. Provided that this occurs over many decades of radius and the jet Mach number does not become too large, this can be achieved without catastrophic heating. Jet powers probably vary from source to source far more than do conditions in the surrounding interstellar medium. We expect that young, powerful jets remain relativistic on the large scale and will therefore be invisible in most luminous extended double sources. As jets become weaker, they become slower and successively one- and two-sided. Jets associated with quasars are much brighter than those found in powerful radio galaxies. We attribute this to the fact that quasar jets interact strongly with the dense circumgalactic gas fueling the nuclear activity and consequently they become more dissipative than the jets in radio galaxies.

Velocity differences across the jet profile provide a source of free energy for particle acceleration through shock waves, hydromagnetic turbulence, and tearing mode magnetic reconnection. Magnetic field frozen into the expanding flow will be amplified to near equipartition strength, and will become aligned with the jet in the innermost parts of the jets and in boundary layers where the velocity shear is large. However, the field will be stretched perpendicular to the flow in the outer jet, where transverse expansion dominates over shear amplification. Large-scale toroidal components of field, perhaps wound up by the central spinning black hole or disk, can be "spun off" at the end of the jet and may contribute to confinement of the jet (see Sec. II.C.4).

Jets are undoubtedly susceptible to hydrostatic and hydromagnetic instability, and most of the departures from linearity that we observe are caused by nonlinear (in the mathematical sense) development of these instabilities (see Sec. II.C.5). However, the striking inversion- and reflection-symmetrical shapes found in some sources are, we believe, caused by precession and acceleration of either the central black hole or the inner parts of the galaxy.

The jets in the more powerful sources appear to terminate at hot spots which we identify with strong shock fronts where particle acceleration can readily occur through the first-order Fermi and other processes. There is almost certainly strong shear in the expanding post-shock flow, and so here again magnetic field amplification can take place (see Sec. II.C.7).

If we were to venture a general classification scheme for galactic nuclei, on the hypothesis that the "central engines" involve black holes, we would obviously expect $M, \dot{M}$, and orientation relative to our line of sight to be essential parameters; the angular momentum of the hole itself, via the quantity $(J/J_{\max})$ (Appendix C Sec. 4), may also be important. It is then natural to identify optical

quasars and (in the case of lower-mass black holes) Seyfert galaxies with supercritical accretion ($\dot{M} > \dot{M}_E$), radio quasars with roughly critical accretion, and radio galaxies with subcritical accretion onto massive spinning holes. Orientation effects may also be important—the most extreme *BL Lac*'s and OVV's (e.g., AO 0235 + 164) may be objects with a beam directed towards us. Beaming effects are also probably responsible for most one-sided jets (especially on pc scales) and for the distinction between core-dominated and lobe-dominated radio sources.

In this scheme, the nucleus of an elliptical galaxy will probably have a large fueling rate initially and be seen as a quasar. As the supply of fuel diminishes, so will the uv continuum and the emission lines, and the galaxy will become a powerful radio galaxy. Further decline in the gas supply will produce a weaker radio source. Spiral galaxies, with their smaller black holes, can likewise evolve through the states QSO, Seyfert, and normal spiral like our own. How much of this evolution is followed by an individual galaxy depends upon the black hole mass and the history of the gas supply. The principal evolutionary properties of active extragalactic objects can clearly be accommodated within this scheme.

Correlations between x-ray, optical, and radio luminosity suggest that there are two distinct mechanisms for x-ray emission. One, operating in all quasars, could be due to flaring or magnetic activity at the photosphere; a second mechanism may be associated with plasma processes near the black hole itself. If this latter mechanism operated only in the radio-loud quasars, it would account for these having a larger $L_x/L_{\rm opt}$ than the radio-quiet quasars.

Optimists might hope eventually for a genuine understanding of active nuclei, on the level of our present knowledge of stellar structure and evolution. Realists, however, are conscious that there may be more independent parameters than the few (mass, age, composition) crucial to stellar evolution, and that most observations tell us less about the primary power source than about secondary reprocessing of this power in the galactic environment—from which we can learn about the central engine only by a chain of uncertain inferences.

3. Charity

We present this rationalization of the principal observed properties of quasars and extragalactic radio sources not so much because we believe there is strong evidence in favor of it, but instead because it provides a framework in which to discuss the observations and to demonstrate that, as yet, active galactic nuclei pose no threat to conventional physics. Of course, as our review must surely have borne out, there is a plethora of alternative possibilities. The observational evidence for massive black holes being the prime movers of active galaxies is largely circumstantial, and our prejudice for them derives as much from theoretical considerations as it does from the discovery of rapid x-ray variability, central light cusps, and radio jets. There is no necessity to invoke black holes on the basis of the radio observation alone, as current limits of resolution are typically $\sim 10^3 - 10^5$ times larger than the radii of the hypothetical event horizons, and we observe substantial collimation occurring on even larger scales than this. (In fact, several authors have suggested that the $\sim 1 - 10$ pc size compact jets are destroyed and recollimated on scales ~ 100 pc—1 kpc to form the observed large-scale sources.) Compact star clusters and spinars remain viable candidates for the central power source in several types of object.

By contrast, the association of observed $\gtrsim 1$ kpc jets with continuous flows seems reasonably secure. In almost every instance where a source has appeared to contain a chain of "knots" interpretable as plasmoids, observations with improved dynamic range have revealed the underlying jet structure. The detailed documentation of the jets from the "local" object SS433 provide a crucial clue that highly collimated, nearly relativistic flow is possible. Unfortunately, despite the discovery of core-jet structure and the spectacular confirmation of superluminal expansion, the observational situation for the compact radio sources is far less certain; several of the highest-dynamic-range maps reveal quite complex radio structure that will take time and more detailed observations to unravel. It was for this reason that we included nonjet models in our discussion in Sec. III.A; however, a wealth of indirect evidence certainly supports the extension of the jet hypothesis to all active galactic nuclei associated with radio sources.

B. Observational prospects

Below we describe some of the *technological* advances in observational capabilities which are likely to advance our understanding of extragalactic radio sources in the next few years.

1. Linked interferometers

As we described in the Introduction, the mapping of large samples of extended radio sources by successively more sensitive linked interferometers has transformed our physical understanding of active galaxies and quasars. The culmination of this research is undoubtedly the set of source structures produced by the VLA and by radio-linked interferometry. As of this writing, the VLA's capability has by no means been exhausted, and we are still several years away from having high-dynamic-range, multifrequency polarization maps of a large flux-limited sample. Such a sample should help to refine the existing morphological classification of the extended sources, clarify the distinction between radio galaxies and quasars, and, we hope, confirm the trends that we reported in Sec. I.C. (Radio-linked interferometry, pioneered at Jodrell Bank, is proving particularly useful in supplying high-resolution maps at low frequencies. A combined direct-linked and radio-linked interferometer is currently under construction in Australia and should become fully operational by

1988. It will enlarge the source sample by producing maps of southern sources comparable in quality to those made by the northern hemisphere interferometers.) Using these maps, it should be possible to understand the flow pattern in the hot spots as well as in the jets themselves by using the magnetic fields as tracers. It should also be possible to use polarization observations of the low-surface-brightness cocoons to determine whether or not jets are confined by toroidal magnetic fields. Most importantly, such a complete sample should allow us to test statistically for Doppler beaming, as well as other effects which serve as diagnostics of the jet velocity (Sec. II.A.4).

Spectral investigations will likewise be important as probes of particle acceleration and the jet speed. This is especially true of hot spots and knots which we associate with shock fronts. In particular, high-frequency observations may allow us to estimate the cooling length of the emitting electrons in the post-shock flow. Dividing this by the equipartition cooling time gives a measure of the post-shock flow speed and hence an independent estimate of the jet speed.

We are more sanguine about the possibility of deriving particle densities from observations of internal depolarization. We believe that many existing estimates are confused by Faraday rotation in the surrounding medium, and field reversals in the source itself can lead to density upper limits which are erroneously low. However, there is the possibility that in the lower-surface-brightness regions of some sources, the degree of polarization is so close to the maximum allowed by the theory of synchrotron radiation that we can severely constrain any departures from long-range order in the magnetic field. Indeed, it may even be possible to reproduce the polarization distribution in detail using simple magnetohydrodynamic models.

Most radio features in the extended components of nearby sources appear to be resolved. However, this is not true of cosmologically distant objects, and high-frequency observations at the highest resolution of the VLA will be necessary to obtain the equipartition pressures. It will be of particular interest to see if these pressures are indeed larger at redshifts $z \gtrsim 2$, indicating strong evolution in the density of circumgalactic gas.

We have described how curved jets may be furnishing valuable probes of both the motion of their sources and of the surrounding gas. Again, the compilation of a large sample of highly symmetric objects should allow us to distinguish these two effects and thereby use the jet shapes as diagnostic tools for the study of galactic dynamics.

2. VLBI

We are probably on the threshold of further advances in VLBI. Current experiments are carried out on an *ad hoc* basis, using telescopes that were designed and are used mostly for other purposes. This inevitably causes a reduction in sensitivity and hinders the comparison of maps produced at different times by different combinations of instruments. There are plans to construct large arrays of telescopes dedicated to VLBI in both North America and Europe. The Australian array, which will ultimately be used for VLBI, will enlarge the area of available sky by $\approx 50\%$. In the United States there is a proposal to establish a ten-station array with telescopes stretching from Hawaii and Alaska to Massachusetts, to be operational in 1988. Good-quality maps of hundreds of compact sources will be made, and the most variable of these will be monitored sufficiently regularly to reveal the detailed kinematics of superluminal expansion. (It should be noted that a VLBI array has a longer active life than a linked array simply because it will be mapping variable sources.) We shall probably have to wait until an array is established before we can perform a completely reliable statistical study of beaming effects in compact sources.

One new type of observation that will be carried out using existing instruments will involve the use of a physically unrelated source that is nearby on the sky as a phase reference for a variable compact extragalactic source. In this way, it will be possible to test the model described above, in which the source consists of a stationary core and a jet which displays moving inhomogeneities. Recent work by Marcaide and Shapiro (1984) and Bartel (1984) that has measured angular velocities ~ 10 μarc sec/yr is particularly encouraging in this respect. It should also be possible to determine whether or not these inhomogeneities move ballistically or are accelerated along established curve tracks.

Further into the future, there are plans to carry out VLBI using one or more antennae orbiting in space. The proposed "Quasat" mission involves a free-flying, 15 m centimeter-wave antenna. Space VLBI will improve the baseline coverage and the dynamic range of the maps, and in particular the angular resolution, as the orbits will extend out to several Earth radii. There is probably not much point in striving for larger baselines, for example by using an Earth-moon baseline, because no evidence exists that there is any structure sufficiently bright to be seen on the micro-arc-second angular scale that could then be achieved; in any case, scattering by interstellar fluctuations would make such observations very difficult.

3. Space Telescope

The Space Telescope, due to be launched in 1986, will have a tenfold improved sensitivity for point sources and a 30-fold improved angular resolution over existing ground-based telescopes. It will therefore be an ideal instrument for discovering compact optical features in radio jets. The resolution will become superior to that of linked interferometers, and the sensitivity will be such that bright compact ($\sim 0.1''$) radio features will be seen in the optical even if the radio-optical spectral index is as large as 0.8. At present, this index must be smaller than 0.5 in order for the optical detection of a typical radio source to be possible. As typical radio spectra indices are roughly 0.7, the prospects seem good for the study of optical jets. This is important to the study of radio sources, because

the detection of nonthermal optical emission from knots and hot spots would place strong constraints on possible particle acceleration mechanisms. However, the most important contribution of the Space Telescope to the study of active galactic nuclei as a class may well turn out to be the correlation of the morphological galaxy type with the nature of the nuclear activity.

Turning to the more distant future, space-borne optical interferometry has been proposed, and if this comes to fruition, it will undoubtedly be a very useful technique for studying galactic nuclei.

4. X-ray astronomy

X-ray observations, particularly those made with the Einstein telescope, have considerable importance for studies of extragalactic radio sources. We now have some knowledge of the x-ray luminosities of quasars and Seyfert galaxies and a partial understanding of their empirical correlation with the radio properties. Of more direct importance are the detections and upper limits on thermal bremsstrahlung emission for circumgalactic and intracluster gas. As we have discussed, in several cases they seem to indicate that jets must either be free or be confined by magnetic stresses. Three jets are now known to be x-ray luminous. If, as we have asserted, the emission is due to the synchrotron process, then electrons must be acclerated to $\sim 10^8$ MeV within the source region. This places very severe constraints on the acceleration mechanism and in our view indicates that strong shock waves are responsible.

We do not expect x-ray astronomy to contribute much more of substance to the study of extragalactic radio sources until the launch of the Advanced X-ray Astrophysical Facility (AXAF), proposed for 1991. However, the ROSAT satellite, being built jointly by West Germany and the United States and intended to be launched in 1986, will have a similar sensitivity to Einstein, but as it will operate in a scanning mode it should greatly enhance our understanding of the statistical properties of extragalactic x-ray sources. With AXAF, it should be possible to detect x-ray emission from several more jets, for the same reasons that the Space Telescope will expand optical coverage. There is also the possibility that inverse Compton emission will be detected from the extended lobes of radio galaxies. It will then be possible to make improved estimates of the magnetic field strengths, and so test the equipartition hypothesis. Another possibility is that we will be able to detect circumgalactic gas that has been shock-heated by the advancing radio component. The expansion velocity could then be estimated from the derived gas temperature, and the gas density could be estimated from the emission measure, using techniques similar to those currently applied to observations of supernova remnants. It will be particularly interesting to see how the derived post-shock pressure compares with the equipartition pressure in the head of the radio source.

C. Experimental prospects

Aerodynamical experiments using cylindrically symmetric supersonic flows may provide valuable insights into purely hydrodynamic aspects of jet physics. They can complement numerical computations (Sec. V.D) by providing higher-resolution simulations of turbulence and instabilities and (more importantly) by displaying fully three-dimensional aspects of the flow which are inaccessible to currently available computer codes. They also have limitations, including their inability to demonstrate the dynamical effects of magnetic fields and relativistic bulk velocity, and the limited ranges of Mach number, density ratio, and adiabatic index which are practicable in the laboratory. Nevertheless, through the judicious choice of different jet gases and the use of wind tunnels and vacuum chambers, it should be possible to spot some of the trends which accompany changes in the various dimensionless quantities that characterize astrophysical jets.

The apparatus for creating a supersonic jet in the laboratory involves a source of gas compressed to some specified pressure (in practice, up to about 10^3 atm), a de Laval nozzle through which the gas is allowed to pass, and a receiving chamber into which the jet propagates. A variety of high-speed diagnostics is available for mapping gas dynamic variables within the jet and surrounding medium at all stages of the jet's development, with minimal disturbance to the flow. The design of the nozzle is crucial, since the ratio of throat to exit area uniquely determines the ratio of exit pressure to "stagnation" pressure, i.e., the pressure far upstream of the nozzle, and also the exit Mach number for gas of a given adiabatic index (Landau and Lifshitz, 1959). Since the exiting gas is supersonic, its pressure initially is independent of the pressure of the ambient medium in the receiving chamber. In most laboratory experiments, these two pressures are not matched, and the jet is therefore *underexpanded* or *overexpanded.* In either case, the jet comes into transverse pressure balance through a series of shocks and rarefactions which result in the production of dissipative *Mach disks* normal to the flow (see Sec. II.C.8). If we desire to model gas pressure confinement of radio jets, then the exit pressure should be matched as closely as possible to the external pressure.

We envision three classes of gas-dynamical experiments relevant to astrophysical jets. The first involves discharging a supersonic jet into still gas. One could observe the structure and stability of the head of the jet as it advances through the ambient medium (Sec. II.B.1), as well as the development of a cocoon (Sec. II.B.3). Once the "transients" have died down, it would be particularly valuable to measure the distance the jet can travel before it becomes fully turbulent, as a function of Mach number, Reynolds's number, and ratio of jet density to ambient density. Existing experimental evidence based on Mach numbers $\lesssim 5$ suggests that this distance (measured in jet diameters at nozzle exit, or "aspect ratio") increases steeply with M_j, and theoretical estimates suggest a further increase at both high and low density ratios.

TABLE I. Some representative Mach numbers, Reynolds numbers, and density ratios which may be attainable in the laboratory for pressure-matched jets discharging into still gas. The terminal Mach number for a jet gas of given composition depends only on the ratio of stagnation pressure to chamber pressure; to obtain the higher values it may be necessary to partially evacuate or cool the receiving chamber. Higher Mach numbers may also be obtained by discharging the nozzle head-on into a wind tunnel. Temperatures of the jet at pressure ratios of 10^3 and 10^4 are taken to be just above the liquefaction points for the respective gases at 1 atm; to avoid liquefaction it is necessary to heat the jet gas before it passes through the nozzle, except in the case of helium at pressure ratios smaller than 10^3. However, heating is necessary even for the lowest pressure ratios, to obtain density ratios substantially less than one. The Reynolds number scales linearly with the jet diameter, which is taken here to be 1 cm.

Jet gas	$\frac{P_{\text{stagnation}}}{P_{\text{chamber}}}$	M_{jet}	P_{chamber} (atm)	$T_{\text{stagnation}}$ (K)	T_{jet} (K)	Reynolds number	Chamber gas	$\frac{\rho_{\text{jet}}}{\rho_{\text{chamber}}}$
Air	10^3	5.57	1.0	567.6	78.8	5.6×10^6	Air	3.5
							He	12.1
							CO_2	1.7
Air	10^4	8.03	0.1	1097.6	78.8	8.0×10^5		
He	10^3	6.69	1.0	249.0	15.6	1.8×10^7	Air	5
							He	17.5
							CO_2	2.5
He	10^4	10.82	0.1	626.3	15.6	2.9×10^6		
He	10^2	3.99	1.0	500	78.8	1.5×10^6	CO_2	0.49
He	30	2.95	1.0	500	127.7	6.5×10^5	CO_2	0.30

M_j is fairly insensitive to the ratio of stagnation to ambient pressure, and there is little hope of achieving Mach numbers larger than 5—10 with standard laboratory techniques. At present, the body of evidence for dynamically important dissipation in jets (see Sec. II.C.6) and against free expansion (Sec. II.C.3) points to jet Mach numbers $\lesssim 10$; if jet Mach numbers are indeed this low, then experiments can feasibly explore the entire range of jet Mach numbers. Density ratios ranging from ~ 0.1 to 100 are potentially accessible to laboratory experiments. As both high and low density ratios have been proposed for individual jets, it seems worthwhile exploring the full range. Some characteristic Mach numbers, density ratios, and Reynolds numbers attainable in the laboratory are tabulated in Table I. Some of the seemingly slow jets which display mirror symmetry, as a result of orbital motion of the parent galaxy, may be as dense or denser than their surroundings. There are two ways to achieve low-density jets. Technically the simplest is to choose a jet gas with small molecular weight and fire it into a receiving chamber filled with dense gas at a sufficiently *low* pressure ratio. A second way to decrease the density ratio is to cool the ambient gas and heat the jet gas. However, since the density ratio depends linearly on the temperature ratio, large temperature differences are required to change the density ratio appreciably, and it is not clear that this is practicable in an experiment of modest cost.

It may be feasible to study the behavior of jets with density ratios as low as 10^{-3} by firing supersonic jets underwater. Jets wider than a few millimeters will be unaffected by the surface tension of the water. At small depths, the stagnation pressure should be set to produce a matched jet upon firing into an ambient pressure of 1 atm. The resulting Mach numbers are the same as those for the gas into gas experiment. If the water depth is $\gtrsim 10$ m, it may be possible to study the response of the jet to pressure gradients along its trajectory, by firing vertically. Two technical requirements of such an experiment are (1) that the jet be sufficiently wide to traverse an adequate range of ambient pressures (since the range of the jet scales with diameter), and (2) that the head of the jet plow through the water faster than the rise speed of a bubble with comparable transverse dimensions. The second condition will generally be satisfied, but the first may be rather difficult to meet in practice. In interpreting the results of an underwater experiment it must be remembered, first, that the advance of the head is highly subsonic with respect to the water, and second, that the water is nearly incompressible. The latter implies that, unlike jets moving through dense gas, supersonic jets in water may be subsonic or mildly trans-sonic with respect to the ambient medium, and the consequent modifications of the stability properties will limit the direct applicability of these experiments to astrophysical jets.

List (1982) gives a good summary of experiments, with particular relevance to the lower-Mach-number case relevant to the later stages in the evolution of large radio sources.

The second and third classes of experiment involve discharging supersonic jets into a wind tunnel, either head-on into the wind or at an angle. By discharging the jet nearly head-on, it is possible to study jets with higher Mach numbers than those obtainable from a nozzle fired into still gas. Furthermore, it is possible to slow down the advance of the head or stop it altogether in the laboratory frame, thus making its structure and stability easier to study. The main drawback of this class of experiments is that the experimental chambers of most wind tunnels are quite small. Thus nozzle openings must be correspondingly narrower to produce jets with sufficiently large aspects ratios, and also to avoid interference (e.g., reflected sound waves) with the walls of the cavity. Experiments

with jets fired transversely into the wind, relevant to radio trails (Sec. II.D.1), are subject to the same drawbacks. In addition, fine tuning of the tunnel Mach number is necessary to prevent the stream's bending too close to the wall of the chamber or the mouth of the nozzle and thus being subject to edge effects and the flow downstream of a rigid obstacle. In addition to verifying the basic scaling relations used in theoretical analyses of radio trails, useful observations would concentrate on the structure and stability of the bowshock upstream of the curved jet (and its dependence upon angle of attack), the mixing region downstream, and the stability of the jet itself as it is being bent.

A different type of experiment which could achieve higher Mach numbers than "traditional" wind tunnels would involve the propagation of intense particle beams—or, alternatively, laser beams—into the atmosphere (see Bekefi *et al.*, 1980). Although the internal dynamics of such beams differ crucially from those in the cosmic-scale beams, they would provide a much higher momentum density than an ordinary gas jet. The interaction with the external medium as such a beam advances may simulate the structure of "hot spots" and cocoons in very strong sources.

One final word of caution is necessary regarding the applicability of studies of laboratory jets to jets in extragalactic radio sources. There is a great temptation to relate the morphological features of laboratory flows—large-scale eddies, etc.—to what we see in the sky. However, one must bear in mind that there may be no simple relation between local flow variables and radio emissivity. Until the particle acceleration mechanisms in radio sources are understood in much greater detail, the generation of synthetic radio maps based on hydrodynamic flows should not be taken too seriously.

D. Theoretical prospects

What can we expect in the way of matching theoretical progress? This we find the most difficult to discuss because theory often develops on a shorter time scale than observations and experiments, and so we cannot foresee most future developments. Although many of the features now observed in extragalactic radio sources (especially jets and superluminal expansion) were anticipated by theoretical discussions, the recent burst of observational discovery has left theory lagging behind. However, there are some topics on which we do believe that there will be steady work of direct relevance to interpreting the observations.

Foremost amongst these topics is the development and use of sophisticated hydrodynamical codes for numerical simulation of radio sources. As we have described, existing two-dimensional codes have already uncovered some gas-dynamical properties of supersonic flows that were unanticipated by analytical models and may have counterparts in radio maps. Useful and affordable three-dimensional simulations are perhaps five years off, and we must wait for these before we can hope to simulate the nonlinear development of instabilities and the production of the symmetric bends in jets. The other important future computational development will be the use of magnetohydrodynamic codes. Only in this way will we be able to see if it really is practical to confine jets magnetically and whether or not the polarization patterns observed in jets can be explained in terms of the kinematics of expanding shear flows.

Another topic on which further work seems practicable concerns the kinematics of superluminal expansion. While it seems probable that we are using the right ingredients of special relativity and a collimated outflow, it is equally true that no detailed model yet commands majority support. We can still expect some surprises from studies of the appearance of relativistic shocks in unsteady jets.

Particle acceleration is another problem that seems ripe for a more sophisticated treatment. Perhaps the most successful approach will be to extrapolate our understanding of particle acceleration in interplanetary space (as obtained by spacecraft), and within supernova remnants. Because of their relative proximity, these environments can be studied in far greater detail than extragalactic sources.

However, the most interesting problem for a theorist remains the nature of the central engine and the means of extracting power in a useful, collimated form. We have just outlined a particular scheme that we believe to be logically self-consistent but for which there is not a shred of *direct* evidence. Alternative possibilities exist, as we have indicated in Sec. III, and these have only been subjected to perfunctory scrutiny. Perhaps the best defined problem in this context is the study of the viability, structure, and evolution of radiation-supported accretion disks and tori. This is somewhat analogous to the problem of stellar structure in the days when astronomers were ignorant of the nuclear processes responsible for the energy release and their dependence on density and temperature. In the case of accretion disks it is the viscosity of which we are ignorant. If these restricted models are combined with realistic atmospheres, then it may be possible to synthesize the continuum spectra of the optical quasars and Seyfert galaxies. Although this may not be directly relevant to the production of jets, it would at least provide strong support for the black hole hypothesis.

The final class of problems on which we expect progress involves modeling the fueling of quasars and active galaxies. As we have described, a choice still cannot be made between a local source of gas, such as a central star cluster or gas cloud left over from the formation of the central object, and an external source, such as a cannibalized galaxy or infalling intergalactic or even interstellar gas. More refined estimates that properly take account of the influence of a bright nucleus on its surroundings should help us to interpret optical observations that we anticipate from the Space Telescope.

ACKNOWLEDGMENTS

We are indebted to a considerable number of observational and theoretical colleagues for their advice and encouragement during the preparation of this review and for their comments on earlier drafts of this manuscript. We acknowledge, in particular, the contributions of Dr. Bridle, Dr. Cohen, Dr. Fabian, Dr. Norman, Dr. Perley, Dr. Phinney, Dr. Readhead, Dr. Scheuer, and Dr. Smarr. Major portions of this review were written at the Aspen Center for Physics; Institute for Advanced Study, Princeton; Institute for Theoretical Physics, Santa Barbara; National Radio Astronomy Observatory, Charlottesville; Kilt Peak National Observatory, Tucson; Nordita, Copenhagen; and the University of California, Berkeley. We thank the directors of these institutions for their generous hospitality. R.D.B. was supported in part by National Science Foundation Grants Nos. AST76-10375, 73-05484, 80-17752, and 82-13001 and the Alfred P. Sloan Foundation. M.C.B. was supported in part by National Science Foundation Grants Nos. AST 78-21070, 79-23243, 82-15456, and 82-16481 and the Science and Engineering Research Council of Great Britain.

APPENDIX A: RADIATION PROCESSES

The best general reference for the details of the relevant radiation processes is Rybicki and Lightman (1979). Other more specific references are given below.

1. Synchrotron radiation

Most of the nonthermal radio emission from extragalactic radio sources is believed to be produced by the *synchrotron* mechanism. In this process, ultrarelativistic electrons of energy $\gamma m_e c^2$ are accelerated in a magnetostatic field of strength B (e.g., Jackson, 1977; Pacholczyk, 1970; Moffet, 1975; Lang, 1978). Individual electrons orbit about the field with frequency ν_L/γ (where $\nu_L = eB/2\pi m_e c$ is the *Larmor frequency*), radiating a total (Lorentz invariant) power given by the relativistic Larmor formula

$$P_S = 2\gamma^2 \sigma_T c (B_\perp^2/8\pi) , \tag{A1}$$

where $B_\perp$ is the field component resolved perpendicular to the electron momentum and σ_T is the Thomson cross section. Averaging over an isotropic distribution of electrons, $B_\perp^2 = (2/3)B^2$. We can define an electron cooling time

$$t_S = \gamma m_e c^2/P_S = 8\times 10^8 B^{-2}\gamma^{-1} s , \tag{A2}$$

where we measure B here and henceforth in gauss.

An ultrarelativistic electron radiates high harmonics of the gyrofrequency. The characteristic frequency radiated ν_c can be estimated as follows: Relativistic aberration gives a beam pattern for an individual electron of angular width $\sim\gamma^{-1}$, and so radiation is emitted in the direction of an observer lying in the orbital plane for a time $\delta t_{\rm em}\sim(\nu_L)^{-1}$. The pulse seen by the observer, however, has duration $\delta t_{\rm ob}\sim\gamma^{-2}\delta t_{\rm em}$, and so $\nu_c\sim\gamma^2\nu_L$. Numerically,

$$\nu_c = 1.2\gamma^2 B_\perp \text{ MHz} . \tag{A3}$$

For $\nu \ll \nu_c$, the spectral power radiated by an individual electron satisfies $P_{S\nu}\propto\nu^{1/3}$. For $\nu\gg\nu_c$, $P_{S\nu}\propto\nu^{1/2}e^{-\nu/\nu_c}$.

The character of the observed radiation changes somewhat if the electrons are streaming along the field with small pitch angles (O'Dell and Sartori, 1970). The characteristic frequency radiated is still given by Eq. (A3), as long as the pitch φ exceeds γ^{-1}. However, the radiation is beamed within a hollow cone of vertex angle $\sim\varphi$. When $\varphi\lesssim\gamma^{-1}$, the electrons are nonrelativistic in the guiding center frame, and Doppler-shifted cyclotron radiation is observed.

Radio spectra are usually power laws with the *spectral flux* S_ν conventionally measured in janskys (Jy) (1 Jy $=10^{-23}$ ergs s^{-1} cm^{-2} Hz^{-1}). If the electron energy distribution function satisfies $dN_\gamma/d\gamma = K\gamma^{-p}$, then

$$S_n \propto \int (dN_\gamma/d\gamma) P_S \delta(\nu-\nu_c) d\gamma \propto K B^{1+\alpha}\nu^{-\alpha} , \tag{A4}$$

where α, the *spectral index,* is given by

$$\alpha = (p-1)/2 . \tag{A5}$$

Synchrotron radiation is linearly polarized with the observed E vector oscillating perpendicular to the projection on the sky of the magnetostatic field. For a uniform field the degree of polarization is ~ 0.7, depending weakly on p.

Synchrotron radiation is also circularly polarized. The radiation emitted on opposite sides of the orbital plane has opposite senses of angular momentum. Thus the observed degree of circular polarization is given roughly by the fractional change in the emissivity as the pitch angle of the electron's orbit changes by $\sim\gamma^{-1}$, the width of the radiation pattern. Numerically the degree of circular polarization at frequency ν_6 MHz is roughly

$$C\sim 3B^{1/2}\nu_6^{-1/2} . \tag{A6}$$

2. Equipartition energy

When we observe an optically thin source of known volume V and power P, we usually do not know the magnetic field strength independent of the relativistic electron energy. However, using Eqs. (A1) and (A3), we can express the relativistic electron energy as $U_e\propto PB^{-3/2}\nu^{-1/2}$. If we assume that the field is randomly oriented, the pressure is $p\sim B^2/8\pi + U_e/3V$, which is therefore minimized when $U_e\sim B^2V/2\pi$, that is to say, when there is approximate equipartition between particle and magnetic energy density (Burbidge, 1958). This calculation is weakly sensitive to the shape and extent of the radio spectrum. If, as is commonly assumed, the spectrum extends over three decades of frequency with a spectral index $\alpha\sim 0.7$, then

the *minimum* pressure in a synchrotron source is given roughly by

$$p_{\min} \sim 10^{-12}(T_5/l_{\rm kpc})^{4/7} \text{ dyn cm}^{-2} , \quad \text{(A7)}$$

where T_5 is the source's *brightness temperature* in K measured at 5 GHz (Appendix C Sec. 2 below) and $l_{\rm kpc}$ is the extent of the source along the line of sight in kiloparsecs (see Moffet, 1975 for more accurate expressions). Additional contributions to the energy, such as relativistic ions or thermal gas, will increase $p_{\min}$.

3. Synchrotron self-absorption

The brightness temperature of a synchrotron source is limited by the kinetic temperature of the emitting electrons, i.e., $T \lesssim \gamma m_e c^2/3k$. The flux observed from an optically thick synchrotron source then satisfies $S_\nu \propto \nu^2 T \propto \nu^{5/2}$. Numerically the limiting brightness temperature is, to within a model-dependent coefficient of order unity,

$$T_{\max} = 10^9 \nu_{\rm MHz}^{1/2} B^{-1/2} \text{ K} . \quad \text{(A8)}$$

The polarization vector from an optically thick source lies parallel to the projected magnetic field direction.

4. Propagation effects

A synchrotron source may also contain thermal plasma which causes the radio waves to become dispersive. The dispersion relation for a high-frequency mode is easily shown to be (e.g., Jackson, 1977)

$$\nu = (c/\lambda)(1+\nu_p^2/2\nu^2+\cdots) , \quad \text{(A9)}$$

where $\nu_p = (n_e e^2/\pi m_e)^{1/2} = 9\times 10^{-3} n_e^{1/2}$ MHz is the plasma frequency and n_e (cm^{-3}) is the electron density. In the presence of a weak magnetic field, making an angle Ψ with the ray, the propagating modes are circularly polarized, and a term $\pm \nu_L \nu_p^2 \cos\Psi/2\nu^2$ must be added to the right-hand side of (A9) where the sign corresponds to the helicity of the wave. Radio waves emitted by the synchrotron process are linearly polarized. We decompose them into two circularly polarized components whose phase velocities differ by $c\nu_L/\nu_p^2/\nu^3$, as a result of which the plane of polarization rotates. This is the phenomenon of *Faraday rotation*. The amount of rotation for radiation of wavelength $\lambda_m m$ is

$$\Delta\varphi = \text{RM}\lambda_m^2 , \quad \text{(A10)}$$

where $\text{RM} = 810 \int n_e \mathbf{B}\cdot\mathbf{dl}_{\rm kpc}$ rad m^{-2} is the *rotation measure*.

If the total rotation across the source is $\Delta\varphi \gtrsim 1$ rad, then waves from the back of the source will be differently polarized from those at the front of the source, and the net emission will have a reduced polarization even if the field is uniform. This is *Faraday depolarization*. Faraday rotation and depolarization can be measured by making observations at three or more frequencies. If the magnetic field is known, then the rotation measure provides an estimate of the mean electron density.

Plasma dispersion can also influence the emission of synchrotron radiation. The waves emitted by the electron can be approximated as traveling with speed c only if their phase velocity differs from c by less than the particle velocity. Equivalently we require $(\nu_p/\nu)^2 \lesssim \gamma^{-2}$, or using Eq. (A3) $\nu \gtrsim \nu_p^2/\nu_L$. Numerically,

$$\nu \gtrsim \nu_R = 2\times 10^{-5} n_e B^{-1} \text{ MHz} . \quad \text{(A11)}$$

ν_R is the *Razin* frequency below which synchrotron radiation is suppressed.

5. Free-free absorption

A further constraint on the physical parameters within and around a synchrotron source is that the radio waves not be absorbed by *inverse bremsstrahlung*. The free-free spectral emissivity at a given frequency $\nu \ll kT/h$ for an ionized gas with electron density n_e and temperature T is $j_\nu \sim e^2 \sigma_T n_e^2 (m_e c^2/kT)^{1/2}$ (Moffet, 1975). The absorption coefficient is furnished by Kirchhoff's law, and in the Rayleigh-Jeans limit, the absorption coefficient μ (Appendix C Sec. 2) is given by $\mu \sim j_\nu c^2/\nu^2 kT$. A radio spectrum should therefore be cut off exponentially below a frequency given by

$$\nu_{ff} = 15 n_e (T/10^4 \text{ K})^{-3/4} l_{\rm kpc}^{1/2} \text{ MHz} , \quad \text{(A12)}$$

where l is the path length through the source.

6. Compton scattering

Photons are scattered by free electrons with the Thomson cross section, σ_T, for frequencies in the rest frame $\nu \lesssim m_e c^2/h$. At higher frequencies, the Klein-Nishina formula is appropriate: $\sigma = \sigma_T (3m_e c^2/8h\nu)[2\ln(h\nu/m_e c^2)^{1/2}]$ (Blumenthal and Gould, 1970). Scattering of photons in nonspherical sources can lead to substantial linear polarization depending upon the shape of the source and the observer's orientation (Angel, 1970). Photons that are more energetic than the scattering electrons will on balance lose energy due to Compton recoil by an amount $\Delta\nu \sim h\nu^2/m_e c^2$ each scattering. Thus electrons exposed to a flux of higher-energy photons of spectral energy density u_ν will be *Compton heated* at a net rate

$$W_e^+ = \int u_\nu \frac{h\nu}{m_e c^2} \sigma_T c \, d\nu . \quad \text{(A13)}$$

Alternatively, when the electrons are hotter, the photons will be scattered to higher energy. Individual scatterings will Doppler-shift photon frequencies up or down by an amount $|\delta\nu/\nu| \sim (kT/m_e c^2)^{1/2}$. However, blueshifts (approaching collisions) outweigh redshifts (receding collisions) by a fractional amount also $\sim (kT/m_e c^2)^{1/2}$. Thus the net *Compton cooling* of the electrons is given by

$$W_e^- = -4(kT/m_e c^2) v_r \sigma_T c , \quad \text{(A14)}$$

where $u_r = \int u_\nu d\nu$ is the integrated energy density of the radiation.

Compton cooling of relativistic electrons is known as the *inverse Compton effect.* In the rest frame of the electron, most incoming photons appear to have a frequency $\sim\gamma\nu$. Provided that this does not exceed $m_e c^2/h$, the photons will be scattered elastically. Lorentz transforming back to the original frame gives a net average boosted frequency $(\frac{4}{3})\gamma^2 h\nu$, where we have assumed that either the electrons or the photons are isotropic. Compton losses by relativistic electrons are therefore similar to synchrotron losses with $B^2/8\pi$ in Eqs. (A1) and (A2) replaced by u_r. If, in a source, the synchrotron photons have an energy density $u_r^s \gtrsim B^2/8\pi$, then they will be scattered to give a larger Compton energy density that exceeds the synchrotron energy density by a factor $(u_r^C)/(B^2/8\pi)$ and so on, until the photon frequency becomes so large that the Klein-Nishina regime is approached or the electrons are catastrophically cooled. Electrons in compact radio sources are generally believed not to be losing more power through Compton than synchrotron processes. This implies that in a self-absorbed source (see Appendix A Sec. 3), $u_r \sim kT_b(\nu/c)^3 \lesssim B^2/8\pi \propto (\nu/T_b^2)^2$, where T_b is the brightness temperature and we have used Eq. (A8). The corresponding limit on the source's radio brightness temperature is fairly insensitive to the spectral details; $T_b \lesssim 10^{12}$ K. Where this limit appears to be violated, as in some compact variable sources, theorists have worried about the so-called "inverse Compton catastrophe" (see Secs. III.A.2 and III.A.3).

Radiation can also exchange momentum with an ionized gas, resulting in a net pressure. In order that the net radiation pressure acting on an electron-proton plasma not exceed the gravitational force due to a mass M, the total radiation flux must stay below the *Eddington limit,*

$$L_E = 4\pi GMM_p c/\sigma_T \ . \tag{A15}$$

The condition $L < L_E$ must be satisfied by gas accreting in a spherically symmetric fashion onto black holes in galactic nuclei; related constraints apply for more general flow patterns.

Under conditions of high radiation intensity, *induced Compton scattering* can enhance the photon-electron energy transfer rate (D. B. Wilson, 1982). In the Rayleigh-Jeans limit the photon occupation number is $n \sim kT_b/h\nu$, and the rate of stimulated scatterings $\mathbf{k} \rightarrow \mathbf{k}'$ will exceed the rate of spontaneous scatterings by n. However, these stimulated scatterings will be largely canceled by inverse stimulated scatterings $\mathbf{k}' \rightarrow \mathbf{k}$. Electron recoil with $\delta\nu/\nu \sim h\nu/m_e c^2$ leads to an imperfect cancellation, and the effective induced scattering rate is a factor $n(h\nu/m_e c^2) \sim (kT_b/m_e c^2)$ times larger than the spontaneous rate. Induced scattering by nearby free electrons will distort the spectrum when the radio brightness temperature of a compact source exceeds $10^{10}\tau_T^{-1}$ K (where τ_T is the Thomson optical depth, assumed to be less than unity; Levich and Sunyaev, 1970).

APPENDIX B: FLUID MECHANICS

The best general reference for fluid mechanics is Landau and Lifshitz (1959). Other, more specific references are given below.

1. Nonrelativistic gas dynamics

When the effective particle mean free path is much smaller than the size of the system astrophysical plasmas can be approximated as fluids, at least insofar as their bulk properties are concerned. The fluid is usually characterized by a scalar pressure p, a density ρ, and a bulk velocity $\mathbf{v}$. If we ignore viscosity and thermal conductivity, the motion is adiabatic and the flow is determined by the conservation laws of mass, momentum, and energy (Liepmann and Roshko, 1957):

$$\frac{\partial\rho}{\partial t} + \nabla\cdot\mathbf{j} = 0 \ , \tag{B1}$$

where $\mathbf{j} = \rho\mathbf{v}$ is both the *mass flux*[4] and the momentum density;

$$\frac{\partial(\rho\mathbf{v})}{\partial t} + \nabla\cdot\mathbf{\Pi} = 0 \ , \tag{B2}$$

where $\Pi_{ij} = p\delta_{ij} + \rho v_i v_j$ is the *momentum flux tensor,* and

$$\frac{\partial u}{\partial t} + \nabla\cdot\mathbf{F} = 0 \ , \tag{B3}$$

where $u = \varepsilon + \frac{1}{2}\rho v^2$ is the total *energy density* in terms of the internal energy per unit volume ε and the kinetic energy density $\frac{1}{2}\rho v^2$ and $\mathbf{F} = (u+p)\mathbf{v}$ is the *energy flux.* For fully ionized plasma, $p = (2/3)\varepsilon$, and for adiabatic changes, $p \propto \rho^{5/3}$. The *sound speed* is $s = (5p/3\rho)^{1/2}$. In the presence of a Newtonian gravitational potential φ, a term $-\rho\nabla\varphi$ must be added to the right-hand side of Eq. (B2), and $\mathbf{F}$ must be augmented by $\mathbf{j}\varphi$.

2. Relativistic gas dynamics

Analogous conservation laws hold in the case of relativistic gas dynamics (e.g., Landau and Lifshitz, 1959; Königl, 1980). The relevant equations of motion are obtained by setting to zero the divergence of the stress tensor $T_{ij} = (e+p)u_i u_j + p g_{ij}$, where e is the *internal energy per unit volume* including rest mass, $u_i = (\gamma, \mathbf{u})$ is the four-velocity, and g_{ij} is the metric tensor (with signature $-+++$).

The *momentum flux three-tensor is*

$$\Pi = (e+p)\mathbf{u}\mathbf{u} + p\mathbf{I} \ . \tag{B4}$$

The *energy flux* (equal to c^2 times the *momentum density*) is

[4]Fluxes are consistently interpreted as quantities per unit area (except in the case of magnetic field lines).

$$\mathbf{F}=(e+p)\gamma\mathbf{u}c\ , \tag{B5}$$

and the *total energy density* is

$$u=e\gamma^2+pu^2\ . \tag{B6}$$

In a flat (Minkowski) space the analogs of Eqs. (B2) and (B3) apply.

A conserved particle species (e.g., baryons) of proper density n satisfies the conservation law

$$\frac{\partial\gamma n}{\partial t}+\nabla\cdot n\mathbf{u}=0\ , \tag{B7}$$

which is the analog of Eq. (B1).

For ultrarelativistic matter (e.g., photons, relativistic electrons), $p=(1/3)e$, and the adiabatic equation is $p\propto n^{4/3}$. The *sound speed* is $s=c/\sqrt{3}$, and the corresponding proper velocity is $\bar{s}\equiv s[1-(s^2/\ c^2)]^{-1/2}=c/\sqrt{2}$.

3. One-dimensional adiabatic motion

For stationary adiabatic motion in the absence of gravitational fields, conservation of energy and particle fluxes implies the *Bernoulli equation.* In the nonrelativistic limit, $(\varepsilon+p)/\rho+\frac{1}{2}v^2$, and in the relativistic limit, $(e+p)\gamma/n$, are conserved along streamlines. If we introduce p_0, the (stagnation) pressure when the fluid is at rest, and the *Mach number M,* then

$$M\equiv v/s=3^{1/2}[(p_0/p)^{2/5}-1]^{1/2} \tag{B8}$$

in the nonrelativistic limit, and

$$M\equiv u/\bar{s}=2^{1/2}[(p_0/p)^{1/2}-1]^{1/2} \tag{B9}$$

in the extreme relativistic limit.

A (sufficiently narrow) jet may be considered as a quasi-one-dimensional flow (Owczarek, 1964; Thompson, 1978). There should be approximate pressure equilibrium across flow lines. In addition, if different streamlines have similar entropies and stagnation pressures, then the velocity shear across the flow may be small and the jet can be characterized by a single speed that varies along its length. If we regard the pressure as fixed by the surrounding gas, then the cross-sectional area A should vary as

$$A\propto(p_0/p)^{4/5}[(p_0/p)^{2/5}-1]^{-1} \tag{B10}$$

in the nonrelativistic case. A is minimized when the flow is trans-sonic, i.e., $M=1$ (a general result) and $p=0.49p_0$. This is the *de Laval nozzle.* For the relativistic case,

$$A\propto(p_0/p)^{3/4}[(p_0/p)^{1/2}-1]^{-1/2}\ . \tag{B11}$$

In this case the pressure at the trans-sonic nozzle is $4/9p_0$. In such a jet, the *discharge* $J\equiv jA$ and the power $L\equiv FA$ are separately conserved. However, the thrust $P=\Pi A$ decreases when $M<1$ and increases for $M>1$.

In the supersonic regime ($M\gg1$) the velocity saturates. Nonrelativistically, $A\propto p^{-2/5}$ and $P\sim 2L/v$. Relativistically, $A\propto p^{-1/2}$, $P\sim L/c$.

4. Shock waves

A *shock wave* is a mathematical discontinuity across which the fluxes of mass, momentum, and energy are conserved (e.g., Zel'dovich and Raizer, 1966). The entropy of the gas increases as bulk kinetic energy is converted into internal energy, and the flow speed changes from supersonic ahead of the shock (region 1) to subsonic behind the shock (region 2). Conservation of j,Π,F [Eqs. (B1)—(B5)] leads to the *Rankine-Hugoniot relations* (e.g., Zel'dovich and Raizer, 1966; Courant and Friedrichs, 1948). For a strong adiabatic shock (in which $p_2\gg p_1$) we obtain

$$\begin{aligned}&\rho_2=4\rho_1\ ,\\ &p_2=(3/4)\rho_1 v_1^2\ ,\end{aligned} \tag{B12a}$$

for a post-shock specific heat ratio of 5/3 and nonrelativistic velocity, and

$$\begin{aligned}&\rho_2=7\rho_1\ ,\\ &p_2=(6/7)\rho_1 v_1^2\ ,\end{aligned} \tag{B12b}$$

for a specific heat ratio 4/3. For the relativistic case,

$$\begin{aligned}&u_2=1/\sqrt{8}\ ,\\ &p_2=(2/3)\gamma_1^2(e+p)\ .\end{aligned} \tag{B13}$$

5. Stationary axisymmetric flow in a gravitational field

The equations of general-relativistic hydrodynamics for a perfect fluid are obtained by setting the covariant divergence of the stress tensor to zero, i.e., $T^j_{i;j}=0$ (Misner, Thorne, and Wheeler, 1973; Weinberg, 1972). In the Boyer-Lindquist coordinate system, $x^i=(t,r,\theta,\varphi)$, appropriate to a spinning black hole, with $\partial/\partial t=\partial/\partial\varphi=0$, it is convenient to introduce $E(r,\theta)=-u_0$, the *energy at infinity* (rest mass + kinetic + gravitational) of a particle of unit mass moving with the fluid four-velocity u^i. We then define $\Omega(r,\theta)=u^\varphi/u^0$, the angular velocity of the flow, and $l(r,\theta)=-u_\varphi/u_0$ as a convenient definition of the angular momentum of a particle of unit rest mass, moving with angular velocity Ω. We ignore poloidal motion. A knowledge of the metric tensor g_{ij} together with the relation $u^iu_i=-1$ allows one to calculate any two of the quantities E,l,Ω from a knowledge of the third. The hydrodynamical equations of motion can now be cast in the form

$$-\frac{\nabla p}{e+p}=\nabla\ln E-\frac{\Omega\nabla l}{1-\Omega l}\ , \tag{B14}$$

where $\nabla=(\partial/\partial r,\partial/\partial\theta)$. For a *barytropic* equation of state, there exists a functional relation $p(e)$, and the right-hand side of Eq. (B14) is then the gradient of a scalar function. This implies the existence of a function $\Omega(l)$ which, when specified, dictates the shape of *equipotential surfaces* $E=$const on which the pressure and entropy are also constant (Abramowicz, Jaroszyński, and Sikora, 1978; Jaroszyński, Abramowicz, and Paczyński, 1980). Simple models of radiation-supported and ion-supported tori can be constructed by solving Eq. (B14) in a Kerr metric.

6. Magnetohydrodynamics

When a highly conducting fluid, like astrophysical plasma, moves through a magnetic field, it will change the field. The magnetic field in turn will react back on the flow. In the limit of high magnetic Reynolds number (perfect conductivity) there will be zero electric field in the comoving frame. So, in the inertial frame, $\mathbf{E}=-(\mathbf{v}/c)\times\mathbf{B}$. Using Faraday's law, we then obtain the *induction equation* (e.g., Parker, 1979)

$$\frac{\partial\mathbf{B}}{\partial t}=\nabla\times(\mathbf{v}\times\mathbf{B})\ . \tag{B15}$$

We combine Eq. (B15) with the mass conservation equation (B1) and $\nabla\cdot\mathbf{B}=0$ to obtain

$$\left[\frac{\partial}{\partial t}+\mathbf{v}\cdot\nabla\right]\frac{\mathbf{B}}{\rho}=\left[\frac{\mathbf{B}}{\rho}\cdot\nabla\right]\mathbf{v}\ . \tag{B16}$$

Equation (B16) can be interpreted physically by saying that magnetic lines of force are "frozen" into the fluid.

The major dynamical effect of the field is that of the Lorentz force, $(\frac{1}{4}\pi)(\nabla\times\mathbf{B})\times\mathbf{B}$. This force can be written as the divergence of the *Maxwell stress tensor,* and so $\mathbf{\Pi}$ in Eq. (B2) must be augmented by

$$\mathbf{\Pi}_{\rm mag}=-(\mathbf{BB}-\tfrac{1}{2}B^2\mathbf{I})/4\pi\ . \tag{B17}$$

The two terms in (B17) can be separately identified as a *magnetic tension* $B^2/4\pi$ acting parallel to the magnetic field and an isotropic *magnetic pressure* of strength $B^2/8\pi$. The energy flux $\mathbf{F}$ in Eq. (B3) must similarly be augmented by *the Poynting flux,*

$$\mathbf{F}_{\rm mag}=\frac{\mathbf{E}\times\mathbf{B}c}{4\pi}\ . \tag{B18}$$

APPENDIX C: RELATIVITY

1. Special relativistic kinematics of a moving source

Consider a source moving with velocity $\mathbf{v}=\beta c$ at an angle θ to the line of sight $\mathbf{n}$ to a distant observer. The time of reception $t_{\rm ob}$ of a photon of frequency ν is related to the proper time t' of emission with frequency ν' by

$$\frac{dt'}{dt_{\rm ob}}=\frac{\nu}{\nu'}=D=\frac{1}{\gamma(1-\boldsymbol{\beta}\cdot\mathbf{n})}\ . \tag{C1}$$

The observed photons are emitted along a direction $\mathbf{n}'$ in the source frame where

$$\boldsymbol{\beta}\cdot\mathbf{n}'=\frac{\boldsymbol{\beta}\cdot\mathbf{n}-\beta^2}{(1-\boldsymbol{\beta}\cdot\mathbf{n})}\ . \tag{C2}$$

The *observed* transverse velocity of the source is then (Rees, 1966; Blandford, McKee, and Rees, 1977)

$$\beta_{\rm ob}=\frac{\mathbf{n}\times(\boldsymbol{\beta}\times\mathbf{n})}{(1-\boldsymbol{\beta}\cdot\mathbf{n})}\ . \tag{C3}$$

For given $\beta<1$, $\beta_{\rm ob}$ has a maximum value of $\gamma\beta$ which exceeds unity when $\beta>1/\sqrt{2}$. The source then undergoes apparent *superluminal* motion. If the source is of finite size and its shape does not change, then its observed appearance will be the same as that observed along the direction $\mathbf{n}'$ in the source frame (Terrell, 1966). If the source is a uniformly expanding sphere, starting from zero radius, the locus of the points from which radiation is received at time $t_{\rm ob}$ after the expansion is observed to start, will be ellipsoidal, with a semimajor axis of length $\gamma^2\beta ct_{\rm ob}$ parallel to $\mathbf{n}$ and eccentricity β. The minor axis has length $\gamma\beta ct_{\rm ob}$, and so the radius of the observed source will expand superluminally in this case as well.

2. Lorentz transformation of radiation formulas

The *intensity* $\mathbf{I}_\nu$ of unpolarized radiation measures the power per unit frequency ν and solid angle Ω flowing normally through unit area. In terms of the Lorentz-invariant occupation number n,

$$I_\nu=2h\nu^3n/c^2\ . \tag{C4}$$

The *brightness temperature* T_b is defined by

$$n=(e^{h\nu/kT_b}-1)^{-1}\simeq kT_b/h\nu\ , \tag{C5}$$

where the approximation is almost always valid at radio frequencies. The *emission coefficient* j_ν measures the power per unit volume (V), frequency, and solid angle emitted by a source. The *absorption coefficient* μ is the fraction of the intensity absorbed per unit length.

Using these definitions, the transformation properties of these quantities from the source (primed) frame to the observer (unprimed) frame can be written down (e.g., Pauli, 1958; Lightman and Rybicki, 1979)

$$\begin{aligned}
&\nu=D\nu'\ ,\\
&d\Omega=D^{-2}d\Omega'\ ,\\
&I_\nu(\nu)=D^3I'_{\nu'}(\nu')\ ,\\
&T(\nu)=DT'(\nu')\ ,\\
&dV=D\,dV'\ ,\\
&j_\nu(\nu)=D^2j'_{\nu'}(\nu')\ ,\\
&\mu(\nu)=D^{-1}\mu'(\nu')\ .
\end{aligned} \tag{C6}$$

These transformations ensure that blackbody radiation remains blackbody, and that the *optical depth* along a ray $\tau=\int \mu\, dl$ is Lorentz invariant.

The *flux* S_ν is the power per unit frequency flowing normally through unit area. The observed flux from an optically thin source at a large distance d is given by

$$\begin{aligned} S_\nu &= \int I_\nu d\Omega = \int j_\nu dV/d^2 \\ &= D^3 \int j'_\nu(\nu')dV'/d^2 \\ &= D^{2+\alpha} \int j'_{\nu'}(\nu)dV/d^2 , \end{aligned} \tag{C7}$$

where the final equality holds if the source has a spectral index α and if it is more convenient to perform the volume integration in the observer frame (e.g., for a jet). Note that the total power observed does not equal the (Lorentz-invariant) power emitted because there is a change in the radiation energy density between the source and the observer. The observed flux from an optically thick source depends on its shape.

3. Cosmography

The preceding formulas are appropriate for Lorentz transformations in a flat spacetime. For cosmologically distant sources we must also take account of the expansion of the universe. This is best achieved conceptually by introducing a cosmologically comoving observer (*) along the line of sight, sufficiently distant from the source for the formulas (C5) to be appropriate, but sufficiently local to the source for the effects of cosmological expansion to be unimportant.

It is conventional to parametrize the time and distance of a source observed now by the *redshift* z of the photons (measured by known spectral lines), i.e.,

$$\nu = \nu^*/(1+z) . \tag{C8}$$

On the cosmological scale, $(1+z)^{-1}$ therefore replaces D, and formulas equivalent to (C6) can be written down (e.g., Weinberg, 1972; Misner, Thorne, and Wheeler, 1973).

Two convenient distance measures are the *angular diameter distance* d_A, defined such that the actual size of a comoving object subtending an angle δ is δd_A, and the *luminosity distance* d_L, defined such that the flux observed from a comoving isotropic source of total power L is $L/4\pi d_L^2$. Using Eq. (C7),

$$d_L = (1+z)^2 d_A . \tag{C9}$$

In a homogeneous, isotropic cosmology obeying general relativity (a Friedmann universe), d_L can be expressed in terms of the current *Hubble constant* H_0, defined so that the distance to a cosmologically local but comoving source is zc/H_0 and *density parameter* $\Omega = 8\pi G\rho_0/3H_0^2$, where ρ_0 is the local mean mass density:

$$\begin{aligned} d_L &= \frac{2\{\Omega z-(2-\Omega)[(1+\Omega z)^{1/2}-1]\}}{H_0\Omega^2} \\ &\simeq (c/H_0)[z+(1-\Omega/2)z^2/2+\cdots] . \end{aligned} \tag{C10}$$

If the universe is inhomogeneous on small scales, Eq. (C10) must be modified.

Using Eqs. (C6)—(C9), we obtain the flux observed from a cosmologically distant moving source,

$$S_\nu(\nu) = (1+z)^{1-\alpha} D^{2+\alpha} \int j'_{\nu'}(\nu)dV/d_L^2 . \tag{C11}$$

Similarly, for a source expanding superluminally according to Eq. (C3), the observed angular expansion rate is

$$\frac{d\delta}{dt_{\rm ob}} = \frac{(1+z)[\mathbf{n}\times(\boldsymbol{\beta}\times\mathbf{n})]c}{(1-\boldsymbol{\beta}\cdot\mathbf{n})d_L} . \tag{C12}$$

4. Black holes

The best general reference for the physics of Kerr black holes is Misner, Thorne, and Wheeler (1973; see also Shapiro and Teukolsky, 1983). More detailed discussion is contained in Novikov and Thorne (1973) and Bardeen, Press, and Teukolsky (1972). A modified Newtonian approach to the properties of black holes is summarized by Thorne and Blandford (1982).

If the angular momentum is zero, then the metric is given by the Schwarzschild solution, which can be written

$$\begin{aligned} ds^2 = &-\left[1-\frac{2m}{r}\right]c^2dt^2+\left[1-\frac{2m}{r}\right]^{-1}dr^2 \\ &+r^2(d\theta^2+\sin^2\theta\, d\varphi^2) . \end{aligned} \tag{C13}$$

The coordinate radius r is defined so that the proper area of a sphere of radius r is $4\pi r^2$. The quantity $m = GM/c^2$ is the mass of the hole expressed as a length. This quantity is sometimes referred to as the "gravitational radius" r_g in the text. The gravitational redshift factor for a body stationary at radius r is $(1-2m/r)^{-1/2}$; this becomes infinite as r approaches the event horizon (Schwarzschild radius) at $r=2m$.

The more general Kerr metric, corresponding to a hole of mass M and angular momentum J, can be written

$$\begin{aligned} ds^2 = &-\frac{\Delta}{\rho^2}(c\,dt-a\sin^2\theta\, d\varphi)^2 \\ &+\frac{\sin^2\theta}{\rho^2}[(r^2+a^2)d\varphi-ac\,dt]^2 \\ &+\frac{\rho^2}{\Delta}dr^2+\rho^2 d\theta^2 , \end{aligned} \tag{C14}$$

where

$$\Delta = r^2-2mr+a^2,$$

$$\rho = r^2+a^2\cos^2\theta ,$$

$$a = \frac{J}{Mc} .$$

The quantity a specifies the ratio of angular momentum to mass, and the Kerr metric is therefore a one-parameter family of solutions (with $J=0$ reducing to the

Schwarzschild case). Note that this metric has a $dt\,d\varphi$ term. This reflects the fact that it is no longer *static* though it is still *stationary* (in the sense that the metric components are themselves independent of t). The presence of the $dt\,d\varphi$ term reflects the fact that space near the hole is, in a sense, being dragged around with the hole. The event horizon in the Kerr solution occurs when $\Delta=0$ and has a radius

$$r_+ = m + (m^2 - a^2)^{1/2} . \tag{C15}$$

This horizon disappears if $J = J_{\max} = GM^2/c$ (corresponding to $a = a_{\max} = r_g$). The so-called "cosmic censorship hypothesis" would imply that holes always form with $J < J_{\max}$. The Kerr solution has a critical radius called the *static limit,* within which particles must rotate with the same sense as the hole, relative to nonrotating, distant observers, even though they can still escape—this is a consequence of the fact that the dragging of inertial frames can be so strong that even light cones necessarily point in the φ direction. This critical radius is

$$r_{\rm stat} = m + (m^2 + a^2\cos^2\theta)^{1/2} ; \tag{C16}$$

it corresponds to the radius at which g_{00} vanishes. The region $r_+ < r < r_{\rm stat}$ is called the *ergosphere* because one can in principle extract energy from it by the following process (Penrose, 1969). If a particle enters the ergosphere and splits in two, in such a way that one fragment falls into the hole, then the other may leave the ergosphere with more energy than the original particle. This is possible because energy is being extracted from the hole. A Kerr hole can thus be considered to have two kinds of mass-energy (Christodoulou, 1970): a fraction associated with its spin, which can in principle be extracted via the Penrose process, and an irreducible mass. The fraction of the mass which can be extracted is $1-2^{-1/2}\{1+[1-(a/m)^2]^{1/2}\}^{1/2}$, which is 29% for a maximally rotating hole. The above limit is an instance of a general theorem in black hole physics, according to which the area of the event horizon (a quantity analogous to entropy) cannot decrease: a Kerr hole has a smaller surface area than a Schwarzschild hole of the same mass.

The energy per unit rest mass of a prograde circular orbit of radius r around a Kerr black hole is

$$e = c^2 \left[\frac{r^2 - 2mr + a(mr)^{1/2}}{r[r^2 - 3mr + 2a(mr)^{1/2}]^{1/2}} \right] . \tag{C17}$$

For $r \gg m$, this reduces to $c^2 - GM/2r$, which is just the Newtonian orbital energy. For a Schwarzschild hole, the binding energy has a *maximum* of $0.057c^2$ at $r = 6m$. Circular orbits closer than this have *more* angular momentum and are less tightly bound (as is the case for orbits in Newtonian theory when the effective force law is r^{-n} with $n > 3$); the orbits have zero binding energy for $r = 4m$, and for $r = 3m$ the binding energy diverges (implying that photons can move in circular orbits at this radius). For corotating equatorial orbits in a Kerr metric, the innermost stable orbit moves inward compared to the Schwarzschild case and becomes more tightly bound. As $a \to m$ the stable orbits extend inwards towards $r = r_+$ and the binding energy approaches $(1 - 1/\sqrt{3})c^2 \simeq 0.42c^2$. These numbers determine the maximum theoretical efficiency of accretion disks (see Sec. III.C.3). A related inference is that there are no stationary bound orbits whose angular momentum is less than a definite threshold value—this important qualitative feature of the orbits means the axisymmetric flow patterns cannot extend very close to the rotation axis.

If the orbit does not lie in the equatorial plane then it will precess with the Lense-Thirring angular velocity, $2GJ/r^3c^2$ (Bardeen and Petterson, 1975). For $r \gg m$, the precessional period equals $r^{3/2}/2am^{1/2}$ orbital periods.

REFERENCES

Abramowicz, M. A., M. Calvani, and L. Nobili, 1980, Astrophys. J. **242**, 772.

Abramowicz, M. A., M. Jaroszyński, and M. Sikora, 1978, Astron. Astrophys. **63**, 221.

Abramowicz, M. A., and T. Piran, 1980, Astrophys. J. (Lett.) **241**, L7.

Abramowicz, M. A., and N. A. Sharp, 1983, Astrophys. Space Sci. **96**, 431.

Achterberg, A., 1979, Astron. Astrophys. **76**, 276.

Achterberg, A., 1980, Astron. Astrophys. **98**, 161.

Achterberg, A., 1982, Astron. Astrophys. **114**, 233.

Achterberg, A., R. D. Blandford, and P. Goldreich, 1983, Nature **304**, 607.

Alfvén, H., and N. Herlofson, 1950, Phys. Rev. **78**, 616.

Allan, P. M., 1984, Astrophys. J. Lett. **276**, L31.

Allen, A. J., and P. A. Hughes, 1983, Mon. Not. R. Astron. Soc. **202**, 935.

Aller, H. D., P. Hodge, and M. Aller, 1981, Astrophys. J. (Lett.) **248**, L5.

Aller, H. D., and J. E. Ledden, 1979, Astrophys. J. (Lett.) **227**, L117.

Altschuler, D. R., and J. F. C. Wardle, 1976, Mem. R. Astron. Soc. **82**, 1.

Altschuler, D. R., and J. F. C. Wardle, 1977, Mon. Not. R. Astron. Soc. **179**, 153.

Andernach, H., 1982, in *Extragalactic Radio Sources* (IAU Symposium No. 97), edited by D. S. Heeschen and C. M. Wade (Reidel, Dordrecht, Holland), p. 41.

Andrews, B. H., 1973, Astrophys. J. (Lett.) **186**, L3.

Angel, J. R. P., 1970, Astrophys. J. **158**, 219.

Angel, J. R. P., and H. S. Stockman, 1980, Annu. Rev. Astron. Astrophys. **18**, 321.

Arons, J., R. M. Kulsrud, and J. P. Ostriker, 1975, Astrophys. J. **198**, 687.

Arons, J., C. E. Max, and C. A. Norman, 1977, Phys. Fluids **20**, 1302.

Auriemma, C., G. C. Perola, R. D. Ekers, R. Fanti, C. Levi, W. Jaffe, and M. H. Ulrich, 1977, Astron. Astrophys. **57**, 41.

Axford, W. I., 1981, in *Plasma Astrophysics,* edited by T. D. Guyenne and G. Lévy (European Space Agency, Paris), p. 425.

Axford, W. I., E. Leer, and G. Skadron, 1977, in *Proceedings of the 15th International Cosmic Ray Conference* (Bulgarian Academy of Sciences, Plovdiv, Bulgaria), Vol. 2, p. 273.

Baade, W., and R. Minkowski, 1954, Astrophys. J. **119**, 215.

Baan, W. A., 1980, Astrophys. J. **239**, 433.

Bahcall, J. N., and M. Milgrom, 1980, Astrophys. J. **236**, 24.
Bahcall, J. N., and R. A. Wolf, 1976, Astrophys. J. **209**, 214.
Bailey, M. E., 1980, Mon. Not. R. Astron. Soc. **191**, 195.
Bailey, M. E., and S. V. M. Clube, 1978, Nature **275**, 278.
Balbus, S., 1982, Astrophys. J. **252**, 529.
Baldwin, J., 1982, in *Extragalactic Radio Sources* (IAU Symposium No. 97), edited by D. S. Heeschen and C. M. Wade (Reidel, Dordrecht, Holland), p. 21.
Balick, B., and T. M. Heckman, 1982, Annu. Rev. Astron. Astrophys. **20**, 431.
Bardeen, J. M., 1978, Bull. Am. Astron. Soc. **10**, 507.
Bardeen, J. M., and B. Berger, 1978, Astrophys. J. **221**, 105
Bardeen, J. M., and J. A. Petterson, 1975, Astrophys. J. (Lett.) **195**, L65.
Bardeen, J. M., W. Press, and S. A. Teukolsky, 1972, Astrophys. J. **178**, 347.
Bardeen, J. M., and R. V. Wagoner, 1971, Astrophys. J. **167**, 359.
Barnothy, J. E., 1965, Astron. J. **70**, 666.
Bartel, N., 1984, in *VLBI and Compact Radio Sources* (IAU Symposium No. 110), edited by K. I. Kellermann and G. Setti (Reidel, Dordrecht, Holland), in press.
Batchelor, G., and A. Gill, 1962, J. Fluid Mech. **14**, 529.
Bateman, G., 1978, *MHD Instabilities* (MIT Press, Cambridge).
Bautz, C. P., and W. W. Morgan, 1970, Astrophys. J. (Lett.) **162**, L149.
Begelman, M. C., 1978a, Mon. Not. R. Astron. Soc. **184**, 53.
Begelman, M. C., 1978b, Astron. Astrophys. **70**, 583.
Begelman, M. C., 1979, Mon. Not. R. Astron. Soc. **187**, 237.
Begelman, M. C., 1982, in *Extragalactic Radio Sources* (IAU Symposium No. 97), edited by D. S. Heeschen and C. M. Wade (Reidel, Dordrecht, Holland), p. 223.
Begelman, M. C., R. D. Blandford, and M. J. Rees, 1980, Nature **287**, 307.
Begelman, M. C., and C. F. McKee, 1983, Astrophys. J. **271**, 89.
Begelman, M. C., C. F. McKee, and G. A. Shields, 1983, Astrophys. J. **271**, 70.
Begelman, M. C., and D. Meier, 1982, Astrophys. J. **253**, 873.
Begelman, M. C., and M. J. Rees, 1978, Mon. Not. R. Astron. Soc. **188**, 847.
Begelman, M. C., and M. J. Rees, 1983, in *Astrophysical Jets: Proceedings of an international workshop held in Torino, Italy, ... 1982,* edited by A. Ferrari and A. G. Pacholczyk (Reidel, Dordrecht, Holland), p. 215.
Begelman, M. C., and M. J. Rees, 1984, Mon. Not. R. Astron. Soc. **206**, 209.
Begelman, M. C., M. J. Rees, and R. D. Blandford, 1979, Nature **279**, 770.
Begelman, M. C., C. L. Sarazin, S. P. Hatchett, C. F. McKee, and J. Arons, 1980, Astrophys. J. **238**, 722.
Behr, C., E. L. Schucking, C. V. Vishveshwara, and W. Wallace, 1976, Astron. J. **81**, 147.
Bekefi, G., B. T. Field, J. Parmentola, and K. Tsipsis, 1980, Nature **248**, 219.
Bell, A. R., 1977, Mon. Not. R. Astron. Soc. **179**, 573.
Bell, A. R., 1978, Mon. Not. R. Astron. Soc. **182**, 147.
Belvedere, G., and D. Molteni, 1982, Astrophys. J. **263**, 611.
Benford, G., 1977, Mon. Not. R. Astron. Soc. **179**, 595.
Benford, G., 1978, Mon. Not. R. Astron. Soc. **183**, 29.
Benford, G., 1981, Astrophys. J. **247**, 792.
Benford, G., 1983, in *Astrophysical Jets: Proceedings of an international workshop held in Torino, Italy, ... 1982,* edited by A. Ferrari and A. G. Pacholczyk (Reidel, Dordrecht, Holland), p. 271.
Benford, G., A. Ferrari, and E. Trussoni, 1980, Astrophys. J. **241**, 98.
Bicknell, G. V., and R. N. Henriksen, 1980, Astrophys. Lett. **21**, 29.
Bicknell, G. V., and D. B. Melrose, 1982, Astrophys. J. **262**, 511.
Biermann, P., P. P. Kronberg, E. Preuss, R. T. Schilizzi, and D. B. Shaffer, 1981, Astrophys. J. (Lett.) **250** L49.
Biretta, J., M. H. Cohen, S. C. Unwin, and I. I. K. Pauliny-Toth, 1983, Nature **306**, 42.
Biretta, J., F. N. Owen, and P. E. Hardee, 1983, Astrophys. J. (Lett.) **274**, L27.
Bisnovatyi-Kogan, G. S., and S. I. Blinnikov, 1977, Astron. Astrophys. **59**, 111.
Bisnovatyi-Kogan, G. S., and S. I. Blinnikov, 1980, Mon. Not. R. Astron. Soc. **191**, 711.
Bisnovatyi-Kogan, G. S., and R. A. Sunyaev, 1972a, Sov. Astron. AJ **15**, 881.
Bisnovatyi-Kogan, G. S., and R. A. Sunyaev, 1972b, Sov. Astron. AJ **16**, 206.
Bjornsson, C. I., 1982, Astrophys. J. **260**, 855.
Blake, G. M., 1970, Astrophys. Lett. **6**, 201.
Blake, G. M., 1972, Mon. Not. R. Astron. Soc. **156**, 67.
Blandford, R. D., 1973a, Ph.D. thesis (University of Cambridge).
Blandford, R. D., 1973b, Astron. Astrophys. **26**, 161.
Blandford, R. D., 1976, Mon. Not. R. Astron. Soc. **176**, 465.
Blandford, R. D., 1979, in *Particle Acceleration Mechanisms in Astrophysics, La Jolla Institute—1979* (AIP conference proceedings No. 56), edited by J. Arons, C. Max, and C. McKee (AIP, New York), p. 333.
Blandford, R. D., 1981, in *Supernovae: A Survey of Current Research,* edited by M. J. Rees and R. J. Stoneham (Reidel, Dordrecht, Holland), p. 459.
Blandford, R. D., 1984, in *VLBI and Compact Radio Sources* (IAU Symposium No. 110), edited by K. I. Kellermann and G. Setti (Reidel, Dordrecht, Holland), in press.
Blandford, R. D., and V. Icke, 1978, Mon. Not. R. Astron. Soc. **185**, 527.
Blandford, R. D., M. Jaroszyński, and S. Kumar, 1984 (in preparation).
Blandford, R. D., and A. Königl, 1979a, Astrophys. Lett. **20**, 15.
Blandford, R. D., and A. Königl, 1979b, Astrophys. J. **232**, 34.
Blandford, R. D., and C. F. McKee, 1977, Mon. Not. R. Astron. Soc. **180**, 343.
Blandford, R. D., C. F. McKee, and M. J. Rees, 1977, Nature **267**, 211.
Blandford, R. D., and J. P. Ostriker, 1978, Astrophys. J (Lett.) **221**, L29.
Blandford, R. D., and D. G. Payne, 1982, Mon. Not. R. Astron. Soc. **199**, 883.
Blandford, R. D., and J. E. Pringle, 1976, Mon. Not. R. Astron. Soc. **176**, 443.
Blandford, R. D., and M. J. Rees, 1972, Astrophys. Lett. **10**, 77.
Blandford, R. D., and M. J. Rees, 1974, Mon. Not. R. Astron. Soc. **169**, 395.
Blandford, R. D., and M. J. Rees, 1978a, in *Pittsburgh Conference on BL Lac Objects,* edited by A. M. Wolfe (Department of Physics and Astronomy, University of Pittsburgh, Pittsburgh), p. 328.
Blandford, R. D., and M. J. Rees, 1978b, Phys. Scr. **17**, 625.
Blandford, R. D., and R. L. Znajek, 1977, Mon. Not. R. As-

tron. Soc. **179**, 433.
Blumenthal, G. R., and R. J. Gould, 1970, Rev. Mod. Phys. **42**, 237.
Blumenthal, G. R., and W. G. Mathews, 1975, Astrophys. J. **198**, 517.
Bodo, G., and A. Ferrari, 1982, Astron. Astrophys. **114**, 394.
Bodo, G., A. Ferrari, and S. Massaglia, 1981, Mon. Not. R. Astron. Soc. **196**, 481.
Bondi, H., 1952, Mon. Not. R. Astron. Soc. **112**, 195.
Boroson, T., J. B. Oke, and R. F. Green, 1982, Astrophys. J. **263**, 32.
Bradshaw, P., 1977, Annu. Rev. Fluid Mechanics **9**, 33.
Bridle, A. H., 1982, in *Extragalactic Radio Sources* (IAU Symposium No. 97), edited by D. S. Heeschen and C. M. Wade (Reidel, Dordrecht, Holland), p. 121.
Bridle, A. H., and G. W. Brandie, 1973, Astrophys. Lett. **15**, 21.
Bridle, A. H., K. L. Chan, and R. N. Henriksen, 1981, J. R. Astron. Soc. Can. **75**, 69.
Bridle, A. H., M. M. Davies, E. B. Fomalont, A. G. Willis, and R. G. Strom, 1979, Astrophys. J. (Lett.) **228**, L9.
Bridle, A. H., R. N. Henriksen, K. L. Chan, E. B. Fomalont, A. G. Willis, and R. A. Perley, 1980, Astrophys. J. **241**, L145.
Bridle, A. H., and R. A. Perley, 1984, Annu. Rev. Astron. Astrophys. **22** (in press).
Browne, I. W. A., 1983, Mon. Not. R. Astron. Soc. **204**, 23p.
Browne, I. W. A., M. J. L. Orr, R. J. Davis, A. Foley, T. W. B. Muxlow, and P. Thomasson, 1982, Mon. Not. R. Astron. Soc. **198**, 673.
Burbidge, G. R., 1958, Astrophys. J. **129**, 841.
Burbidge, G. R., 1961, Nature **190**, 1053.
Burbidge, G. R., 1967, Nature **216**, 1287.
Burbidge, G. R., T. W. Jones, and S. L. O'Dell, 1974, Astrophys. J. **193**, 43.
Burch, S. F., 1977a, Mon. Not. R. Astron. Soc. **180**, 623.
Burch, S. F., 1977b, Mon. Not. R. Astron. Soc. **181**, 599.
Burch, S. F., 1979, Mon. Not. R. Astron. Soc. **187**, 187.
Burn, B. J., 1966, Mon. Not. R. Astron. Soc. **133**, 67.
Burn, B. J., 1976, Astron. Astrophys. **45**, 435.
Burns, J. O., 1981, Mon. Not. R. Astron. Soc. **195**, 523.
Burns, J. O., J. A. Eilek, and F. N. Owen, 1982, in *Extragalactic Radio Sources* (IAU Symposium No. 97), edited by D. S. Heeschen and C. M. Wade (Reidel, Dordrecht, Holland), p. 45.
Burns, J. O., and S. A. Gregory, 1982, Astron. J. **87**, 1245.
Burns, J. O., S. A. Gregory, and G. O. Holman, 1981, Astrophys. J. **250**, 450.
Burns, J. O., F. N. Owen, and L. Rudnick, 1978, Astrophys. J. **84**, 11.
Burns, J. O., E. Schwendeman, and R. A. White, 1983, Astrophys. J. **271**, 575.
Burns, J. O., R. A. White, and D. H. Hough, 1981, Astron. J. **86**, 1.
Burns, M. L., 1981, Ph.D. thesis (Cornell University).
Burns, M. L., and R. V. E. Lovelace, 1982, Astrophys. J. **262**, 87.
Butcher, H., W. J. M. van Breugel, and G. Miley, 1980, Astrophys. J. **235**, 749.
Callahan, P. S., 1975, Mon. Not. R. Astron. Soc. **173**, 111.
Callahan, P. S., 1977, Astron. Astrophys. **59**, 127.
Carter, B., 1979, in *General Relativity: an Einstein Centenary Survey*, edited by S. W. Hawking and W. Israel (Cambridge University, Cambridge), p. 294.
Cassen, P., 1978, Astrophys. J. **219**, 336.
Cassen, P., and D. Pettibone, 1976, Astrophys. J. **208**, 500.
Cavaliere, A. G., P. Morrison, and F. Pacini, 1970, Astrophys. J. (Lett.) **162**, L133.
Cavaliere, A. G., P. Morrison, and L. Sartori, 1971, Science **173**, 525.
Cavaliere, A. G., F. Pacini, and G. Setti, 1969, Astrophys. Lett. **4**, 103.
Cesarsky, C., 1980, Annu. Rev. Astron. Astrophys. **18**, 289.
Chan, K. L., and R. N. Henriksen, 1980, Astrophys. J. **241**, 534.
Chandrasekhar, S., 1961, *Hydrodynamic and Hydromagnetic Stability* (Clarendon, Oxford).
Cheng, F. T., and P. C. W. Fung, 1977a, Astrophys. Space Sci. **49**, 427.
Cheng, F. T., and P. C. W. Fung, 1977b, Astrophys. Space Sci. **52**, 243.
Cheng, A. Y. S., and S. L. O'Dell, 1981, Astrophys. J. (Lett.) **251**, L49.
Chitre, D. M., and J. V. Narlikar, 1979, Mon. Not. R. Astron. Soc. **187**, 655.
Chitre, D. M., and C. V. Vishveshwara, 1975, Phys. Rev. D **12**, 1538.
Christiansen, W. A., 1969, Mon. Not. R. Astron. Soc. **145**, 327.
Christiansen, W. A., 1971, Astrophys. Lett. **7**, 233.
Christiansen, W. A., 1973, Mon. Not. R. Astron. Soc. **164**, 211.
Christiansen, W. A., A. G. Pacholczyk, and J. S. Scott, 1976, Astrophys. J. **210**, 311.
Christiansen, W. A., A. G. Pacholczyk, and J. S. Scott, 1977, Nature **266**, 503.
Christiansen, W. A., A. G. Pacholczyk, and J. S. Scott, 1981, Astrophys. J. **251**, 518.
Christiansen, W. A., G. Rolison, and J. S. Scott, 1979, Astrophys. J. **234**, 456.
Christiansen, W. A., and J. S. Scott, 1977, Astrophys. J. (Lett.) **216**, L1.
Christiansen, W. A., J. S. Scott, and W. T. Vestrand, 1978, Astrophys. J. **223**, 13.
Christodoulou, P., 1970, Phys. Rev. Lett. **25**, 1596.
Cioffi, D. F., and T. W. Jones, 1980, Astron. J. **85**, 368.
Cocke, W. J., M. S. Giampapa, and A. G. Pacholczyk, 1975, Astrophys. J. **195**, 279.
Cocke, W. J., M. S. Giampapa, and A. G. Pacholczyk, 1979, Astrophys. J. **229**, 503.
Cocke, W. J., and A. G. Pacholczyk, 1975, Astrophys. J. **195**, 279.
Cocke, W. J., and A. G. Pacholczyk, 1977, Nature **265**, 608.
Cocke, W. J., A. G. Pacholczyk, and F. A. Hopf, 1978, Astrophys. J. **226**, 26.
Cohen, M. H., W. Cannon, G. H. Purcell, D. B. Shaffer, J. J. Broderick, K. I. Kellermann, and D. L. Jauncey, Astrophys. J. **170**, 207.
Cohen, M. H., T. J. Pearson, A. C. S. Readhead, G. A. Seielstud, R. S. Simon, and R. C. Walker, 1979, Astrophys. J. **231**, 293.
Cohen, M. H., and A. C. S. Readhead, 1979, Astrophys. J. (Lett.) **233**, L101.
Cohen, M. H., and S. C. Unwin, 1984, in *VLBI and Compact Radio Sources* (IAU Symposium No. 110), edited by K. I. Kellermann and G. Setti (Reidel, Dordrecht, Holland), in press.
Cohn, H., 1983, Astrophys. J. **269**, 500.
Cohn, H., and R. M. Kulsrud, 1978, Astrophys. J. **226**, 1087.
Colgate, S. A., 1967, Astrophys. J. **150**, 163.
Colgate, S. A., and A. G. Petschek 1976, in *Supernovae: Proceedings of a special IAU session . . .*, jointly sponsored by IAU Commissions No. 35 and 48, edited by D. N. Schramm (Reidel, Dordrecht, Holland), p. 73.

Condon, J. J., and D. C. Backer, 1975, Astrophys. J. **197**, 31.
Condon, J. J., and L. L. Dressel, 1973, Astrophys. Lett. **15**, 703.
Condon, J. J., and L. L. Dressel, 1974, Astrophys. J. (Lett.) **15**, 203.
Condon, J. J., and L. L. Dressel, 1978, Astrophys. J. **221**, 456.
Condon, J. J., D. L. Jauncey, M. G. Smith, A. J. Turlte, and A. E. Wright, 1981b, Astrophys. J. **244**, 5.
Condon, J. J., J. E. Ledden, S. L. O'Dell, and B. Dennison, 1979, Astron. J. **84**, 1.
Condon, J. J., S. L. O'Dell, J. J. Puschell, and W. A. Stein, 1981a, Astrophys. J. **246**, 624.
Cook, D. B., and S. R. Spangler, 1980, Astrophys. J. **240**, 751.
Cornwell, T. S., and R. A. Perley, 1984 (in preparation).
Coroniti, F. V., 1981, Astrophys. J. **244**, 587.
Coroniti, F. V., 1983, in Proceedings of IAU Symposium No. 107, edited by M. R. Kundu and G. D. Holman (Reidel, Dordrecht, Holland), in press.
Cotton, W. D., J. J. Wittels, I. I. Shapiro, J. Marcaide, F. N. Owen, S. R. Spangler, A. Rius, C. Angulo, T. A. Clark, and C. A. Knight, 1980, Astrophys. J. (Lett.) **238**, L123.
Courant, R., and K. O. Friedrichs, 1948, *Supersonic Flow and Shock Waves* (Interscience, New York).
Cowie, L. L., and C. F. McKee, 1975, Astron. Astrophys. **43**, 337.
Cowie, L. L., J. P. Ostriker, and A. A. Stark, 1978, Astrophys. J **226**, 1041.
Cowie, L. L., and A. Songaila, 1978, Nature **266**, 501.
Cunningham, C., 1973, Ph.D. thesis (University of Washington).
Curtis, H. D., 1918, Lick Obs. Publication **13**, 11.
Damour, T., 1976, Ann. NY Acad. Sci. **262**, 113.
Damour, T., 1978, Phys. Rev. D **18**, 3598.
Davidson, K., and H. Netzer, 1979, Rev. Mod. Phys. **51**, 715.
de Bruyn, A. G., 1976, Astron. Astrophys. **52**, 439.
de Bruyn, A. G., and A. S. Wilson, 1978, Astron. Astrophys. **64**, 433.
De Young, D. S., 1971a, Astrophys. J. **167**, 541.
De Young, D. S., 1971b, Astrophys. Lett. **9**, 43.
De Young, D. S., 1972, Astrophys. J. **177**, 573.
De Young, D. S., 1976, Annu. Rev. Astron. Astrophys. **14**, 447.
De Young, D. S., 1977, Astrophys. J. **211**, 329.
De Young, D. S., 1980, Astrophys. J. **241**, 81.
De Young, D. S., 1981, Nature **293**, 43.
De Young, D. S., 1982, in *Extragalactic Radio Sources* (IAU Symposium No. 97), edited by D. S. Heeschen and C. M. Wade (Reidel, Dordrecht, Holland), p. 69.
De Young, D. S., and W. I. Axford, 1967, Nature **216**, 129.
De Young, D. S., J. J. Condon, and H. Butcher, 1980, Astrophys. J. **242**, 511.
Dennison, B., and J. J. Condon, 1980, Astrophys. J. **246**, 91.
Dent, W. A., 1965, Science **148**, 1458.
Dent, W. A., 1972, Science **175**, 1105.
Dobrowolny, M., A. Ferrari, and S. Massaglia, 1978, Mon. Not. R. Astron. Soc. **185**, 335.
Downes, A. J. B., 1982, in *Extragalactic Radio Sources* (IAU Symposium No. 97), edited by D. S. Heeschen and C. M. Wade (Reidel, Dordrecht, Holland), p. 393.
Dreher, J. W., 1979, Astrophys. J. **230**, 687.
Dreher, J. W., 1981, Astron. J. **86**, 883.
Dreher, J. W., and E. D. Feigelson, 1984, *Nature* (in press).
Dressel, L., 1981, Astrophys. J. **245**, 25.
Duncan, M. J., and S. L. Shapiro, 1983, Astrophys. J. **268**, 565.
Dyson, J. E., S. A. E. G. Falle, and J. J. Perry, 1980, Mon. Not. R. Astron. Soc. **191**, 785.
Eardley, D. M., and A. P. Lightman, 1975, Astrophys. J. **200**, 187.
Earl, J. A., 1976, Astrophys. J. **206**, 301.
Edgar, B., and L. Rudnick, 1983 (University of Minnesota preprint).
Edge, D. O., and M. J. Mulkay, 1976, *Astronomy Transformed: The Emergence of Radio Astronomy in Britain* (Wiley, New York).
Edwards, A. L., 1980, Mon. Not. R. Astron. Soc. **190**, 757.
Eichler, D., 1979, Astrophys. J. **229**, 419.
Eichler, D., 1981, Astrophys. J. **247**, 1089.
Eichler, D., 1982, Astrophys. J. **263**, 571.
Eichler, D., 1983, Astrophys. J. **272**, 48.
Eilek, J., 1979, Astrophys. J. **230**, 373.
Eilek, J., 1982, Astrophys. J. **254**, 472.
Eilek, J., J. O. Burns, C. P. O'Dea and F. N. Owen, 1983, Astrophys. J. (in press).
Eilek, J. and R. N. Henriksen, 1984, Astrophys. J. (in press).
Eikers, R. D., 1982, in *Extragalactic Radio Sources* (IAU Symposium No. 97), edited by D. S. Heeschen and C. M. Wade (Reidel, Dordrecht, Holland), p. 465.
Eikers, R. D., R. Fanti, C. Levi, and P. Parma, 1978, Nature **276**, 588.
Epstein, R. I., 1973, Astrophys. J. **183**, 593.
Epstein, R. I., and M. J. Geller, 1977, Nature **265**, 219.
Fabian, A. C., E. M. Hu, L. L. Cowie, and J. Grindlay, 1981, Astrophys. J. **248**, 47.
Fabian, A. C., J. E. Pringle, and M. J. Rees, 1975, Mon. Not. R. Astron. Soc. **172**, 15p.
Fanaroff, B., and J. M. Riley, 1974, Mon. Not. R. Astron. Soc. **167**, 31p.
Feigelson, E. D., 1983, in *Extragalactic Radio Sources* (IAU Symposium No. 97), edited by D. S. Heeschen and C. M. Wade (Reidel, Dordrecht, Holland), p. 465.
Feigelson, E. D., T. Maccacaro, and G. Zamorani, 1982, Astrophys. J. **256**, 397.
Feigelson, E. D., E. J. Schreier, J. P. Delvaille, R. Giaconni, J. E. Grindlay, and A. P. Lightman, 1981, Astrophys. J. **251**, 31.
Federenko, V. N., 1980, Sov. Astron. AJ **24**, 294.
Ferrari, A., S. Massaglia, and M. Dobrowolny, 1980, Astron. Astrophys. **92**, 246.
Ferrari, A., S. Massaglia, and E. Trussoni, 1982, Mon. Not. R. Astron. Soc. **198**, 1065.
Ferrari, A. E., and E. Trussoni, 1983, Mon. Not. R. Astron. Soc. **205**, 515.
Ferrari, A., E. Trussoni, and L. Zaninetti, 1978a, Mon. Not. R. Astron. Soc. **182**, 49.
Ferrari, A., E. Trussoni, and L. Zaninetti, 1978b, Astron. Astrophys. **64**, 43.
Ferrari, A., E. Trussoni, and L. Zaninetti, 1979, Astron. Astrophys. **79**, 190.
Ferrari, A., E. Trussoni, and L. Zaninetti, 1980, Mon. Not. R. Astron. Soc. **193**, 469.
Ferrari, A., E. Trussoni, and L. Zaninetti, 1981, Mon. Not. R. Astron. Soc. **196**, 1051.
Fiedler, R., 1982, Ph.D. thesis (University of Minnesota)
Fishbone, L. G., and V. Moncrief, 1976, Astrophys. J. **207**, 962.
Flammang, R. A., 1982, Mon. Not. R. Astron. Soc. **199**, 833.
Flasar, P. M., and P. Morrison, 1976, Astrophys. J. **204**, 352.
Fomalont, E. B., 1981, in *Origin of Cosmic Rays* (IAU Symposium No. 94), edited by G. Setti, G. Spada, and A. W. Wolfendale (Reidel, Dordrecht, Holland), p. 111.
Fomalont, E. B., A. H. Bridle, A. G. Willis, and R. A. Perley, 1980, Astrophys. J. **237**, 418.

Fomalont, E. B., B. J. Geldzahler, R. M. Hjellming, and C. M. Wade, 1983, Astrophys. J. (Lett.) **275**, 802.
Fowler, W. A., 1966, Astrophys. J. **144**, 180.
Frank, J., 1978, Mon. Not. R. Astron. Soc. **184**, 87.
Frank, J., 1979, Mon. Not. R. Astron. Soc. **187**, 883.
Frank, J., and M. J. Rees, 1976, Mon. Not. R. Astron. Soc. **176**, 633.
Fukue, J., 1982, Publ Astron. Soc. Japan **34**, 163.
Fukue, J., 1983, Publ Astron. Soc. Japan (in press).
Gailitis, A., and V. N. Tsytovich, 1964, Zh. Eksp. Teor. Fiz. **46**, 1726 [Sov. Phys.—JETP **19**, 1165 (1964)].
Galeev, A. A., R. Rosner, and G. S. Vaiana, 1979, Astrophys. J. **229**, 318.
Geldzahler, B., T. Pauls, and C. Salter, 1980, Astron. Astrophys. **84**, 237.
Gerwin, R. A., 1968, Rev. Mod. Phys. **40**, 652.
Getmansev, G. G., 1971, Nature Phys. Sci. **229**, 199.
Gilden, D. L., and J. C. Wheeler, 1980, Astrophys. J. **239**, 705.
Gill, A. E., 1965, Phys. Fluids **8**, 1428.
Ginzburg, V. L., and L. M. Ozernoi, 1967, Astrophys. J. **144**, 599.
Gioia, I. M., L. Gregorini, and G. Veltolani, 1981, Astron. Astrophys. **96**, 58.
Gisler, G., 1976, Astron. Astrophys. **51**, 137.
Goldreich, P., and W. H. Julian, 1969, Astrophys. J. **157**, 869.
Goldreich, P., F. Pacini, and M. J. Rees, 1971, Comments Astrophys. Space Phys. **3**, 185.
Goldreich, P., and G. Schubert, 1967, Astrophys. J. **150**, 571.
Gopal-Krishna, 1977, Mon. Not. R. Astron. Soc. **181**, 247.
Gopal-Krishna, 1980a, Astron. Astrophys. **81**, 328.
Gopal-Krishna, 1980b, Astron. Astrophys. **86**, L3.
Gott, J. R., and J. E. Gunn, 1972, Astrophys. J. **176** 1.
Gould, R. J., 1981, Phys. Fluids **24**, 102.
Gould, R. J., 1982a, Astrophys. J. **254**, 755.
Gould, R. J., 1982b, Astrophys. J. **263**, 879.
Gower, A. C., P. C. Gregory, J. B. Hutchings, and W. G. Unruh, 1982, Astrophys. J. **262**, 478.
Gower, A. C., and J. B. Hutchings, 1982a, Astrophys. J. (Lett.) **253**, L1.
Gower, A. C., J. B. Hutchings, 1982b, Astrophys. J. (Lett.) **258**, L63.
Green, R. F., and M. Schmidt, 1978, Astrophys. J. (Lett.) **220**, L1.
Gull, S. F., 1974, Observatory **94**, 266.
Gull, S. F., 1975, Ph.D. thesis (University of Cambridge).
Gull, S. F., and K. J. E. Northover, 1973, Nature **224**, 80.
Gunn, J. E., 1978, in *Active Galactic Nuclei,* edited by C. Hazard and S. Mitton (Cambridge University, Cambridge), p. 213.
Gunn, J. E., and J. P. Ostriker, 1970, Astrophys. J. **157**, 1395.
Gurzadyan, V. G., and L. M. Ozernoi, 1982, Astron. Astrophys. **95**, 39.
Guthrie, B. N. G., 1979, Mon. Not. R. Astron. Soc. **187**, 581.
Hardee, P. E., 1979, Astrophys. J. **234**, 47.
Hardee, P. E., 1981, Astrophys. J. (Lett.) **250**, L9.
Hardee, P. E., 1982, Astrophys. J. **257**, 509.
Hardee, P. E., 1983, Astrophys. J. **269**, 94.
Hardee, P. E., 1984, Astrophys. J. **277**, 106.
Hardee, P. E., J. Eilek, and F. N. Owen, 1980, Astrophys. J. **242**, 502.
Hargrave, P. J., and M. McEllin, 1975, Mon. Not. R. Astron. Soc. **173**, 37.
Hargrave, P. J., and M. Ryle, 1974, Mon. Not. R. Astron. Soc. **166**, 305.
Hargrave, P. J., and M. Ryle, 1976, Mon. Not. R. Astron. Soc. **175**, 481.
Harris, A., 1974, Mon. Not. R. Astron. Soc. **106**, 449.
Harris, D. E., 1982, in *Extragalactic Radio Sources* (IAU Symposium No. 97), edited by D. S. Heeschen and C. M. Wade (Reidel, Dordrecht, Holland), p. 77.
Hausman, M. A., and J. P. Ostriker, 1979, Astrophys. J. **224**, 320.
Hawley, J. F., and L. L. Smarr, 1984, in Proceedings of the Toulouse Conference on Numerical General Relativity (Reidel, Dordrecht, Holland) (in press).
Hawley, J. F., L. L. Smarr, and J. R. Wilson, 1984a, Astrophys. J. **277**, 296.
Hawley, J. F., L. L. Smarr, and J. R. Wilson, 1984b, Astrophys. J. Suppl. **55** (in press).
Haynes, M. P., and M. S. Roberts, 1979, Astrophys. J. **227**, 769.
Hazard, C., and S. Mitton, 1979, Eds., *Active Galactic Nuclei* (Cambridge University, Cambridge).
Heckman, T. M., 1980, Astron. Astrophys. **87**, 152.
Heeschen, D. S., and C. M. Wade, 1982, Eds., *Extragalactic Radio Sources* (IAU Symposium No. 97) (Reidel, Dordrecht, Holland).
Henriksen, R. N., A. H. Bridle, and K. L. Chan, 1982, Astrophys. J. **257**, 63.
Henriksen, R. N., J. P. Vallée, and A. H. Bridle, 1981, Astrophys. J. **249**, 40.
Hey, J. S., 1971, *The Radio Universe* (Pergamon, Oxford).
Hills, J. G., 1975, Nature **254**, 295.
Hills, J. G., 1978, Mon. Not. R. Astron. Soc. **182**, 517.
Hine, R. G., and M. S. Longair, 1979, Mon. Not. R. Astron. Soc. **188**, 111.
Hine, R. G., and P. A. G. Scheuer, 1980, Mon. Not. R. Astron. Soc. **193**, 285.
Hirasawa, T., and H. Tabara, 1970, Astrophys. Lett. **7**, 121.
Hirth, 1970, Astrophys. J. (Lett.) **7**, 153.
Hjellming, R. M., and K. L. Johnston, 1981, Astrophys. J. (Lett.) **246**, L141.
Hodge, P. E., 1982, Astrophys. J. **263**, 595.
Holman, G., J. A. Ionson, and J. S. Scott, 1979, Astrophys. J. **228**, 576.
Hooley, A., 1976, Mon. Not. R. Astron. Soc. **167**, 31p.
Hooley, A., M. S. Longair, and J. M. Riley, 1978, Mon. Not. R. Astron. Soc. **182**, 127.
Hoyle, F., and W. A. Fowler, 1963a, Mon. Not. R. Astron. Soc. **125**, 169.
Hoyle, F., and W. A. Fowler, 1963b, Nature **197**, 533.
Hoyle, F., G. R. Burbidge, and W. L. W. Sargent, 1966, Nature **209**, 751.
Hughes, P. A., 1979, Mon. Not. R. Astron. Soc. **186**, 853.
Hughes, P. A., 1980, Mon. Not. R. Astron. Soc. **193**, 277.
Hughes, P. A., and A. J. Allen, 1981, Mon. Not. R. Astron. Soc. **196**, 339.
Hummel, E., 1981, Astron. Astrophys. **96**, 111.
Hunstead, R. W., 1972, Astrophys. Lett. **12**, 193.
Icke, V., 1977, Nature **266**, 699.
Icke, V., 1980, Astron. J. **85**, 329.
Icke, V., 1981, Astrophys. J. (Lett.) **246**, L65.
Icke, V., 1983, Astrophys. J. **265**, 648.
Ikeuchi, S., 1981, Pub. Astron. Soc. Japan **33**, 211.
Ingham, W., and P. Morrison, 1975, Mon. Not. R. Astron. Soc. 173, 569.
Jackson, J. D., 1977, *Classical Electrodynamics* (Wiley, New York).
Jaffe, W. J., 1980, Astrophys. J. **241**, 925.

Jaffe, W. J., and G. C. Perola, 1973, Astron. Astrophys. **26**, 423.
Jaffe, W. J., and G. C. Perola, 1975, Astron. Astrophys. **42**, 163.
Jaroszyński, M., M. A. Abramowicz, and B. Paczynski, 1980, Acta Astron. **30**, 1.
Jauncey, D. L., 1977, Ed., *Radio Astronomy and Cosmology* (Reidel, Dordrecht, Holland).
Jenkins, C. J., and P. A. G. Scheuer, 1976, Mon. Not. R. Astron. Soc. **174**, 327.
Jenkins, C. J., and M. McEllin, 1977, Mon. Not. R. Astron. Soc. **180**, 219.
Jenkins, C. R., 1981, Mon. Not. R. Astron. Soc. **196**, 987.
Jennison, R. C., and M. S. Das Gupta, 1953, Nature **172**, 996.
Jennison, R. C., 1958, Mon. Not. R. Astron. Soc. **118**, 276.
Jones, T. W., and G. R. Burbidge, 1973, Astrophys. J. **186**, 791.
Jones, T. W., and P. E. Hardee, 1979, Astrophys. J. **228**, 268.
Jones, T. W., and S. L. O'Dell, 1977a, Astron. Astrophys. **61**, 291.
Jones, T. W., and S. L. O'Dell, 1977b, Astrophys. J. **214**, 522.
Jones, T. W., and S. L. O'Dell, 1978, Astrophys. J. **215**, 236.
Jones, T. W., S. L. O'Dell, and W. A. Stein, 1974a, Astrophys. J. **188**, 353.
Jones, T. W., S. L. O'Dell, and W. A. Stein, 1974b, Astrophys. J. **192**, 261.
Jones, T. W., and F. N. Owen, 1979, Astrophys. J. **234**, 818.
Jones, D. L., R. A. Sramek, and Y. Terzian, 1981, Astrophys. J. (Lett.) **247**, L57.
Jones, T. W., and D. Tobin, 1977, Astrophys. J. **215**, 474.
Kafka, P., and P. Mészáros, 1977, Gen. Relativ. Gravitation **7**, 84.
Kahn, F. D., 1983, Mon. Not. R. Astron. Soc. **202**, 553.
Kandrup, H., 1982, Astrophys. J. **255**, 691.
Kapahi, V., and R. Schilizzi, 1979, Nature **277**, 610.
Kapahi, V. K., and C. R. Subrahmanya, 1982, in *Extragalactic Radio Sources* (IAU Symposium No. 97), edited by D. S. Heeschen and C. M. Wade (Reidel, Dordrecht, Holland), p. 401.
Kardashev, N., 1966, Sov. Astron. AJ **89**, 217.
Katgert-Meikelijn, J., C. Levi, and L. Padrielli, 1980, Astron. Astrophys. Suppl. **40**, 91.
Katz, J. I., 1980, Astrophys. J. **236**, L127.
Keel, W. C., 1983, Astrophys. J. **269**, 466.
Kellermann, K. I., and I. I. K. Pauliny-Toth, 1966, Astrophys. J. **146**, 632.
Kellermann, K. I., and I. I. K. Pauliny-Toth, 1968, Annu. Rev. Astron. Astrophys. **6**, 417.
Kellermann, K. I., and I. I. K. Pauliny-Toth, 1981, Annu. Rev. Astron. Astrophys. **19**, 373.
Kellermann, K. I., and G. Setti, 1984, Eds., *VLBI and Compact Radio Sources* (IAU Symposium No 110) (Reidel, Dordrecht, Holland), in press.
Kellermann, K. I., R. Sramek, D. Shaffer, M. Schmidt, and R. Green, 1983, in *Quasars and Gravitational Lenses: Proceedings No. 24 International Astrophysics Colloquium, Liege* (Université de Liège, Institut d' Astrophysique), p. 81.
Kerr, A. J., P. Birch, R. G. Conway, R. J. Davis, and D. Stannard, 1981, Mon. Not. R. Astron. Soc. **197**, 921.
King, A. R., J. P. Lasota, and W. Kundt, 1976, Phys. Rev. D **12**, 3037.
Kirk, J. G., 1980, Astron. Astrophys. **82**, 262.
Kirshner, R. P., A. Oemler, and P. L. Schechter, 1979, Astron. J. **84**, 951.
Knapp, G. R., F. J. Kerr, and B. Williams, 1978, Astrophys. J. **222**, 800.
Kogure, T., 1971, Publ. Astron. Soc. Japan **23**, 449.
Kompaneets, A. S., 1960, Sov. Phys. Dok. **5**, 46.
Königl, A., 1978, Astrophys. J. **225**, 732.
Königl, A., 1980, Phys. Fluids **23**, 1083.
Königl, A., 1981, Astrophys. J. **243**, 700.
Kotanyi, C. G., and R. D. Ekers, 1979, Astron. Astrophys. **73**, L1.
Kozlowski, M., M. Jaroszyński, and M. A. Abramowicz, 1978, Astron. Astrophys. **63**, 209.
Kraichnan, R. H., 1965, Phys. Fluids **8**, 1385.
Krantter, A., R. N. Henriksen, and K. Lake, 1983, Astrophys. J. **269**, 81.
Kraus, J. D., 1976, *Big Ear* (Cygnus-Quasar Books).
Krimigis, S. M., 1979, in *Particle Acceleration Mechanisms in Astrophysics, La Jolla Institute—1979* (AIP Conference Proceedings No. 56), edited by J. Arons, C. Max, and C. McKee (AIP, New York), p. 179.
Krimsky, G. F., 1977, Dokl. Akad. Nauk SSSR **234**, 1306.
Krolik, J. H., and R. A. London, 1983, Astrophys. J. **267**, 18.
Krolik, J. H., C. F. McKee, and B. Tarter, 1981, Astrophys. J. **249**, 422.
Kulsrud, R. M., and J. Arons, 1975, Astrophys. J. **198**, 709.
Kulsrud, R. M., and A. Ferrari, 1971, Astrophys. Space Sci. **12**, 302.
Kurilchik, V. N., 1972, Astrophys. Lett. **10**, 115.
Lacombe, C., 1976, Astron. Astrophys. **48**, 11.
Lacombe, C., 1977, Astron. Astrophys. **54**, 1.
Lacombe, C., 1979, Astron. Astrophys. **71**, 169.
Laing, R. A., 1980a, Mon. Not. R. Astron. Soc. **193**, 427.
Laing, R. A., 1980b, Mon. Not. R. Astron. Soc. **193**, 439.
Laing, R. A., 1981, Astrophys. J. **248**, 87.
Laing, R. A., 1982, in *Extragalactic Radio Sources* (IAU Symposium No. 97), edited by D. S. Heeschen and C. M. Wade (Reidel, Dordrecht, Holland), p. 161.
Laing, R. A., and J. A. Peacock, 1980, Mon. Not. R. Astron. Soc. **190**, 903.
Landau, L. D., and E. M. Lifshitz, 1959, *Fluid Mechanics* (Pergamon, Oxford).
Lang, K. R., 1978, *Astrophysical Formulae* (Springer, Berlin).
Lea, S. M., and G. Holman, 1978, Astrophys. J. **222**, 29.
Lessen, M., and P. J. Singh, 1973, J. Fluid Mech. **60**, 433.
Levich, E. V., and R. A. Sunyaev, 1970, Astrophys. Lett. **7**, 69.
Levy, E. H., 1971, Astrophys. J. **164**, 23.
Liepmann, H., and A. Roshko, 1957, *Elements of Gas Dynamics* (Wiley, New York).
Lightman, A. P., 1982, Astrophys. J. **253**, 842.
Lightman, A. P., and D. M. Eardley, 1976, Astrophys. J. Lett. **187**, L1.
Lightman, A. P., and S. L. Shapiro, 1977, Astrophys. J. **211**, 244.
Linfield, R. P., 1981a, Astrophys. J. **244**, 436.
Linfield, R. P., 1981b, Astrophys. J. **250**, 464.
Linfield, R. P., 1982, Astrophys. J. **254**, 465.
List, E. J., 1982, Annu. Rev. Fluid Mech. **14**, 189.
Lo, K. Y., and M. J. Claussen, 1983, Nature (in press).
Lo, K. Y., and W. L. W. Sargent, 1979, Astrophys. J. **227**, 756.
Longair, M. S., 1978, in *Observational Cosmology: 8th advanced course of the Swiss Society of Astronomy and Astrophysics,* edited by A. Maeder, L. Martinet, and G. Tammann (Geneva Observatory, Sauverny, Switzerland), p. 127.
Longair, M. S., 1982, Astrophysical Cosmology Study Week.
Longair, M. S., and J. M. Riley, 1979, Mon. Not. R. Astron. Soc. **183**, 625.

Longair, M. S., M. Ryle, and P. A. G. Scheuer, 1973, Mon. Not. R. Astron. Soc. **164**, 243.
Longair, M. S., and M. Seldner, 1979, Mon. Not. R. Astron. Soc. **189**, 433.
Lovelace, R. V. E., 1976, Nature **262**, 649.
Lovelace, R. V. E., J. MacAuslon, and M. L. Burns, 1979, in *Particle Acceleration Mechanisms in Astrophysics* (AIP Conference Proceedings No. 56), edited by J. Arons, C. Max, and C. McKee (AIP, New York).
Lupton, R. H., and J. R. Gott, 1982, Astrophys. J. **255**, 408.
Lynden-Bell, D., 1969, Nature **223**, 690.
Lynden-Bell, D., 1977, Nature **270**, 396.
Lynden-Bell, D., 1978, Phys. Scr. **17**, 185.
Lynden-Bell, D., and J. E. Pringle, 1974, Mon. Not. R. Astron. Soc. **108**, 603.
Macdonald, D., 1984, Mon. Not. R. Astron. Soc. (in press).
Macdonald, D., and K. S. Thorne, 1982, Mon. Not. R. Astron. Soc. **198**, 345.
Macdonald, J., and M. E. Bailey, 1981, Mon. Not. R. Astron. Soc. **197**, 995.
Mackay, C. D., 1971a, Mon. Not. R. Astron. Soc. **151**, 421.
Mackay, C. D., 1971b, Mon. Not. R. Astron. Soc. **154**, 209.
Mackay, C. D., 1973, Mon. Not. R. Astron. Soc. **162**, 1.
Maltby, P., and A. T. Moffet, 1963, Astrophys. J. Suppl. **7**, 141.
Maraschi, L., C. Reina, and A. W. Treves, 1976, Astrophys. J. **206**, 295.
Marcaide, J., and I. I. Shapiro, 1984, Astrophys. J. **276**, 56.
Margon, B., 1982, Science **215**, 247.
Marscher, A. P., 1977, Astrophys. J. **216**, 244.
Marscher, A. P., 1978a, Astrophys. J. **219**, 392.
Marscher, A. P., 1978b, Astrophys. J. **224**, 816.
Marscher, A. P., 1979, Astrophys. J. **228**, 27.
Marscher, A. P., 1980a, Astrophys. J. **235**, 386.
Marscher, A. P., 1980b, Astrophys. J. **239**, 296.
Marscher, A. P., 1983, Astrophys. J. **264**, 296.
Marscher, A. P., and J. J. Broderick, 1982, Astrophys. J. (Lett.) **255**, L11.
Marscher, A. P., and J. S. Scott, 1980, Publ. Astron. Soc. Pac. **92**, 127.
Mathews, W. G., 1983, Astrophys. J. **272**, 390.
Mathews, W. G., and J. C. Baker, 1971, Astrophys. J. **170**, 241.
Mathews, W. G., and J. C. Bregman, 1978, Astrophys. J. **224**, 308.
Mathewson, D. S., M. N. Cleary, and J. D. Murray, 1975, Astrophys. J. (Lett.) **195**, L97.
Max, C. E., 1972, Phys. Rev. Lett. **29**, 1731.
McHardy, I. M., 1979, Mon. Not. R. Astron. Soc. **188**, 495.
McMillan, S. L. W., A. P. Lightman, and H. Cohn, 1981, Astrophys. J. **251**, 436.
McNaughton, K., and P. Sinclair, 1966, J. Fluid Mech. **25**, 367.
Meier, D. L., 1979, Astrophys. J. **233**, 664.
Meier, D. L., 1982a, Astrophys. J. **256**, 386.
Meier, D. L., 1982b, Astrophys. J. **256**, 681.
Meier, D. L., 1982c, Astrophys. J. **256**, 693.
Melrose, D. B., 1971a, Astrophys. Lett. **8**, 35.
Melrose, D. B., 1971b, Astrophys. Lett. **8**, 227.
Melrose, D. B., 1980, *Plasma Astrophysics,* Vols. I,II (Gordon and Breach, New York).
Mészáros, P., 1975, Astron. Astrophys. **44**, 59.
Michel, F. C., 1972, Astrophys. Space Sci. **15**, 153.
Miles, J. W., 1958, J. Fluid Mech. **4**, 538.
Miley, G. K., 1971, Mon. Not. R. Astron. Soc. **152**, 477.
Miley, G. K., 1980, Annu. Rev. Astron. Astrophys. **18**, 165.
Miley, G. K., T. Heckman, H. Butcher, and W. J. M. van Breugel, 1981, Astrophys. J. (Lett.) **247**, L5.
Miley, G. K., and H. van der Laan, 1973, Astron. Astrophys. **28**, 359.
Miley, G. K., and J. S. Miller, 1979, Astrophys. J. **228**, L55.
Miley, G. K., G. C. Perola, P. C. van der Krint, and H. van der Laan, 1972, Nature **237**, 209.
Miley, G. K., and C. M. Wade, 1971, Astrophys. J. (Lett.) **8**, 11.
Milgrom, M., 1979, Astron. Astrophys. **78**, L17.
Milgrom, M., and J. N. Bahcall, 1978, Nature **274**, 349.
Mills, D. M., and P. A. Sturrock, 1970, Astrophys. Lett. **5**, 105.
Misner, C. W., K. S. Thorne, and J. A. Wheeler, 1973, *Gravitation* (Freeman, San Francisco).
Moffet, A. T., J. Gubbay, D. S. Robertson, and A. J. Legg, 1971, in *External Galaxies and Quasi-Stellar Objects* (IAU Symposium No. 44), edited by D. S. Evans (Reidel, Dordrecht, Holland), p. 228.
Moffet, A. T., 1975, in *Stars and Stellar Systems, IX: Galaxies and the Universe,* edited by A. Sandage, M. Sandage, and J. Kristran (University of Chicago, Chicago), p. 211.
Mollenhoff, C., 1976, Astron. Astrophys. **50**, 105.
Moore, P. K., I. W. A. Browne, E. J. Daintre, R. G. Noble, and D. Walsh, 1981, Mon. Not. R. Astron. Soc. **197**, 325.
Moore, R. L., A. C. S. Readhead, and L. Baåth, 1983, Nature **306**, 44.
Morrison, P., 1969, Astrophys. J. (Lett.) **157**, L73.
Morrison, P., and A. Cavaliere, 1971, in *Nuclei of Galaxies,* edited by D. J. K. O'Connell (North-Holland, Amsterdam), p. 485.
Morrison, P., and L. Sartori, 1968, Astrophys. J. **152**, L139.
Mundt, R., and J. W. Fried, 1983, Astrophys. J. Lett. **274**, L83.
Mushotzky, R. F., 1984, in *Proceedings of the 12th Texas Symposium on Relativistic Astrophysics* (in press).
Narayan, R., R. Nityanda, and P. J. Wiita, 1983, Mon. Not. R. Astron. Soc. **205**, 1103.
Neill, A. E., T. G. Lockhart, R. A. Preston, and D. C. Backer, 1982, in *Extragalactic Radio Sources* (IAU Symposium No. 97), edited by D. S. Heeschen and C. M. Wade (Reidel, Dordrecht, Holland), p. 207.
Nepveu, M., 1979a, Astron. Astrophys. **75**, 149.
Nepveu, M., 1979b, Astron. Astrophys. **79**, 40.
Nepveu, M., 1980, Astron. Astrophys. **84**, 14.
Nepveu, M., 1982a, Astron. Astrophys. **105**, 15.
Nepveu, M., 1982b, Astron. Astrophys. **112**, 223.
Nityanda, R., and R. Narayan, 1982, Mon. Not. R. Astron. Soc. **201**, 697.
Noerdlinger, P. D., 1978, Phys. Rev. Lett. **41**, 135.
Norman, C. A., and D. ter Haar, 1975, Phys. Rep. C **17**, 307.
Norman, C. A., and J. Silk, 1979, Astrophys. J. (Lett.) **233**, L1.
Norman, C. A., and J. Silk, 1983, Astrophys. J. **266**, 502.
Norman, M. L., L. L. Smarr, J. R. Wilson, and M. D. Smith, 1981, Astrophys. J. **247**, 52.
Norman, M. L., L. L. Smarr, K.-H. A. Winkler, and M. D. Smith, 1982, Astron. Astrophys. **113**, 285.
Norman, M. L., K.-H. A. Winkler, and L. L. Smarr, 1983, in *Astrophysical Jets: Proceedings of an international workshop held in Torino, Italy, ... 1983,* edited by A. Ferrari and A. G. Pacholczyk (Reidel, Dordrecht, Holland), p. 227.
Novikov, I. D., and K. S. Thorne, 1973, in *Black Holes* (Les Houches, 1972), edited by C. De Witt and B. S. De Witt (Gordon and Breach, New York), p. 343.
O'Dea, C. P., and F. N. Owen, 1984 (in preparation).
O'Dell, S. L., 1981, Astrophys. J. (Lett.) **243**, L147.
O'Dell, S. L., J. J. Puschell, W. A. Stein, F. N. Owen, R. W. Porcas, S. Mufson, T. J. Moffet, and M. H. Ulrich, 1978, As-

trophys. J. **224**, 22.
O'Dell, S. L., and L. Sartori, 1970, Astrophys. J. (Lett.) **161**, L63.
Okoye, S. E., 1976, Astrophys. J. **209**, 362.
Onuora, L. I., and S. E. Okoye, 1983, Astrophys. J. **270**, 360.
Oort, J. H., 1982, in *Extragalactic Radio Sources* (IAU Symposium No. 97), edited by D. S. Heeschen and C. M. Wade (Reidel, Dordrecht, Holland), p. 1.
Opher, R., 1975, Astrophys. J. **201**, 527.
Orr, M. J. L., and I. W. A. Browne, 1982, Mon. Not. R. Astron. Soc. **200**, 1067.
Osterbrock, D. E., 1978, Phys. Scr.**17**, 137.
Ostriker, J. P., 1983, Astrophys. J. **273**, 99.
Ostriker, J. P., and L. L. Cowie, 1981, Astrophys. J. (Lett.) **243**, L127.
Ostriker, J. P., R. McCray, R. Weaver, and A. Yahil, 1976, Astrophys. J. (Lett.) **208**, L61.
Owczarek, J. A., 1964, *Fundamentals of Gas Dynamics* (International Textbook Company, Scranton).
Owen, F. N., J. O. Burns, and L. Rudnick, 1978, Astrophys. J (Lett.) **226**, L119.
Owen, F. N., J. O. Burns, and L. Rudnick, 1979, Astrophys. J (Lett.) **229**, L59.
Owen, F. N., P. E. Hardee, and R. C. Bignell, 1980, Astrophys. J. Lett. **239**, L11.
Ozernoi, L. M., and V. E. Chertoprid, 1966, Sov. Astron. AJ **10**, 15.
Ozernoi, L. M., and V. E. Chertoprid, 1969, Sov. Astron. AJ **46**, 940.
Ozernoi, L. M., and V. N. Sazonov, 1969, Nature **219**, 467.
Ozernoi, L. M., and V. Ulanovskii, 1974, Sov. Astron. AJ **18**, 4.
Ozernoi, L. M., and V. V. Usov, 1971, Astrophys. Space Sci. **12**, 267.
Ozernoi, L. M., and V. V. Usov, 1973a, Astrophys. Space Sci. **25**, 149.
Ozernoi, L. M., and V. V. Usov, 1973b, Astrophys. Lett. **13**, 209.
Pacholczyk, A. G., 1970, *Radio Astrophysics* (Freeman, San Francisco).
Pacholczyk, A. G., 1973, Mon. Not. R. Astron. Soc. **163**, 29p.
Pacholczyk, A. G., and J. S. Scott, 1976, Astrophys. J. **203**, 313.
Pacholczyk, A. G., and T. L. Swihart, 1970, Astrophys. J. **161**, 145.
Pacholczyk, A. G., and T. L. Swihart, 1971a, Mon. Not. R. Astron. Soc. **153**, 3p.
Pacholczyk, A. G., and T. L. Swihart, 1971b, Astrophys. J. **170**, 405.
Pacholczyk, A. G., and T. L. Swihart, 1973, Astrophys. J. **179**, 21.
Pacholczyk, A. G., and T. L. Swihart, 1974, Astrophys. J. **192**, 591.
Pacholczyk, A. G., and T. L. Swihart, 1975, Astrophys. J. **196**, 125.
Pacini, F., and M. Salvati, 1974, Astrophys. J. (Lett.) **188**, L55.
Pacini, F., and M. Salvati, 1978, Astrophys. J. (Lett.) **225**, L99.
Paczyński, B., 1977a, Acta Astron. **28**, 91.
Paczyński, B., 1977b, Astrophys. J. **216**, 822.
Paczyński, B., and M. A. Abramowicz, 1982, Astrophys. J. **253**, 897.
Paczyński, B., and P. Wiita, 1980, Astron. Astrophys. **88**, 23.
Page, D. N., and K. S. Thorne, 1974, Astrophys. J. **191**, L99.
Palimaka, J. J., A. H. Bridle, E. B. Fomalont, and G. W. Brandie, 1979, Astrophys. J. (Lett.) **231**, L7.
Papaloizou, J. C. B., and J. E. Pringle, 1983, Mon. Not. R. Astron. Soc. **202**, 1181.
Papaloizou, J. C. B., and J. E. Pringle, 1984, Mon. Not. R. Astron. Soc. (in press).
Palimaka, J. J., A. H. Bridle, E. B. Fomalont, and G. W. Brandie, 1979, Astrophys. J. (Lett.) **231**, L7.
Parker, E. N., 1979, *Cosmical Magnetic Fields* (Clarendon, Oxford).
Pauli, W., 1958, *Theory of Relativity* (Pergamon, Oxford).
Pauliny-Toth, I. I. K., 1981, in *Origin of Cosmic Rays* (IAU Symposium No. 94), edited by G. Setti, G. Spada, and A. W. Wolfendale (Reidel, Dordrecht, Holland), p. 127.
Peacock, J. A., 1982, Mon. Not. R. Astron. Soc. **199**, 295.
Peacock, J. A., and S. F. Gull, 1981, Mon. Not. R. Astron. Soc. **196**, 611.
Pearson, T., S. Unwin, M. H. Cohen, R. Linfield, A. C. S. Readhead, G. A. Seielstad, R. S. Simon, and R. C. Walker, 1981, Nature **290**, 365.
Peckham, R. J., 1973, Nature Phys. Sci. **246**, 54.
Peebles, P. J. E., 1972, Astrophys. J. **178**, 371.
Penrose, R., 1969, Nuovo Cim. **1**, 252.
Perley, R. A., and A. H. Bridle, 1984 (in preparation).
Perley, R. A., A. H. Bridle, and A. G. Willis, 1984, Astrophys. J. Suppl. (in press).
Perley, R. A., J. J. Cowan, and J. W. Dreher, 1984 (in preparation).
Perley, R. A., E. B. Fomalont, and K. J. Johnston, 1980, Astron. J. **85**, 649.
Perley, R. A., E. B. Fomalont, and K. J. Johnston, 1982, Astrophys. J. (Lett.) **255**, L93.
Perley, R. A., A. G. Willis, and J. S. Scott, 1979, Nature **281**, 437.
Peterson, F. W., and W. A. Dent, 1973, Astrophys. J. **186**, 421.
Peterson, F. W., C. B. Foltz, and P. L. Byard, 1981, Astrophys. J. **251**, 4.
Peterson, F. W., and C. King, 1975, Astrophys. J. **195**, 753.
Phinney, E. S., 1982, Mon. Not. R. Astron. Soc. **198**, 1109.
Phinney, E. S., 1983a, Ph.D. thesis (University of Cambridge).
Phinney, E. S., 1983b, Mon. Not. Astrophys. Soc. (in press).
Pineault, S., 1984, Astron. Astrophys. (in press).
Piddington, J. H., 1970, Mon. Not. R. Astron. Soc. **148**, 131.
Piddington, J. H., 1981, *Cosmic Electrodynamics* (Krieger, Melbourne, Florida).
Piran, T., 1978, Astrophys. J. **221**, 652.
Piran, T., 1982, Astrophys. J. **257**, L23.
Porcas, R. W., 1981, Nature **294**, 47.
Potash, R. I., and J. F. C. Wardle, 1979, Astron. J. **84**, 707.
Potash, R. I., and J. F. C. Wardle, 1980, Astrophys. J. **239**, 42.
Pringle, J. E., 1981, Annu. Rev. Astron. Astrophys. **19**, 137.
Pringle, J. E., and M. J. Rees, 1972, Astron. Astrophys. **21**, 1.
Pringle, J. E., M. J. Rees, and A. G. Pacholczyk, 1973, Astron. Astrophys. **29**, 179.
Pudritz, R. E., 1981, Mon. Not. R. Astron. Soc. **195**, 881.
Pudritz, R. E., and G. G. Fahlman, 1982, Mon. Not. R. Astron. Soc. **198**, 689.
Ray, T. P., 1981, Mon. Not. R. Astron. Soc. **196**, 195.
Ray, T. P., and A. Ershkovich, 1983, Mon. Not. R. Astron. Soc. **204**, 821.
Rayburn, D., 1977, Mon. Not. R. Astron. Soc. **179**, 603.
Readhead, A. C. S., 1980, in *Objects of High Redshift* (IAU Symposium No. 92), edited by G. O. Abell and P. J. E. Peebles (Reidel, Dordrecht, Holland), p. 165.
Readhead, A. C. S., M. H. Cohen, and R. D. Blandford, 1978, Nature **272**, 131.
Readhead, A. C. S., M. H. Cohen, T. J. Pearson, and P. Wilkin-

son, 1978, Nature **276**, 768.
Readhead, A. C. S., and A. Hewish, 1976, Mon. Not. R. Astron. Soc. **176**, 571.
Readhead, A. C. S., and M. Longair, 1975, Mon. Not. R. Astron. Soc. **170**, 393.
Readhead, A. C. S., and T. Pearson, 1983 (preprint).
Readhead, A. C. S., and T. Pearson, 1984, in *VLBI and Compact Radio Sources* (IAU Symposium No. 110), edited by K. I. Kellermann and G. Setti (Reidel, Dordrecht, Holland), in press.
Readhead, A. C. S., T. J. Pearson, M. H. Cohen, M. S. Ewing, and A. T. Moffet, 1979, Astrophys. J. **231**, 299.
Readhead, A. C. S., T. J. Pearson, and S. C. Unwin, 1984, in *VLBI and Compact Radio Sources* (IAU Symposium No. 110), edited by K. I. Kellermann and G. Setti (Reidel, Dordrecht, Holland), in press.
Readhead, A. C. S., and P. N. Wilkinson, 1978, Astrophys. J. **223**, 25.
Readhead, A. C. S., and P. N. Wilkinson, 1980, Astrophys. J. **235**, 11.
Rees, M. J., 1966, Nature **211**, 468.
Rees, M. J., 1967a, Mon. Not. R. Astron. Soc. **135**, 345.
Rees, M. J., 1967b, Mon. Not. R. Astron. Soc. **137**, 429.
Rees, M. J., 1971, Nature **229**, 312 (errata p. 510).
Rees, M. J., 1976, Comments Astrophys. Space Sci. **6**, 113.
Rees, M. J., 1978a, Mon. Not. R. Astron. Soc. **184**, 61p.
Rees, M. J., 1978b, Nature **275**, 516.
Rees, M. J., 1978c, Phys. Scr. **17**, 193.
Rees, M. J., 1980, in *Origin of Cosmic Rays* (IAU Symposium No. 94), edited by G. Setti, G. Spada, and A. W. Wolfendale (Reidel, Dordrecht, Holland), p. 139.
Rees, M. J., M. C. Begelman, R. D. Blandford, and E. S. Phinney, 1982, Nature **295**, 17.
Rees, M. J., and G. Setti, 1968, Nature **219**, 127.
Rees, M. J., and M. Simon, 1968, Astrophys. J. (Lett.) **152**, L145.
Rees, M. J., and M. Simon, 1970, Nature **227**, 1303.
Reynolds, S. P., 1982a, Astrophys. J. **256**, 13.
Reynolds, S. P., 1982b, Astrophys. J. **256**, 38.
Reynolds, S. P., and C. P. McKee, 1980, Astrophys. J. **239**, 893.
Richter, G. M., 1976, Astron. Nachr. **297**, 5.
Rickett, B. J., W. A. Coles, and G. Bourgois, 1983 (U. C. San Diego preprint).
Riegler, G. R., and R. D. Blandford, 1982, Eds., *The Galactic Center* (AIP Conference Proceedings No. 83) (AIP, New York).
Riley, J. M., 1973, Mon. Not. R. Astron. Soc. **161**, 167.
Roos, N., 1981, Astron. Astrophys. **104**, 218.
Roos, N., and C. A. Norman, 1979, Astron. Astrophys. **76**, 75.
Rose, J. A., 1982, Mon. Not. R. Astron. Soc. **201**, 1015.
Rosenberg, H., 1972, Astron. Astrophys. **19**, 104.
Rudnick, L., 1982, in *Extragalactic Radio Sources* (IAU Symposium No. 97), edited by D. S. Heeschen and C. M. Wade (Reidel, Dordrecht, Holland), p. 47.
Rudnick, L., and J. O. Burns, 1981, Astrophys. J. (Lett.) **246**, L69.
Rudnick, L., W. C. Saslaw, P. O. Crane, and J. A. Tysoni, 1981, Astrophys. J. **246**, 677.
Rybicki, G. B., and A. P. Lightman, 1979, *Radiative Processes in Astrophysics* (Wiley, New York).
Ryle, M., and A. C. Brodie, 1981, Mon. Not. R. Astron. Soc. **196**, 567.
Ryle, M., and M. S. Longair, 1967, Mon. Not. R. Astron. Soc. **136**, 123.
Ryle, M., P. C. Waggett, and C. O'Dell, 1975, Mon. Not. R. Astron. Soc. **173**, 9.
Saikia, D. J., 1981, Mon. Not. R. Astron. Soc. **197**, 11p.
Saikia, D. J., and V. K. Kulkarni, 1979, Mon. Not. R. Astron. Soc. **189**, 393.
Saikia, D. J., and P. J. Wiita, 1982, Mon. Not. R. Astron. Soc. **200**, 83.
Sakimoto, P. J., and F. Coroniti, F. V., 1981, Astrophys. J. **247**, 19.
Salpeter, E. E., 1964, Astrophys. J. **140**, 796.
Salpeter, E. E., 1971, Nature Phys. Sci. **233**, 5.
Salpeter, E. E., and R. V. Wagoner, 1971, Astrophys. J. **164**, 557.
Salvati, M., 1979, Astrophys. J. **233**, 11.
Sanders, R. H., 1970, Astrophys. J. **162**, 784.
Sanders, R. H., 1974, Nature **248**, 390.
Sanders, R. H., 1976, Astrophys. J. **205**, 135.
Sanders, R. H., 1983, Astrophys. J. **266**, 73.
Sarazin, C. L., M. C. Begelman, and S. P. Hatchett, 1980, Astrophys. J. (Lett.) **238**, L129.
Saslaw, W. C., and S. A. Mitton, 1973, Comments Astrophys Space Phys. **5**, 133.
Saslaw, W. C., J. C. Tyson, and P. C. Crane, 1978, Astrophys. J. **222**, 435.
Saslaw, W. C., M. Valtonen, and S. Aarseth, 1974, Astrophys. J. **190**, 253.
Saunders, R., J. E. Baldwin, G. G. Pooley, and P. J. Warner, 1981, Mon. Not. R. Astron. Soc. **197**, 287.
Sazanov, V. N., 1969, Sov. Astron. AJ **13**, 396.
Sazanov, V. N., 1973a, Astrophys. Space Sci. **19**, 3.
Sazanov, V. N., 1973b, Sov. Astron. AJ **16**, 774.
Scheuer, P. A. G., 1967, in *Plasma Astrophysics, Proceedings of the International School of Physics "Enrico Fermi" Course 39*, edited by P. A. Sturrock (Academic, New York/London), p. 262.
Scheuer, P. A. G., 1974, Mon. Not. R. Astron. Soc. **166**, 513.
Scheuer, P. A. G., 1982, in *Extragalactic Radio Sources* (IAU Symposium No. 97), edited by D. S. Heeschen and C. M. Wade (Reidel, Dordrecht, Holland), p. 163.
Scheuer, P. A. G., and A. C. S. Readhead, 1979, Nature **277**, 182.
Schilizzi, R. T., and A. G. de Bruyn, 1983, Nature **303**, 26.
Schmidt, G. D., B. M. Petersen, and E. A. Beaver, 1978, Astrophys. J. (Lett.) **220**, L31.
Schmidt, M., 1963, Nature **197**, 1040.
Schmidt, M., 1978, Phys. Scr. **17**, 135.
Schmidt, M., and R. F. Green, 1983, Astrophys. J. **269**, 352.
Schmitt, J., 1968, Nature **218**, 663.
Schreier, E. J., J. Burns, and R. Feigelson, 1981, Astrophys. J. **251**, 523.
Schreier, E. J., E. Feigelson, J. Delvaille, R. Giacconi, J. Grindlay, D. A. Schwartz, and A. C. Fabian, 1980, Astrophys. J. (Lett.) **234**, L39.
Schwarz, D. A., and W. M. M. Ku, 1983, Astrophys. J. **266**, 469.
Schwartz, R. D., 1983, Annu. Rev. Astron. Astrophys. **21**, 209.
Scott, M. A., 1977a, Mon. Not. R. Astron. Soc. **178**, 329.
Scott, M. A., 1977b, Mon. Not. R. Astron. Soc. **179**, 377.
Scott, M. A., and R. V. E. Lovelace, 1981, Astrophys. J. **252**, 765.
Scott, M. A., and A. C. S. Readhead, 1977, Mon. Not. R. Astron. Soc. **180**, 539.
Seaquist, E. R., 1972, Astrophys. Space Sci. **15**, 284.
Segal, I. E., 1979, Astrophys. J. **227**, 15.
Seguin, F. H., 1975, Astrophys. J. **197**, 745.

Seidl, A. G. P., and A. G. W. Cameron, 1972, Astrophys. Space Sci. **15**, 44.
Seielstad, G. A., 1974, Astrophys. J. **193**, 55.
Seldner, M., and P. J. E. Peebles, 1978, Astrophys. J. **225**, 7.
Setti, G., 1978, in *Proceedings of Pittsburgh Conference on BL Lac Objects,* edited by A. M. Wolfe (Department of Physics and Astronomy, University of Pittsburgh, Pittsburgh), p. 385.
Seyfert, C. K., 1943, Astrophys. J. **97**, 28.
Shaffer, D. B., and A. P. Marscher, 1979, Astrophys. J. (Lett.) **233**, L105.
Shakura, N. I., and R. A. Sunyaev, 1973, Astron. Astrophys. **24**, 337.
Shakura, N. I., and R. A. Sunyaev, 1976, Mon. Not. R. Astron. Soc. **175**, 613.
Shakura, N. I., R. A. Sunyaev, and A. Zilitinkovich, 1978, Astron. Astrophys. **62**, 179.
Shapiro, P. R., 1979a, Astrophys. J. **233**, 831.
Shapiro, P. R., 1979b, in *Particle Acceleration Mechanisms in Astrophysics* (AIP Conference Proceedings No. 56), edited by J. Arons, C. Max, and C. McKee (AIP, New York), p. 295.
Shapiro, P. R., 1980, Astrophys. J. **236**, 958.
Shapiro, P. R., M. Milgrom, and M. J. Rees, 1982, in *Extragalactic Radio Sources* (IAU Symposium No. 97), edited by D. S. Heeschen and C. M. Wade (Reidel, Dordrecht, Holland), p. 209.
Shapiro, S. L., 1973a, Astrophys. J. **180**, 531.
Shapiro, S. L., 1973b, Astrophys. J. **185**, 69.
Shapiro, S. L., and S. A. Teukolsky, 1983, *Black Holes, White Dwarfs and Neutron Stars* (Wiley, New York).
Shaver, P. A., I. J. Danzinger, R. D. Ekers, R. A. E. Fosbury, W. M. Goss, D. Malin, A. F. M. Moorwood, and J. V. Wall, 1982, in *Extragalactic Radio Sources* (IAU Symposium No. 97), edited by D. S. Heeschen and C. M. Wade (Reidel, Dordrecht, Holland), p. 55.
Sherman, R. D., 1981, Astrophys. J. **246**, 365.
Shields, G. A., and J. C. Wheeler, 1976, Astrophys. J. **17**, 69.
Shields, G. A., and J. C. Wheeler, 1978, Astrophys. J. **222**, 667.
Shirie, J. W., and J. G. Seubold, 1967, AIAA J. **5**, 2062.
Shklovsky, I. S., 1953, Dokl. Akad. Nauk SSSR **90**, 983.
Shklovsky, I. S., 1960, Astron. Zh. **37**, 256.
Shklovsky, I. S., 1971, Sov. Astron. AJ **14**, 594.
Shklovsky, I. S., 1977, Sov. Astron. AJ **21**, 4.
Shklovsky, I. S., 1982, in *Extragalactic Radio Sources* (IAU Symposium No. 97), edited by D. S. Heeschen and C. M. Wade (Reidel, Dordrecht, Holland), p. 475.
Shull, J. M., 1983, Astrophys. J. **264**, 446.
Siah, M. J., and P. J. Wiita, 1983, Astrophys. J. **270**, 427.
Sikora, M., 1981, Mon. Not. R. Astron. Soc. **196**, 257.
Sikora, M., and D. B. Wilson, 1981, Mon. Not. R. Astron. Soc. **197**, 529.
Silk, J., and C. A. Norman, 1979, Astrophys. J. **234**, 86.
Simkin, S., 1978, Astrophys. J. (Lett.) **222**, L55.
Simkin, S., 1979, Astrophys. J. **234**, 56.
Simkins, S., and R. Ekers, 1979, Astron. J. **84**, 56.
Simon, A., 1979, Mon. Not. R. Astron. Soc. **188**, 637.
Simon, M., 1969, Astrophys. J. **158**, 865.
Simon, M., and W. I. Axford, 1967, Astrophys. J. **150**, 105.
Simon, R. S., A. C. S. Readhead, and P. N. Wilkinson, 1984, in *VLBI and Compact Radio Sources* (IAU Symposium No. 110), edited by K. I. Kellermann and G. Setti (Reidel, Dordrecht, Holland), in press.
Slingo, A., 1974a, Mon. Not. R. Astron. Soc. **166**, 101.
Slingo, A., 1974b, Mon. Not. R. Astron. Soc. **168**, 307.
Smak, 1976, Acta. Astron. **76**, 277.
Smarr, L. L., 1978, Ed., *Sources of Gravitational Radiation,* (Cambridge University, Cambridge).
Smith, D. F., 1976, Astrophys. Space Sci. **42**, 261.
Smith, D. F., 1977, Astrophys. J. **212**, 891.
Smith, M. D., and C. A. Norman, 1981, Mon. Not. R. Astron. Soc. **194**, 771, 785.
Smith, M. D., L. L. Smarr, M. L. Norman, and J. R. Wilson, 1983, Astrophys. J. **264**, 432.
Smith, M. G., and A. E. Wright, 1980, Mon. Not. R. Astron. Soc. **191**, 871.
Smith, M. D., L. L. Smarr, M. L. Norman, and J. Wilson, 1981, Nature **293**, 277.
Soltan, A., 1982, Mon. Not. R. Astron. Soc. **200**, 115.
Southwood, D. J., 1968, Planet. Space Sci. **16**, 587.
Spangler, S., 1979, Astrophys. J. (Lett.) **232**, L7.
Spangler, S., 1983, Astrophys. J. (Lett.) **271**, L49.
Sparke, L. S., 1982a, Astrophys. J. **254**, 456.
Sparke, L. S., 1982b, Astrophys. J. **260**, 104.
Sparke, L. S., and F. H. Shu, 1980, Astrophys. J. (Lett.) **241**, L65.
Spitzer, L., 1971, Astrophys. J. (Lett.) **158**, L139.
Spitzer, L., 1978, *Physical Processes in the Interstellar Medium* (Wiley, New York).
Spitzer, L., and W. C. Saslaw, 1966, Astrophys. J. **143**, 400.
Spitzer, L., and M. E. Stone, 1967, Astrophys. J. **147**, 519.
Stewart, P., 1971, Astrophys. Space Sci. **14**, 261.
Stocke, J., 1978, Astron. J. **83**, 348.
Stocke, J., 1979, Astrophys. J. **230**, 40.
Stocke, J., W. A. Tifft, and M. A. Kaftan-Kassim, 1978, Astron. J. **83**, 322.
Stockman, H. S., J. R. P. Angel, and G. K. Miley, 1979, Astrophys. J. (Lett.) **227**, L55.
Stoeger, W. R., 1977, Astrophys. J. **261**, 659.
Strittmatter, P. A., P. Hill, I. I. K. Pauliny-Toth, M. Steppe, and A. Witzel, 1980, Astron. Astrophys. **88**, L12.
Strom, R. G., J. R. Baker, and A. G. Willis, 1981, Astron. Astrophys. **100**, 220.
Sturrock, P. A., 1965, Nature **205**, 861.
Sturrock, P. A., 1971, Astrophys. J. **170**, 85.
Sturrock, P. A., and C. Barnes, 1972, Astrophys. J. **176**, 31.
Sturrock, P. A., and P. A. Feldman, 1968, Astrophys. J. (Lett.) **152**, L39.
Sunyaev, R. A., 1970, Astrophys. Lett. **7**, 19.
Svennson, R., 1982a, Astrophys. J. **258**, 131.
Svennson, R., 1982b, Astrophys. J. **258**, 321.
Svennson, R., 1984, Mon. Not. R. Astron. Soc. (in press).
Takahara, F., 1979, Prog. Theor. Phys. **62**, 629.
Takaroda, K., 1970, Publ. Astron. Soc. Japan **22**, 551.
Taylor, J. B., 1974, Phys. Rev. Lett. **33**, 1139.
Terrell, J., 1966, Science **154**, 1281.
Thompson, P. A., 1978, *Compressible Fluid Dynamics* (McGraw-Hill, New York).
Thorne, K. S., 1974, Astrophys. J. **191**, 507.
Thorne, K. S., and R. D. Blandford, 1982, in *Extragalactic Radio Sources* (IAU Symposium No. 97), edited by D. S. Heeschen and C. M. Wade (Reidel, Dordrecht, Holland), p. 255.
Thorne, K. S., and D. Macdonald, 1982, Mon. Not. R. Astron. Soc. **198**, 339.
Tubbs, A., 1981, Astrophys. J. **241**, 969.
Turland, B. D., and P. A. G. Scheuer, 1976, Mon. Not. R. Astron. Soc. **176**, 421.
Tyson, J. A., P. Crane, and W. C. Saslaw, 1977, Astron. Astrophys. **59**, 127.

Ulfbeck, O., 1978, Ed., *Quasars and Active Nuclei of Galaxies,* Phys. Scr. **17**, 3.
Unno, W., 1971, Publ. Astron. Soc. Japan **23**, 123.
Unwin, S. C., M. H. Cohen, T. J. Pearson, G. A. Seielstad, R. S. Simon, R. P. Linfield, and R. C. Walker, 1983, Astrophys. J. **271**, 536.
Vallée, J. P., A. H. Bridle, and A. S. Wilson, 1981, Astrophys. J. **250**, 66.
Vallée, J. P., and A. S. Wilson, 1976, Nature **259**, 451.
Valtonen, M. J., 1979, Astrophys. J. (Lett.) **227**, L79.
Valtonen, M. J., and G. G. Byrd, 1980, Astrophys. J. **240**, 442.
van Albada, T. S., C. E. Kotanyi, and M. Schwarzschild, 1982, Mon. Not. R. Astron. Soc. **198**, 303.
van Breugel, W. J. M., 1980, Astron. Astrophys. **88**, 248.
van Breugel, W. J. M., T. Heckman, M. Batcher, and G. Miley, 1984, Astrophys. J. **277**, 82.
van Breugel, W. J. M., and G. Miley, 1977, Nature **265**, 315.
van Groningen, E., G. Miley, and C. A. Norman, 1980, Astron. Astrophys. J. Lett. **90**, L7.
van den Heuvel, E. P. J., J. Ostriker, and J. A. Petterson, 1980, Astron. Astrophys. **81**, L7.
van der Kruit, P. C., J. H. Oort, and D. S. Mathewson, 1972, Astron. Astrophys. **21**, 169.
van der Laan, H., 1963, Mon. Not. R. Astron. Soc. **126**, 535.
van der Laan, H., 1966, Nature **211**, 1131.
van der Laan, H., 1971, in *Nuclei of Galaxies,* edited by D. J. K. O'Connell (North-Holland, Amsterdam), p. 245.
Vestrand, W. T., J. S. Scott, A. P. Marscher, and W. A. Christiansen, 1981, Astrophys. J. **245**, 811.
Vitello, P., and F. Pacini, 1977, Astrophys. J. **215**, 452.
Vitello, P., and F. Pacini, 1978, Astrophys. J. **220**, 756.
Waggett, P. C., P. J. Warner, and J. E. Baldwin, 1977, Mon. Not. R. Astron. Soc. **181**, 465.
Wall, J. V., 1979, Philos. Trans. R. Soc. London **111**, 99.
Wall, J. V., T. J. Pearson, and M. S. Longair, 1981, Mon. Not. R. Astron. Soc. **196**, 597.
Walmsey, C. M., 1971, Astrophys. Lett. **8**, 27.
Wardle, J. F. C., 1977, Nature **269**, 563.
Wardle, J. F. C., 1978, in *Pittsburgh Conference on BL Lac Objects,* edited by A. M. Wolfe (Department of Physics and Astronomy, University of Pittsburgh, Pittsburgh), p. 39.
Wardle, J. F. C., A. H. Bridle, and M. J. L. Kesteven, 1981, Astron. J. **86**, 848.
Wardle, J. F. C., and R. I. Potash, 1982, in *Extragalactic Radio Sources* (IAU Symposium No. 97), edited by D. S. Heeschen and C. M. Wade (Reidel, Dordrecht, Holland), p. 129.
Weedman, D. W., 1977, Annu. Rev. Astron. Astrophys. **15**, 69.
Weedman, D. W., 1983, Astrophys. J. **266**, 479.
Weiler, K. W., and K. J. Johnston, 1980, Mon. Not. R. Astron. Soc. **190**, 269.
Weinberg, S., 1972, *Gravitation and Cosmology* (Wiley, New York).
Wellington, K. J., G. K. Miley, and H. van der Laan, 1973, Nature **244**, 502.
Wesson, P. S., and A. Lenmann, 1977, Astrophys. Space Sci. **46**, 51.
Whitney, A. R., I. I. Shapiro, A. E. E. Rogers, D. S. Robertson, C. A. Knight, T. A. Clark, R. M. Goldstein, G. E. Marandino, and N. R. Vandenburg, 1971, Science **173**, 225.
Wiita, P. J., 1978a, Astrophys. J. **221**, 41.
Wiita, P. J., 1978b, Astrophys. J. **221**, 436.
Wiita, P. J., 1982, Astrophys. J. **256**, 666.
Wiita, P. J., and M. J. Siah, 1981, Astrophys. J. **243**, 710.
Wilkinson, A., R. G. Hine, and W. L. W. Sargent, 1981, Mon. Not. R. Astron. Soc. **196**, 669.
Willis, A. G., R. G. Strom, A. H. Bridle, and E. B. Fomalont, 1981, Astron. Astrophys. **95**, 250.
Willis, A. G., R. G. Strom, R. A. Perley, and A. H. Bridle, 1982, in *Extragalactic Radio Sources* (IAU Symposium No. 97), edited by D. S. Heeschen and C. M. Wade (Reidel, Dordrecht, Holland), p. 141.
Willis, A. G., R. G. Strom, and A. S. Wilson, 1974, Nature **250**, 625.
Wilson, A. S., 1982, in *Extragalactic Radio Sources* (IAU Symposium No. 97), edited by D. S. Heeschen and C. M. Wade (Reidel, Dordrecht, Holland), p. 179.
Wilson, A. S., and J. S. Ulvestad, 1982, Astrophys. J. **263**, 576.
Wilson, A. S., and A. G. Willis, 1980, Astrophys. J. **240**, 429.
Wilson, D. B., 1980, Mon. Not. R. Astron. Soc. **192**, 787.
Wilson, D. B., 1982, Mon. Not. R. Astron. Soc. **200**, 881.
Wilson, J. R., 1976, Ann. N.Y. Acad. Sci. **262**, 123.
Wilson, M. J., and P. A. G., Scheuer, 1983, Mon. Not. R. Astron. Soc. **205**, 449.
Windsor, R. D., and P. J. Kellogg, 1974, Astrophys. J. **190**, 167.
Wirth, A., L. L. Smarr, and J. S. Gallagher, 1982, Astron. J. **87**, 602.
Wittels, J. J., I. I. Shapiro, and W. D. Cotton, 1982, Astrophys. J. (Lett.) **262**, L27.
Wolfe, A., 1978, Ed., *Pittsburgh Conference on BL Lac Objects* (Department of Physics and Astronomy, University of Pittsburgh, Pittsburgh).
Woltjer, L., 1966, Astrophys. J. **146**, 597.
Woltjer, L., 1971, in *Nuclei of Galaxies* edited by D. J. K. O'Connell (North-Holland, Amsterdam), p. 477.
Woltjer, L., 1972, Annu. Rev. Astron. Astrophys. **10**, 129.
Wyckoff, S., P. A. Wehinger, and T. Gehren, 1981, Astrophys. J. **247**, 750.
Yokosawa, M., and S. Sakashita, 1980, Astrophys. Space Sci. **82**, 491.
Yokosawa, M., S. Ikeuchi, and S. Sakashita, 1983, Publ. Astron. Soc. Japan (in press).
Young, P. J., 1977, Astrophys. J. **212**, 227.
Young, P. J., G. A. Shields, and J. C. Wheeler, 1977, Astrophys. J. **212**, 367.
Young, P. J., J. A. Westphal, J. Kristian, C. P. Wilson, and F. P. Landaner, 1978, Astrophys. J. **221**, 721.
Zel'dovich, Ya. B., and I. D. Novikov, 1964, Usp. Fiz. Nauk **84**, 377 [Sov. Phys.—Usp. **7**, 763 (1965)].
Zel'dovich, Ya. B., and Yu. P. Raizer, 1966, *Physics of Shock Waves and High-Temperature Hydrodynamic Phenomena* (Academic, New York).
Zheleznyakov, V. V., 1969, Astrophys. J. **155**, 1129.
Znajek, R. L., 1978, Mon. Not. R. Astron. Soc. **185**, 833.

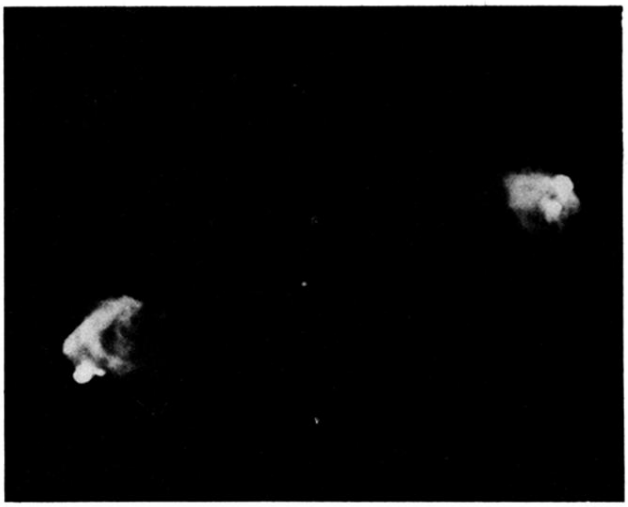

FIG. 1. Prototypical "edge-brightened" strong double source Cygnus A (3C405), showing the characteristic hot spots, lobes, and nucleus (cf. Fig. 10). This radio image, made with the VLA operating at $\lambda = 6$ cm, has a resolution of 0".7. Data from Perley, Cowan, and Dreher, in preparation; image supplied by R. A. Perley.

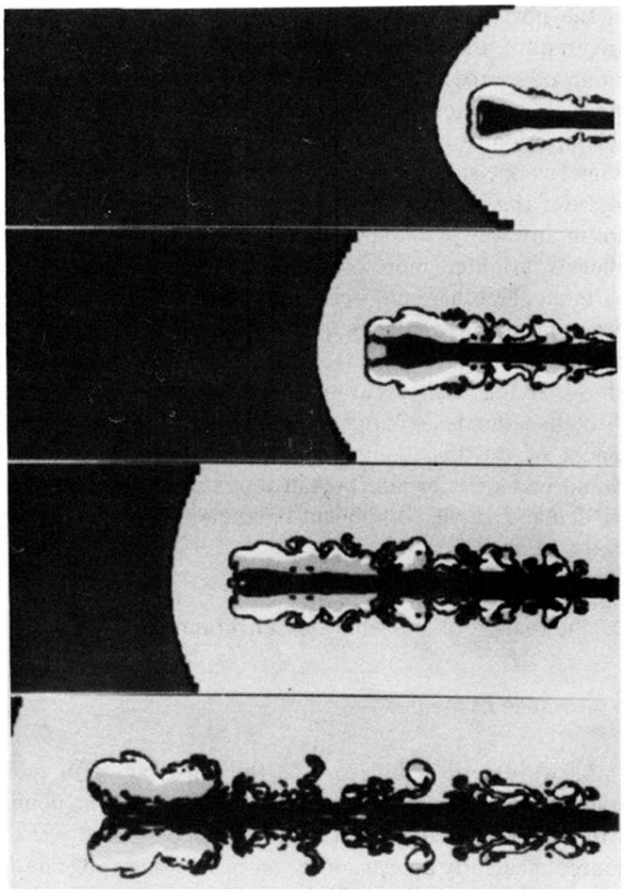

FIG. 11. Evolution of a Mach 3 pressure-matched jet of $\frac{1}{10}$ the ambient density, as determined by the two-dimensional hydrodynamical simulations of Norman, Winkler, and Smarr (1983). Various flow features are represented by different shades of grey as follows: unperturbed ambient medium, dark grey; bow shock, black; perturbed ambient medium, light grey; supersonic jet, black; backflowing cocoon gas, white; forward-flowing cocoon gas, grey; jet boundary, black. At early times a well-developed cocoon exists, which becomes Kelvin-Helmholtz unstable at later times. Reproduced, with permission, from Norman, Winkler, and Smarr (1983), © 1983 by D. Reidel Publishing Company.

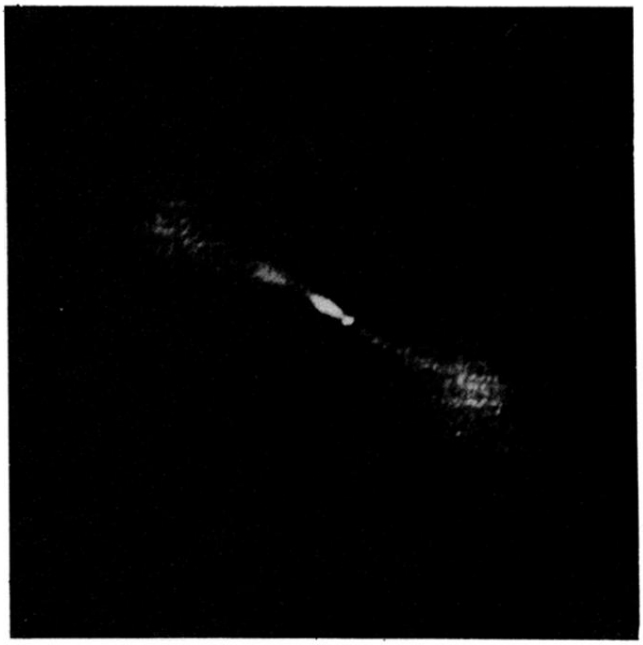

FIG. 2. Image of the weak "edge-darkened" radio source $2354+471$, made using the VLA at $\lambda=20$ cm. Data from Burns and Gregory (1982), image supplied by J. O. Burns.

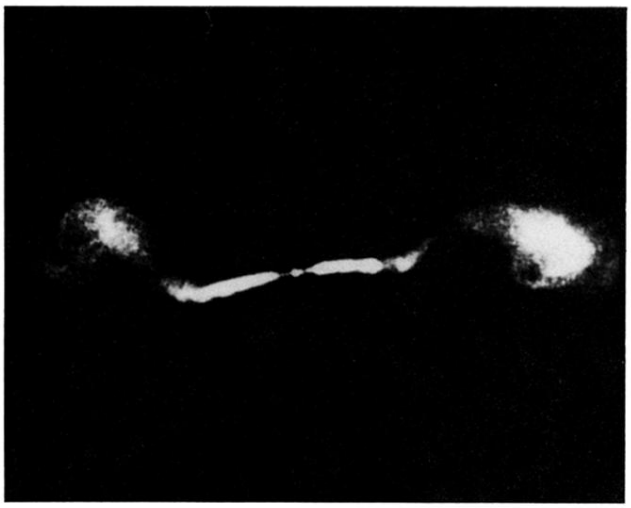

FIG. 3. Prominent jets and a high degree of symmetry are characteristic of the weaker radio sources, such as 3C449. The reflection (*C*-type) symmetry may result from the orbital motion of the parent galaxy around a companion, which is visible on optical photographs. This VLA image, made at $\lambda = 22$ cm, has a resolution of 1".4. Data from Cornwell and Perley, in preparation; image supplied by R. A. Perley.

(b)

FIG. 4. *(Continued).*

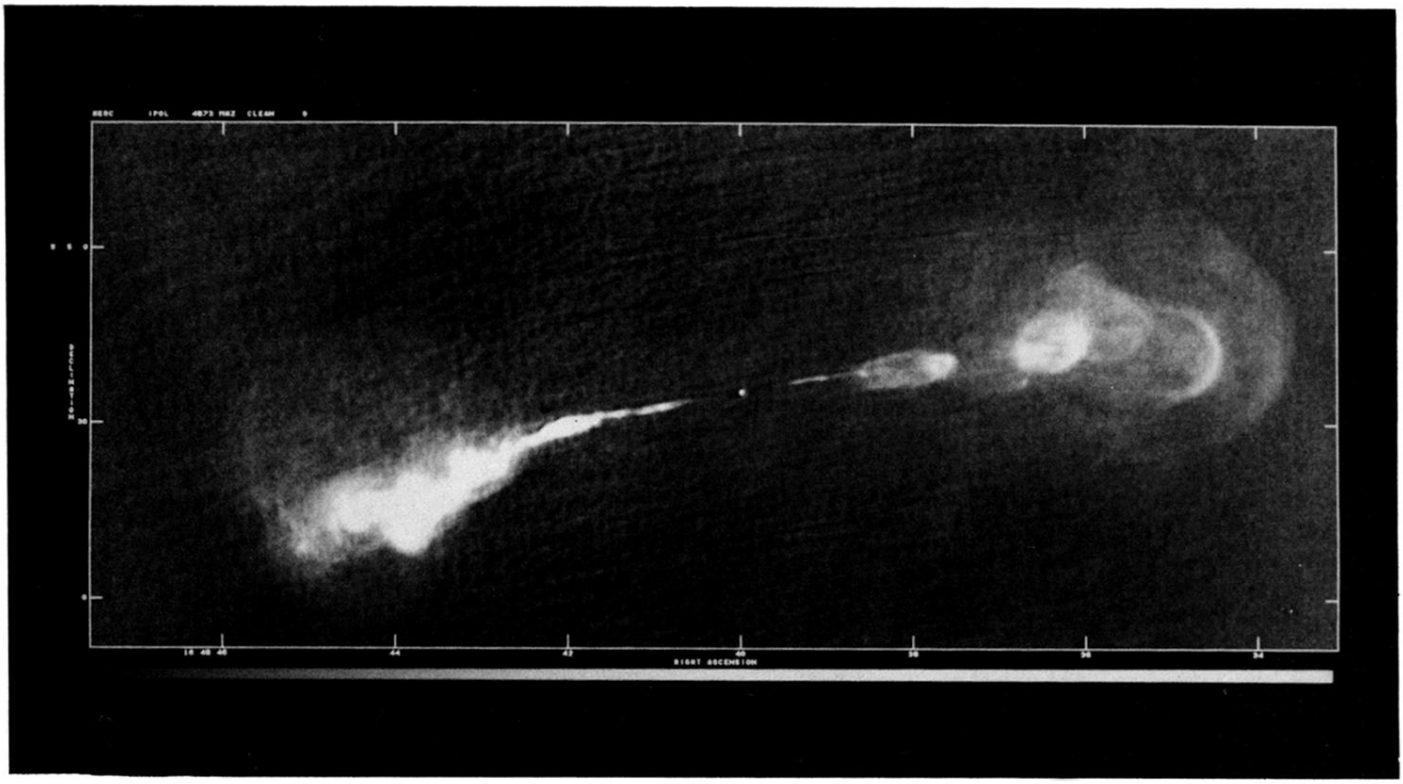

FIG. 5. The puzzling object Hercules A (3C348) displays characteristics of both the strong ("edge-brightened") and weak ("edge-darkened") sources, and may represent a transitional case. This 6-cm VLA image has a resolution of 0".5. Data from Dreher and Feigelson (1984); image supplied by E. D. Feigelson.

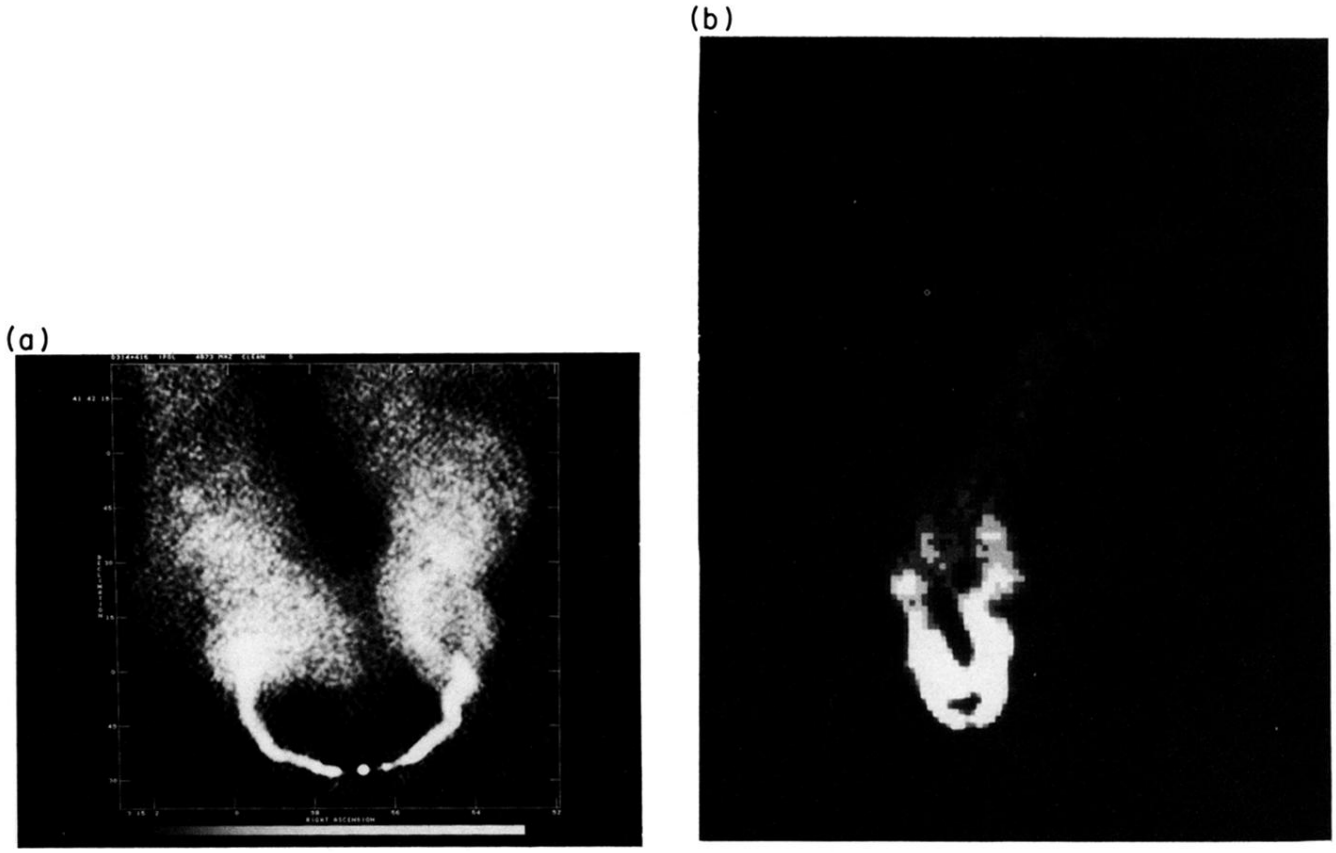

FIG. 6. (a) The jets in the prototypical radio trail NGC 1265 (3C83.1B) are believed to be swept back by the ram pressure of the intergalactic medium. The sharp edges above and below the inner jets are artifacts of the reproduction process. (VLA image at $\lambda=6$ cm, 1".2 resolution.) (b) Traced over hundreds of kiloparsecs, the source has a tadpole-like appearance. (VLA image at $\lambda=20$ cm, $13''\times11''$ resolution.) Data from O'Dea and Owen, in preparation; images supplied by C. P. O'Dea.

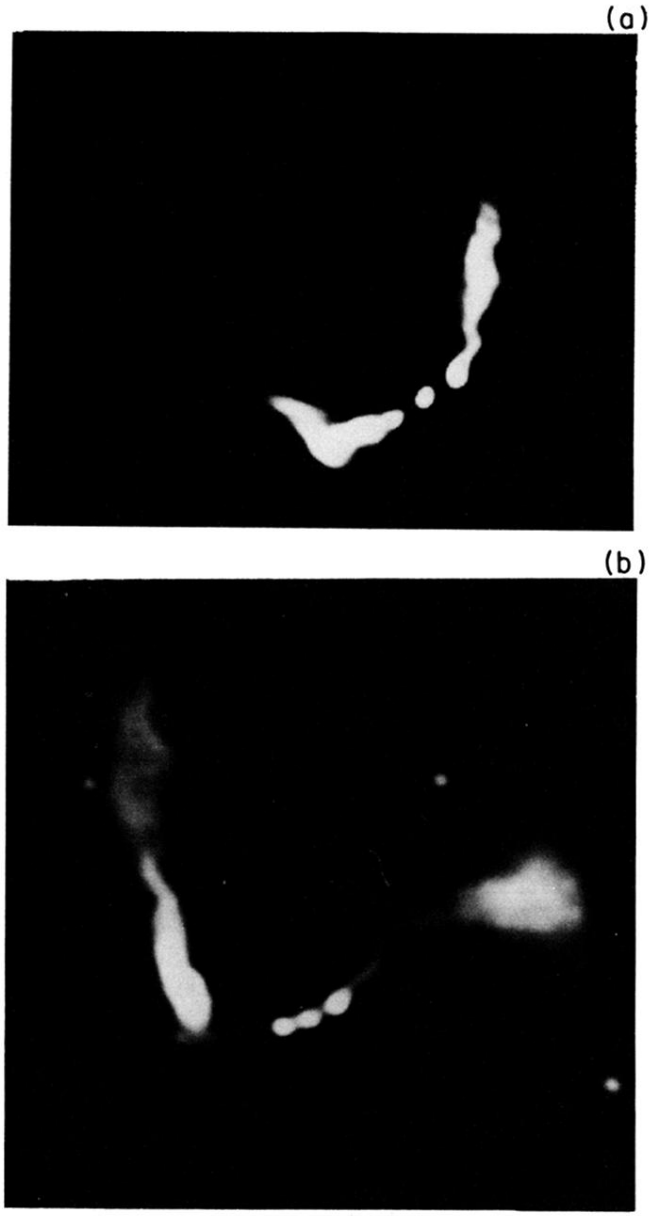

FIG. 7. 3C465 (a) and 1919 + 479 (b) are typical of the sources known as "wide-angle tails." Like radio trails (Fig. 6), wide-angle tails are found almost exclusively in rich clusters of galaxies, and the curvature is believed to result from interaction between the jets and the intracluster medium. Data on 3C465 (VLA at $\lambda=20$ cm with $9''.5\times12''$ resolution) from Eilek, Burns, O'Dea, and Owen, 1984; image supplied by C. P. O'Dea. Data on 1919 + 479 (VLA at $\lambda=20$ cm with $5''$ resolution) from J. O. Burns (1981); image supplied by J. O. Burns.